

RELATION OF COAL LIQUEFACTION CATALYST PROPERTIES TO PERFORMANCE

R. J. Bertolacini, L. C. Gutberlet, D. K. Kim and K. K. Robinson

Amoco Oil Company
P. O. Box 400
Naperville, Illinois 60540

INTRODUCTION

In March 1975, Amoco Oil Research, under contract with EPRI, began a three-year project on liquefaction catalysis (1,2). The specific purpose was to develop one or more superior catalysts for hydroliquefaction processes in advanced stages of development, such as the H-Coal process. The primary interest was in the conversion of coal to a clean-burning boiler fuel, low in sulfur and ash.

The hydroliquefaction of coal is a complex process which involves close interaction between the solubilized coal, hydrogen donor solvent, and catalyst. An improved catalyst for coal liquefaction must satisfy several requirements, but two key aspects are high initial activity for liquefaction-desulfurization and good aging characteristics.

Initial catalyst performance was determined in a batch test unit. A large number of catalysts, both commercially available and experimental, have been screened for initial performance. Catalysts selected on the basis of their physical and chemical properties as well as initial performance in the screening test were then subjected to continuous flow operation for approximately one week to determine their early deactivation behavior. Good initial performance of a catalyst may rapidly decline due to factors such as coking, sintering and metals deposition. Therefore a crucial aspect in developing a coal liquefaction catalyst is continuous operation for extended periods.

EXPERIMENTAL

Batch Screening Unit

The screening of catalysts for initial performance was carried out in a one-liter stirred autoclave. A mixture of 10 grams of catalyst (60-100 mesh granules, predried), 150 g coal and about 300 g liquefaction solvent was charged to the autoclave at ambient conditions. The coal was Illinois No. 6 from Burning Star Mine, ground to pass a 40 mesh screen. The solvent consisted primarily of mono-, di-, and trimethylnaphthalenes derived from petroleum refining and was essentially free of sulfur, nitrogen and oxygen. Pressure, hydrogen flow rate and mixing speed were set and reactor temperature was raised to 750°F in about 60 minutes. After

reaction at that temperature for 40 to 60 minutes, the reactor was cooled rapidly for removal of the reactor contents at ambient conditions. The test conditions are listed below.

Catalyst Screening Conditions

Catalyst	10g, 60-100 mesh
Coal, Illinois No. 6	150g
Solvent	300g
Pressure	2000 psig
Hydrogen flow rate	3 ft ³ /hr
Mixing speed	1800 rpm
Temperature (maximum)	750°F
Reaction time at 750°F	40-60 minutes

Product Workup and Analysis--Batch Unit

Evaluation of catalyst performance was based on the following procedure for separating liquid product from solid residue. The reactor contents were vacuum filtered and the filtrate segregated. Residual material was recovered from the reactor with benzene and washed through the filter cake. After additional washing with benzene, the filter cake and paper were Soxhlet extracted for 16 hours with benzene. The benzene solutions were combined and distilled to recover an extract that was added to the original filtrate. The final liquid which contains coal product, liquefaction solvent and a small amount of residual benzene was subjected to elemental analysis to determine product quality. The analysis was corrected for water and benzene present. The solid residue was dried at 160°C in a vacuum oven. A moisture and ash free conversion was defined on the basis of solid residue with the assumption that any change in the weight of the catalyst, which was not separated from the coal residue, would be of minor importance. Conversion, thus defined, has been referred to as benzene soluble conversion although, strictly speaking, the filtered product initially segregated in the product workup contained some converted material that is insoluble in benzene.

Catalyst Performance Indices--Batch Unit

Liquefaction conversion and the sulfur content of the coal liquid were used as the primary indicators of catalyst performance. The results obtained in the absence of catalyst provided the reaction baseline while Filtrol cobalt-molybdenum on alumina was selected as the reference for comparing initial catalyst performance.

Under otherwise constant conditions, conversion of coal to liquid product depends on reaction time and whether or not a hydrogenation catalyst is present. Simple reaction kinetics do not define the increase in conversion with increasing reaction time. Hence, some means other than the reaction rate constant is needed to assess catalyst activity. If the conversion obtained without added catalyst can be viewed as the result of noncatalyzed or thermal reaction, then at any given reaction time the increased conversion obtained with catalyst present is indicative of catalyst performance. The ratio of this increase to that obtained with the reference catalyst, Filtrol HPC-5, is defined as the conversion index.

There is also a corresponding decrease in product sulfur content as reaction time is increased. As with conversion, a desulfurization index can be defined as the decrease in product sulfur from the noncatalyzed baseline relative to that obtained with the reference catalyst at the same reaction time.

Continuous Testing Unit

The continuous pilot plant consists of three main sections as shown in the flow diagram (Figure 1). The first section called the feed module contains all equipment for feeding coal slurry and high pressure hydrogen. The center section which is the reactor module contains a 1-liter stirred autoclave and liquid product recovery system. The third module contains the gas let-down, metering and sampling facilities. The design conditions include a maximum working pressure and temperature of 4000 psig and 900°F. Once-through hydrogen is used in the catalyst activity test, but gas recycle has been provided. The once-through operation is preferred for aging tests since hydrogen pressure is maintained constant, independent of the light ends production.

The combined stream of coal slurry and hydrogen gas is continuously introduced into the bottom of the liquefaction reactor and reaction products withdrawn through a vertical overflow tube. A schematic of the reactor is given in Figure 2. Reactor holdup can be varied by changing the overflow tube height. A 60 cc catalyst charge is retained in a stationary annular basket. A specially designed blade impeller plus high agitation rate assures good mixing and contacting of the coal slurry with the catalyst.

Test Conditions--Continuous Unit

The nominal operating conditions used for catalyst testing in the continuous pilot plant are as follows:

Catalyst Test Conditions

Pressure	137 atm (2000 psig)
Temperature	427°C (800°F)
Hydrogen feed rate	170 liters/hr (6 scfh)
Slurry feed rate	400 gm/hr
Slurry concentration	20 wt%, -400 mesh coal (Ill. #6)
LHSV	1.33 gm coal/hr - cc cat
Residence time	48 minutes
Catalyst charge	60 cc
Mixing speed	1500 rpm

Product Workup--Continuous Unit

Product workup required considerable attention in this catalyst development program. To measure catalyst performance, one needs information on coal conversion and product quality. However, the information must satisfy certain requirements specific to the development program. This includes control of the aging test, a rapid measurement based on a small sample, and evaluation of the product quality, using a larger sample.

Coal liquids are normally characterized by solubility in a given solvent. Insolubles in coal product may be determined by different procedures which vary in extraction solvent; therefore, the solvent used defines conversion.

The product workup methods selected include two micro and one macro residue method using benzene and tetrahydrofuran (THF). Conversion based on the micro-benzene method (pressurized filtration using millipore cartridge filter) provides a quick index of product quality. Benzene soluble materials, such as asphaltenes and oils, represent the upgraded fraction of boiler fuel. Conversion based on the micro-THF method measures boiler fuel yield. Detailed evaluation of the liquid coal product requires a larger sample for boiling range determination and elemental analysis. The macro-THF residue method (Soxhlet extraction) is used for this purpose.

DISCUSSION BATCH SCREENING RESULTS

Cobalt-Molybdenum Composition

The effect of varying the cobalt-molybdenum composition was examined to determine if the optimum catalyst composition for coal liquefaction might be different than that typically used in commercial desulfurization catalysts and to gain an indication of the impact of differences in catalyst composition on performance in the screening test. The study was made with two alumina supports having different surface properties--Cyanamid PA (ca. 300 m²/g, 60 Å) and Kaiser KSA Light (ca. 180 m²/g, 160 Å).

With both aluminas, conversion index increased rapidly up to about 10 wt% MoO₃ and then very slowly at higher molybdena contents (Figure 3). Both catalyst systems responded similarly to cobalt with the optimum lying between 2 and 4 wt% CoO. The Kaiser alumina, however, provided a more active catalyst than Cyanamid PA.

For desulfurization, the two supports were indistinguishable (Figure 4). Like conversion, desulfurization index increased rapidly up to about 10 wt% MoO₃ but then leveled off as molybdena content was increased further. The optimum cobalt content for desulfurization was also between 2 and 4 wt% CoO. However, desulfurization was much more sensitive than conversion when the cobalt content was reduced to zero.

Since catalysts made with two supports having different surface properties showed a similar relationship of performance to composition, it appears reasonable that a single composition of, say, 3 wt% CoO and 15% MoO₃ would be appropriate for studying the effects of the support on initial catalyst performance. Furthermore, small deviations from this composition should have only a minor effect on catalyst performance.

Surface Property Effects

The study on surface properties of cobalt-molybdenum catalysts focused primarily on the surface area and average pore diameter. These surface properties are considered important because the number of catalytic sites available depends on surface area and the accessibility of these sites is limited by the pore structure. Average pore diameter is an indicator of pore structure although the distribution of pore sizes may well be more important.

Consider, for example, the relationship of initial performance to the structural properties of the alumina supported catalysts. With respect to surface area, conversion index (CI) is relatively constant over a wide range while desulfurization index (SI) increases with increasing surface area (Figure 5). A corresponding disparity of performance is shown with respect to average pore diameter (Figure 6). The preferred average pore diameter for desulfurization appears to be smaller than for conversion.

These observations provide a basis for selecting catalysts for continuous testing. There is admittedly some scatter in the data which might be resolved by a closer look at such factors as pore size distribution. However, appropriate choices for determining the relation of activity maintenance to surface properties should include aluminas with average pore diameters in the range of 100 to 200 Å.

DISCUSSION-- CONTINUOUS TESTING RESULTS

The short-term aging behavior will now be discussed for a variety of catalysts tested in the continuous pilot plant. The main catalyst parameters we have focused on are surface properties, impregnating procedures, and type of catalytic metals.

Surface Properties and Impregnation Procedures

The effect of surface properties and impregnating methods was investigated by impregnating a series of alumina supports with cobalt and molybdenum. A phosphoric acid impregnating aid was used in some cases to adjust the acidity of the impregnating solution. Again, to facilitate data interpretation, surface area and average pore diameter were the two parameters used to characterize the surface properties, although the distribution of pore sizes should also be considered. The various CoMo on alumina catalysts tested are listed in Table I.

Table I. CoMo on Alumina Catalysts

<u>Catalyst ID*</u>	<u>Major Pores</u> <u>Å</u>	<u>APD</u> <u>Å</u>	<u>SA</u> <u>m²/g</u>	<u>PV</u> <u>cc/g</u>	<u>ABD</u> <u>g/cc</u>
HDS-1442 (ref)	30-110	58	323	.56	.57
KSA-LP	50-250	105	195	.70	.59
Grace-100UP	60-200	118	140	.54	.69
Grace-200UP	110-300	187	78	.44	.75
Grace-100U	60-200	122	167	.59	.68
Grace-200U	110-300	202	92	.52	.73

*U: unimodal; P: phosphorus addition

Referring to Figure 7, we compare liquefaction conversion for the various catalysts to the reference catalyst, HDS-1442A. First of all, the larger pore catalyst, Grace-200UP, results in higher conversion than the smaller pore version, Grace-100UP. The catalyst based on Kaiser KSA-LP alumina exhibits a rapid decline in activity even though its APD is around 100 Å. Closer inspection of the pore size distribution reveals that the KSA-LP alumina has a broad distribution of pore sizes.

The elimination of the phosphoric acid impregnating aid causes an upward shift in conversion for the catalyst prepared with Grace-100U alumina. However, no improvement was observed on the large pore Grace-200U alumina by eliminating the phosphoric acid. Therefore the best liquefaction performance is achieved with an alumina having an APD and surface area of 100 Å and 200 m²/gm, respectively. Furthermore, a phosphoric acid impregnating aid is detrimental to the liquefaction performance.

Desulfurization performance of the catalysts was evaluated by monitoring the sulfur content of the resid fraction (975°F+) of the coal liquid product. Referring to Figure 8, the lowest sulfur level was achieved with the catalyst prepared on Grace-100U alumina. We again conclude that the Grace-100U alumina gives the best overall performance.

Alternate Catalytic Metals

A series of catalyst tests to explore the effects of varying hydrogenation and cracking activity was also performed. Alternate hydrogenation metals tested include Ni-W, Ni-Mo, Ni-Mo-Re, all supported on the small pore Grace 100 alumina. Cracking activity was increased by impregnating the alumina with silica prior to impregnation with the catalytic metals. The specific version tested was a Ni-Mo on a silica promoted alumina. Inspections for the catalysts employing alternate catalytic metals are listed in Table II.

Table II. Catalyst Inspections--Alternate Hydrogenation Metals

Catalyst	Composition	APD Å	SA m ² /g	PV cc/g	ABD g/cc
HDS-1442A	3.1 CoO-13.2 MoO ₃	58	323	.64	.57
Grace-100U	2.9 CoO-16.8 MoO ₃	122	167	.59	.68
NiW-100U	3 NiO-25 WO ₃	118	140	.52	.75
NiMo-100U	2.0 NiO-16.2 MoO ₃	119	163	.62	.67
NiMoRe-100U	3 NiO-16 MoO ₃ -2.3 Re	113	158	.58	.69
NiMo-100U/Si	3 NiO-16 MoO ₃	---	---	---	.66

Benzene soluble conversion is plotted against time on stream in Figure 9 for all of the catalysts in Table II. Compared to the cobalt-molybdenum catalyst (Grace-100U), both NiMo and NiMoRe gave lower benzene soluble conversion and faster decline rates. Addition of rhenium to NiMo had little effect. The more acidic support, silica promoted alumina,

did not improve performance of nickel-molybdenum. The increase in benzene soluble conversion of NiMo catalysts over the reference HDS-1442A catalyst can probably be explained by more favorable surface properties and higher density. Nickel-tungsten gave the lowest benzene soluble conversion which confirmed previous batch screening results.

CONCLUSIONS

Effective tests have been developed to evaluate coal liquefaction catalysts and relate their performance to catalytic properties. Initial performance in the batch unit was related to metals loading of cobalt and molybdenum and surface properties, specifically average pore diameter and surface area. Aging behavior of liquefaction catalysts was established for several catalysts in a continuous pilot plant unit. Surface properties had the most pronounced effect on aging performance; type of catalytic metals appeared to be a secondary effect.

REFERENCES

1. Brooks, J. A., Bertolacini, R. J., Gutberlet, L. C., Kim, D. K., "Catalyst Development for Coal Liquefaction," Electric Power Research Institute First Annual Report AF-190, February, 1976.
2. Bertolacini, R. J., Gutberlet, L. C., Kim, D. K., Robinson, K. K., "Catalyst Development for Coal Liquefaction," Electric Power Research Institute Second Annual Report, October, 1977.

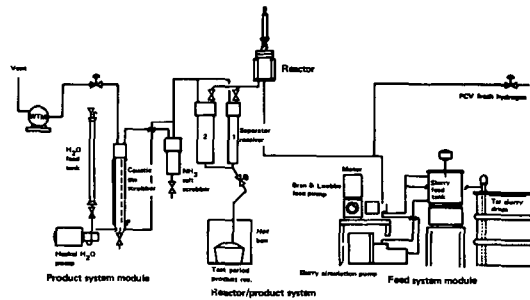


Fig 1 Unit flow diagram

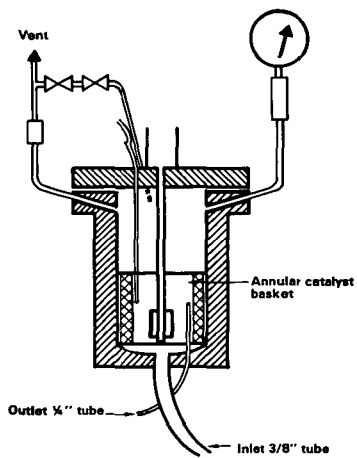


Fig 2 Liquefaction reactor

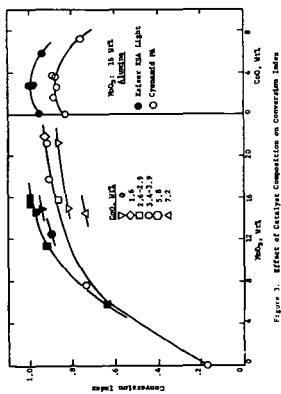


Figure 3. Effect of Catalyst Composition on Conversion Index

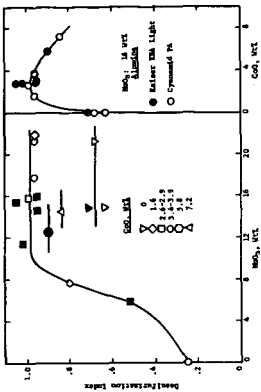


Figure 4. Effect of Catalyst Composition on Desulfurization Index

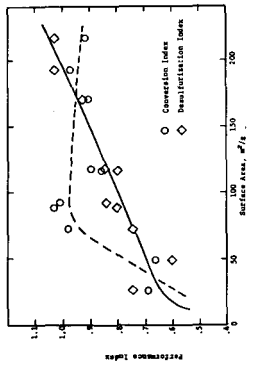


Figure 5. Relation of Catalyst Performance to Surface Area (A. 10 wt% Alumina)

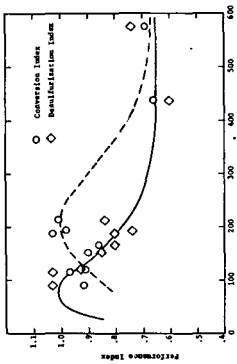
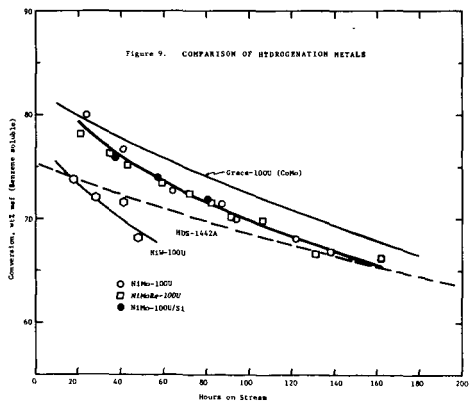
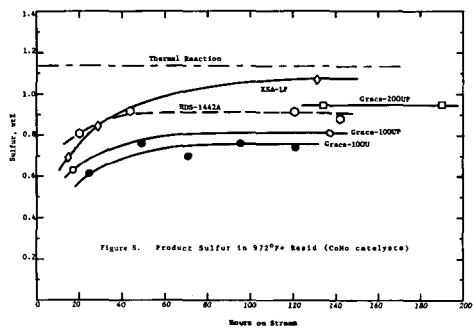
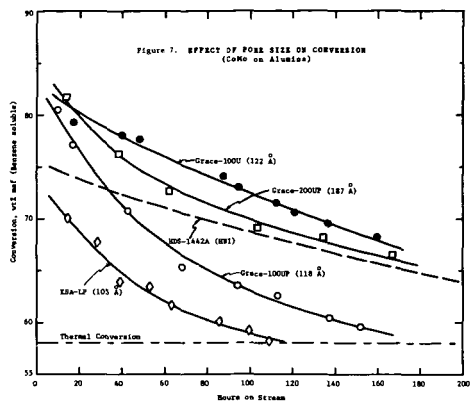


Figure 6. Relation of Catalyst Performance to Average Pore Diameter (B. 10 wt% Alumina)



BATCH SCREENING OF COAL LIQUEFACTION CATALYSTS
WITH A FALLING BASKET REACTOR

William R. Alcorn, George E. Elliott, and Leonard A. Cullo

The Harshaw Chemical Co., Box 22126, Beachwood, Ohio 44122

The Harshaw Chemical Company and Battelle Columbus Laboratories have been studying coal liquefaction catalysts in a joint program sponsored by the Dept. of Energy. Its objective is the development of catalysts of improved life and selectivity for direct liquefaction processes.

Harshaw's specific objective is to identify catalysts of superior activity and selectivity, i.e. those that most efficiently use hydrogen in forming coal liquids with low heteroatom content. These will then be tested by Battelle for longer term aging characteristics. This paper is a report of progress with about half of the planned screening tests completed.

Experimental System

The test system, diagrammed in Figure 1, is based on an Autoclave Engineers 1-liter Magnedrive reactor and is designed to run whole formed catalysts in an environment of coal slurry with continuous hydrogen flow.

Illinois No. 6 coal from Consolidation Coal Company's Burning Star Mine No. 2 was analyzed as follows after grinding and drying.

	<u>Wt %</u>
Moisture	1.3
Ash	12.0
Carbon	68.3
Hydrogen	4.7
Nitrogen	1.2
Sulfur	3.2
Oxygen (by diff.)	9.3

The coal is charged to the reactor as 30% MAF coal in a vehicle. Two vehicles have been used. The first is a "heavy oil" cut of a coal tar from Koppers Co. Analyses of this vehicle and the coal are shown below.

	<u>Wt % Components</u>	
	<u>Coal</u>	<u>Heavy Oil</u>
Oil	1.0	76.9
Asphaltenes	0.3	22.8
Pre-asphaltenes	7.8	} 0.3
Residue	90.9	}
	<u>100.0</u>	<u>100.0</u>
% Sulfur	3.2	0.44
% Nitrogen	1.2	0.96

In the second series of runs the vehicle is tetralin. Run conditions for the two series are as follows:

Vehicle	Heavy Oil	Tetralin
Pressure, psig	4000	2500
Temperature, °C	425	425
Activation in H ₂ /H ₂ S, hr	1.5	1.5
Thermal Reaction Period, hr*	0.5	1.0
Catalytic Reaction Period, hr	2.0	2.0
Inlet H ₂ Flow, SCFH	5	10
Catalyst Charge, cc	25	25
Wt Coal, g	188	162
Wt Vehicle, g	355	306
Volume of Slurry, cc	471	471

*After heatup to 425°C

Falling Basket Reactor

It is desirable that a catalyst screening test simulate continuous operating conditions as far as possible. In this case, five requirements were set in advance.

1. Batch operation for rapid screening.
2. Pre-activate the catalyst in situ with H₂/H₂S.
3. Use formed catalyst (tablets and extrudates) rather than powder.
4. Avoid contact of catalyst with slurry during heatup.
5. Separate thermal from catalytic conversion experimentally.

The Falling Basket Reactor, illustrated in Figure 2, was developed to meet these requirements. With this device, the catalyst is suspended in the gas phase during the initial stages of the run, then lowered into the liquid for the catalytic reaction portion. Catalyst (25 cc) is loaded in the four arms of the basket assembly which moves along a grooved sleeve attached to the agitator shaft. In operation the basket is held at the top of the shaft by a horizontal notched groove as long as the shaft is rotated at a constant RPM. (Rotation speed was set at 300 RPM after a preliminary mixing study.) When rotation is stopped and momentarily reversed, the basket travels down the groove to the bottom position where it remains for the rest of the run. The point at which the basket drops is recorded by a temporary drop in batch temperature.

Pre-activation of the catalyst, heatup, pressurization, and a period of thermal reaction are accomplished after sealing the reactor, but before contacting catalyst and slurry. The catalytic period starts when the basket is dropped into the liquid and stops when the heater is removed from the autoclave. Figure 3, a typical temperature history of a run, shows that this sequence results in a well defined reaction period. Figure 3 also shows the endotherm that always occurs during heatup as the coal undergoes thermal dissolution.

Product Analysis

Product analysis schemes are similar for the two vehicles except for the addition of a distillation step in the tetralin runs (Figure 4). The vehicle remained with the coal liquefaction products in the heavy oil runs. The techniques used to separate oil (pentane soluble),

asphaltenes (benzene soluble, pentane insoluble), and pre-asphaltenes (pyridine soluble, benzene insoluble) are well known.

Effluent gas was monitored by GC for 50 runs, enough to establish that there were no significant differences among catalysts in the gases formed, nor between catalysts and no catalyst. It was concluded that light hydrocarbons come from the coal (not the vehicle) at the test operating conditions, whether or not catalyst is present.

Samples of the separator condensate and the distillate obtained during product workup were analyzed by GC for the tetralin runs. Particular attention was paid to the relative amounts of decalin, tetralin, and naphthalene as indicators of hydrogenation activity.

The results are presented in terms of elemental analyses of product (%S, %N, and H/C atomic ratio); extraction analyses (oil/asphaltene ratio and % pre-asphaltenes); the decalin/naphthalene ratios of distillate and separator product (for tetralin runs); and conversion. Conversion is defined as 100 less the percent MAF coal charged that remains benzene insoluble. Note that the chemical analyses refer to coal plus vehicle in the heavy oil runs, but only to coal products in the tetralin runs.

Catalysts

Eight 1/8 in. tabletted catalysts were tested in the heavy oil series at 4000 psig. Four of these tablets and ten 1/16 in. extrudates have been tested to date in the runs with tetralin at 2500 psig. Various blank and duplicate runs were made with both vehicles.

The reference catalyst is Harshaw's CoMo-0402 T 1/8, which has been reported in connection with work on the Synthoil process and other studies. Other catalysts are designated either by their commercial name (as HT-400) or by a simple chemical notation (as NiMo). The catalysts tested to date represent a variety of chemical compositions and support structures. For example, two sets of NiMo extrudates were made to have systematically varying pore structure; these are designated on Table 2 as A-1, B-1, etc.

Catalysts are loaded on a volume basis (25 cc). Packed densities cover a wide range, tablets running 1.0 - 1.1 g/cc and extrudates 0.6 - 0.8 g/cc. Weight of catalyst charged therefore ranges from about 15 to 28 g.

General Results

Test results from runs with heavy oil vehicle are summarized in Table 1, and from tetralin runs in Table 2. All runs were at the operating conditions given above except for the few special run times indicated by notes to the tables. The runs are listed in order of decreasing oil/asphaltene ratio in the product.

Mass recoveries typically run 97 to 99% with heavy oil and higher with tetralin; the small variations do not affect the conclusions. "Conversion" of coal to liquids also falls within a narrow range for standard runs and does not differentiate among catalysts. Thermal conversion (no catalyst present) is about 2-3% lower than the average catalytic conversion with heavy oil, and about 6-7% lower with tetralin. The fact that the catalytic conversions are close attests to the reproducibility of the test, for conversion varied widely when time was varied as in Runs 18, 19, and 20. Excellent reproducibility

is also demonstrated by the similar results found in duplicate Runs 32 and 50, and 29 and 52 (Table 2).

As noted earlier, the amount and composition of effluent gases do not appear to be influenced by the presence of a catalyst. Similarly, the amount of separator condensate is essentially constant for a fixed run time. However, its composition is related to the activity of the catalyst used, as may be seen from the decalin/naphthalene ratios given in Table 2. The data show that separator product is more saturated than the solvent which remains in the reactor and becomes "distillate".

Special Runs

The marked effect of a catalyst on sulfur removal, H/C ratio, and conversion of asphaltenes to oils is seen from comparison of Run 9 (no catalyst) with any of the catalytic runs on Table 1. However, removal of nitrogen heteroatoms from the coal appears to be nearly as difficult with a catalyst as without.

Comparison of Runs 24 and 27 (Table 2) shows the effect of catalyst on tetralin in the absence of coal. Much more decalin was made in the presence of a catalyst: 1.4% in Run 24, but 48% in Run 27.

In three instances run time was varied with the same catalyst. Runs 19, 20, and 18, with the reference CoMo catalyst, had catalytic run times of 0.4, 2.0, and 2.5 hrs. Without exception, as run time increases, H/C and oil/asphaltene ratios increase and % pre-asphaltene and % S decrease.

In the tetralin series, Run 43 had 0.5 hr more thermal exposure than Run 42, other things being equal, and showed more reaction in each of the variables tabulated. Similarly, Run 36 (1 hr thermal, 2 hr catalytic) shows more reaction than Run 35 (2 hr thermal, 1 hr catalytic) with the same catalyst.

Comparison of Catalysts

In general, the data indicate that all the measures of catalytic activity are interrelated. Inspection of Tables 1 and 2 shows that the following properties coincide:

- high oil/asphaltene and H/C ratios, both measuring the extent of hydrogen addition to the coal,
- low S and N in the product (the latter less definitely) and lower % pre-asphaltene, all measures of catalytic action on the liquefied coal,
- high decalin/naphthalene ratio in both distillate and separator products, showing activity in solvent hydrogenation.

The correlation between H/C and oil/asphaltene ratios is shown graphically in Figures 5 and 6. With respect to the heavy oil runs (Fig. 5), all the points except Run 19 (0.4 hrs) appear to fit a correlation. It is concluded that some kind of thermalequilibrium between coal, solvent, and hydrogen has been reached in the standard length runs, and more hydrogen addition is achieved either by longer contact time or a better catalyst. The activity differences among catalysts in the heavy oil runs are relatively small in spite of the variety of compositions employed. It is believed that the uniformity of

results is due, in part, to the fact that the vehicle is not separated from the coal and plays a major role in the observed results. Another reason may be the use of tablets in this series. Tablets tend to have similar pore structures at their external surfaces which may mask chemical differences.

Table 2 and Figure 6 show a wider range of results with tetralin and extruded catalysts. Certain NiMo catalysts have demonstrated very good relative performance in this test. However, the six NiMo catalysts tested in Runs 37 - 43, differing primarily in pore structure, show little difference in performance. It is premature to draw firm conclusions regarding the key factors that affect catalyst activity, and more work is required before relating performance to properties.

NiW catalysts have not shown up well vs. NiMo in the few tests completed. Regarding CoMo, the best comparison so far between similar NiMo and CoMo catalysts is in Runs 32 and 50 vs. 33; the NiMo catalyst appears to be somewhat more active in each category. It is interesting, however, that the CoMo causes less saturation of the solvent than expected from its position on the table. The same thing may be said of the tableted version (Run 31). This may be an advantage.

The four tablets tested on tetralin gave similar results (Table 2). As expected, they are less active than corresponding 1/16 in. extrudates. The similarity of tablet results parallels the same finding on the heavy oil feed.

Principal Conclusions

Conversion of coal to benzene soluble liquids is primarily a thermal reaction dependent on temperature and time, only secondarily on catalyst. Addition of hydrogen to the coal liquids and solvent and removal of heteroatoms are greatly influenced by the catalyst, and these characteristics tend to correlate with each other. This suggests that one mechanism such as rehydrogenation of the solvent may be the dominating process which separates good from bad catalysts.

If this picture of the process is valid, the catalysts selected by this screening test are likely to be effective not only in direct liquefaction processes, but also in processes where catalytic upgrading of the coal liquids is separated from the liquefaction step.

Several catalysts have been identified which show better short-term performance than the reference CoMo tablet. The properties which lead to better catalyst performance have not yet been clarified, nor have aging tests been carried out.

The falling basket reactor solves a number of experimental problems in batch screening of catalysts for continuous processes, especially in separating thermal from catalytic effects and in providing a well defined reaction period. Reproducibility of results is excellent.

TABLE 1 RUNS WITH HEAVY OIL VEHICLE - RANKED BY OIL/ASPHALTENE RATIO

Run	Catalyst (1)	Conversion %	Pre-asphaltenes %	Benzene Solubles(2)		
				%S	%N	H/C(At.)
22 (3)	CoMo-0402	-	-	0.04	0.42	1.02
18 (4)	CoMo-0402	77.0	0.6	0.11	0.79	0.99
16	HT-400 CoMo/Al	75.6	0.2	0.18	0.81	0.96
21	CoMo-0402 + 0.1% Re	75.0	0.4	0.17	0.82	0.96
20	CoMo-0402	69.3	1.4	0.14	0.80	0.96
17	NiW/Al	74.1	0.8	0.10	0.94	0.94
12	NiMo/Si-Al	73.7	0.3	0.10	0.83	0.94
11 (6)	NiW/Al	74.7	0.2	0.11	0.95	0.98
15	CoMo/Al	75.1	0.6	0.14	0.79	0.95
14	CoMo/Al-Si	72.9	0.4	0.16	0.94	0.93
23	CoMo/SiMg-Al	65.6	1.0	0.23	1.01	0.90
19 (5)	CoMo-0402	52.9	2.1	0.30	1.00	0.83
9	No Catalyst	72.8	0.6	0.37	0.94	0.87

(1) All 1/8 in. tablets. Al = Al₂O₃ and Si = SiO₂

(2) Bz sols. = vehicle + liquefied coal.

(3) No coal.

(4) 2.5 hr. catalytic reaction time instead of 2.0 hr.

(5) 0.4 hr. catalytic reaction time.

(6) Carbonaceous material left in catalyst. Sample of same was used in Run 17 after complete calcination.

TABLE 2 RUNS WITH TETRALIN VEHICLE - RANKED BY OIL/ASPHALTENE RATIO

Run	Catalyst(1)	Conversion %	Pre-asphaltenes %	COAL LIQUEFACTION PRODUCT				decalin/naphthalene Separator Product
				\$S	\$N	H/C (At.)	Oil/Asph.	Distillate
32	HT-500 NiMo/Al E	77.9	0.0	0.02	0.96	1.10	2.6	2.7
34	HT-115 NiMo/Al E	79.4	0.1	0.06	1.04	1.07	2.3	1.6
50	HT-500 NiMo/Al E	77.8	0.2	0.02	0.02	1.06	2.1	2.7
37	NiMo/Al E A-1	78.6	0.1	0.05	1.15	1.06	1.9	1.6
43	NiMo/Al E B-2	78.8	0.0	0.02	0.02	1.08	1.9	1.6
33	HT-400 CoMo/Al E	75.7	0.0	0.04	1.19	1.05	1.8	0.8
38	NiMo/Al E B-1	78.1	0.2	0.06	1.05	1.05	1.8	1.7
40	NiMo/Al E B-3	78.0	0.0	0.02	0.02	1.08	1.7	1.4
41	NiMo/Al E A-2	78.9	0.0	0.05	1.05	1.05	1.7	2.0
42(2)	NiMo/Al E B-2	78.1	0.0	0.04	1.06	1.06	1.7	1.2
31	HT-400 CoMo/Al T	76.1	0.4	0.09	1.21	1.06	1.6	0.8
26	NiMo/Al T	77.5	0.3	0.07	1.10	1.05	1.5	2.1
30	NiW/Al T	73.6	0.5	0.12	1.28	1.04	1.4	0.9
39	NiMo/Al E A-3	78.6	0.1	0.04	1.04	1.04	1.3	0.7
29	CoMo-0402 T Ref.	78.0	0.2	0.09	1.24	1.03	1.1	0.8
52	CoMo-0402 T Ref.	77.7	0.3	0.10	1.01	1.01	1.1	0.9
36	NiW/Al E C-1	77.9	0.2	0.07	1.28	1.01	1.1	0.4
35(3)	NiW/Al E C-1	75.5	0.6	0.09	1.37	1.01	0.9	0.2
45	NiW/Al E C-2	74.6	0.9	0.18	1.01	1.01	0.8	0.8
28	No Catalyst	71.9	2.4	0.46	1.66	0.94	0.4	0.1
44	Alumina E	70.8	1.5	0.53	0.93	0.93	0.4	0.1
24(4)	No Catalyst	-	-	-	-	-	-	5.0
27(4)	CoMo-0402 T Ref.	-	-	-	-	-	-	206.0
								12.3

(1) Al = Al₂O₃. E = 1/16 in. extrudate. T = 1/8 in. tablet.

(2) 0.5 hr. thermal reaction time instead of 1.0 hr. as in Run 43.

(3) 2.0 hr. thermal and 1.0 hr. catalytic instead of 1.0 and 2.0 as in Run 36.

(4) No coal.

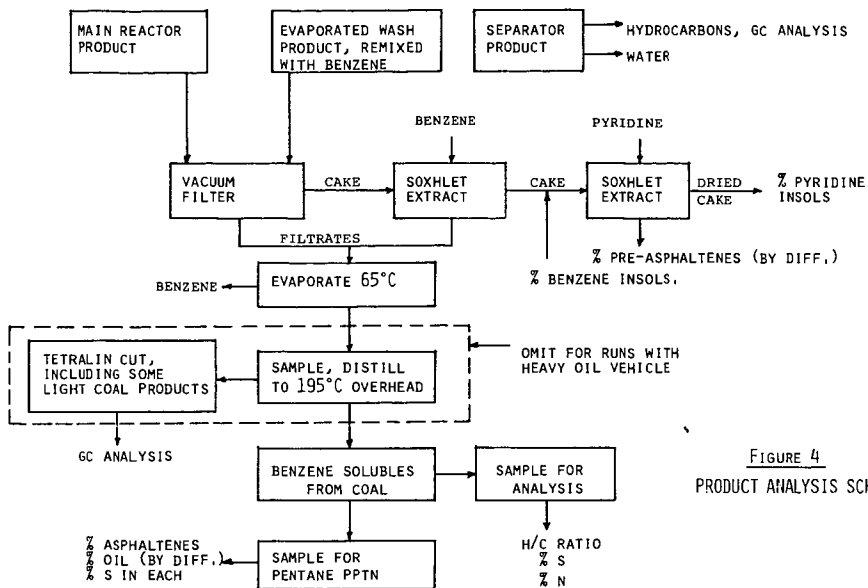


FIGURE 4
PRODUCT ANALYSIS SCHEME

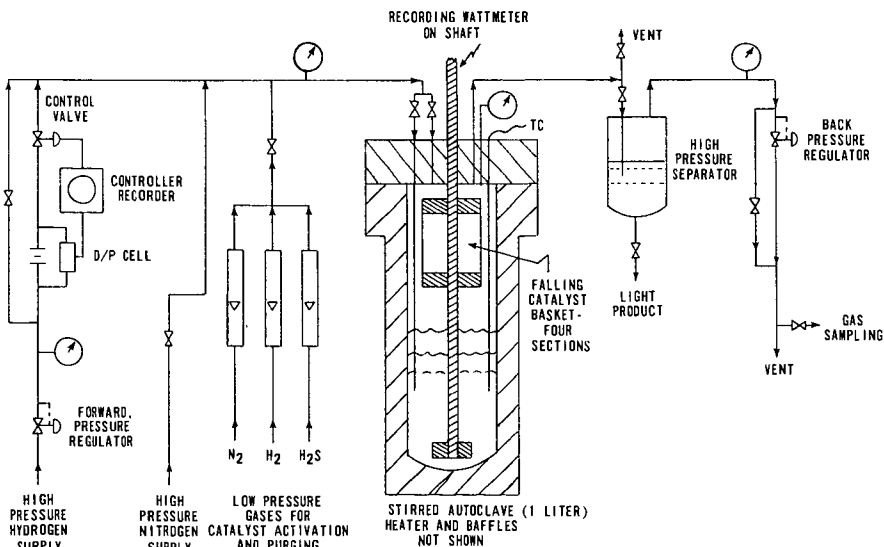


FIGURE 1

HARSHAW CATALYST SCREENING UNIT
SIMPLIFIED SCHEMATIC DIAGRAM

FIGURE 3
 TEMPERATURE-TIME HISTORY
 OF TYPICAL RUN
 (HEAVY OIL VEHICLE)

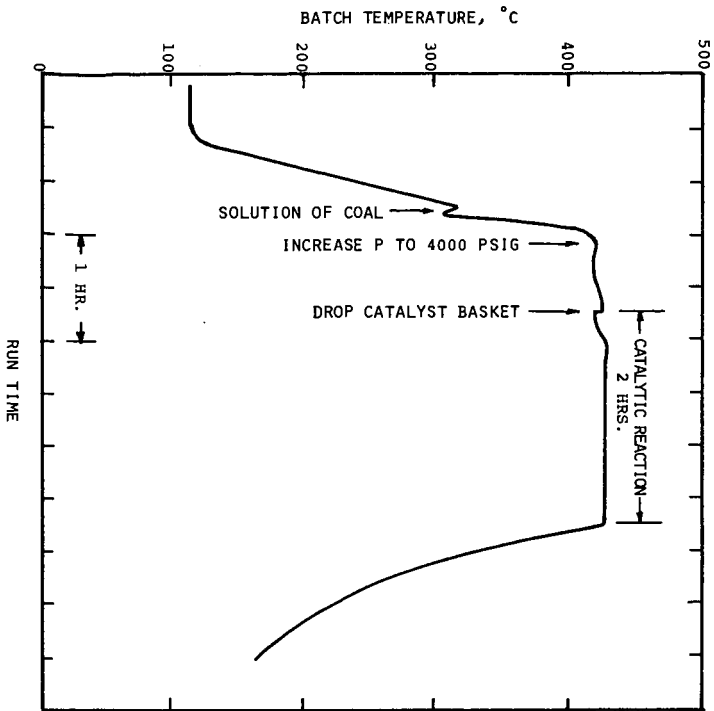
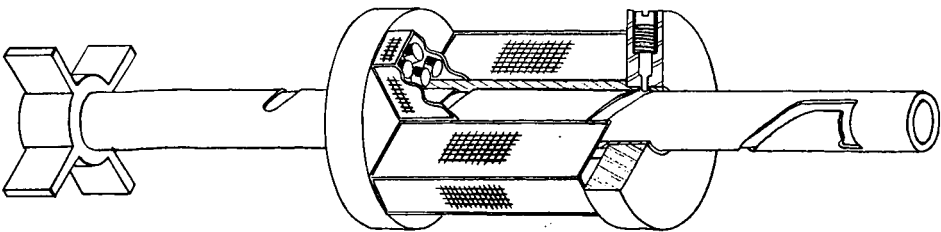
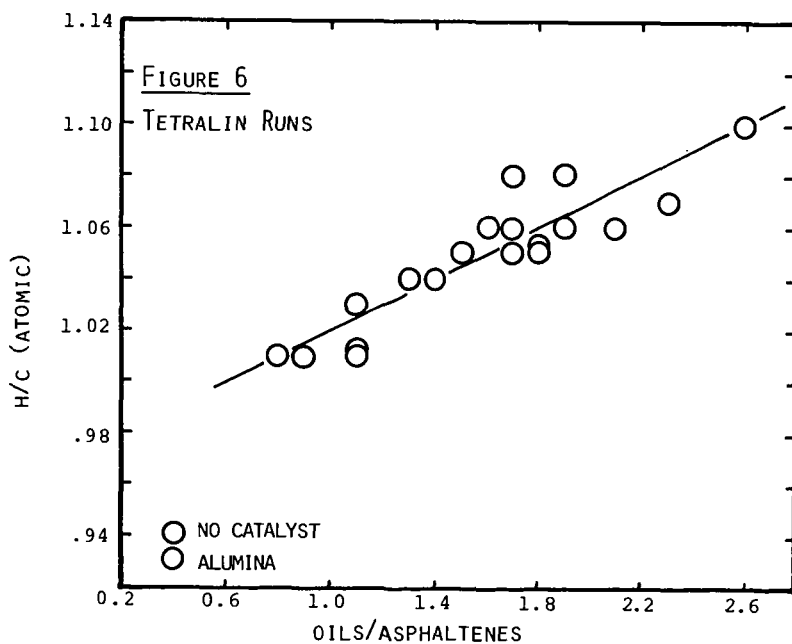
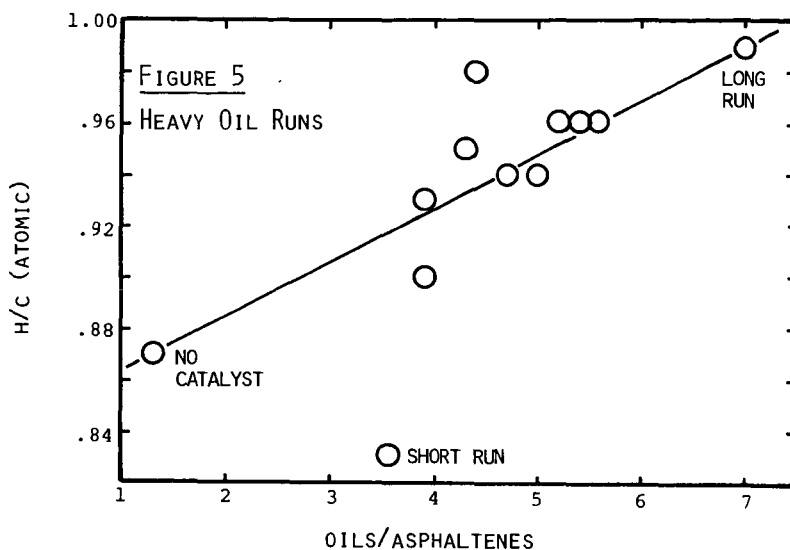


FIGURE 2
 FALLING BASKET ASSEMBLY



CORRELATION OF H/C AND OIL/ASPHALTENE RATIOS
IN LIQUEFACTION PRODUCTS



Catalyst Development for Hydroliquefaction of Coal¹

E. W. Stern and S. G. Hindin
ENGELHARD INDUSTRIES DIVISION
ENGELHARD MINERALS AND CHEMICALS CORP.
Menlo Park, Edison, NJ 08817

Abstract

This paper summarizes observations made during the development of a catalyst screening test in the initial phases of a program which has as its objective the development of improved catalysts for the direct hydroliquefaction of coal.

The test is carried out batchwise in a stirred autoclave and employs Illinois #6 coal and a commercial petroleum based solvent (Panasol AN3). Uncertainties in reaction time and temperature are normally encountered in this mode of operation due to substantial coal conversions during heating and cooling. These uncertainties have been reduced significantly by injecting coal after a slurry of solvent and catalyst has reached operating temperature and by rapid cooling at the termination of the reaction period.

Products are separated into benzene insoluble, pentane insoluble (asphaltene) and pentane soluble (oil) fractions. Data obtained with a commercial CoMo catalyst in a study of the effect of reaction variables on hydrogen consumption, coal conversion, asphaltene and oil yields, and sulfur removal indicate the following:

Hydrogen absorption is linear with time and continues after maximum coal conversion (93%) is reached. It is also linear with pressure in the range investigated (760-3000 psi) indicating a process first order in hydrogen and therefore independent of coal conversion which becomes zero order in hydrogen above 2000 psi.

A clearcut distinction between first and zero order dependence on coal in the 50-80% conversion range cannot be made. The reaction tends toward first order at higher conversion levels. Substantial conversion of coal is observed in the absence of catalyst and at very short reaction times.

Asphaltene yields are proportional to conversion until about 80% conversion and remain relatively constant thereafter. Oil yields increase with conversion to maximum conversion (93%).

¹ ERDA Contract No. EF-76-C-01-2335

Sulfur levels in asphaltene and oil decline with increasing yields of these fractions.

The relationship between asphaltene and oil yields and sulfur contents is not affected by temperature or catalyst loading.

Most of these observations can be rationalized via a model in which the major role of catalyst is to maintain the solvent in a suitable state of hydrogenation. Moreover, the data support a branching mechanism for formation of asphaltenes and oil rather than the generally assumed sequence of first order reactions.

EFFECTS OF MINERAL MATTER ON THE HYDROLIQUEFACTION OF COAL

by

Barry Granoff, Michael G. Thomas, Paul M. Baca
and George T. Noles

Geo Energy Technology Department
Sandia Laboratories
Albuquerque, New Mexico 87115

INTRODUCTION

Several previously published studies have shown that the naturally occurring minerals in coal may play a significant role in hydroliquefaction (1-6). The extent of conversion was shown to correlate with total mineral content (1,2,4). Iron - in the form of pyrite, pyrrhotite and liquefaction residue - has been shown to affect conversion and hydrogenation (2-4). Coal ash, pyrrhotite and liquefaction residues have all exhibited some activity for the desulfurization of coal (2,5), and pyrrhotite has been shown to be more active than pyrite for the desulfurization of thiophene (5). Pyrite and several clays were shown to catalyze the isomerization of tetralin to methyl indane and the transfer of hydrogen from hydroaromatic to aromatic structures (6).

We have shown, for a series of high-volatile bituminous coals having similar maceral contents, that the extent of conversion, product viscosity and hydrogen consumption could be correlated with the mineral content (4). The combined role of pyrite, clays and organic sulfur was shown, but the independent effect of each of these components was not investigated in our previous work. To better understand the role of minerals in the hydroliquefaction of coal, we decided to carry out a number of experiments, in a stirred autoclave, in which pure minerals, liquefaction residues and a commercial catalyst were added to the feed coal. The experimental conditions (temperature, heating rate, pressure, residence time and solvent-to-coal ratio) were held constant for each run. Illinois No. 6 coal was selected for this work because of its moderate liquefaction reactivity (4). It was assumed that greater differences in conversion and product composition would be observed by augmenting the mineral content of a moderately reactive coal than by utilizing a very reactive (e.g., western Kentucky) coal.

EXPERIMENTAL PROCEDURES

The coal used in all of the experiments was Illinois No. 6 (Orient 4 Mine), which was pulverized to minus 100 mesh. Proximate, ultimate and sulfur forms analyses are given in Table 1. The mineral matter composition, also shown in Table 1, was obtained from the x-ray diffraction analysis of low temperature ash (7,8). The percentages of pyrite and mixed layer clays were approximately

one-half the corresponding values that were reported for the more reactive Kentucky No. 11 (Fies Mine) coal (4).

The solvent used was creosote oil, No. 4 cut, which was obtained from the Reilly Tar & Chemical Co. This oil had a specific gravity of 1.12 and a boiling range of 270-400°C. The solvent-to-coal (daf) ratio used in all runs was 2.50.

The minerals, catalyst and residue used for the spiking experiments are described in Table 2. Pyrite, pyrrhotite (FeS), clay and the liquefaction residue were included in this study because of their potential catalytic importance (1-6). Zinc sulfide was included because several Illinois coals have been found to have extremely high zinc contents (8). The zinc presumably occurred in the form of the mineral sphalerite (zinc sulfide). The commercial Co/Mo hydrodesulfurization catalyst was included as a reference "standard" with which to compare the activity of the other added species. The minerals were blended with the dry coal by milling in a mortar and pestle for a minimum of 15 min. In each of the spiking experiments, 2.50 g of the mineral, residue or catalyst was used; this was equivalent to 5% of the daf coal charge.

All of the liquefaction runs were carried out in a one-liter, stirred autoclave. The reactants were placed in a stainless-steel liner that had a volume of 0.7 liter. Nominal reaction conditions were:

Initial (cold) pressure	:	1000 psig hydrogen
Heatup time	:	1.0 hr
Temperature	:	405°C
Residence time at temperature:	:	0.5 hr
Cooldown time	:	overnight (18 hr)

At the end of each run, following cooldown, the overhead gases were vented through caustic scrubbers, and the liquid product was removed. Material accountability was routinely 95% or better. Solids separation was effected by centrifugation at 2200 rpm for 45 min. Product analysis included viscosity (Brookfield), elemental composition and Soxhlet solvent extraction. Conversion was calculated on the basis of both pyridine and benzene insolubles. The former was calculated from a forced ash balance (9), the latter was obtained from the expression:

$$\text{Percent conversion} = 100 \left[1 - (\text{OBI}_f / \text{OBI}_i) \right]$$

where OBI_f and OBI_i are the weight fractions of organic benzene insolubles in the final liquid product and initial reactants, respectively.

A crude estimate of hydrogen consumption was made by calculating the difference between the initial pressure (1000 psig in all cases) and the final pressure after cooldown. The pressure difference, ΔP , was normalized to that of the experiment in which no mineral or catalytic agent was added. A pressure ratio was then defined as:

$$\text{Pressure ratio} = \Delta P / \Delta P_0$$

where ΔP_0 was the pressure difference for the control (no added minerals) run. As defined above, the greater the pressure ratio, the greater was the hydrogen consumption. The formation of hydrocarbon gases could have had an effect on the ratio, but it was assumed that this would not alter the observed trends.

RESULTS AND DISCUSSION

Data from the autoclave experiments are given in Table 3. It has been shown in the literature that coal can be converted to greater than 90% pyridine solubles in less than three minutes under the proper reaction conditions (9,10). In the present case of relatively long heatup and residence times, reaction temperatures in excess of 400°C and use of a good liquefaction solvent, it is clear that transformation to pyridine solubles reached a plateau (92 to 94% conversion) that was independent of any added species.

The conversion of the initially solubilized coal to molecular constituents that are soluble in benzene is a slower process (9). This, in part, may be seen by the lower conversions to benzene solubles as shown in Table 3. Whereas the addition of mineral matter did not affect the conversion to pyridine solubles, certain species such as FeS, liquefaction residue and Co/Mo did have an effect upon the conversion to benzene solubles. It is of some interest to note that pyrite did not affect conversion, but pyrrhotite - both as FeS and as the predominant form of iron in the liquefaction residue (3,6,11) - did result in an increase in conversion. The Co/Mo catalyst had the greatest positive effect on conversion, and ZnS seemed to have a slightly negative effect as seen by the decrease in conversion.

Significant decreases in the viscosity of the liquid products were observed for the runs in which pyrite, pyrrhotite (FeS) and Co/Mo had been added. A smaller decrease in viscosity, which is probably not statistically significant, was noted when the liquefaction residue had been used. In the experiment with kaolinite, the viscosity of the product increased. This increase could have been caused by suspended particulate matter that was not removed by centrifugation. Zinc sulfide did not have any effect on product viscosity.

We have previously shown, for West Virginia coal, that the viscosity of a coal-derived liquid was dependent upon the organic benzene insolubles and asphaltenes content, but the benzene insolubles had a significantly greater effect on viscosity than did asphaltenes (4,12). The largest decrease in viscosity in the spiking experiments (Table 3) was observed when Co/Mo had been added to the feed. In this case, the asphaltene content of the resulting liquid product was essentially the same as that obtained in the control experiment, in

which no mineral or catalyst had been added. The addition of Co/Mo, however, resulted in a significant reduction in organic benzene insolubles, and the large decrease in viscosity was probably a direct consequence of this. The addition of pyrite resulted in the largest decrease in asphaltene content in the entire test series, but did not affect the benzene insolubles. The addition of pyrrhotite (FeS and residue) resulted in decreases in both the asphaltenes and organic benzene insolubles. The observed decreases in viscosity in these cases were attributed to corresponding shifts in the relative quantities of the asphaltenes and benzene insolubles. An interesting selectivity has been observed in which pyrite significantly affected only the asphaltene content, whereas pyrrhotite affected both the organic benzene insolubles and asphaltenes.

The hydrogen-to-carbon ratios of the centrifuged liquid products were quite similar (Table 3). The present data show that hydrogen consumption, as indicated by changes in the pressure ratio, increased in all of the spiking experiments. This increase was particularly significant in the run with Co/Mo, in which the pressure ratio increased almost three-fold. Since the H/C ratios of the liquid products were similar, it is proposed that hydrogen was primarily consumed for heteroatom removal, conversion of (initially solubilized) coal to benzene solubles and production of hydrocarbon gases. In the case of Co/Mo, the high hydrogen consumption, without a concomitant increase in the hydrogen content of the liquid product, would appear to be undesirable with respect to process economics.

Significant decreases in the sulfur content of the liquid products were found in the runs with FeS, ZnS and Co/Mo. In the experiment with pyrite, the sulfur content of the product was higher than the corresponding product from the control run where no minerals or catalysts had been added. This may have been due to the presence of extremely fine particles of inorganic sulfur that could not be removed by centrifugation. On the other hand, this could have been a consequence of the fact that pyrite is not an effective desulfurization catalyst. Work at Auburn University has shown that pyrite was less effective than no catalyst at all for the desulfurization of creosote oil (2). We have shown that pyrrhotite, FeS, was considerably more active for sulfur removal than either pyrite or the liquefaction residue (Table 3). This is in good agreement with the Auburn work (2), and with the data from a recent pulse microreactor study, where it was demonstrated that pyrrhotite was approximately four times more active than pyrite for the hydrodesulfurization of thiophene (5). It is conceivable, therefore, that the non-stoichiometric iron sulfides, which are formed from the pyrite during coal hydroliquefaction (6,11), are the active species for desulfurization.

SUMMARY

Batch autoclave experiments have been carried out with Illinois No. 6 coal (Orient 4 Mine) in creosote oil. Various minerals, a dry liquefaction residue and a Co/Mo catalyst were added to the feed coal, while all process parameters (pressure, temperature, residence time, heating rate and solvent-to-coal ratio) were held constant. Significant increases in conversion to benzene solubles were observed when pyrrhotite (FeS), residue and Co/Mo had been used. Decreases in the viscosity of the liquid products were found in the spiking runs with pyrite, pyrrhotite and Co/Mo. The largest decrease in viscosity occurred in the experiment with Co/Mo and, in this case, a concomitant decrease in the organic

benzene insolubles was found. A selectivity was observed in which pyrite affected only the asphaltene content of the liquid product, but pyrrhotite affected both the asphaltenes and the organic benzene insolubles. The data have shown that pyrrhotite and Co/Mo were active for desulfurization, but pyrite and most of the other minerals were not. Hydrogen consumption, as estimated from differences in the venting pressure, increased in all spiking experiments - especially when Co/Mo had been added to the feed. The H/C ratios of the liquid products, however, were similar. This would imply that hydrogen had been utilized primarily for heteroatom removal, conversion to benzene solubles and hydrocarbon gas formation.

REFERENCES

1. D. K. Mukherjee and P. B. Chowdhury, *Fuel* 55, 4 (1976).
2. A. R. Tarrer, J. A. Guin, W. S. Pitts, J. P. Henley, J. W. Prather and G. A. Styles, Preprints, Div. of Fuel Chemistry, Amer. Chem. Soc., 21 (5), 59 (1976).
3. C. H. Wright and D. E. Severson, *ibid.*, 16 (2), 68 (1972).
4. B. Granoff and M. G. Thomas, *ibid.*, 22 (6), 183 (1977).
5. C. E. Hamrin, Jr., "Catalytic Activity of Coal Mineral Matter," Interim Report for the Period April-September 1976, FE-2233-2, February 1977.
6. P. H. Given, "The Dependence of Coal Liquefaction Behavior on Coal Characteristics," presented at the Short Course on Coal, The Pennsylvania State University, June 1976.
7. F. W. Frazer and C. B. Belcher, *Fuel* 52, 41 (1973).
8. C. P. Rao and H. J. Gluskoter, "Occurrence and Distribution of Minerals in Illinois Coals," Illinois State Geological Survey, Circular 476 (1973).
9. R. C. Neavel, *Fuel* 55, 237 (1976).
10. D. D. Whitehurst, M. Farcasiu and T. O. Mitchell, "The Nature and Origin of Asphaltenes in Processed Coals," EPRI AF-252, February 1976.
11. J. T. Richardson, *Fuel* 51, 150 (1972).
12. M. G. Thomas and B. Granoff, *Fuel* (accepted for publication).

Table 1. Analysis of Illinois No. 6 Coal^a

<u>Proximate Analysis</u>		<u>Sulfur Forms</u>	
Volatile Matter	36.69	Pyritic	1.27
Fixed Carbon	52.60	Sulfate	0.09
Ash	10.71	Organic	1.64
<u>Ultimate Analysis</u>		<u>Mineral Matter</u>	
Carbon	71.48	Pyrite	2.80
Hydrogen	4.89	Quartz	2.20
Nitrogen	1.45	Calcite	0.78
Sulfur	3.00	Kaolinite	0.82
Oxygen (difference)	8.47	Mixed Clays	6.35
Ash	10.71		

^aAll data given as a percent of the coal on a dry basis.

Table 2. Minerals and Catalysts Used for the Spiking Experiments

<u>Mineral</u>	<u>Description</u>
FeS ₂	Single crystal pyrite from Sinaloa, Mexico. Pulverized to minus 200 mesh.
FeS	Obtained from Cerac/Pure, Inc. as minus 100 mesh powder. Identified as pyrrhotite, Fe _{1-x} S, by x-ray diffraction (x = 0.14).
ZnS	Obtained from Cerac/Pure, Inc. as minus 325 mesh powder.
Kaolinite	Obtained from a clay deposit in Lewiston, Montana. Pulverized to minus 100 mesh.
Co/Mo	Commercial hydrodesulfurization catalyst (Harshaw O402T). Crushed and screened to 45 x 100 mesh.
Residue	Acetone-washed filter cake obtained from previous run with Illinois No. 6 coal in creosote oil. Used in the form of a dry, minus 100 mesh powder. (Ash = 48.4%; sulfur = 4.9%).

Table 3. Data from the Autoclave Experiments

	Added Minerals or Catalyst						
	None	Pyrite	FeS	ZnS	Kaolinite	Residue	Co/Mo
Conversion (% , daf)							
Pyridine Solubles	93	94	93	93	92	92	93
Benzene Solubles	38	38	46	34	38	44	63
Viscosity ^a (cps @ 60°C)	355	271	290	351	418	338	112
Solvent Analysis (% , daf)							
Organic Benzene Insol.	17.7	17.6	15.4	18.9	17.8	16.1	10.4
Asphaltenes	19.6	15.3	16.8	16.2	19.6	18.9	19.8
Pentane-soluble Oils	62.7	67.1	67.8	64.9	62.6	65.0	69.8
Elemental Analysis ^a (% , daf)							
Carbon	87.93	88.04	88.02	88.09	87.40	87.99	87.95
Hydrogen	5.84	6.00	5.92	5.92	5.83	5.89	6.02
Nitrogen	1.34	1.32	1.38	1.30	1.37	1.25	1.23
Sulfur	0.75	0.86	0.57	0.67	0.73	0.72	0.49
Oxygen (difference)	4.14	3.78	4.11	4.03	4.67	4.15	4.31
H/C	0.80	0.82	0.81	0.81	0.80	0.80	0.82
Pressure Ratio ^b	1.0	1.3	1.2	1.1	1.1	1.3	2.9

^aCentrifuged liquid product.

^b $\Delta P/\Delta P_0$ as defined in text.

EVALUATION OF USE OF SYNGAS FOR COAL LIQUEFACTION

Rand F. Batchelder and Yuan C. Fu

Pittsburgh Energy Research Center
U.S. Department of Energy
4800 Forbes Avenue, Pittsburgh, Pennsylvania 15213

INTRODUCTION

With the feasibility of coal liquefaction having been demonstrated over forty years ago, the major emphasis since then has been on process modifications and catalyst development to improve the process economics [1]. Cost analysis of a typical coal liquefaction process [2] reveals that as much as 30 percent of the overall cost is related to hydrogen production. The proposed modification is to use syngas ($H_2 + CO$) and steam instead of H_2 as feed gas to the reactor. The advantages of this modification are presented.

The bench scale approach in the direct liquefaction of coal consists of treating a slurry of coal in solvent under high H_2 pressure at temperatures of 400-475° C. The large coal molecules fragment thermally and are hydrogenated via hydrogen transfer from a donor solvent. The liquid product is formed as the H/C atomic ratio of coal increases from 0.7 to an approximate value of 0.9-1.0. Lighter liquid products could be formed with additional H_2 uptake. A catalyst would serve to promote hydrogenation and desulfurization processes during liquefaction. The required H_2 , usually 3-6 weight percent of the coal feed, is produced by gasification of coal and residual char to produce a synthesis gas. The synthesis gas as produced is a mixture of H_2 , CO, H_2O , and some CO_2 . The "raw" syngas is then passed through a shift converter to produce CO_2 and additional H_2 . Since the gas still contains about 2-3 percent residual CO, further processing will be required before the gas can be used with a CO-sensitive catalyst [3].

SYNTHESIS GAS CONCEPT

The syngas approach is to bypass the expensive gas purification and shift conversion step and send the product from the gasifier directly to the liquefaction reactor along with the recycle gas and added steam. The CO in the feed gas reacts with steam to form H_2 ($CO + H_2O \rightarrow H_2 + CO_2$) in the liquefaction reactor rather than separately in the water-gas shift system. This can be accomplished by utilizing a bifunctional catalyst in the liquefaction reactor, consisting of the conventional CoMo-SiO₂-Al₂O₃ for liquefaction and desulfurization, which is impregnated with K_2CO_3 to catalyze^{2,3} the shift reaction.

The obvious advantage of this modification is the elimination of the capital and operating cost of the purification and shift steps. In addition there will be a slight improvement in the thermal efficiency of the process. There is a need, however, for a larger recycle gas cleanup step capable of removing both H_2S and CO_2 . Before the process can be considered viable it must be proven that the liquefaction activity in the presence of CO, H_2 and H_2O is comparable to that with H_2 .

To evaluate the effect of substituting synthesis gas for H_2 , we decided at first to look at the SYNTHOIL process. The experimental section explains how the direct catalytic coal liquefaction performance using H_2 and H_2 -CO was compared in a set of autoclave experiments. The results of a batch reactor cannot be simply used to predict the steady state conditions in a continuous commercial reactor. An attempt was made, however, to calculate flow conditions for coal liquefaction processes using H_2 and H_2 -CO on the same basis using autoclave data. The objective is a preliminary study to evaluate and compare the potential merit of using syngas rather than to calculate the accurate results for a commercial process. The evaluation of SYNTHOIL by Kattel [2] was used as the basis for the conceptual design.

EXPERIMENTAL AND RESULTS

The concept of liquefying coal with syngas was tested in a stirred autoclave. The autoclave was charged with 30 grams of West Virginia bituminous coal, 70 grams of Solvent Refined Coal process solvent, 10 grams of H_2O , and 2-3 grams of crushed CoMo- K_2CO_3 catalyst. The autoclave was then charged with a 2:1 H_2 -CO gas mixture to 1500 psi (gage), heated to 450° C (operating pressure 2800-3000 psi), held at 450° C for 15 min. and then rapidly cooled by running water through an immersed cooling coil.

The CoMo- K_2CO_3 catalysts were prepared in three ways: (1) by blending ground CoMo- SiO_2 - Al_2O_3 catalyst (Harshaw 0402T) with K_2CO_3 powder, (2) by impregnating the CoMo catalyst with aqueous carbonate solution, (3) by introducing K_2CO_3 early in the preparation of CoMo catalyst in place of silicated alumina and keeping the ratios of Co and Mo to alumina constant. We have also tested CoMo catalysts impregnated with sodium carbonate, potassium acetate and barium acetate, NiMo catalyst impregnated with K_2CO_3 , and NH_4Mo catalyst. Some results have been presented previously [2]. Table I shows some representative results as well as hydrotreating data obtained with pure H_2 and CoMo- SiO_2 - Al_2O_3 catalyst. The performances with H_2 -CO and H_2 compare very closely in all categories.

PROCESS EVALUATION

Using the yields obtained from the autoclave experiments and the process parameters of the SYNTHOIL process, material balances were derived for both the H_2 -CO and H_2 systems. An energy balance was then calculated for the H_2 -CO process scheme. Finally an economic comparison of the two alternatives was performed, based on an economic evaluation of the SYNTHOIL process made by Kattel, et al [2]. The benefit of using a high pressure gasifier (such as in the Texaco process) and a modification of the Exxon Donor Solvent Process using syngas were also examined.

A. Direct Catalytic Liquefaction of Coal

The flowsheet for the modified direct catalytic liquefaction process is shown in Figure 1. Synthesis gas from the gasifier is sent directly to the liquefaction reactor eliminating the shift and purification steps. Steam is added to the liquefaction reactor to promote the water-gas shift reaction. Now that this reaction is taking place in the liquefaction reactor, the CO_2 produced there must be removed in the recycle gas cleanup step. Therefore, the recycle gas cleanup step must be designed to remove both CO_2 and H_2S . It is desirable to produce a concentrated stream of H_2S to allow efficient use of the Claus process for converting H_2S to sulfur. The concept employed in the Giammarco-Vetrocoke process [5] for acid-gas removal meets these requirements. It will remove both CO_2 and H_2S from a gas stream and process it into two separate streams of CO_2 and H_2S .

The aqueous stream from the vapor-liquid separators is sent to an ammonium sulfate and sulfuric acid recovery process. The product slurry from the high temperature separator is centrifuged. The underflow from the centrifuge is sent to a char de-oiling process for recovery of oil entrained in the solids. Unconverted char from this step is sent to the gasifier for further carbon utilization.

TABLE 1. Hydrotreating of Bituminous Coal^a

(Coal: SRC Liquid = 1:2.5, 3000 psi, 450° C, 15 min)

Catalyst	Syngas (H ₂ :CO = 2:1)						H ₂		
	CoMo-K ₂ CO ₃ ^b	CoMo-K ₂ CO ₃ ^b	CoMo-K ₂ CO ₃ ^c	CoMo-BaAc ^b	NiMo-K ₂ CO ₃ ^b	NH ₄ Mo ^b	CoMo ^d	CoMo ^e	NH ₄ Mo
% K ₂ CO ₃	11.2	5.0	7.7	(9.9) ^f	10.1	-	-	-	-
Surf. Area m ² /g	74	133	136	141	140	-	123	153	-
Conversion, %	94	90	90	89	89	90	94	91	93
Oil yield, %	68	60	63	61	59	57	71	62	62
Asphaltene formed, %	42	42	32	24	32	19	30	25	37
S in oil product, %	0.40	0.44	0.41	0.41	0.40	0.37	0.39	0.33	0.44
Kinematic viscosity, CS* at 60° C	20	18	18	16	21	13	15	13	20
Syngas or H ₂ consumed, SCF/lb maf coal	8.6	9.9	10.0	10.0	9.0	11.2	10.7	11.6	10.2

^aData are given in weight percent of maf coal

^bCoMo or NiMo impregnated with K₂CO₃ solution

^cLaboratory prepared sample with K₂CO₃ substituted for alumina

^dHarshaw 0402

^eLaboratory prepared sample with the same composition as Harshaw 0402

^fPercent barium acetate

Mass Balance - The basis of the flowsheet calculation is briefly described in the Appendix. There are two major problems associated with the batch autoclave data: (1) the solvent is not a recycle solvent derived at the identical steady state condition, and (2) the material balance is usually poor with a recovery in the range of 94-98%. Batch data from the autoclave experiments were used in the calculation as shown in the Appendix. The conversion of CO is calculated by assuming water-gas shift equilibrium at 475° C (28° C approach) with a $H_2:CO:H_2O$ feed of 2:1:0.4. The resulting yields for a continuous reaction are shown in Table 2. The flowsheet derived from these yields is shown in Figure 1.

The overall mass balances for the H_2 -CO and H_2 processes were obtained on the basis of one ton of West Virginia bituminous coal feed (See Table 3). The mass balance over the reactor, which operates at 4000 psig and 450° C, is based on the simulated yields. The design parameters used in the study are listed in the Appendix. It was assumed that the recycle gas scrubber provided complete removal of CO_2 and H_2S . The flow and composition of the off-gas from the vapor-liquid separators were estimated from vapor-liquid equilibria of the various components with the liquid oil at the separator temperatures of 150 and 40° C. The gasifier mass balance was based on the total gas demand, coal and char feed, operating condition of 450 psi and 982° C, 95% carbon conversion and a water-gas shift equilibrium at 1010° C (28° C approach).

Energy Balance - The thermal efficiency of the SYNTHOIL Process has been estimated by Akhtar et al [6]. The energy balance for the H_2 -CO process was computed and is shown in Figure 2. It is based on the net heats of combustion at the specified temperature of each stream, neglecting pressure effects. The net heats of combustion of the coal (12,390 Btu/lb), oil (16,300 Btu/lb), and the char (4,500 Btu/lb) were obtained experimentally. The heat capacities for coal, char, ash and oil were obtained from IGT's Coal Conversion Data Book. The energy balance across the reactor was calculated using eqn. 6 in the Appendix, assuming an adiabatic reaction with an estimated heat loss. The conceptualized plant is totally self-sufficient with the coal being the only energy input. The plant contains its own steam and electricity plant. The overall thermal efficiency is 75.6 percent as compared to values of 67.8 [2] and 74.9 [6] percent for the SYNTHOIL process using H_2 . The advantage of the syngas system is a result of the elimination of the inefficient two-stage shift reactors.

Economics - The methods used to perform the economic analysis of the two alternative cases followed those used in Katell's report. The main objective of this economic evaluation is to obtain a relative cost comparison of the two processes rather than to yield accurate estimates. The sequence of steps in the evaluation was as follows: (1) size major equipment, (2) cost major equipment, (3) use standard factors to cost miscellaneous equipment, (4) calculate utility balance, (5) size and cost utility sections, (6) determine operating costs and (7) do a discounted cash flow analysis over the life of the plant to determine the product selling price at various rates of return and coal prices. The analysis was carried out for both the $CO-H_2$ and H_2 cases. A unit cost table, which shows the cost distribution among the various sections of the process, is shown in Table 4. Two major differences are apparent in the unit cost table. The recycle gas cleanup and byproduct recovery sections in the H_2 -CO process are more expensive than that in the H_2 process because of the necessity of removing CO_2 in addition to H_2S in this stage.² The cost of the shift and purification section is \$1.90/bbl in the H_2 process, but is totally absent in the H_2 -CO system. Thus the H_2 -CO system results in a net cost advantage of \$1.59/bbl or about 14% of the total process cost.

TABLE 2. Product Yields and Analysis at Steady State
(Basis 100 lb of maf coal feed)

Input		<u>Syngas</u>	<u>H₂</u>
maf coal		100.00	100.00
H ₂		1.17	3.79
CO		35.20	0.00
H ₂ O		<u>25.81</u>	<u>0.00</u>
Total		162.18	103.79
H ₂ or H ₂ + CO consumption, SCF		661	675
Output			
C ₁ -C ₄		11.37	10.80
Oil		77.38	77.87
H ₂ O		9.08	5.99
CO ₂		55.31	0.00
H ₂ S		2.54	2.54
NH ₃		0.50	0.59
Char		<u>6.00</u>	<u>6.00</u>
		162.18	103.79
Elemental	Coal	Product Oil	Product Oil
C	73.8	88.3	88.3
H	5.2	7.5	7.7
O	7.2	2.6	2.5
N	1.3	1.2	1.1
S	3.8	0.4	0.4
Ash	8.2	-	-
Moisture	0.5	-	-

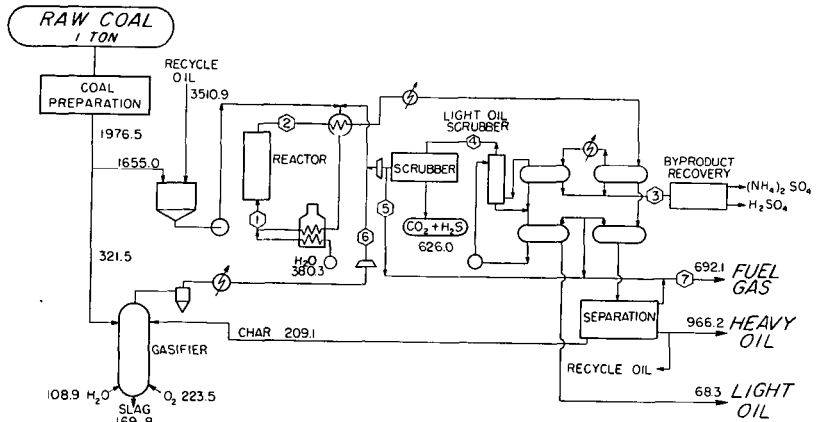


Figure 1-Process flow diagram using SYNGAS.

STREAM COMPOSITION

STREAM	①		②		③		④		⑤		⑥		⑦	
	lbs	(vol %)	lbs	(vol %)	lbs	(vol %)	lbs	(vol %)	lbs	(vol %)	lbs	(vol %)	lbs	(vol %)
MAF COAL	1511.4		0											
ASH	160.0		160.0											
CHAR	16.6		107.3											
OIL	3478.2		4647.8				26.1		0.2				144.8	
GAS COMPOSITION														
H ₂ O	390.0	(9.50)	137.2	(3.58)	137.2						1.4	(0.22)		
H ₂	239.3	(5.208)	221.5	(5.165)			217.0	(57.16)	4.3	(57.83)	26.6	(36.37)	11.5	(26.37)
CO	1628.1	(25.50)	1096.1	(18.40)			1052.8	(19.96)	21.1	(20.19)	596.4	(58.67)	643	(11.60)
C1	391.9	(10.72)	452.4	(13.26)			399.8	(13.23)	8.0	(13.39)			65.0	(18.71)
C2	72.2	(1.06)	111.5	(1.75)			73.6	(1.31)	1.5	(1.32)			39.3	(6.06)
C3	33.8	(0.34)	81.2	(0.88)			34.5	(0.42)	0.7	(0.43)			47.4	(5.03)
C4	5.7	(0.04)	30.2	(0.24)			5.8	(0.05)	0.1	(0.05)			24.5	(1.94)
H ₂ S	36.3	(0.47)	74.8	(1.03)	15.1		17.9	(0.53)	0		36.3	(2.94)	41.8	(4.38)
CO ₂	202	(0.20)	856.1	(9.15)			608.1	(7.34)	0		20.2	(1.26)	247.9	(26.00)
NH ₃	0	(0)	7.6	(0.21)	7.6									
N ₂	5.5	(0.09)	5.5	(0.09)							5.5	(0.54)	5.5	(0.90)
Total	7989.2	(100)	7989.2	(100)	1599		2435.6	(100)	35.9	(100)	686.4	(100)	692.0	(100)
scf....		81820		76350				67610		330		13030		7780

TABLE -3 OVERALL MASS BALANCE

In:	H ₂	H ₂ /CO
Raw Coal	2000.0	2000.0
Gasifier Steam Feed	141.4	108.9
Gasifier O ₂ Feed	187.0	223.5
Shift Converter Steam	558.2	0
Reactor Water Feed	0	380.3
Total	2886.6	2712.7
Out:		
Water Condensate	249.1	30.4
Waste Water	118.9	159.9
Slog	169.6	169.8
Fuel Gas	365.0	692.1
H ₂ S + CO ₂	946.4	626.0
Oil Product	1037.6	1034.5
Total	2886.6	2712.7

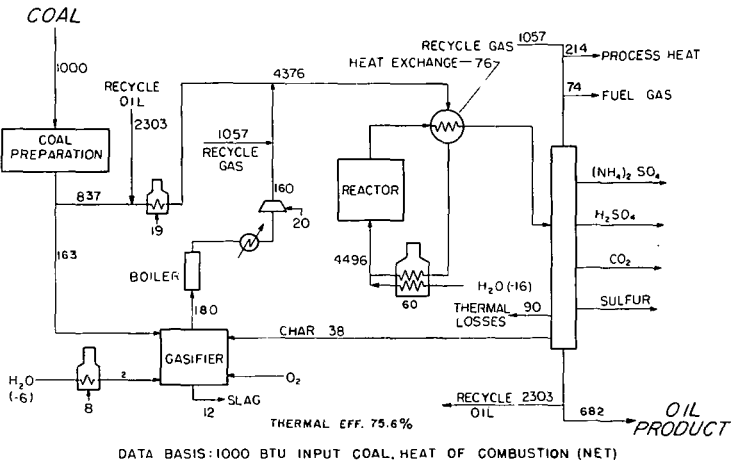


Figure 2 - Thermal balance.

9-7-77 L-15579

TABLE 4. Unit Cost, \$/bbl Product Oil

<u>Cost</u>	<u>Operating</u>	<u>Capital</u>	<u>Credits</u>	<u>Total</u>
Coal + Paste Preparation	0.899	0.670	0	1.569
Hydrogenation	2.102	2.180	-2.366	1.916
Heat Exchange	0.666	1.178	0	1.844
Char De-oiling	.205	.362	-0.315	.252
Gasification	1.985	.174	0	2.159
Gas Cleanup + Byproduct Recovery	.819	.837	-.105	1.551
	<u>.593</u>	<u>.750</u>	<u>-.105</u>	<u>1.238</u>
Shift + Purification	0	0	0	0
	<u>1.206</u>	<u>.694</u>	<u>0</u>	<u>1.900</u>
Flue Gas Processing	.431	.431	-.232	0.630
Total	7.107	5.832	-3.018	
	<u>8.087</u>	<u>7.439</u>	<u>-3.018</u>	9.921
				<u>11.508</u>
		Processing Cost		
		Coal Cost		9.453
		Oil Cost		19.374
				<u>20.961</u>

Underline - Cost using H₂
 Otherwise both H₂ and
 H₂-CO systems have the
 same cost.

Basis: 25,000 BBL/D
 Cost based on April 1977 CE index
 WVa Coal - \$25/T
 15% return on investment

High Pressure Gasifier - A beneficial modification to the H_2 -CO process is to employ a high pressure gasifier to be operated at a pressure in the range of 2500-3000 psi, equivalent to that required in a liquefaction reactor. This change would further increase the thermal efficiency and improve the economics. From the energy balance (Figure 2) we see that 2% of the input energy exists as latent heat in the hot gasifier output. Also 2% of the input energy is used to compress the gasifier product gas. By employing a high pressure gasifier all of the latent heat is recovered, the inefficient gasifier heat exchanger is eliminated, the make-up gas compressor is not required and the reactor preheat duty is reduced. Thus the use of higher pressure gasifier increases thermal efficiency by about 4 percent. A minor offsetting change is the increased pressure of O_2 and steam necessary to feed the gasifier.

B. Extractive Hydrogenation of Coal

Coal liquefaction processes by extractive hydrogenation such as the Exxon Donor Solvent Process can also be benefited economically by using syngas in place of H_2 . A conceptual process scheme is presented in Figure 3. Coal is dissolved in a recycling solvent in the absence of catalyst under H_2 -CO pressure, and part of the liquid product is subsequently hydrotreated with syngas and steam in the presence of $CoMo-K_2CO_3$ catalyst to make the recycle solvent. Experimental data were obtained by initially hydrotreating an SRC solvent with syngas and steam in the presence of $CoMo-K_2CO_3$ catalyst and subsequently using this hydrotreated solvent to extract coal in the absence of catalyst. Table 5 shows the autoclave experimental results of hydrotreating the SRC solvent with syngas and H_2 . Table 6 shows the comparison of using the syngas hydrotreated solvent and the H_2 hydrotreated solvent for coal solvolysis under H_2 -CO and H_2 pressures respectively. From both tables, no significant difference in the quality of the product oil or solvent was observed between the syngas and H_2 systems.

REFERENCES

1. Bergius, F., German Patent 303272 (1922).
2. Kattel, S., "SYNTHOIL Process-Liquid Fuel from Coal Plant," Report No. 75-20, Bu. of Mines, Morgantown, WVa., Jan. 1975.
3. Vernon, L. W., Pennington, R. E., U.S. Patent 3,719,588 (1973).
4. Fu, Y. C., Illig, E. G., Ind. Eng. Chem., Proc. Des. Dev., Vol. 15, No. 3, 392, 1976.
5. Riesenfeld, F. C., Mallowney, J. F., Oil and Gas J., Vol. 57, No. 20, 86, 1959.
6. Akhtar, S., Lacey, J. J., Weintraub, M., Reznik, A. A., Yavorsky, P.M., "The SYNTHOIL Process -- Material Balance and Thermal Efficiency," Paper No. 356, Bu. of Mines, Pittsburgh Energy Research Center, Dec. 1974.
7. IGT, "Preparation of a Coal Conversion Systems Technical Data Book," Final Report FE-1730-21, 1976.

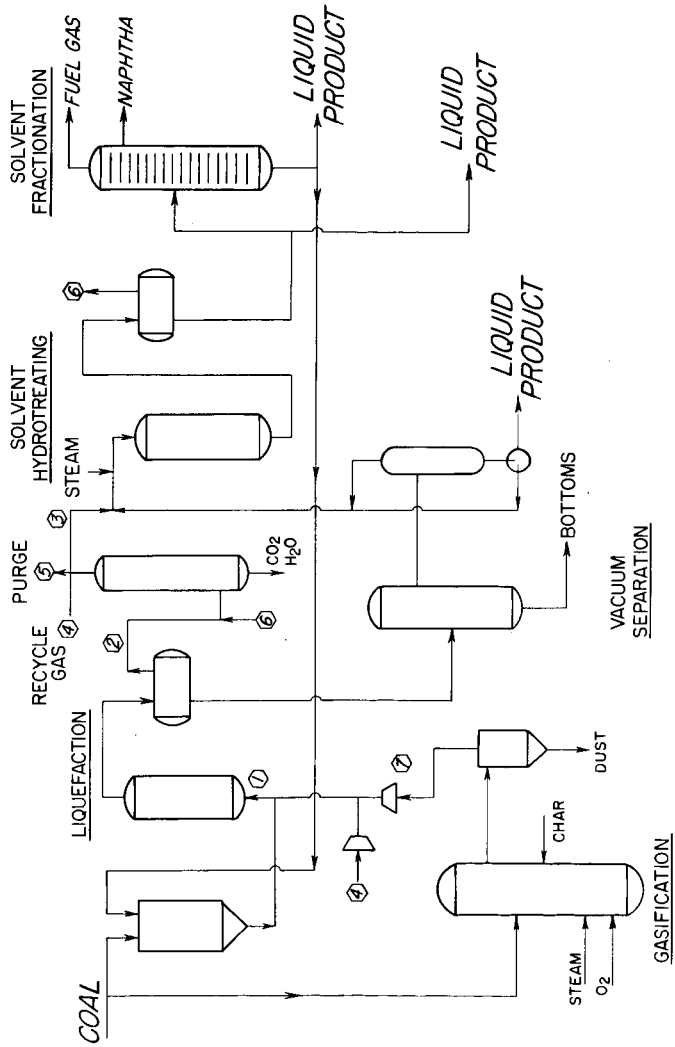


Figure 3--Solvolysis of coal using SYNGAS.

5-19-77 L-15382

TABLE 5. Hydrotreating of SRC Solvent
(425° C, 60 min)

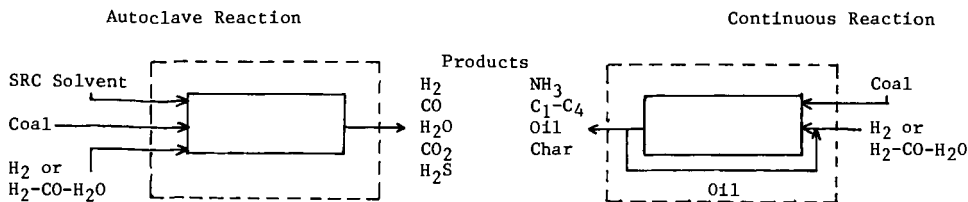
	Original	Syngas (H ₂ :CO = 2:1)	H ₂
Catalyst	-	CoMo-K ₂ CO ₃	CoMo
H ₂ O added pts/100 pts		10	0
Initial Press, psi		1220	1520
Operating Press, psi		2600	2450
Product Analysis, %			
C	88.8	89.1	89.4
H	7.4	7.6	8.0
N	1.1	1.0	0.8
S	0.65	.42	.14
O	2.05	1.88	1.66
Kinematic Viscosity, CS at 60° C	12.2	7.8	5.4

TABLE 6. Coal Liquefaction by Solvolysis
(solvent: coal = 2.3:1, 3000 psi, 450° C, 15 min)

	Syngas (H ₂ :CO = 2:1)		H ₂	
	SRC	Treated SRC	SRC	Treated SRC
Conversion, %	89	90	89	91
Asphaltene formed, %	42.7	32.6	49.3	25.6
S in oil prod., %	0.64	0.54	0.65	0.44
Kinematic viscosity, CS at 60° C	30.1	22.7	30.8	14.8

APPENDIX

Design Calculations



Elemental Balance for Continuous Reaction

Y_i = yield, (lbs of i out - lbs of i in) / lb maf coal

F_i^k = wt. fraction of element k in component i

$$C \quad F_{\text{Coal}}^C - (Y \cdot F^C)_{\text{CO}} = (Y \cdot F^C)_{\text{C}_1\text{-C}_4} + (Y \cdot F^C)_{\text{CO}_2} + (Y \cdot F^C)_{\text{Oil}} + (Y \cdot F^C)_{\text{Char}} \quad (1)$$

$$H \quad F_{\text{Coal}}^H - Y_{\text{H}_2} = (Y \cdot F^H)_{\text{C}_1\text{-C}_4} + (Y \cdot F^H)_{\text{H}_2\text{O}} + (Y \cdot F^H)_{\text{NH}_3} + (Y \cdot F^H)_{\text{H}_2\text{S}} + (Y \cdot F^H)_{\text{Oil}} + (Y \cdot F^H)_{\text{Char}} \quad (2)$$

$$O \quad F_{\text{Coal}}^O - (Y \cdot F^O)_{\text{CO}} = (Y \cdot F^O)_{\text{H}_2\text{O}} + (Y \cdot F^O)_{\text{CO}_2} + (Y \cdot F^O)_{\text{Oil}} + (Y \cdot F^O)_{\text{Char}} \quad (3)$$

$$N \quad F_{\text{Coal}}^N = (Y \cdot F^N)_{\text{NH}_3} + (Y \cdot F^N)_{\text{Oil}} + (Y \cdot F^N)_{\text{Char}} \quad (4)$$

$$S \quad F_{\text{Coal}}^S = (Y \cdot F^S)_{\text{H}_2\text{S}} + (Y \cdot F^S)_{\text{Oil}} + (Y \cdot F^S)_{\text{Char}} \quad (5)$$

Energy Balance for Continuous Reactor

H_i = net enthalpy of combustion of component i , BTU

$$\sum_i^{\text{in}} H_i T_i^{\text{in}} = \sum_i^{\text{out}} H_i T_i^{\text{out}} + \text{heat loss} \quad (6)$$

Assumptions

- The yields of $\text{C}_1\text{-C}_4$ gas ($Y_{\text{C}_1\text{-C}_4}$) and char (Y_{Char}) and the elemental compositions of $\text{C}_1\text{-C}_4$, oil, and char observed in the autoclave experiment are used in the continuous reaction design.
- The yield of carbon monoxide is calculated assuming the water-gas shift reaction to be at equilibrium at 477°C (28°C approach) with a $\text{H}_2:\text{CO}:\text{H}_2\text{O}$ reactor feed of 2.05:1:0.4. It is also assumed that carbon dioxide is involved only in the water-gas shift reaction, thus $Y_{\text{CO}_2} = -Y_{\text{CO}}$.
- The remaining unknowns are Y_{H_2} , $Y_{\text{H}_2\text{O}}$, $Y_{\text{H}_2\text{S}}$, Y_{NH_3} , and Y_{Oil} . These are determined by solving eqns. 1-5 simultaneously. The other unknown, T_{out} , is solved from eqn. 6.

Design Parameters

Oil:Coal Recycle Ratio = 2.12
 SCF/lb Slurry Reactor Feed = 15.8
 Reactor Feed Rate = 280 lb/hr-ft³ catalyst
 Reactor Inlet Temp = 425°C
 Reactor Inlet Press = 4200 psig
 Reactor Exit Temp = 449°C
 Reactor Exit Press = 4000 psig
 Process Heater Eff = 80%
 Electric Generation Eff = 40%

Economic Evaluation

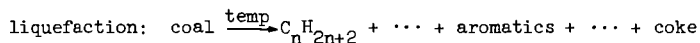
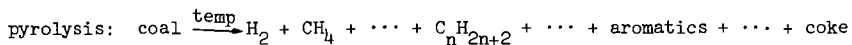
Based on April 1977 CE Index
 15% Discounted Cash Flow

Hydrogen Consumption in Non-Catalyzed Coal Liquefaction

M. G. Thomas, Barry Granoff, G. T. Noles and P. M. Baca
Sandia Laboratories
Albuquerque, New Mexico 87115

INTRODUCTION

Liquefaction, in general, refers to the thermal reactions experienced by coals at temperature usually above 400°C in suitable solvents. These reactions produce a complex mixture of solubilized (liquefied) and gasified products in high yield over short time intervals (1). The interaction of hydrogen in these reactions is not well understood, but the presence of H₂ has been observed to increase the yields of liquefaction products (2). Hydrogen also provides a reductive pathway to allow for the removal of hetero-atoms as H₂S, H₂O and NH₃. Though the implication of these beneficial uses of hydrogen is net consumption, it has recently been shown that H₂ is also produced in these thermal reactions in non-H₂ atmospheres (3). The thermal reactions of coal in solvent, then, are best represented schematically as a set of two competing reactions (4); i.e.,



where H₂, the light hydrocarbons and coke are maximized in pyrolysis and minimized in liquefaction. It can be seen then how hydrogen can be produced in the pyrolysis reaction, and how its presence can favor one reaction over the other without being consumed; the H₂ gas may merely inhibit the pyrolysis. Obviously, maximizing the rate of liquefaction/pyrolysis is an important consideration in the efficient use of hydrogen. We will attempt to show how each of these competing reactions respond to changing conditions and some of the effects that the various conditions produce with respect to hydrogen consumption.

EXPERIMENTAL

Data reported in this presentation have been obtained from analysis of products from 1.) a 1-liter stirred batch autoclave operating between 395°-430°C, and H₂ pressure of 1000-1750 psi measured prior to reaction at 24°C, and 2) a four-stage continuous (non-cycling) reactor operating at 425°C and 4000 psi. In the autoclave experiments, a charge of 50 g daf coal and 115 g #4 cut creosote oil was employed (5). Samples for gas analyses were obtained at ~ 25°C by venting through gas sampling tubes before scrubbing. The GC columns used were 6' x 1/8" O.D., 80-100 mesh poropak Q in teflon lined aluminum. The continuous reactor was packed with glass spheres; each stage was a 10 ft length, .203 inch I.D., void volume ~ 50%. The packing was intended to improve heat transfer and maintain mixing. The reactor was charged with a fixed slurry of #4 cut creosote oil and 30% by weight coal. The coal used in the continuous reactor was -60 mesh West Virginia, Ireland Mine coal. Block diagrams of the autoclave and reactor are shown in Figure 1a and Figure 1b. Analyses of the West Virginia, Ireland Mine coal used for both autoclave and continuous reactor experiments: ultimate (dry)

C 62.83; H 4.45; N 0.90; Cl 0.03; S 6.93; Ash 19.06; O (diff) 0.577; sulfur forms-pyrite 4.55; sulfate 0.25; organic 2.13. A description of the liquid analyses is given in block diagram form, in Figure 2. Data on other coals used in this study can be obtained from Reference 5.

RESULTS AND DISCUSSION

Comparisons of liquefaction products from different coals are not generally successful because of the variations in composition (of the coals), but can serve to illustrate the nature of the products and the role of hydrogen. Table 1 contains data from six different high volatile bituminous coals and the liquefaction products obtained in each case at 430° and .5 hour reaction times. The amount of reactive macerals varied between 89-95%, but the mineral content changed from 5 to 21%. Although the conversion varies (62-94%), the H/C ratios of the filtered (organic) products are basically the same, about 0.8. Analysis of the gas data certainly show consumption of hydrogen and production of H₂S and hydrocarbon gases. The H₂ consumption parallels conversion as does the H₂S produced. However, the production of methane, reflecting the pyrolysis reaction, does not vary in any readily apparent fashion. The H₂ consumed apparently accompanies conversion of the primary liquefaction products to benzene solubles among the several coals, as suggested by Neaval based upon the behavior of one coal in time (6).

Data obtained from the continuous reactor at 425°C shown in Table 2 clearly show two additional features of coal liquefaction 1.) the rapid initial desulfurization followed by a much slower removal of the more resistant organic sulfur; and 2.) accompanying pyrolysis reactions seen here as formation of CH₄. One conclusion based on these data is that most of the H₂S (removed sulfur) is produced in the early stages of the reactor (as is the H₂ needed for H₂S formation). Although organic sulfur is being removed, it is removed in a very specific fashion.

Reactor Stage	Asphaltene %S	Preasphaltene %S
1	1.33	1.68
2	1.24	1.59
3	1.20	1.66
4	1.22	1.68

As shown above, the percentage sulfur in the asphaltenes and the preasphaltenes is not changing significantly in time. The interconversions of the liquefaction products (as preasphaltene → asphaltene + oil) are accompanied by sulfur removal (consistent with H₂ consumption for the conversion to benzene solubles as noted earlier). Thus, sulfur removal does not occur to any significant extent without a concurrent change in solubility properties. This type of reaction is consistent with data published on hetero-atom removal from model aromatic compounds; the molecule is usually saturated with hydrogen, followed by ring opening and then removal of the hetero-atom (7). The resulting products thus, have different structures, solubility characteristics, and molecular weights and are not merely the initial molecule minus a S, N or O atom. For coal derived molecules then, this reductive cracking occurs simultaneously with defunctionalization, and both of these reactions are accompanied by hydrogen consumption.

It is necessary to examine the responses to temperature, time, and pressure to understand the process more fully. Using the same coal as in the continuous reactor, a number of autoclave experiments were performed at residence times between .25 and 1 hour, 395°-430°, and 1000-1750 psi initial pressures (pressure charges measured at 24°C before the heat cycle). Data obtained from these experiments are plotted in Figure 3, and in contrast to the data presented in Table 1, the C/H ratio of the products is changing. In Figure 3a it is seen that as time increases sulfur is removed and the amount of hydrogen in the liquefied product increases, data consistent with results drawn from the reactor runs. Likewise, sulfur decreases and hydrogen in the product increases with higher pressures, Figure 3b. However as temperature increases, the sulfur is lowered but the C/H ratio increases, Figure 3c. Figure 3d shows the amounts of H₂ gas consumed versus temperature. Though a cursory examination of Figure 3d would suggest greater hydrogenation at the higher temperature we know this is not consistent with the liquid analyses, Figure 3c. A more consistent picture is obtained by examination of the quantity of hydrogen in the gas from all sources (H₂, C₁-C₄'s, and H₂S) at two temperatures:

Gas	Moles Produced at 414°C	Moles Produced at 429°C
CH ₄	.06	.11
C ₂ H ₆	.02	.05
H ₂ S	.03	.04
H ₂ (consumed)	.30	.50

It can be seen that the total hydrogen in the gases produced is greater at higher temperature (approximately twice as large at 429° than at 414°) and indicates that temperature increases favor the pyrolysis reaction (4).

The effects observed in these experiments must not be evaluated without a description of solvent behavior under similar conditions. Table 3 shows both liquid and gas analyses of #4 creosote oil before and after reaction at 407° and 427°C. The H₂ gas consumption and CH₄ production are low compared to data obtained with coals. Also, no desulfurization is observed, though a slight increase in hydrogen content of the oil is observed. The magnitude of the differences observed in the gas data (H₂ consumption, H₂S and CH₄ formation) between the solvent and the solvents with coal would seem to indicate that the contribution of solvent to these specified (gasification and H₂ consumption) reactions was minimal (8).

SUMMARY

The discussion has considered liquefaction as two competing reactions; one which produces solubilized defunctionalized products, and a pyrolysis reaction which consumes hydrogen. Responses of the reactions to the independent variables of pressure, temperature, and time have been described and suggest that hydrogen pressure and time favor the liquefaction reactions (decreases in C/H ratio, decreases in sulfur, and increases in conversion), but that temperature seems to preferentially favor pyrolysis. These conclusions are in general agreement with

literature data. Additionally it has been shown that 1.) sulfur removal occurs concurrent with conversions among the various solvent extraction fractions, 2.) conversion varies with H₂ consumption among a number of similar but different coals and 3.) hydrogen consumption must be evaluated on the basis of a total balance, not just a change in concentration of H₂ gas.

REFERENCES

1. U.S. Bureau of Mines 646; also S. Weller, M. G. Pelipitz, E. S. Friedman, *Ind. Eng. Chem.* 43, 1572 (1951).
2. M. Farcasiu, T. O. Mitchell, and D. D. Whitehurst, 1st Yearly Report, RP-410-1 to EPRI (1976).
3. D. D. Whitehurst, M. Farcasiu, T. O. Mitchell, and J. J. Dickert, Jr., 2nd Yearly Report, RP-410-1 to EPRI (1977).
4. W. H. Wiser, L. L. Anderson, S. A. Quaged, G. R. Hill, *J. Appl. Chem. Biotechnol.* 21, 82 (1971).
5. Barry Granoff and Michael G. Thomas, Preprints, Div. of Fuel Chemistry, *Amer. Chem. Soc.*, 22 (6), 183 (1977).
6. R. C. Neavel, *Fuel*, 55, 237 (1976).
7. M. Houalla, D. Brodirich, V. H. J. De Deer, B. C. Gates, H. Kwart, "Structure and Reactivity," Preprints, Petroleum Chemistry Symposia, *Amer. Chem. Soc.*, March 1977.
8. Arthur R. Tarrer, James A. Guin, Wallace S. Pitts, John P. Henley, John W. Prather and Gary A. Styles, Preprints, Div. of Fuel Chem., 21 (5) 59 (1976).

FIGURE 1. BLOCK DIAGRAMS OF a. AUTOCLAVE, AND b. 4-STAGE REACTOR.

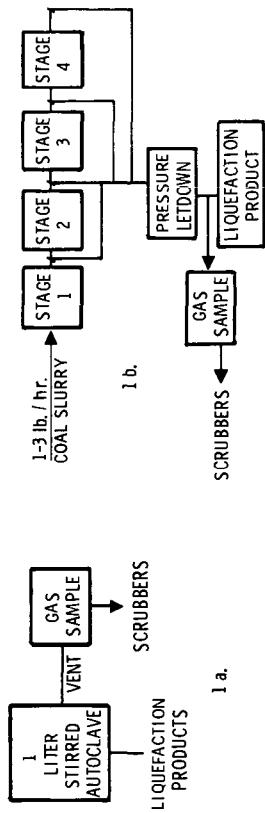


FIGURE 2. BLOCK DIAGRAM OF LIQUID ANALYSIS.

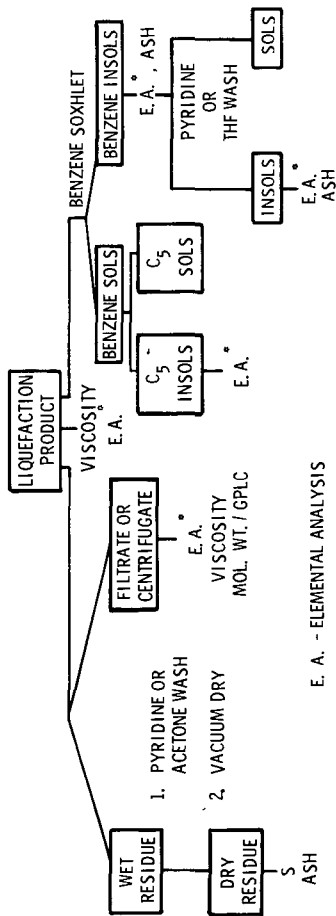


Table 1. Selected data of several coals and respective liquefaction products.

Coal %S	Reactive Macerals	Mineral Matter	Conv.	OBI	Filtered Product H/C	Mole % H ₂ S	Mole % CH ₄	Moles H ₂ Consumed
Kent. 11, Fies	93	20.9	93	7.8	.82	6.6	2.87	.57
Kent. 11, Homestead	92	15.7	94	10.3	.83	3.2	2.71	.53
West Va.	91	13.8	88	10.6	.80	2.44	3.70	.41
Ill. 6	95	13.0	87	14.8	.80	1.62	2.16	.40
Pennsylvania	90	5.2	84	16.5	.81	0.38	1.82	.33
Kent. Elkhorn 3	89	5.6	62	22.9	.81	0.36	1.85	.31

Table 2. Reactor products from a run at 425°C, 4000 psi H₂, 1 lb/hr coal.

Product %S	Benzene Insols	Asphaltene	THF Preasphaltene	% of Total S in THF Insols	Moles CH ₄ / lbs. Coal
Reed	30.0	-	-	92.0	-
Stage 1	18.9	11.8	9.9	39.0	.68
Stage 2	15.4	13.1	8.5	40.5	1.47
Stage 3	10.9	15.5	5.3	-	2.18
Stage 4	9.8	13.4	4.8	40.8	3.10

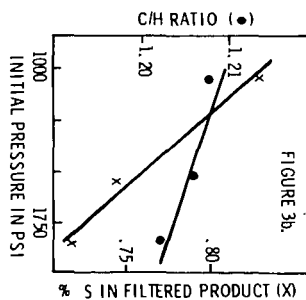
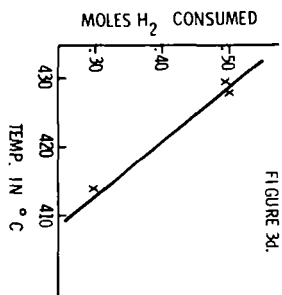
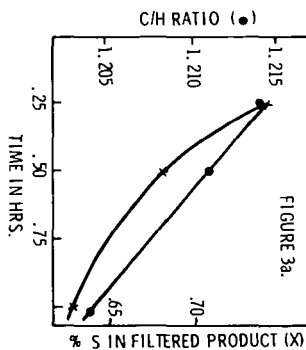
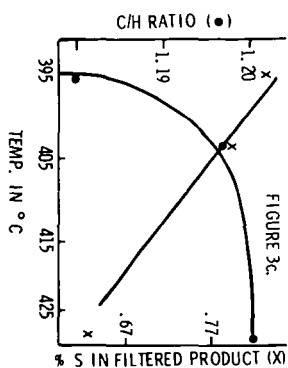


FIGURE 3. a. C/H RATIO AND S vs. TIME (430°C, Initial H₂ Pressure 1500 psi)
 b. C/H RATIO AND S vs. PRESSURE (405°, time 1 hour)
 c. C/H RATIO AND S vs. TEMPERATURE (time 1 hour, Initial H₂ Pressure 1500 psi)
 d. MOLES H₂ CONSUMED vs. TEMPERATURE (time and Pressure as in 3c)

Table 3. Analyses of #4 Cut Creosote Oil

	Initial	1800 psi, .5 hr 407°	1800 psi, .5 hr 427°
Pyridine Insols	0.0	0.0	0.0
Benzene Insols	0.3	1.0	1.6
Asphaltene	7.3	3.9	3.2
Oil	92.7	95.1	95.2
C	90.77	91.03	-
H	5.8	5.93	-
S	.4	.4	.4
Moles CH ₄	-	.0029	.0097
Moles H ₂ Consumed	-	.004	.015

CONCEPT AND USE OF HYDROGEN PERMEABLE CATALYSTS

Clarence Karr, Jr. and Kenneth B. McCaskill

U.S. Energy Research and Development Administration
Morgantown Energy Research Center
P.O. Box 880, Collins Ferry Road
Morgantown, WV 26505

INTRODUCTION

The concept of a hydrogen-permeable catalyst has not previously been reduced to practice for any gaseous or liquid mixture of coal-derived compounds, including sulfur compounds. The only known instance of the use of this concept is that described in a U.S. Patent by Rudd (1). In his work hydrogen was diffused under pressure through a palladium coil into a vessel containing ethylene. The ethylene was readily reduced to ethane, presumably by reaction with the hydrogen at the palladium surface, the palladium acting as a catalyst. The hydrogen for this reaction was apparently limited to that which had diffused just to the surface of the palladium, and was present as atomic hydrogen. In another experiment, Rudd demonstrated that an oxide coating produced on one side of a Hastelloy B disc could be completely removed by diffusing hydrogen through the disc from the non-oxidized side. The self-cleaning effects of a hydrogen permeable catalyst are implied in this demonstration, although Rudd did not try to use Hastelloy B as a catalyst.

The successful implementation of the concept of hydrogen permeable catalysts to coal-derived gases or liquids, and even coal or coal/recycle oil slurries, may offer several technical and economic advantages. These could include the virtual absence of unused hydrogen that has to be purified, recompressed and recycled at considerable expense, because essentially all the hydrogen could be consumed at the catalyst surface, without forming hydrogen bubbles. Another advantage, as suggested by Rudd's work, is that the catalyst surface could be kept free of carbon deposits because, just as oxides were removed by reaction with hydrogen diffusing up through the metal, so coking precursors would be converted by hydrogenation, preventing the formation of carbonaceous deposits. Finally, it may be possible to prevent the buildup of mineral deposits when coal or coal slurries are used, because the presence of a mono-molecular or monoatomic layer of hydrogen at the surface would prevent the adhesive forces between the mineral particles and the catalyst surface from being effective.

EXPERIMENTAL PROCEDURE

Reactor Design and Function

The general reactor design is briefly as follows. The shell of the hydrogen permeable catalyst reactor consisted of 3-inch O.D. schedule 80 stainless steel pipe, 4-feet and 7-inches in length. One end of the pipe was adapted to accept tubing from one inch to 3/8 inches in diameter. The other end was modified to accept tubing from 1/2 to 3/8 inches in diameter. One quarter inch openings were made in the reactor walls to permit inlet and venting of gases. Catalyst tubes were connected at each end to short lengths of stainless steel tubing. The stainless steel tubing, holding the catalyst tube, was inserted into the reactor at the end containing the larger opening, and allowed to protrude from the lower end of the reactor for a length of about 8 inches. The reactor, containing the catalyst tube, was suspended vertically in a high temperature furnace. Connections were made to the walls of the shell to permit inlet and venting of gases. Connections were made to the stainless steel tubing at the bottom of the reactor to permit hydrogen sulfide and hydrogen

for presulfiding, and liquid feed to enter the tube, with appropriate valving. The upper end of the tube went directly into a product receiver (gas liquid separator). Lines from the gas-liquid separator were connected to a cold trap, and then into a wet test meter for measuring any gas flow.

Hydrogen Permeable Catalyst Tubes

The thin-wall nickel-200 tubing was composed of 99.5 wt. % Ni, with small amounts of iron and manganese. Dimensions of the tubes were 17-7/8 inch length by 3/8-inch O.D., with wall thickness reduced from 0.035-inch to 0.017-inch to a point approximately one inch from each end. Samples of finely porous nickel-molybdenum and cobalt-molybdenum tubing were fabricated at Oak Ridge National Laboratory from micron-range powders by flame spraying on a mandrel, followed by high-temperature sintering to densities in excess of 95% of the natural density. The dimensions after sintering were 16.5-inches length, 0.181-inches I.D., and 0.396-inches O.D. The total length was 21-inches after brazing on nickel tips for ease of mounting in the reactor.

Catalyst tube permeability measurements were made by determining the hydrogen flow from the shell side through the permeable tubing by the wet test meter connected to the tube side of the reactor.

The internal surfaces of all catalyst tubes were coated with a metal sulfide layer by passage of a 50% hydrogen sulfide and 50% hydrogen mixture through the tube for four hours at a catalyst tube temperature of 400°C. After sulfiding, the entire reactor system was cooled to 100°C, purged with nitrogen to remove all traces of hydrogen sulfide.

Hydrogenation of liquid feed was accomplished by pumping the feed at a predetermined rate up through the catalyst tube to react with hydrogen diffusing from the shell through the catalyst tube wall. Experimental runs were made at catalyst tube temperatures from 250°C to 450°C and shell side pressures of 655 psig hydrogen to 1510 psig hydrogen. Hydrogen pressures inside the tube varied from 650 psig to 1,495 psig. Temperatures inside the tube were determined with a thermocouple in an axially positioned well.

Analyses

The identities of the metal sulfides were determined by x-ray diffraction analysis, while the compositions of the liquid feeds and liquid products, and the composition of the gaseous products, were determined by gas chromatography/mass spectrometry, and gas chromatography. Other analyses were employed, as required. The hydrogen permeability values for nickel metal are known (2).

DISCUSSION OF RESULTS

Thin Wall Nickel Tubing Reactors

1. Runs with Tar Oil in Ni Tubes. X-ray diffraction analyses of the various samples of sulfided nickel tubing showed that in each instance the coating on the inner wall consisted of a mixture of Ni_3S_4 and Ni_3S_2 . The latter compound, nickel subsulfide, was very likely the only form present soon after the start of each hydrogenation run. According to Weisser and Landa (3) all nickel sulfides are rapidly converted to the subsulfide by hydrogen in any use of the sulfides for hydrogenation reactions. In any event, a large amount of Ni_3S_2 was observed for both the fresh and used tubing. Weisser and Landa also describe the use of nickel subsulfide as a catalyst for hydrogenation, including the hydrogenolysis of thiophene-type compounds. That the Ni_3S_2

present was actually functioning as a catalyst was demonstrated by the decreases in the amounts of six major components of the feed, and the increases in the amounts of eleven probable product compounds, as shown in Table 2 for runs 1 through 5, according to the conditions shown in Table 1. The reactants, R, and probable products, P, are arranged into four groups, following the possible reaction mechanisms shown in Figure 1. The reaction intermediates, indicated in Figure 1 by brackets, were not detected. All other compounds shown were identified, and their amounts determined, by combined gas chromatography and mass spectrometry. The observed m/e values are given in Table 2, along with the number of millimoles of each compound per 100 g sample, and the change in millimoles per 100 g sample in going from the feed to the product. No benzothiophene was added to the feed in run 4.

Most of the possible reaction mechanisms shown in Figure 1 for the thin-wall nickel tubing reactors have been studied in depth by other researchers under various conditions other than with nickel subsulfide catalyst. Qader and Hill (4) have shown the sequence naphthalene \rightarrow tetralin \rightarrow methylindan \rightarrow indan \rightarrow alkylbenzene. Penninger and Slotboom (5) have further detailed the steps leading from tetralin to alkylbenzenes. Rollman (6) has defined the steps in the conversion of benzothiophene to alkylbenzene, as have Furinsky and Amberg (7). Oltay *et al.* (8) have shown the steps in the conversion of 2-methylnaphthalene to tetralin and alkylbenzene as have Qader *et al.* (9). The two conversion sequences: 1) phenanthrene \rightarrow dihydrophenanthrene \rightarrow ethylbiphenyl \rightarrow biphenyl; 2) phenanthrene \rightarrow tetrahydrophenanthrene \rightarrow alkylnaphthalene \rightarrow tetralin have been detailed by Wu and Haynes (10). The sequence fluorene \rightarrow methylbiphenyl \rightarrow biphenyl has been shown by Oltay *et al.* in a second paper (11), as well as Penninger and Slotboom (5).

The hydrogen permeable catalyst tube in run 2, which was regenerated with air oxidation after being used in run 1, and then resulfided, showed the greatest activity of the five tubes used. The lowest activity was shown for the tube in run 1, lower than the tubes used in runs 4 and 5, which were not presulfided with the $H_2 + H_2S$ mixture. In these latter two runs a more effective nickel subsulfide coating was obtained by the reaction of the organic sulfur compounds present in the tar oil (0.64 weight percent sulfur), and the reaction of the benzothiophene added to the tar oil feed. The small amount of sulfur in the tar oil was as effective in run 4 as was the much larger amount of benzothiophene added to the tar oil in run 5. The used tubes from all runs did not have any noticeable carbon deposits, even after 13 hours operation. The relatively low operating temperature of 400°C was probably helpful in this regard, and it seems reasonable to assume that the cleansing action of the diffusing hydrogen, as described by Rudd (1), was operative. Only small amounts of hydrocarbon gases were detected in the gas in the tubing, indicating that limited cracking has occurred, whether hydrocracking or thermal cracking. Typical concentrations observed were 0.14 volume percent methane and 0.03 volume percent ethane, the remainder being the hydrogen required to maintain the 1,000 psig tube-side pressure.

2. Runs with Pure Compounds in Ni Tubes. A series of six test runs (runs 6 through 11) on the hydrogen permeability of thin wall nickel-200 tubing at various temperatures and differential pressures, and on the degree of hydrogenation of four different pure polycyclic aromatic compounds used as model compounds was likewise conducted. The hydrogen diffusivities were measured from the shell side to the inner tubing side over the shell to tubing pressure differential range of 300 to 1,700 psig, and temperatures of 400° and 450°. At both temperatures the amount of hydrogen diffusing through the wall at a Δp of 300 psig was essentially zero. The H_2 flow through the wall increased rapidly with increasing Δp , leveling off at about 0.45 liters/hr at 400°C and 1,500 psig Δp , and about 0.65 liters/hr at 450°C and 1,700 psig Δp .

The inside of the nickel tubing was sulfided by reacting at 400°C with about 8 cu. ft. of a 50-50 mixture of hydrogen sulfide and hydrogen. X-ray diffraction analysis showed the principal component to be nickel subsulfide. The inner surface was covered with a very rough texture of tiny, dark grey crystallites of this

material. There was no significant decrease in hydrogen permeability after sulfiding. Benzothiophene was added to all liquid feeds in order to ensure maintenance of this sulfided surface. SEM analysis gave 0.2 μm as a typical crystallite size.

Phenylcyclohexane was chosen as the solvent for the model compounds because of its presumed relative inertness and because it is a liquid at room temperature. Runs were made with about 5 to about 13 weight percent of each of the four model compounds dissolved in this solvent. The Δp was 700 or 750 psig, with the inner tube pressure about 1,000 psig. Temperatures of 290, 340, 400 and 450°C were used, generally with a feed residence time of about 1 hour, and usually somewhat less than the stoichiometric hydrogen required for complete hydrogenation of the components present. Table 3 shows the results for gas chromatographic analyses of the products. There was a general trend to greater hydrogenation with higher temperature and longer residence time, as would be expected.

Porous Nickel-Molybdenum Reactors

1. Runs with Pure Compounds in Ni-Mo Tubes. The run conditions are summarized in Table 4 for the Ni-Mo tubing reactors. The results for the gas chromatographic analysis of the receiver product for runs 12 and 13 with pure compounds are shown in Table 5. At low hydrogen pressure (650 psig) inside the tubing, with about 4.5 psig differential pressure for diffusing the hydrogen through the pores of the tubing from the shell side, there was substantial reaction of the phenanthrene (45% conversion) and the benzothiophene (27% conversion). Biphenyl in the product probably came from hydrogenolysis of dihydrophenanthrene. The alkylbenzenes came in part from the phenanthrene and benzothiophene but probably also from hydrogenolysis of the solvent, phenylcyclohexane. High yields of alkylbenzenes were obtained in the thin-wall nickel tube runs in the absence of phenylcyclohexane (Table 2). At the higher hydrogen pressure (1,350 psig) enough of the intermediate di- and tetrahydrophenanthrenes were produced to be detected, and the amount of biphenyl increased. The apparent increase in the amounts of phenanthrene and benzothiophene was due to loss of volatiles, probably mostly benzene, as shown by the unexpectedly low yield of this product. As will be seen for the results from the comparable runs at these pressures with tar oil as feed, the most reasonable estimate is that the amount of conversion was doubled upon doubling the pressure, as indicated by the yields of toluene, xylenes, and biphenyl.

In two runs with pure compounds, designated 13-S and 14-S, at the run conditions shown for runs 13 and 14 in Table 4, product from the top (exit) end of the catalyst tube drained down the outside of the tube into the cold lower portion of the pressurized shell, from which it was drained at the conclusion of the run, rather than from the product receiver. It was observed in these runs under these particular operating conditions there was even greater conversion to benzene, alkylbenzenes, and biphenyl. The dihydrophenanthrene was largely converted to biphenyl under these conditions, but in so doing the intermediate methylbiphenyl was produced in large enough amount for detection. The amount of conversion was increased upon decreasing the LHSV from 20.0 to 13.3, i.e., upon increasing the residence time from 3.0 to 4.5 minutes, as indicated by the yields of toluene, xylenes, and biphenyl. The production of naphthalene in this run would indicate the formation of the intermediate tetrahydrophenanthrene, but none could be detected.

2. Runs with Tar Oil Feed in Ni-Mo Tubes. The results for the gas chromatographic analysis of the receiver product for runs 15 and 16 with coal tar creosote oil feeds are shown in Table 6. In run 15 considerable total hydrogen sulfide was evolved, showing that the 0.6 wt. % sulfur in the feed was insufficient to maintain a heavy sulfide coating inside the nickel-molybdenum tubing. This was probably because the hydrogen permeability of the Ni-Mo tubing was so high as indicated by the pressure differentials of only 5 to 10 psig (Table 4), compared to 700 psig for the thin-wall nickel tubing (Table 1). Nevertheless, a significant conversion of various feed components was observed. MoS_2 , molybdenum disulfide, a known hydrogenation catalyst,

was present in the Ni-Mo tube, as well as Ni_3S_2 . The presence of $MoNi_4$ alloy was also shown.

Analysis of the product gas from run 15 showed 0.29 vol. % hydrogen sulfide, whereas the gas from run 16 had no detectable H_2S , showing that the metal sulfide layer had stabilized with the small sulfur content of the feed. The hydrocarbon in largest quantity in the gas from run 15 was propane at 0.14 vol. %. This would seem to indicate hydrocracking of the saturated rings of hexahydropyrene to yield propane and naphthalene, or propane, ethane, and methyl-naphthalene. Table 6 shows that the primary product was methyl-naphthalene in run 15. The product gas from run 16 showed methane at 2.67 vol. %, and ethane at 0.26 vol. % to be the hydrocarbon gases in the largest quantities. This would seem to indicate hydrocracking of the saturated rings of tetrahydroacenaphthene to produce these gases and alkylbenzenes. Table 6 shows that the primary reactant was acenaphthene, with tetrahydroacenaphthene and alkylbenzene the major products.

These possible reaction mechanisms, and others, are shown in Figure 2. The hydrogenated derivatives of pyrene and fluoranthene could not be detected, and so are shown in brackets. However, tetrahydroacenaphthene (Table 6), dihydrophenanthrene (Table 5), and tetrahydrophenanthrene (Table 5) were all found in significant quantities when using the porous nickel-molybdenum tubing reactors. The only reasonable source for the pentane found by GC would be the hydrocracking of phenylcyclohexane. Qader and Hill (4) have shown the sequence pyrene \rightarrow hydroxyrenes \rightarrow naphthalenes \rightarrow tetralin \rightarrow benzenes. As mentioned previously, Wu and Haynes (10) have outlined the two conversion sequences for phenanthrene. Fluoranthene also has the sequence leading to tetrahydrofluoranthene and then, by hydrocracking, to methylbiphenyl.

Porous Cobalt-Molybdenum Reactors

Runs were made using the porous cobalt-molybdenum tubing fabricated at ORNL and pure compounds (phenanthrene and benzothiophene) dissolved in phenylcyclohexane. The inner surface of the tubing was sulfided before use in the same manner as for the nickel-molybdenum tubing. The operating conditions and the results for gas chromatographic analysis of the products, are summarized in Table 7.

The respective run numbers, weight of feed material (g), pump rate (g/hr), and total run time (hr) were: 17, 32.82, 45, 2.00; 18, 189.4, 50.49, 2.25; 19, 239.2, 26.3, 2.50. The hydrogen flows for the Co-Mo reactors were very similar to those for the Ni-Mo reactors, the respective run numbers, average hydrogen flow (l/hr), and total hydrogen flow (l) being: 17, 4.7, 9.4; 18, 7.2, 16.3; 19, 5.64, 14.1.

A comparison of the results for the porous Ni-Mo reactors in Table 5 with those for the porous Co-Mo reactors in Table 7 shows that the reactions of the pure compounds were similar, but the sulfided Co-Mo appeared to have a little greater activity than the sulfided Ni-Mo, at the same approximate temperature and pressure, for the production of dihydrophenanthrene and its hydrocracking products, dimethylbiphenyl, methylbiphenyl, and biphenyl, and the production of tetrahydrophenanthrene, and its cracking product, naphthalene.

Hydrogen Permeability

It was not possible to measure hydrogen permeability of thin-wall nickel tubing during a run, because of the relatively low rate of hydrogen flow, and permeabilities had to be measured beforehand with the empty tubing, making hydrogen stoichiometry calculations difficult. However, direct hydrogen flow measurements could be made during the runs with the porous nickel-molybdenum tubing (Table 4) for comparison with the amounts required for any presumed set of hydrogenation reactions. Neglecting certain reactions, such as the hydrocracking of the phenylcyclohexane solvent, from 54 to 89% of the available hydrogen was consumed in the pure compound runs, and 85

to 90% in the tar oil runs. When estimations are allowed for these neglected reactions, it appears that essentially all hydrogen was consumed except that required to maintain pressure on the inside of the tubing. The high hydrogen flow rates with the porous Ni-Mo tubing allowed economically low feed residence times of only 3.0 to 12.6 minutes. A similar situation existed for the Co-Mo tubing.

As long as hydrogen flow was maintained through the tubing wall, there was never any indication of carbon deposits, even after many hours use on successive runs. However, in one instance, at the termination of run 16 at 400°C, the pressure differential of 10 psig H₂ from the shell-side to the tubing-side was lost, allowing the tar oil feed to penetrate the pores under conditions of poor contact with hydrogen. A heavy carbonaceous deposit was produced, typical of extensive cracking.

ACKNOWLEDGEMENTS

The authors wish to thank Richard L. Heestand, Metals Processing Laboratory, Oak Ridge National Laboratory, for the fabrication of the porous Ni-Mo and Co-Mo tubes, Robert E. Lynch for conducting the hydrogen permeable catalyst runs, Margaret H. Mazza for the X-ray diffraction analyses of the catalytic coatings, Clyde C. Kyle for the gas chromatographic analyses of the liquid feeds and products, and Derry A. Green for scanning electron microscope analyses.

REFERENCES

1. Rudd, David W., "Apparatus for Use in Effecting Chemical Reactions," U.S. Patent 3,210, 162, Oct. 2, 1965.
2. International Critical Tables, Vol. 5, p. 76, McGraw-Hill Book Co., Inc., NY, 1933.
3. Weisser, Otto, and Stanislav Landa, "Sulfide Catalysts, Their Properties and Applications," Pergamon Press, NY, 1973.
4. Qader, S.A., and G.R. Hill, "Development of Catalysts for the Hydrocracking of Polynuclear Aromatic Hydrocarbons," Amer. Chem. Soc., Div. Fuel Chem. Prepr. 1972, vol. 16, no. 2, pp. 93-106.
5. Penninger, Johannes M.L., and Hendrik W. Slotboom, "Mechanism and Kinetics of the Thermal Hydrocracking of Single Polyaromatic Compounds," Chap. 25 in "Industrial and Laboratory Pyrolysis," L.F. Albright and B.L. Crynes, eds., ACS Symposium Series 32, Amer. Chem. Soc., Washington, DC, 1976, pp. 444-456.
6. Rollman, Louis D., "Competitive Hydrogenation of Model Heterocycles and Polynuclear Aromatics," Amer. Chem. Soc., Div. Fuel Chem. Prepr. 1976, vol. 21, no. 7, pp. 59-66.
7. Furimsky, E. and C.H. Amberg, "The Catalytic Hydrodesulfurization of Thiophenes. VIII. Benzo thiophene and 2,3-Dihydrobenzothiophene," Can. J. Chem., vol. 54, no. 10, 1507-1511 (1976).
8. Oltay, Ernst, Johannes M.L. Penninger, and Peter G.J. Koopman, "Thermal High-Pressure Hydrogenolysis of 2-Methylnaphthalene," *Chimia*, vol. 27, no. 6, 318-19 (1973).
9. Qader, S.A., L. Chun Chen, and D.B. McOmber, "Hydrocracking of Polynuclear Aromatic Hydrocarbons over Mordenite Catalysts," Amer. Chem. Soc., Div. Petrol. Chem. Prepr. 1973, vol. 18, no. 1, pp. 60-71.
10. Wu, Wen-Lung and H.W. Haynes, Jr., "Hydrocracking Condensed-Ring Aromatics Over Nonacidic Catalysts," Chap. 4 in "Hydrocracking and Hydrotreating," J.W. Ward and S.A. Qader, eds., ACS Symposium Series 20, Amer. Chem. Soc., Washington, DC, 1975, pp. 65-81.
11. Oltay, Ernst, Johannes M.L. Penninger, and Willem A.N. Konter, "Thermal High Pressure Hydrogenolysis. II. The Thermal High Pressure Hydrocracking of Fluorene," *J. Appl. Chem. Biotechnol.*, vol. 23, 573-579, 1973.

TABLE 1. Operating Conditions for Thin-Wall Nickel Tubing Hydrogen Permeable Catalyst Reactors

Hydrogenation Run No.	1	2	3	4	5
H ₂ Permeability of Cat. Tube - 700 psig Diff. @ 400°C, cc/min	0.77	0.72	0.68	1.83	1.83
Dry Air Oxidation of Catalyst Surface	Non Oxidized	Oxidized 4 Hrs. @ 400°C	Non Oxidized	Non Oxidized	Non Oxidized
Sulfiding Conditions - Internal Surface of Tube	50% H ₂ + 50% H ₂ S 4 Hrs. @ 400°C	50% H ₂ + 50% H ₂ S 4 Hrs. @ 400°C	50% H ₂ + 50% H ₂ S 4 Hrs. @ 400°C	Non Sulfided by Feed Oil	Non Sulfided at Start of Run
H ₂ Permeability of Cat. Tube - 700 psig, 400°C after sulfiding, cc/min	0.79	0.93	0.57	1.83	1.83
Feed Raw Material	Clean Reilly Tar Oil + Benzothio- phenone	Clean Reilly Tar Oil + Benzothio- phenone	Clean Reilly Tar Oil + Benzothio- phenone	Clean Reilly Tar Oil	Benzothio- phenone Mod- ified Reilly Tar Oil
Wt. of Feed Material, g	151.80	131.89	146.76	142.00	187
Pump Rate, cc/hr	7.04	10.65	8.90	15.33	11.49
Catalyst Tube Temperature °C	400	400	400	400	400
Pressure Differential (shell to tube) psig - H ₂	700	700	700	700	700
Tube Side Pressure, psig	1,000	1,000	1,000	1,000	1,000
Residence Time in Catalyst Tube, Hrs.	2.87	1.90	2.27	1.32	1.62
LHSV	0.35	0.53	0.44	0.76	0.62
Total Run Time, Hrs.	12.27	9.0	12.0	9.33	13.08

TABLE 2. Amounts of Reactant and Product Compounds in Feed Oil and Product from Ni Hydrogen Permeable Catalyst Tube; 400°C; 1,000 psig Tube Side

COMPOUND	m/e	Millimoles/100 GRAMS										
		Feed Oil + Benzothiophene	Run 1 Product 0.35 ^a	Change ²	Run 2 Product 0.53 ^a	Change	Run 3 Product 0.44 ^a	Change	Run 4 Product 0.76 ^a	Change	Run 5 Product 0.62 ^a	Change
Naphthalene (R) ¹	128	46.8	37.5	- 9.1	34.06	-12.74	35.00	-11.8	34.37	-18.47	32.19	-14.61
1-Benzothiophene (R)	134	90.3	8.95	-81.3	8.13	-82.17	8.20	-82.10	0.0	0.0	7.68	-82.62
Benzene (P)	78	0.0	0.26	+ 0.26	3.46	+ 3.46	0.89	+ 0.89	1.41	+ 1.41	1.79	+ 1.79
Toluene (P)	92	0.54	2.06	+ 1.52	13.47	+12.93	3.04	+ 2.50	5.65	+ 5.11	7.17	+ 6.63
Xylenes & Ethylbenzene (P)	106	0.0	2.17	+ 2.17	2.73	+ 2.73	3.11	+ 3.11	2.83	+ 2.83	2.45	+ 2.45
Trimethylbenzenes (P)	120	0.08	2.75	+ 2.67	1.83	+ 1.75	1.91	+ 1.83	1.83	+ 1.74	1.58	+ 1.50
2-Methylnaphthalene (R)	142	37.6	25.5	-12.1	24.64	-12.96	22.11	-15.49	21.05	-21.34	22.60	-15.00
Ethylindan (P)	146	0.0	2.39	+ 2.39	2.19	+ 2.19	2.53	+ 2.53	2.67	+ 2.67	2.26	+ 2.26
Indan (P)	118	2.54	3.60	+ 1.06	4.41	+ 1.87	3.05	+ 0.51	3.64	+ 0.77	3.64	+ 1.10
Acenaphthene (R)	154	49.0	33.11	-15.9	30.84	-18.16	27.53	-21.47	29.09	-26.28	29.67	-19.33
Ethyl-naphthalenes (P)	156	4.67	9.20	+ 4.53	10.77	+ 6.1	10.12	+ 5.45	9.23	+ 3.96	10.00	+ 5.33
Dimethylnaphthalenes (P)	156	17.1	22.8	+ 5.70	25.32	+ 8.22	26.79	+ 9.69	25.00	+ 5.68	23.78	+ 6.68
Fluorene (R)	166	36.9	28.2	- 8.70	26.44	-10.46	24.39	-12.51	24.75	-16.94	25.96	-10.94
Phenanthrene (R)	178	90.7	47.8	-42.9	41.23	-49.47	35.88	-54.82	37.75	-64.74	40.56	+50.14
Methylbiphenyls (P)	168	3.33	13.1	+ 9.77	17.79	+14.46	17.62	+14.29	14.46	+10.7	16.72	+13.39
Biphenyl (P)	154	8.31	12.3	+ 3.99	13.31	+ 5.0	13.11	+ 4.8	12.46	+ 3.07	12.59	+ 4.28

¹R = Reactant, P = Product

²+ = Increase, Feed to Product; - = Decrease, Feed to Product

³1-Benzothiophene Free Reilly Tar Oil Feed Used In Run 4

⁴LHSV (Liquid Hourly Space Velocity)

TABLE 3. Reaction of Diffused Hydrogen with Pure Compounds in Thin Wall Ni Tubing with Ni₃S₂ Coating, about 1,000 PSIG

Solvent = Phenylcyclohexane

Run No.	Temp., °C	LHSV	Compound	Weight %		
				Feed	Product	Hydrogenated
6	290	1.0	Benzothiophene	5.74	4.68	19
7	290	1.0	Phenanthrene	7.58	6.36	16
			Benzothiophene	6.22	5.11	18
8	290	1.0	Acenaphthene	7.67	4.98	35
			Benzothiophene	6.25	5.63	10
9	340	1.0	Fluorene	7.79	5.13	21
			Benzothiophene	6.09	5.30	13
10	400	1.2	Phenanthrene	12.97	7.70	41
			Benzothiophene	7.06	4.79	32
11	450	0.51	Phenanthrene	5.21	2.62	50
			Benzothiophene	5.10	2.23	56

TABLE 4. Operating Conditions for Porous Nickel-Molybdenum Tubing Hydrogen Permeable Catalyst Reactors at 400°C

Run No.	12	13	14	15	16
Sulfiding Conditions, Internal Surface	50% H ₂ + 50% H ₂ S, 4 hours at 400°C, total gas flow = 8 feet ³				
Feed Material	Phenylcyclohexane, Phenanthrene Benzothiophene (various proportions)			Filtered Reilly Tar Oil	
Wt. of Feed Material, g	150.0	160.1	205.2	267.7	114.4
Pump Rate, g/hr	56.2	64.0	41.0	48.6	57.2
Total Run Time, hrs	1.63	1.25	1.5	1.9	2.0
Residence Time in Catalyst Tubing, min	3.0	3.0	4.5	12.6	10.2
Pressure Inside Tubing, psig	650	1,350	1,350	767	1,380
Pressure Differential (shell to tubing), psig	4.5	10.0	10.0	8.5	10.0
Hydrogen Flow, liters/hr	6.26	5.56	4.50	5.40	5.10

TABLE 5. Reaction of Pure Compounds at 400°C with Hydrogen Diffusing Through Porous Nickel-Molybdenum Tubing with a Sulfided Inner Wall

Feed: 4.52 wt. % benzothiophene
10.17 wt. % phenanthrene
(solvent: phenylcyclohexane)

Run No.	Receiver Product, Wt. %	
	12	13
Pressure, psig	650	1350
LHSV	20.0	20.0
Benzene	16.56	0.69
Toluene	0.63	1.49
Xylenes	1.77	3.33
Trimethylbenzenes	0.06	0.97
Biphenyl	0.58	1.28
Dihydrophenanthrene	0.00	2.26
Tetrahydrophenanthrene	0.00	1.09
Phenanthrene	5.60	12.03 ¹
Benzothiophene	3.29	7.97 ¹

¹High, due to loss of volatiles, mostly benzene.

TABLE 6. Reaction of Coal Tar Creosote Oil at 400°C with Hydrogen Diffusing Through Porous Nickel-Molybdenum Tubing with Sulfided Inner Wall

Run No.	Composition, Weight %					
	15			16		
LHSV	4.8			5.9		
Pressure, psig	767			1,380		
Reactants	Feed	Receiver Product	Decrease	Feed	Receiver Product	Decrease
Acenaphthene	8.61	8.45	0.16	8.23	4.03	4.20
Phenanthrenes ¹	20.01	19.06	0.95	20.77	18.44	2.33
Pyrene	6.68	4.30	2.38	5.59	3.52	2.07
Fluoranthene	5.83	4.81	1.02	5.99	4.09	1.90
Total			4.51			10.50
Products	Increase			Increase		
Benzene	0.00	0.21	0.21	0.00	1.52	1.52
Toluene	0.10	0.10	0.00	0.33	2.22	1.89
Xylenes	0.16	0.20	0.04	0.21	2.03	1.82
Indan	1.23	1.57	0.34	1.99	3.06	1.07
Tetralin	1.15	1.60	0.45	1.45	2.15	0.70
Methylnaphthalenes	11.70	14.56	2.86	9.29	10.91	1.62
Tetrahydroacenaphthene	0.00	0.34	0.34	0.00	1.85	1.85
Total			4.24			10.47

¹Phenanthrene plus methylphenanthrenes.

TABLE 7. Reaction of Pure Compounds with Hydrogen
Diffusing Through Porous Cobalt-Molybdenum
Tubing with Sulfided Inner Wall

Solvent = Phenylcyclohexane

Run No.	17	18	19
Temp., °C	350	400	400
Pressure inside tube, psig	750	728	1,495
Pressure, diff- erential, psig	20	9.0	7.0
Residence time, min.	11.4	10.2	19.2
LHSV	5.3	5.9	3.1

Composition, Weight %

	Feed	Product	Feed	Product	Feed	Product
Pentane	0.00	0.00	0.00	2.73	0.00	0.00
Benzene	0.64	6.91	0.60	7.54	1.75	0.03
Toluene	0.00	0.02	0.00	4.73	0.00	0.08
Xylenes	0.00	1.93	0.00	6.36	0.00	1.74
Trimethylbenzenes	0.00	0.00	0.00	1.13	0.00	0.59
Naphthalene	0.00	0.62	0.00	4.68	0.00	2.20
Biphenyl	0.00	0.00	0.00	3.46	0.00	4.49
Methylbiphenyl	0.00	0.00	0.00	0.00	0.00	0.99
Dimethylbiphenyl	0.00	0.00	0.00	0.00	0.00	1.12
Dihydrophenanthrene	0.00	0.00	0.00	0.05	0.00	5.97
Tetrahydrophenanthrene	0.00	0.00	0.00	0.00	0.00	2.08
Phenanthrene	11.82	5.05 ¹	12.12	5.70 ¹	13.28	23.74 ¹
Benzothiophene	4.42	4.42 ¹	4.51	5.40 ¹	5.27	5.28 ¹

¹High, due to loss of volatiles, primarily pentane and benzene.

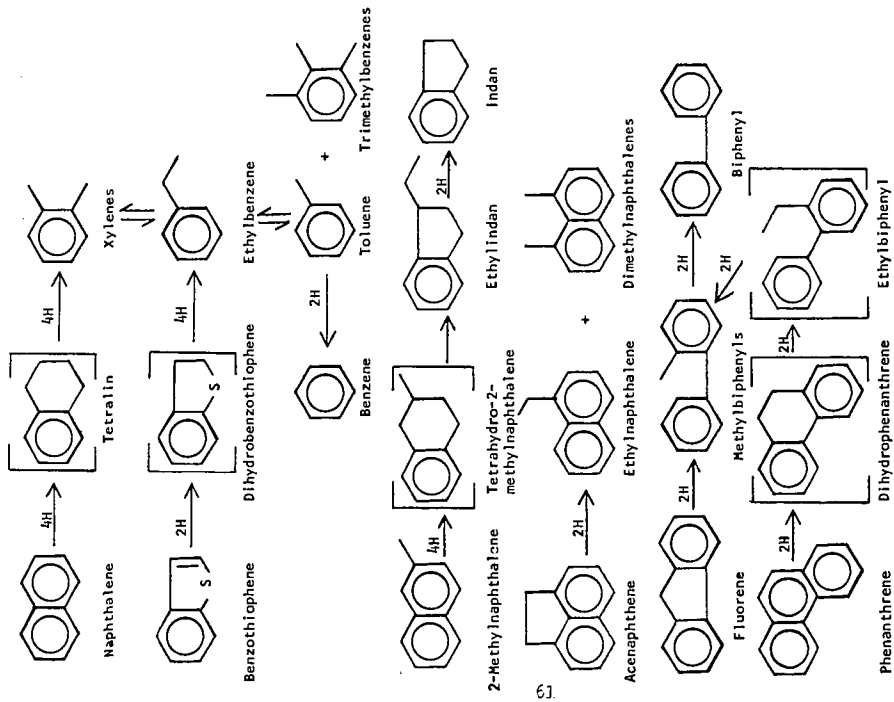


Figure 1. Possible Reaction Mechanisms Involved in Hydrogenation of Tar Oil with Nickel Sulfide Catalyst at 1,000 psig and 400°C

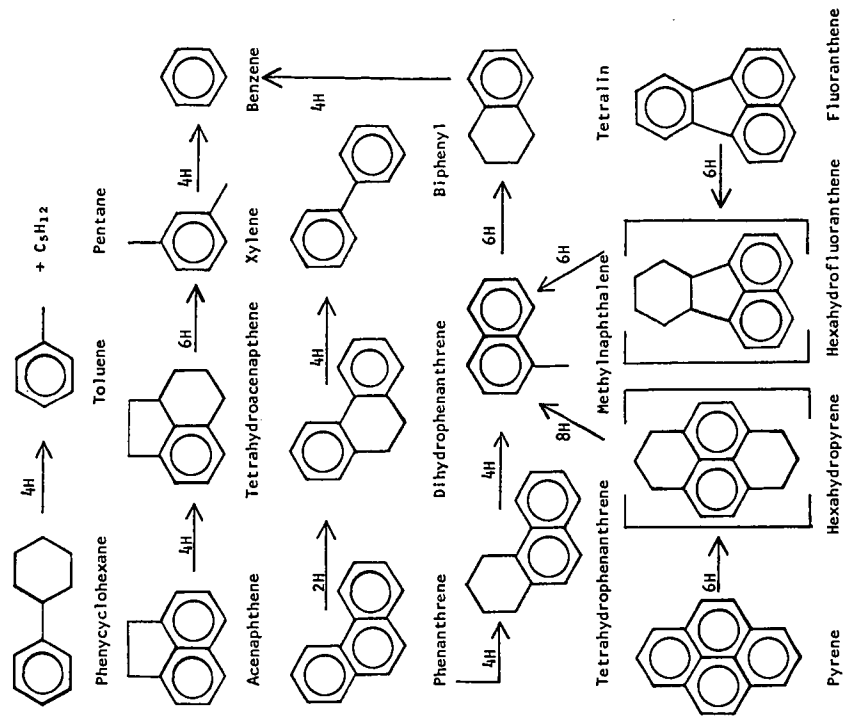


Figure 2. Possible Reaction Mechanisms Involved in Hydrogenation with Sulfided Nickel-Molybdenum at 400°C and 650 to 1,400 psig

CATALYTIC HYDROLIQUEFACTION OF COALS FOR HYDROCARBON-TYPE ANALYSIS IN RELATION TO REFINING

by

W. C. Lanning, J. B. Green, and J. E. Dooley
Department of Energy, Bartlesville Energy Research Center
P. O. Box 1398, Bartlesville, Oklahoma 74003

INTRODUCTION

Small samples of liquids have been prepared from several coals of widely varied rank by catalytic hydrogenation in a batch autoclave. The liquids were prepared at conditions designed to minimize cracking of hydrocarbon components, yet were upgraded to remove nitrogen and to permit detailed determination of hydrocarbon types potentially obtainable for refining. This paper covers the preparation and properties of the liquids; the hydrocarbon analyses will be reported later.

Scattered literature references indicate that the complexity of hydrocarbon groups in coals and in liquefaction products varies substantially with the rank or grade of coal liquefied. Reports of early German technology refer repeatedly to the liquefaction of brown coal (lignite) at about half the hydrogenation pressure required for bituminous coals (9). The asphaltene content of recycled oil in continuous hydrogenation of German coals decreased with decreasing grade of coal and reached an apparent minimum in the range of sub-bituminous coals. Although there were gaps in the data, this trend, combined with greater rates of hydrogenation observed for the product oils, indicated smaller polynuclear hydrocarbon units as well as different chemical structure in brown coals in comparison with bituminous coals. The greater reactivity was also associated with increased oxygen content. Wender (8) suggested that hydrocarbon groups in coal can vary from those which contain little more than one aromatic ring, as in lignite, to virtually one huge fused-ring aromatic in anthracite coal. However, most coal liquefaction research in this country has been done on bituminous coals. U.S. Bureau of Mines work in the 1940 era recognized the greater reactivity of lower-rank coals and the importance of catalysts in promoting formation of hydroaromatic compounds that function as hydrogen donors in liquefaction (6). In fact, low-rank coals were so reactive that high hydrogen pressure was required to avoid repolymerization of reactive fragments to coke at the temperatures used, generally about 430° C. However, almost complete liquefaction and extensive oxygen removal could be obtained at relatively low temperature and with relatively little hydrogen consumption (but with hydrogen transfer from solvent). The rate of conversion of Pittsburgh bituminous-A coal to asphaltenes was considerably greater than conversion of the asphaltenes to oil, while the opposite was true for coal of bituminous-C rank from Rock Springs, WY (9). The wt-pct yield of total oil increased with rank of coal from about 55 for lignite to 65 for sub-bituminous to 70-75 for high-volatile bituminous coal on a moisture- and ash-free (maf) basis. Yields were much less for still higher-rank medium-volatile coals because of low reactivity. These trends were observed in both batch autoclave and continuous-flow units with stannous sulfide catalyst. Characterization of the liquid products was limited to distillate fractions, usually a small part of the product, which were determined to be highly cyclic and aromatic. Phenolics content was greater in distillates from coal of lower rank.

Among more recent studies, the effluent from liquefaction of a Utah sub-bituminous coal with hydrogen donor solvent (3) contained less benzene insoluble material than that from Pittsburgh bituminous coal, and addition of a paraffinic diluent was required to precipitate enough asphaltenes for agglomeration of residual solid particles. Other sub-bituminous coal products behaved similarly. In reports of the HRI, Inc., H-Coal process (7) and the Gulf Science and Technology Co. CCL (catalytic coal liquefaction) process (4), syncrudes produced from sub-bituminous coals contained less heavy ends and less polynuclear aromatics with 4 or more rings. An extensive survey of coals

with respect to liquefaction by hydrogenation (1) confirmed early reports that high volatile bituminous coals gave the best yields, but the products were not characterized in any detail.

EXPERIMENTAL

Materials

Table 1 shows analyses of the coal samples used. The analyses were run by the U.S. Bureau of Mines, Pittsburgh, PA. The lignite was supplied by the Grand Forks, ND, Energy Research Center, the Wyodak coal by Hydrocarbon Research, Inc., Trenton, NJ, and the other four samples by Conoco Coal Development Co., Library, PA. Those samples not already pulverized were ground and screened to -50 mesh. The lignite and Wyodak coal samples were dried under vacuum and kept under nitrogen thereafter. The others were used as received. Note that the nitrogen content of the bituminous coals was about 50 percent greater than that of the sub-bituminous coals and lignite. Indicated oxygen content of the dry coals increased from about 8 to 19 wt pct as the rank or grade decreased. The W. Kentucky coal had a high sulfur content of 4.3 wt pct.

TABLE 1. - Analyses of Coals

Source	PA-WV	Illinois	W. KY	Montana	Wyoming	N. Dakota
Seam	Pittsburgh	No. 6	--	(Colstrip)	(Wyodak)	Beulah Std. II
Rank	hvb A	hvb B or C	hvb B or C	sub-bit. A	sub-bit. C	Lignite
Proximate analysis (as received)						
Moisture	1.7	7.8	2.9	4.2	10.9	28.0
Volatile matter	35.9	34.2	38.4	34.4	39.5	31.0
Fixed carbon	55.1	51.4	48.8	48.5	42.7	33.3
Ash	7.3	6.6	9.9	12.9	6.9	7.7
Ultimate analysis (moisture free)						
Hydrogen	5.1	4.9	4.9	4.3	4.8	4.5
Carbon	76.9	75.2	70.2	65.2	66.8	63.5
Nitrogen	1.5	1.6	1.4	0.6	1.0	0.9
Sulfur	1.6	1.5	4.3	1.8	0.5	1.3
Oxygen (difference)	7.6	9.7	8.8	14.5	19.2	19.1
Ash	7.4	7.1	10.2	13.5	7.8	10.7

Nickel-molybdenum/alumina hydrotreating catalyst, American Cyanamid HDS-3A, was crushed, screened to 60-100 mesh, and dried overnight at 200° C. Elemental sulfur was added in liquefaction runs to provide some sulfiding of the catalyst. For upgrading the crude liquids, the catalyst was presulfided in the autoclave as a slurry in n-octane plus carbon disulfide, 400 psig added hydrogen, and at 285° C maximum temperature. The diluent was flashed off at 225° C to insure elimination of water.

The initial solvent for each preparation was 99 percent tetralin from the Aldrich Chemical Co.

Procedure

Both liquefaction and upgrading runs were made in a 2-liter Magnedrive autoclave from Autoclave Engineers, Inc. A typical liquefaction charge was 325 - 400 g coal, 500 g solvent, 50 g catalyst, and 4 g sulfur. The charged reactor was purged with nitrogen and hydrogen, pressured with hydrogen to about 1,500 psig, leak tested, and heated to 300° C in about one hour. The temperature was then raised slowly over a period of several hours, depending upon the rate and extent of hydrogen consumption, to a maximum of 400° C. Cylinder hydrogen was boosted to about 3,300 psig with a Whitey compressor, and it was added periodically to the reactor from a calibrated surge volume to maintain reactor pressure between about 2,450 and 2,700 psig. At the end of a run the reactor was cooled rapidly to 260° C, and nearly all the gaseous components were bled off to remove water and some light ends. The effluent gas passed through a condenser and ice-cooled trap, a scrubber column filled with 1/4-inch screen saddle-type packing, and a second ice-cooled trap, after which it was sampled and metered. The top section of the packed column was heated to break the fog which passed the first trap. The product slurry, cooled to about 70° C, was removed from the reactor by suction through a dip tube and was filtered through Whatman No. 41 paper in a heated Buchner funnel, at 50 - 60° C. Filtered liquid product was used as diluent for the following run. The filter cake was washed with benzene at 50° C and dried to determine residual solids. Runs were repeated until the calculated tetralin content of the recycled liquid was less than 6 wt pct, and then were continued to accumulate at least 1,200 g of crude liquid (including benzene washings and light ends). The reactor was flushed with hot benzene only at the end of a series, since complete recovery from single runs was not essential. The reactor was opened occasionally to inspect for accumulated deposits, which generally were insignificant.

The crude liquids were upgraded in similar autoclave runs to remove heteroatoms, especially nitrogen. A typical charge was 100 g presulfided catalyst and 850 g crude liquid.

Effluent gases were analyzed by gas chromatography. Hydrogen consumption was taken as the difference between that charged and withdrawn. No attempt was made to account for sulfur, nitrogen, or oxygen, although water recovery was nearly quantitative in later runs. Overall material balances were calculated, recognizing the limitations of the procedures used, but the objective was to obtain liquids which contained most of the hydrocarbons potentially obtainable from the coal, not to provide quantitative process data.

The upgraded liquids were vacuum distilled in a Perkin-Elmer spinning band column to an overhead temperature of 425° C, corrected to atmospheric pressure. Asphaltenes were removed from the > 425° C residuum by pentane precipitation (5), and the asphaltene-free residuum was then vacuum flashed at 540° C, corrected to atmospheric pressure.

RESULTS

The results of the liquefaction experiments are summarized in Table 2. The data for each coal are a composite of those for successive batches from which product liquid was retained. Total products accounted for varied from 90 to 105 wt pct of coal charged. The variations reflected mostly uncertainty in reactor holdup at the start of product accumulation, incomplete recovery of water and possibly removal of sulfur from W. Kentucky coal. Net yields of liquid varied from 69 wt pct from Illinois coal to 55 wt pct from lignite. The yields of C₁ - C₄ light gases decreased and that of CO₂ increased as the rank of coal decreased. Hydrogen consumption increased by about 15 percent as the rank of coal decreased, with the exception of Pittsburgh coal to be noted later. The reaction times briefly summarized in Table 2 show that the major part of the reaction was at temperatures less than 375° C, except for Pittsburgh coal, and that less total time was required to yield a readily filterable product slurry from the lower-rank coals.

TABLE 2. - Batch Liquefaction of Coals
2,450-2,800 psig, NiMo Catalyst

Coal	Pittsburgh	Ill. No. 6	W. Ky.	Colstrip	Wyodak	Lignite
Wt-pct of coal charge:						
Net liquid	66	69	62	58	60	55
Gas: C ₁ - C ₄	5.8	5.0	5.2	3.2	4.2	4.2
C ₅ +	2.8	0.9	1.0	1.3	2.2	2.2
CO ₂	0.1	0.5	0.7	3.2	5.6	5.6
Residual solids	19	19	18	32	21	20
Total products	101	97	90	104	106	102
H ₂ consumed	4.3	4.0	4.0	4.4	4.8	4.6
Reaction time, hrs. at °C:						
325 - 375	5.2	7.6	10.3	6.8	6.8	5.6
376 - 400	<u>5.2</u>	<u>2.6</u>	<u>2.0</u>	<u>2.1</u>	<u>1.9</u>	<u>1.6</u>
Total	10.4	10.2	12.3	8.9	8.7	7.2

Most of the hydrogen consumption also occurred at less than 375° C, again with the exception of Pittsburgh coal.

Averaged temperature-time curves for the liquefaction reactions are shown in Figure 1. Temperatures were increased as needed to maintain a suitable rate of hydrogen consumption. The maximum temperature was set at 400° C to minimize hydrocarbon cracking, except for an initial preparation from Illinois coal for which data are not included. Temperatures up to 415° C were used in that series, and yields of methane increased significantly. The bituminous coals showed no substantial consumption of hydrogen, as indicated by pressure decrease, at less than about 350° C. Pittsburgh coal was the least reactive, with the indicated rate of hydrogen consumption being about half that of the other bituminous coals and one-third that of the lower-rank coals. To overcome this, maximum reactor pressure for Pittsburgh coal was increased to 2,800 psig. Coupled with less production of water, this resulted in sharply increased partial pressure of hydrogen in the reactor. Reaction rates actually increased as the series progressed, in contrast to behavior of the other coals. This improved rate was attributed to the formation of hydroaromatics of higher molecular weight which were better hydrogen donor solvents than the tetralin used as starting solvent. Hydrogen consumption by the sub-bituminous coals and lignite began at 325° C or less, as reflected in the curves of Figure 1, and most of the hydrogen was consumed at less than 350° C. In fact, too rapid an increase in reaction temperature for these coals resulted in an overall decrease in hydrogen consumption and a viscous product which was difficult to handle. Reaction temperature was still programmed to 400° C, however, for increased heteroatom removal from the liquid and resultant molecular weight decrease.

The results of upgrading the crude coal liquids by similar batch hydrogenations with pre-sulfided catalyst are summarized in Table 3. Results for the Wyodak coal were not complete when the manuscript was submitted. The objective was to decrease nitrogen content of the liquids to 0.2 to 0.3 wt pct with a minimum of cracking of hydrocarbons. The ratio of oil to catalyst in the autoclave was far greater than in a typical trickle-flow operation over fixed-bed catalyst, by a factor of up to 50-fold. Thus, longer reaction time was required, and

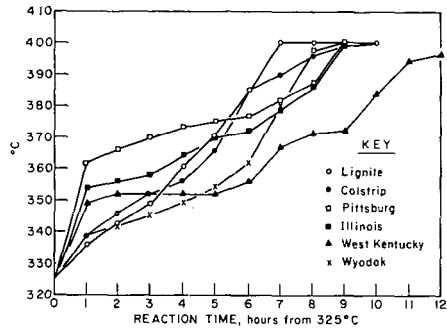


FIGURE 1 LIQUEFACTION OF COALS

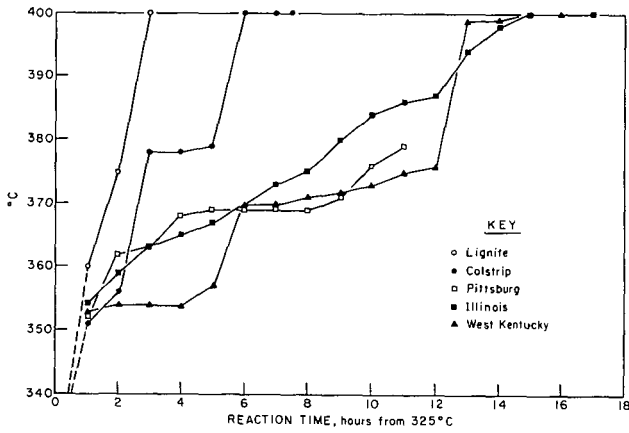


FIGURE 2 UPGRADING OF COAL LIQUIDS

TABLE 3. - Upgrading Coal Liquids
2,450 - 2,650 psig, NiMo Catalyst (Presulfided)

Coal	Pittsburgh	Ill. No. 6	W. Ky.	Colstrip	Lignite
Wt-pct of charge:					
Liquid product	92	92	92	93	95
Gas: C ₁ - C ₄	0.3	1.8	2.0	0.8	0.3
C ₅ +	1.0	0.8	0.8	0.2	0.9
Total products	95	97	97	97	98
H ₂ consumed	1.0	2.3	2.3	1.6	0.9
Reaction time, hrs. at °C:					
325 - 375	9.8	8.7	12.7	4.7	2.0
376 - 400	<u>0.9</u>	<u>9.3</u>	<u>6.4</u>	<u>2.9</u>	<u>0.7</u>
Total	10.7	18.0	19.1	7.6	2.7

increased temperature could not be substituted for time without increased cracking of hydrocarbons originally present. The liquids from Illinois and W. Kentucky coals required up to 19 hours reaction time; however, even in those runs over 60 percent of the hydrogen was consumed at less than 375° C. Much shorter reaction times were required for upgrading the liquids from lower-rank coals and lignite. Recovery of upgraded liquid was 92 to 95 wt pct of the charge, not including C₅+ material in the effluent gas. Hydrogen consumptions and yields of gaseous hydrocarbons were small, except for the two liquids which required extended reaction. Temperature-time curves for the upgrading are shown in Figure 2. No appreciable hydrogenation occurred at less than 350° C, and reactions of all except the Pittsburgh liquid were programmed to 400° C. The Pittsburgh run was cut short when that liquid was found to have been substantially upgraded during the liquefaction as previously noted.

Properties and some elemental analyses of the crude and upgraded liquids are given in Table 4. Nitrogen content of the crude liquids from bituminous coals was 1.1 to 1.3 wt pct, compared to 0.4 to 0.6 wt pct in those from lower-rank coals. The exception, again, was that from Pittsburgh coal, for which more hydrogenation during liquefaction had decreased nitrogen content to 0.4 wt pct. Oxygen content in several of the crude liquids, determined by neutron activation analysis, was 1.3 to 2.1 wt pct. Nitrogen content of all the upgraded liquids was decreased to about the same level, in the range of 0.2 to 0.3 wt pct. Sulfur content was, of course, small in all cases. The upgraded liquid from Pittsburgh coal was the most viscous, but differences were small since the extent of upgrading was controlled to bring all liquids to the same nitrogen content. Pour points of the upgraded liquids varied from less than 5° F for liquids from bituminous coals to +45° F for that from lignite, reflecting increased paraffin content in the latter. However, a few percent of waxy n-paraffins can increase pour point sharply.

Distributions of the upgraded liquids by distillation and asphaltene content are shown in Table 5. Asphaltene contents were in the range of 4.7 to 6.8 wt pct and, thus, correlated well with nitrogen contents to indicate that all liquids had been brought to a similar level of upgrading to a predominantly hydrocarbon product. The distribution by boiling range was similar for all the liquids. This may be surprising in view of the greater reactivity of the lower-rank coals, but relatively little upgrading of the crude liquid was required in those cases.

TABLE 4. - Properties of Crude and Upgraded Coal Liquids

Coal	Pittsburgh	Ill. No. 6	W. Ky.	Colstrip	Lignite
Crude liquid:					
Nitrogen, wt-pct	0.44	1.10	1.28	0.64	0.43
Oxygen, wt-pct	-	1.34	2.09	1.61	-
Upgraded liquid:					
Specific gravity, 60/60° F	0.99	0.99	0.99	0.99	0.98
SSU vis. @ 100° F	441	126	89	263	181
Pour point, ° F	+5	<5	<5	+20	+45
Carbon, wt-pct	89.2	88.6	88.2	88.1	89.0
Hydrogen, wt-pct	10.8	10.3	10.7	10.6	10.8
Sulfur, wt-pct	<.01	.02	.02	<.01	<.01
Nitrogen, wt-pct	.20	.25	.29	.19	.25
Oxygen, wt-pct	-	.19	.32	.32	-

TABLE 5. - Distribution of Upgraded Coal Liquids

Coal	Pittsburgh	Ill. No. 6	W. Ky.	Colstrip	Lignite
Distillation, wt-pct					
<200° C	10.0	11.4	16.6	11.5	12.3
200 - 325° C	21.7	27.9	26.1	21.5	24.0
325 - 425° C	20.3	22.5	22.8	21.1	20.7
425 - 540° C*	26.6	23.7	19.7	21.0	21.0
>540° C*	16.2	7.5	9.3	18.3	15.0
Asphaltenes	4.7	6.8	5.2	6.6	6.7

*Asphaltenes removed from > 425° C resid.

Table 6 gives the specific gravities and nitrogen contents of the distillation fractions. The trends are as expected, with nitrogen concentration greatest in the residuum.

DISCUSSION

The results reported here indicate that a wide variety of coals can be liquefied by catalytic hydrogenation at conditions which permit recovery of most of the hydrocarbons potentially obtainable from a given coal. By control of the extent of upgrading of the crude product, liquids of which about 90 percent can be analyzed for hydrocarbon type have been prepared. Such analyses will provide information on the effect of coal source on the character of potential feedstocks for production of refined fuels. Differences in the required extent of upgrading of the crude liquids may have decreased the spread in complexity of hydrocarbon types recovered, but in view of the relatively low reaction temperatures used and the small yields of gaseous hydrocarbons, not much

TABLE 6. - Distillation Fractions of Upgraded Liquids

Coal	Pittsburgh	Ill. No. 6	W. Ky.	Colstrip	Lignite
<200° C distillate:					
Specific gravity	0.829	0.827	0.832	0.822	0.822
Nitrogen, wt-pct	.003	.001	.096	.023	.007
200 - 325° C distillate:					
Specific gravity	.915	.926	.919	.918	.916
Nitrogen, wt-pct	.016	.021	.062	.030	.104
325 - 425° C distillate:					
Specific gravity	.983	1.001	.993	.982	.983
Nitrogen, wt-pct	.076	.159	.200	.119	.304
425 - 540° C distillate:*					
Specific gravity	1.045	1.061	1.049	1.032	1.032
Nitrogen, wt-pct	.272	0.415	0.415	0.233	0.412
>425° C resid.					
Sulfur, wt-pct	<.01	<.01	.04	.02	<.01
Nitrogen, wt-pct	.37	.56	.57	.33	.50
Asphaltenes, wt-pct	9.9	17.9	15.3	14.3	15.7

*Asphaltenes removed

cracking of heavier hydrocarbons should have occurred. The reaction conditions used for lignite, for example, could not have been applied to Illinois coal to recover any substantial part of the hydrocarbons for analysis. On the other hand, a crude liquid from one of the low-rank coals could be upgraded on the same temperature-time program as was used for Illinois coal, and this is planned.

The upgraded coal liquids described in this paper are being analyzed in detail for hydrocarbon-type composition by methods developed for petroleum and adapted to the analysis of synthetic crude oils (2). The results will be reported later when completed.

ACKNOWLEDGEMENT

We are indebted to Dr. F. W. Steffgen and associates of the Pittsburgh Energy Research Center, DOE, for advice on autoclave techniques and handling of liquid products from coal. We also thank Jane Thomson for assistance in preparation of the liquid samples.

REFERENCES

1. Danis, A., et al. The Influence of the Properties of Coals on Their Conversion into Clean Fuels. ACS Div. Petrol. Chem. Preprints, v. 19, No. 3, 1974, pp. 461-484.

2. Dooley, J. E., and C. J. Thompson. The Analysis of Liquids from Coal Conversion Processes. ACS Div. Fuel Chem. Preprints, v. 21, No. 5, 1976, pp. 243-251.
3. Gorin, E., et al. Deashing of Coal Liquefaction Products Via Partial Deasphalting. Part I. ACS Div. Fuel Chem. Preprints, v. 20, No. 1, 1975, pp. 79-104.
4. Malone, H. P. The Characterization and Upgrading of Coal Liquids to High Value Fuels and Chemicals. ACS Div. Fuel Chem. Preprints, v. 20, No. 1, 1975, p. 142. (Manuscript supplied by author.)
5. Mima, M. J., et al. Method for the Determination of Benzene Insolubles, Asphaltenes, and Oils in Coal-Derived Liquids. PERC/RI-76/6, 1976, 15 pp.
6. Storch, H. H., et al. Hydrogenation and Liquefaction of Coal, Part IV. U.S. BuMines Tech. Paper 654, 1943, 50 pp.
7. Johnson, C. A., et al. Present Status of the H-Coal Process. Symposium on Clean Fuels from Coal, Illinois Inst. of Technology, September 1973, pp. 549-575. .
8. Wender, I. Catalytic Synthesis of Chemicals from Coal. ACS Div. Fuel Chem. Preprints, v. 20, No. 4, 1975, pp. 16-30.
9. Wu, W. R. K., and H. H. Storch. Hydrogenation of Coal and Tar. U.S. BuMines Bull. 633, 1968, 195 pp.

STANNOUS CHLORIDE AND COBALT MOLYBDATE-ALUMINA CATALYSTS
IN HYDROGENOLYSIS OF SOLVENT REFINED COAL

David C. Lovetro and Sol W. Weller*

Department of Chemical Engineering
State University of New York at Buffalo
Buffalo, New York 14214

Abstract

The relative effectiveness of SnCl_2 and $\text{Co/Mo/Al}_2\text{O}_3$ (silica-stabilized) for the hydrogenolysis of solvent-refined coal was studied in a batch autoclave with tetralin as solvent. SnCl_2 was exceptional in higher H_2 consumption, higher liquefaction, and higher ratio of low molecular weight products in the oil fraction than either $\text{Co/Mo/Al}_2\text{O}_3$ or in catalyst-free tests. Discrimination between catalysts with respect to S elimination was difficult because of the low S content of SRC; however, the effectiveness with respect to both N and O elimination decreased in the order $\text{SnCl}_2 > \text{No Catalyst} > \text{Co/Mo/Al}_2\text{O}_3$. Oil production was also lower with $\text{Co/Mo/Al}_2\text{O}_3$ than with no catalyst, an effect which may be due to the SiO_2 present as a stabilizer in the support Al_2O_3 . The results are consistent with the concept that coal ash catalyzes the difficult step of converting asphaltene to oil.

Introduction

One of the intriguing aspects of catalytic coal liquefaction-hydrodesulfurization is that multifunctional catalysts are desirable, as is also true in the well-known cases of naphtha reforming and of hydrocracking in petroleum refining. Most of the individual catalysts best studied in coal processing are at least bifunctional, although this aspect has not received much explicit attention. The role of SnCl_2 (or $\text{Sn} + \text{HCl}$, or $\text{Sn} + \text{NH}_4\text{Cl}$) in coal liquefaction is still not understood after some decades of study, but clearly the catalyst exercises cracking as well as hydrogenative functions. The catalysts consisting of "cobalt molybdate" supported on silica-stabilized alumina are acidic, whatever their detailed action may be in the hydrodesulfurization of coal or coal-derived liquids.

It is an interesting fact that the best catalyst for liquefaction of coal is not best for hydrodesulfurization. The comprehensive catalyst survey of Kawa et al. (1974) provides a recent illustration. Supported SnCl_2 , even in small concentration, was outstanding in its ability to promote both total liquefaction and the production of benzene-soluble oil, but not in desulfurization. Supported "cobalt molybdate" was equally outstanding in giving products of low S content, but not in liquefaction.

The study of catalysts for coal hydrogenolysis is essential, but the catalytic effects of coal ash itself may confound the interpretation of the effects of added catalysts. There is some advantage, therefore, in studying

added catalysts for the hydrogenolysis of solvent-refined coal (SRC) rather than of coal itself. SRC is essentially ash-free.

The present limited study was intended to explore what seem to be extreme cases of catalytic action, with the use of SRC as feed. The study is a comparison of (a) no catalyst, (b) unsupported SnCl_2 at low concentration, and (c) a commercial $\text{Co/Mo/SiO}_2\text{-Al}_2\text{O}_3$ at low concentration. In some ways SRC is a reasonable "model compound" with which to study the difficult steps in coal-to-oil conversion free of the complication of intrinsic catalyst (ash). The sample of SRC was almost completely soluble in pyridine, in Soxhlet extraction; only 17% soluble in either benzene or toluene; and almost insoluble in n-pentane (< 2%). The difficult steps of converting pyridine-solubles to "asphaltene" and "oil", as well as of hydrodesulfurization, may therefore be followed conveniently with SRC as feed.

Experimental

Equipment

All autoclave experiments were conducted with the same 1- $\frac{1}{2}$ stirred autoclave (Autoclave Engineers Model MB-1005 Magnedash) used in the work of Yen et al. (1976). As in the earlier studies, a glass liner was used in the autoclave to eliminate possible catalyst "memory effects". The following changes were made in equipment used for product analyses:

1. At the conclusion of a run, after cooldown, autoclave gas was passed through 2N zinc acetate solution (rather than caustic) in the scrubbing bottles, to remove H_2S and permit subsequent analysis of H_2S by an iodometric method.
2. After the scrubbing bottles, the autoclave gas was passed through an on-line gas chromatograph (Perkin-Elmer Model 810) for analysis of light hydrocarbons. The column was 7 ft. x 1/8 inch Porapak Q, operated at 80°C.; flow rate of the He carrier was 45 ml./min.
3. Analysis of the "oil" samples was performed with a Varian Aerograph gas chromatograph, Model 1420, equipped with 5 ft. x 1/8 inch columns packed with 1.5% OV-101 on 100/120 Chromosorb G-H.P., with a helium carrier flow rate of 25 ml./min. The column was operated isothermally at 125°C. for the first 3 minutes after sample injection, after which the column temperature was increased from 125°C. to (a maximum of) 270°C. at the programmed rate of 15°C./min. The G.C. data were processed with a Varian CDS-111 Data System and visually displayed on a Leeds and Northrup Azar recorder.

Materials

The solvent-refined coal used in this work was obtained, through the courtesy of Mr. E.L. Hoffman, from the pilot plant operated in Wilsonville, Alabama by Southern Services, Inc. Our material, said to have been made from

Kentucky No. 14 coal, has the following elemental analysis: 86.77% C, 6.0% H, 1.3% N, 0.7% S, and 5.3% O (by difference). These values are close to, but differ slightly from, "typical values" reported for the Wilsonville plant. Ash was about 0.2%.

The tin chloride used as catalyst was ACS grade $\text{SnCl}_2 \cdot 2\text{H}_2\text{O}$, obtained from Fisher Scientific Co. The $\text{Co/Mo/Al}_2\text{O}_3$ catalyst was Harshaw Type 0402T, containing approximately 15 wt.% MoO_3 and 3 wt.% CoO on silica-stabilized alumina (5% SiO_2). Its properties are given in greater detail in Yen et al. (1976).

Procedures

Procedures for the autoclave experiments were essentially the same as those used by Yen et al. (1976), except for the addition of a solid-state temperature controller (Barber-Colman Model 520) for the 2 kw. furnace. Internal temperatures were monitored by a chromel-alumel couple, inserted in the autoclave thermowell, connected to a millivolt potentiometer. Initial (cold) H_2 pressure was 1000 psig in all experiments. The autoclave "dasher" was operated during heatup and the reaction period of 1 hr. at 450°C. ($\pm 5^\circ\text{C}$.) at the constant frequency of 180 strokes per minute.

The procedures for analyzing the letdown gases at the conclusion of a run have been described above. A series of eight gas samples was taken during the letdown period for G.C. analysis; the analyses for any single run were integrated to obtain total gas composition.

After the autoclave was unsealed, the glass liner with its contents was removed for analysis. Some material, found outside the liner in the bottom of the autoclave, was removed by aspiration, collected, and weighed; it was denoted as "autoclave residue". Although the average amount of "autoclave residue" was approximately 14 wt.% of the total initial charge (75g. SRC + 300g. tetralin), it was not included in the mass balance or in the product separation scheme because of possible catalytic effects of the metal autoclave walls.

The separation scheme used for liquid and solid products is summarized in Figure 1. Distillations in Run 1 (see Table I) were performed at atmospheric pressure, as was done by Furlani et al. (1976). In all other runs, the distillations were generally conducted at 30-35 Torr. under a N_2 atmosphere. Separation of "asphaltols" (toluene-insoluble, pyridine-soluble material) was effected in only a few runs; the results are therefore not included in this paper. Occasionally naphthalene was observed to be condensing during the tetralin distillation. When this occurred, the vacuum distillation was carried to a vapor temperature somewhat in excess of 105°C., cooling water was drained from the condenser, and a heat gun was employed to drive the naphthalene into the tetralin distillate. The pot temperature was always kept below 250°C. in this distillation. Further details of the separation scheme are to be found in Lovetro (1977).

Analyses for C, H, and N were performed with a Perkin-Elmer Model 240 Analyzer in the Department of Chemistry of this university. Analyses for S were very kindly provided through the courtesy of the Hooker Chemical Co.

Results and Discussion

The catalysts used in the various autoclave runs are summarized in Table I. Also shown are the weights of H₂ consumed in each run, calculated by difference, and the weights of H₂S absorbed in the zinc acetate scrubbers.

Table I
Autoclave Tests: H₂ Consumed and H₂S Discharged*

Run No.	Catalyst	Hydrogen (g.)			H ₂ S
		Charged	Discharged	Consumed**	Discharged (g.)
1	None	3.56	2.43	1.13	0.0154
1A	None	4.44	3.42	1.02	0.0528
2	SnCl ₂ ***	4.45	Not detnd.	Not detnd.	0.0139
2A	SnCl ₂	4.53	2.78	1.75	0.0219
2B	SnCl ₂	4.53	2.71	1.82	0.0416
3	Co/Mo/Al ₂ O ₃ ****	4.43	3.43	1.00	0.0487
3A	Co/Mo/Al ₂ O ₃	4.49	3.31	1.18	0.0416

*75g. SRC + 300g. tetralin charged to glass liner.

**H₂ consumption by difference.

***1g. SnCl₂ · 2H₂O charged.

****1g. Harsshaw 0402T (Co/Mo/SiO₂-Al₂O₃) charged as 40-60 mesh particles.

There was considerable scatter in the H₂S data. However, the S measured as H₂S was in all cases less than 10% of that charged in the 75g. of SRC. Substantially more elimination of S actually occurred, based on the analyses of asphaltene and oil shown in Table II. Sulfur analyses of the toluene and tetralin distillates show the presence of small amounts of low-boiling sulfur compounds, and the "missing" S is probably to be accounted for in these cuts.

Of particular interest is the H₂ consumption in the run with SnCl₂ catalyst (Series 2). It was much higher than in the blank runs (Series 1) or in the runs with Co/Mo/Al₂O₃ (Series 3). This result may be correlated with the relatively poor material balances in the SnCl₂ runs (cf. Table IV, below) and with the relatively rich content of low-boiling constituents in the "oil" fraction from the SnCl₂ runs (cf. Figure 2, below).

The difference between average values for H₂S discharged, for the blank runs and for those with SnCl₂ or Co/Mo/Al₂O₃, was found by application of the "t" test to be significant only at the 80% level. Values for the weight of CH₄ discharged are not shown in Table I. These showed almost no variation, run to run, and the average value for CH₄ produced was about 1.7g. This corresponds to a conversion to CH₄ of about 2% of the carbon in the 75g. of SRC charged.

Table II contains the elemental analyses for the oil and asphaltene fractions from each run.

Table II
Elemental Analyses

Run No.	Product	Atom Ratio (H/C)	Wt. % C	Wt. % H	Wt. % N	Wt. % S	Wt. % O (by dif.)
Feed	--	0.83	86.66	5.99	1.33	0.70	5.32
SRC							
1	Oil	1.20	87.57	8.74	0.05	0.09	3.55
	Asphaltene	0.77	89.62	5.77	1.82	0.38	2.41
1A	Oil	1.11	88.32	8.20	0.24	0.27	2.97
	Asphaltene	0.87	88.28	6.38	1.82	0.41	3.11
2	Oil	1.10	88.58	8.10	0.63	0.26	2.43
	Asphaltene	0.87	89.87	6.52	0.73	0.37	2.51
2A	Oil	1.12	89.22	8.30	0.81	0.24	1.43
	Asphaltene	0.86	89.69	6.46	1.32	0.39	2.14
2B	Oil	1.08	88.97	8.02	2.38	< 0.15	~ 0.48
	Asphaltene	0.87	89.35	6.47	1.13	0.37	2.68
3	Oil	1.12	87.49	8.20	0.15	< 0.15	~ 4.01
	Asphaltene	0.88	88.28	6.49	1.70	0.40	3.13
3A	Oil	1.18	83.70	8.26	0.37	0.23	7.44
	Asphaltene	0.87	87.96	6.38	1.49	0.46	3.71

With the exception of Run 1, which involved distillations at atmospheric pressure, the H/C atom ratios were almost the same for all of the oil samples, and almost the same for all of the asphaltene samples. The S contents of all fractions were lower than that of the SRC feed, which occasions no surprise. Furthermore, within the limitations of the lower bound for the S analyses, all oil samples had approximately the same S content, as was also true for all asphaltene samples.

The interesting features of the elemental analyses relate to the questions of N elimination and of O elimination from the SRC as a function of catalyst. The average N elimination for Series 1 (blank) was 9%; for Series 2 (SnCl_2), 38%; and for Series 3 ($\text{Co/Mo/Al}_2\text{O}_3$), 1%. The rank ordering, therefore was $\text{SnCl}_2 \gg \text{No catalyst} > \text{Co/Mo/Al}_2\text{O}_3$ for effectiveness in N elimination. The average O elimination for Series 1 was 57%; for Series 2, 69%; and for Series 3, 42%. Again the rank ordering is $\text{SnCl}_2 > \text{No catalyst} > \text{Co/Mo/Al}_2\text{O}_3$.

Table III compares results reported by Yen et al. (1976) for the hydrogenolysis of Kentucky coal with those obtained in the present studies for the hydrogenolysis of SRC made from Kentucky coal. The same autoclave (Magdash) and conditions were used in both studies; tetralin was used as solvent in both cases; and the $\text{Co/Mo/Al}_2\text{O}_3$ catalyst was the same batch of Harshaw 0402T in both cases.

Table III
Comparison of Coal and SRC

Quantity	Coal*		SRC**	
	Blank Run	Co/Mo/Al ₂ O ₃	Blank Run	Co/Mo/Al ₂ O ₃
% S in Oil	0.25	0.21	0.18	<0.19
% S in Asphaltene	0.27	0.47	0.40	0.43
($\frac{\text{Oil}}{\text{Oil} + \text{Asphaltene}}$)	34	49	19	5

*Data from Yen et al. (1976). "Blank Run" = Run T-3; "Co/Mo/Al₂O₃" = Run T-4.

**Present work. Data given are average values for Runs 1 and 1A for "blank", Runs 3 and 3A for "Co/Mo/Al₂O₃"; see Table IV.

The S contents in both the oil and the asphaltene fractions were slightly lower in the SRC runs than in the corresponding fractions from whole coal. This is not surprising, of course, since the organic S of the coal is already significantly reduced in the process of making SRC. It is surprising that (1) the oil production in the SRC runs (cf. Table IV) was exceptionally low relative to the runs with whole coal, and (2) the oil production from SRC was even lower in the presence of Co/Mo/Al₂O₃ than with no catalyst. Two implications may be suggested:

1. The lower oil production from SRC is consistent with the notion, now generally accepted, that the ash in the coal is catalytically active and its removal is harmful (cf. "SRC I" vs. "SRC II" processes). This result is reminiscent of that reported by Weller and Pelipetz (1951). In the earlier work it was found that under identical experimental conditions with no added catalyst, whole Pittsburgh seam coal showed 50-60% conversion, whereas low-ash (1.4%) hand-picked anthraxylon from the same mine showed only 30% conversion. Since iron pyrite is so important an ash constituent in high-ash coals, this again is not surprising: (a) the commercial development of the Bergius process by I.G. Farbenindustrie included Luxmasse, a high-iron material, in the coal-oil paste; (b) impregnated iron sulfate is known to be an excellent catalyst for coal liquefaction (Weller and Pelipetz, 1951a).
2. The deleterious effect of Harshaw Co/Mo/Al₂O₃ on oil production from SRC, relative to no added catalyst, may reflect an undesired polymerization of feed or products occurring as a result of the acidic support (silica-stabilized alumina). Variation of the support acidity was not studied in the present work, but it should be examined.

Table IV summarizes the material balances, total "liquefaction", and the oil and asphaltene distributions for the individual runs.

Table IV

Product Distributions*

Run No.**	Total Products Recovered (g.)	% Liquefaction***	Oil, % of Total Products	Asphaltene, % of Total Products	$\frac{(\text{Oil}) \times 100}{(\text{Oil} + \text{Asphaltene})}$
1****	61.7	Not detnd.	22.1	77.4	22.2
1A	64.8	93.7	14.0	77.2	15.4
2	50.5	100.0	13.5	86.5	13.5
2A	56.3	99.6	21.8	77.5	22.0
2B	59.8	99.8	20.5	79.1	20.6
3	67.6	94.5	2.7	90.1	2.9
3A	69.9	94.1	5.9	87.2	6.3

*75g. SRC + 300g. tetralin charged in each run.

**See Table I for identification.

***% Liquefaction = $\frac{75 - \text{Toluene insolubles (including catalyst)}}{75} \times 100$

****Distillations in Run 1 made at atmospheric pressure. Vacuum distillation (30-35 Torr.) under N_2 used in all other runs.

Two points should be noted:

1. Although the liquefaction is high in all cases, it is highest in the $SnCl_2$ runs. (Note: Correction for the catalyst in the toluene insolubles would increase the % Liquefaction to 95.8% in Run 3 and 95.5% in Run 3A. The very small amount of toluene insolubles in Runs 2, 2A, and 2B means that the $SnCl_2$ has been somehow "solubilized"; it is not present in the toluene insolubles.)
2. Although the material balances are low in all cases, they are consistently lower in the $SnCl_2$ runs. The losses are tentatively attributed to low-boiling liquid products from the SRC which are lost to the overhead during the toluene and tetralin distillations. The particularly high losses in the $SnCl_2$ runs are consistent with (a) the higher H_2 consumptions observed in these runs (Table I), and (b) the evidence for many low-boiling constituents in the recovered oil fractions (cf. Figures 2 and 3, below). If this interpretation is correct, then the attribution of the "missing" material to distillation of low-boiling fractions of the oil product would mean that all the oil recoveries listed in Table IV may be lower than the true values. This would be particularly true for the $SnCl_2$ runs.

Figures 2 and 3 are illustrative of the gas chromatograms obtained on the oil fractions. Figure 2 is for the oil from Run 2A ($SnCl_2$); Figure 3 is for the oil from Run 3A ($Co/Mo/Al_2O_3$). In both cases there was some residual

(unstripped) solvent, typically a mixture of tetralin and naphthalene. In both cases there was a major, sharp peak with a retention time of 13.5 minutes (at 270°C.) in this temperature-programmed chromatogram. The identity of this component is unresolved. However, correlations of relative retention time vs. carbon number and vs. normal boiling point were used to predict that the 13.5 minute peak could correspond to a compound analogous to an alkane of carbon number C_{20} - C_{21} and a normal boiling point of ca. 365°C. The sharpness of the peak and the estimated carbon number make it tempting to attribute the peak to some dimeric (i.e., C_{20} , with $M \approx 260$) species originating from the tetralin solvent, and not from the SRC. Our determinations, by vapor-phase osmometry, of the molecular weight of the total oil fractions routinely showed an average molecular weight in the range 250-300. The rich mixture of peaks in the $SnCl_2$ run (Figure 2) between naphthalene and the "13.5 minute unknown" presumably represents low-boiling products in the oil, derived from the SRC with $SnCl_2$ catalyst. It is noteworthy that these peaks are almost absent in the $Co/Mo/Al_2O_3$ run (Figure 3). As pointed out above, the chromatogram shown in Figure 2 is consistent with the high H_2 consumption and the very low material balances when $SnCl_2$ is used. Oil constituents with retention times longer than 13.5 minutes at 270°C., the highest temperature chosen for use with the OV-101 columns, would not have been detected; the G.C. analysis was terminated at this point.

Acknowledgment

The authors are grateful to the Energy Research and Development Administration and to the Hooker Chemical Co. for partial support of this research. D. Elmore and M. LaRosa established the solubility of SRC in various solvents; Miss E. Rabcewicz and C. Orcheski measured the molecular weights of oil and asphaltene samples. P. Ho and J. Scinta provided continuous advice and assistance.

Literature Cited

- Kawa, W., Friedman, S., Wu, W.R.K., Frank, L.V., Yavorsky, P.M., 167th National Meeting of the American Chemical Society, Los Angeles, Calif., Mar. 31-Apr. 5, 1974.
- Lovetro, D.C., M.S. Thesis, Department of Chemical Engineering, State University of New York at Buffalo, April 1977.
- Weller, S., Pelipetz, M.G., Proc. 3rd World Petrol. Cong., Sect. IV, Subsect. 1, 91 (1951).
- Weller, S., Pelipetz, M.G., Ind. Eng. Chem. 43, 1243 (1951a).
- Yen, Y.K., Furlani, D.E., Weller, S.W., IEC Prod. Res. Dev. 15, 24 (1976).

Illustrations

Figure 1. Analytical Procedure

Figure 2. Chromatogram of Oil Fraction from Run 2A

Figure 3. Chromatogram of Oil Fraction from Run 3A

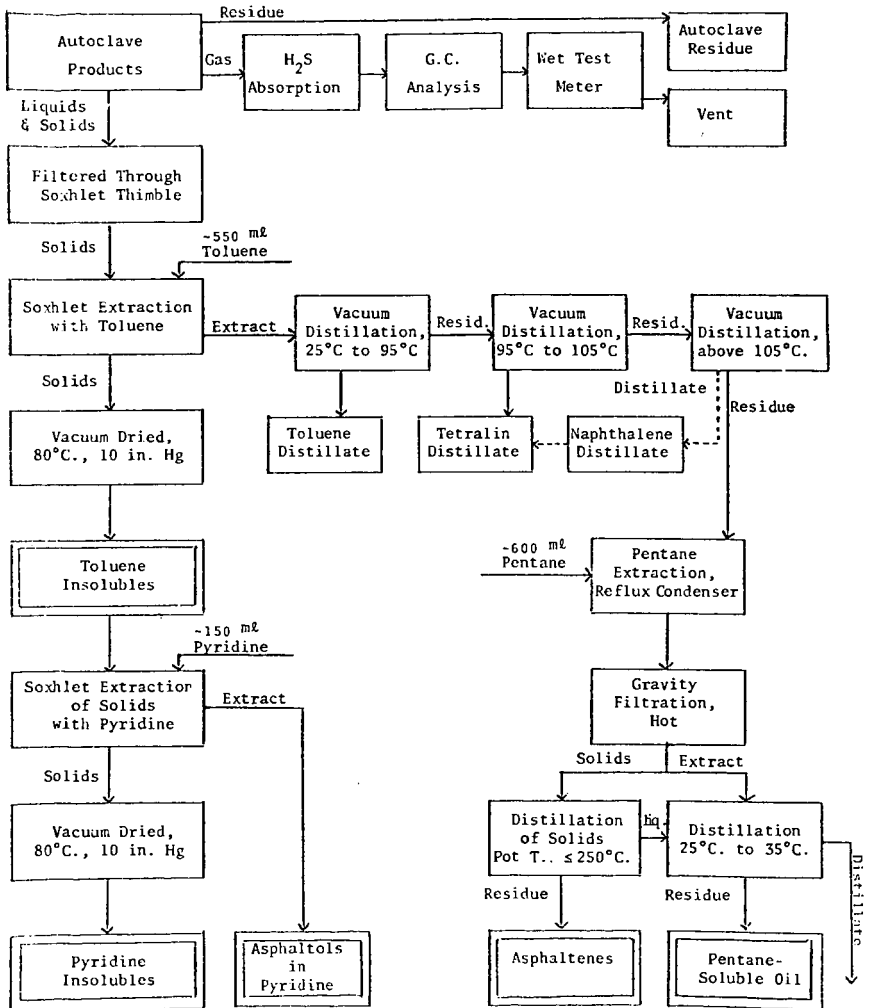


Figure 1. Analytical Procedure

Figure 2
SRC Run #2A Oil Fraction
(1 Time Unit = 0.5 Minutes)

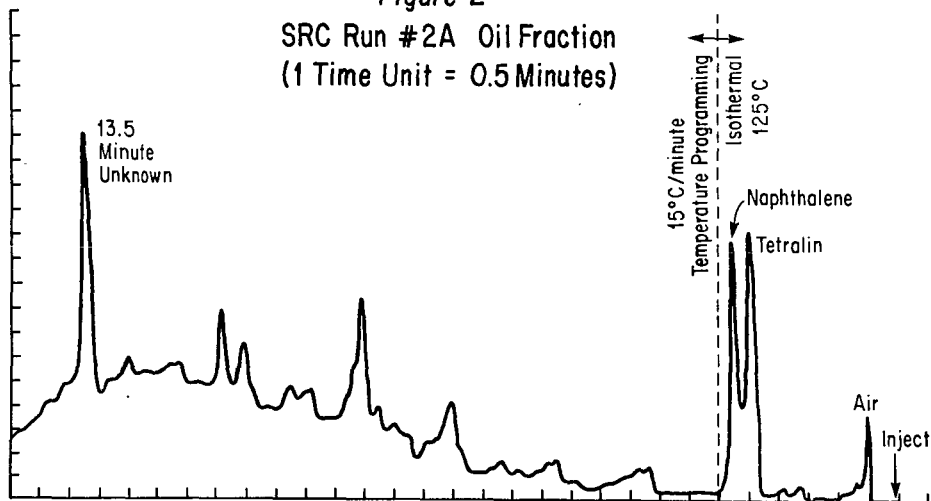
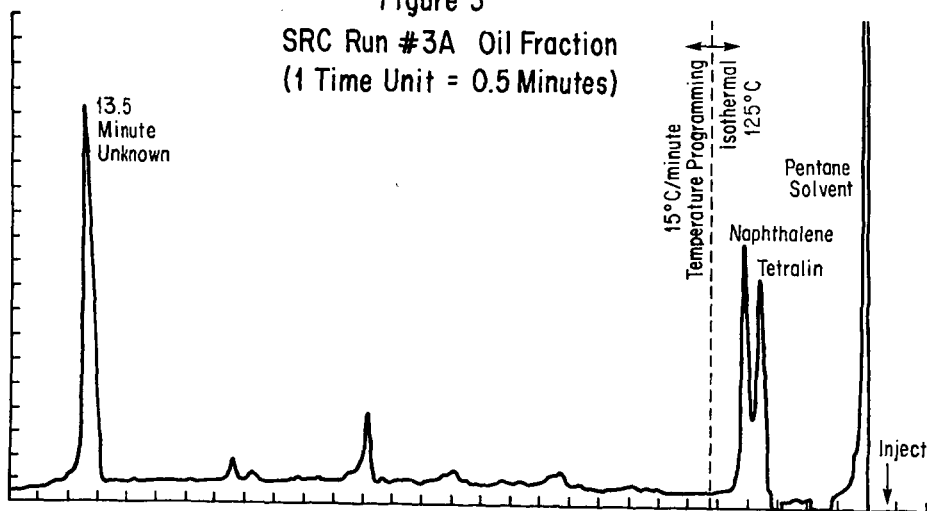


Figure 3
SRC Run #3A Oil Fraction
(1 Time Unit = 0.5 Minutes)



UPGRADING OF SOLVENT REFINED COAL

Yuan C. Fu, Rand F. Batchelder and John C. Winslow

Pittsburgh Energy Research Center
U. S. Department of Energy
4800 Forbes Avenue, Pittsburgh, Pennsylvania 15213

INTRODUCTION

Several coal liquefaction processes are being developed by various organizations. The initial objective appears to be the production of low-sulfur boiler fuels for power generation, but it is obvious that upgrading of these coal liquids will be necessary to make acceptable quality fuels for home, transportation, and industrial sectors of our economy. Studies have been conducted on the upgrading of coal-derived liquids, tar, and anthracene oil in the past. More recently, Eisen (1) hydrogenated syncrudes from a western Kentucky coal and a Utah coal in an attempt to prepare gas turbine engine fuel. Stein et al. (2) reported their exploratory studies on hydroprocessing of Solvent Refined Coal (SRC), H-Coal, and SYNTHOIL. Several institutions are also stepping up their activities in coal liquids upgrading, as evidenced by a recent symposium (3).

This report presents an evaluation study on hydroprocessing of a blend of 30 weight percent SRC and 70 weight percent SRC process solvent. It was chosen as the feed-stock, because in some respects it is typical of coal liquids such as SYNTHOIL or mixtures of atmospheric bottoms and vacuum bottoms of H-Coal. They have similar boiling point ranges and high percentages of asphaltenes, organic sulfur and nitrogen. The single-stage hydrotreating of the SRC liquid over conventional nickel-tungsten or nickel-molybdenum catalysts does not give very effective hydrogenation even under severe conditions, whereas the hydrogenation effect, as measured by the increase of H/C atomic ratio, N-removal, and S-removal, is substantially improved in the second-stage hydroprocessing of the hydrotreated SRC liquid.

EXPERIMENTAL

The hydroprocessing of coal liquid was studied in a 500-ml magnetically-stirred autoclave. A series of factorial experiments for single-stage hydrotreating of SRC liquid was conducted using Ni-W supported on silica-alumina (Harshaw Ni-4301E) as the catalyst. The feed was a blend of 30 parts SRC solid and 70 parts SRC solvent, with 5 parts of catalyst added per hundred parts of the feed. Ranges of conditions were: temperature 375°-475°C, initial H₂ pressure 600-1,800 psig (to give operating pressure 900-2,900 psig at reaction temperatures), and reaction time 1-4 hours. The autoclave was stirred at 600-700 rpm during the reaction. The reaction time was measured after the autoclave reached the reaction temperature in about 60-70 minutes, and the autoclave was quenched rapidly after the reaction by an internal water cooling coil. Total products were filtered to obtain liquid oils. Asphaltenes and benzene insolubles were determined according to procedures established by the Chemical and Instrumental Analysis Division of the Pittsburgh Energy Research Center (4). Boiling range distributions of selected oil products were obtained by gas chromatography (ASTM D2887). Gaseous products were analyzed by mass spectrometry.

Various commercial catalysts have been tested for comparison. Most catalysts, excepting ZnCl₂ and noble metal catalysts, were reduced, sulfided, and crushed to pass through a #60 mesh sieve prior to use.

For a two-stage hydroprocessing, the SRC blend was hydrotreated over a Ni-Mo catalyst (Nalco NM-504), in the first stage, in a 5-liter rocking autoclave. The product was then hydroprocessed over a Ni-W catalyst (Harshaw Ni-4301) in the 500-ml magnetically stirred autoclave. The experimental conditions are described further on.

RESULTS AND DISCUSSION

Single-Stage Hydrotreating. Table 1 shows the design and the results of a series of factorial experiments with three variables of temperature, initial H_2 pressure, and time at three levels. The experiments were carried out in random order. The feed was a blend of SRC solid and SRC process solvent (for the composite analyses, see Table 6), and the catalyst was Ni-W supported on silica-alumina (Harshaw Ni-4301E). The data analysis was made by computer, and the dependence of various measured characteristics (Y), such as conversion of pentane insolubles, C_1-C_4 hydrocarbon yield, S-reduction, N-reduction, oil viscosity, and H_2 consumption on processing variables (X) of pressure, temperature, and time was represented by the following quadratic polynomial

$$Y = \beta_0 + \sum \beta_{1i} X_i + \sum \beta_{ij} X_i^2 + \sum \beta_{ij} X_i X_j$$

The statistical significance of the regression coefficients (β) has been tested, and it was observed that, except for N-reduction and viscosity, most characteristics correlate well and pass the F-test for fit with 95% confidence. The quadratic approximation yielded plots showing the effects of initial H_2 pressure and temperature on the conversion of pentane insolubles (benzene insoluble + asphaltene) and on S-reduction in Figures 1 and 2, respectively.

Further, this equation can be used to represent characteristic response surfaces during an optimization analysis. The analysis is made by finding an optimum point over the response surface of the characteristic being optimized, while simultaneously keeping other characteristics within specified levels. The main objective of the coal liquids upgrading in the first stage of a two-stage concept is hydrodesulfurization and hydrodenitrogenation. These reactions can be better achieved at higher temperatures, but H_2 consumption and C_1-C_4 hydrocarbon formation could become uneconomically high. Table 2 shows the optimum conditions for (1) achieving a maximum S-reduction while limiting H_2 consumption to 2.8 weight percent (1740 scf/bbl) and C_1-C_4 yield to 5 weight percent,² (2) achieving a minimum C_1-C_4 hydrocarbon formation while realizing S-reduction of at least 80% and N-reduction of 35%, and (3) achieving a maximum conversion of pentane insolubles without any characteristic constraints. It appears that temperature is the controlling factor for achieving a desired optimum. Figure 3 shows the change of various characteristics with temperature at an optimum condition of 1,800 psi and 3.18 hours.

Elemental analyses were obtained for some selected oil products. In general, the hydrotreated products were not sufficiently rich in hydrogen, and N and O contents were still too high. The S-removal was relatively satisfactory. Figure 4 shows that the H/C ratio increases only from 0.92 to 1.1, regardless of the increase in H_2 consumption. It appears that, under severe conditions at high temperatures, additional H_2 is consumed in C_1-C_4 hydrocarbon gases formation. The decrease of the N/C ratio is only moderate with rising H_2 consumption.

Various hydroprocessing catalysts (Table 3) were evaluated at one standard set of conditions used in the factorial experiments. The results in Table 4 show that Ni-Mo type catalyst exhibited the best overall activity.

TABLE 1. Factorial experiments - hydrotreating SRC liquid with Ni-W catalyst

Controlled factors			Measured characteristics					
Pressure psi	Temp, °C	Time hr	Pentane insoluble conversion, wt %	C ₁ -C ₄ yield, wt %	% S reduction	% N reduction	Viscosity, cs at 60°C	H ₂ Consumed, wt %
600	375	2.5	10.2	0.6	40.9	9.8	113	0.43
1800	375	2.5	23.4	0.9	60.0	19.6	66	1.10
600	475	2.5	-65.6	12.7	63.5	21.0	65	1.16
1800	475	2.5	65.8	13.5	89.6	31.5	4.3	3.76
600	425	1	20.9	2.2	46.1	3.9	58	0.71
1800	425	1	48.6	2.3	72.2	21.7	18	1.69
600	425	4	4.6	6.7	53.0	5.6	33	1.11
1800	425	4	73.7	5.3	86.1	41.3	6.2	3.08
1200	375	1	-3.8	0.4	42.6	7.7	183	0.60
1200	475	1	1.5	10.3	61.7	10.5	45	1.85
1200	375	4	24.5	0.8	60.0	18.2	59	1.18
1200	475	4	8.9	14.8	77.4	23.8	37	2.94
1200	425	2.5	53.7	2.9	73.9	21.0	14	1.51
1200	425	2.5	45.0	3.6	68.7	22.4	14	1.73
1200	425	2.5	50.3	3.7	73.9	21.0	14	1.67

TABLE 2. Characteristic optimization

Factors	Value at maximum		Value at minimum		Value at maximum	
	% S-reduction	C ₁ -C ₄ yield	C ₁ -C ₄ yield	PI conversion	PI conversion	PI conversion
Pressure, psi	1800	1800	1800	1800	1800	1800
Temperature, °C	429.2	406.4	406.4	438.4	438.4	438.4
Time, hr	3.12	3.12	3.18	4	4	4
Characteristics						
S-reduction, %	86.4	80 ^a	80 ^a	88.8	88.8	88.8
N-reduction, %	38.0	36.8 ^a	36.8 ^a	38.6	38.6	38.6
Pentane insoluble conversion, %	80.8	66.7	66.7	85.6	85.6	85.6
C ₁ -C ₄ yield, wt %	5 ^a	2.4	2.4	7.4	7.4	7.4
H ₂ consumed, wt % (scf/bbl)	2.8 ^a (1740)	2.2 (1360)	2.2 (1360)	3.5 (2170)	3.5 (2170)	3.5 (2170)

^a Limiting characteristics in optimization.

TABLE 3. Hydroprocessing catalysts

Catalyst No.	1	2	3	4	5	6	7	8	9
	Harshaw Ni-4301	Harshaw Ni-4303	Harshaw 0402T	Harshaw HT-100E	Nalco NM-504	Girdler T-826	Harshaw Pd-0501	Linde SK-120	Girdler T-309B
Chemical composition, wt %									
NiO	6 ^a	6 ^a	-	3.8	5.5	2.5	-	-	-
WO ₃	19 ^a	19 ^a	-	-	-	-	-	-	-
CoO	-	-	3	-	-	2.5	-	-	-
MoO ₃	-	-	15	16.8	19	10	-	-	-
Pd	-	-	-	-	-	-	0.3	0.5	-
Pt	-	-	-	-	-	-	-	-	0.5
P ₂ O ₅	-	-	-	-	7	-	-	-	-
SiO ₂	50	-	5	1.5	1.6	-	-	64.5	-
Al ₂ O ₃	25	75	77	78	64	85	99.7	22.7	99.5
RE ₂ O ₃	-	-	-	-	-	-	-	10.7	-
<u>Physical properties</u>									
Surface area, m ² /g	228	152	200	175	170	232	186	> 550	190
Pore volume, cc/g	0.37	0.54	0.4	0.54	0.41	-	0.38	-	0.27
Avg. pore diameter, Å	65	142	100	123	97	-	82	-	57

^a Values listed are metal contents of Ni or W.

TABLE 4. Comparative performance of catalysts

Catalyst No.	Type	(1,800 psi, 425°C, 1 hr)							
		Pentane insoluble conversion, wt % (480°C+)	350°C- C ₁ -C ₄ yield, wt %	% S reduction	% N reduction	H ₂ consumed, wt %	Viscosity, cs at 60°C		
1	NiW on silicated alumina	48.6	83.8	58.3	2.32	72.2	21.7	1.69	18.0
2	NiW on alumina	57.4	87.0	58.2	1.70	75.7	21.6	1.88	18.0
3	CoMo on silicated alumina	52.6	85.7	60.5	1.94	63.5	16.7	1.60	21.7
4	NiMo on silicated alumina	60.3	82.5	59.1	1.66	73.9	27.2	2.03	14.5
5	NiMo on P ₂ O ₅ -alumina	63.0	83.7	56.6	2.03	77.4	30.0	2.08	13.6
6	NiCoMo on alumina	55.3	87.4	61.4	1.82	68.7	15.3	1.90	19.0
7	Pd on alumina	15.7	91.8	60.7	1.76	28.7	2.0	1.23	54.1
8	Pd on Y-type molecular sieve	24.9	85.0	57.3	2.30	27.0	16.7	1.32	44.2
9	Pt on alumina	12.4	75.2	46.7	1.86	30.4	2.0	1.12	47.6
10	ZnCl ₂	64.9	86.5	59.1	2.39	37.4	38.4	2.11	10.7
11	None	-10.2	8.2	40.3	1.53	13.0	-	0.40	172

Two-Stage Hydroprocessing. A two-stage hydroprocessing was conducted. In the first stage, the SRC blend was hydrotreated in a 5-liter rocking autoclave at an initial H₂ pressure of 2,200 psi and 415°C for 4 hours. It was judged that this condition would give a good compromise of high S and N reduction with low H₂ consumption and C₁-C₄ yield. The catalyst was Ni-Mo on alumina promoted with P₂O₅ and SiO₂ (Nalco NM-504). The product was then used as the feedstock for a hydrocracking study over Ni-W catalyst on silica-alumina (Harshaw Ni-4301). A series of factorial experiments for this second-stage hydrocracking was conducted at 1,800 psi initial H₂ pressure, with temperature in the range of 377°-433°C and reaction time in the range of 40-180 minutes. The results of the factorial experiments are shown in Table 5. Some results of using catalysts other than Ni-W are also included. Through a computerized regression analysis of the second-stage hydrocracking data, we were also able to determine that most characteristics, such as pentane insoluble conversion, S-reduction, N-reduction, H₂ consumption, and C₁-C₄ hydrocarbon yield, could be represented by the quadratic approximation. Figure 5 shows the change of characteristics with temperature for the second-stage hydrocracking at the specified conditions. It is evident that the upgrading is quite effective at the second stage. The benefit of the second-stage hydroprocessing can be better seen in Table 6, which shows the analyses of products obtained from a two-stage hydroprocessing of the SRC blend. The light fractions (IBP-260°C and 260°-350°C, obtained from a Kontes vacuum distiller) of the second-stage product have very low sulfur and nitrogen contents (pass EPA specifications for turbine oil).

Additional experiments were also made to determine the effect of pressure (Figure 6) in the second-stage hydrocracking. As expected, the hydrocracking effect improved with increasing pressure.

REFERENCES

- (1) F. S. Eisen, "Preparation of Gas Turbine Engine Fuel from Synthesis Crude Oil Derived from Coal," Phase 11, Final Report, U.S. Navy Contract N00014-74-C-0568, Mod. P00001, Feb. 1975.
- (2) T. R. Stein, S. E. Voltz, and R. B. Callen, *Ind. Eng. Chem., Prod. Res. Dev.*, vol. 16, No. 1, 61 (1977).
- (3) Symposium on "Refining of Synthetic Crudes," Div. Petrol. Chem., Am. Chem. Soc. Meeting, Chicago, August 1977.
- (4) M. J. Mima, H. Schultz, and W. E. McKinstry, PERC/RI-76/6, ERDA (1976).

Reference to a company or brand name is made to facilitate understanding and does not imply endorsement by the U.S. Department of Energy.

TABLE 5. Factorial experiments - second stage hydroprocessing with Ni-W catalyst

Temp, °C	Time, min	Pentane insoluble conversion, %	350°C-- yield, wt %	C ₁ -C ₄ yield, wt %	% S reduction	% N reduction	H ₂ consumed, wt %	Viscosity, cs at 60°C
377	110	22.9	71.7	0.1	44.4	38.2	0.76	7.8
385	60	12.4	67.5	0.1	22.2	30.2	0.58	8.2
385	160	38.3	65.6	0.1	55.6	41.9	0.94	6.7
405	40	9.8	61.5	0.1	66.7	33.7	0.58	7.5
405	110	41.4	58.7	0.4	44.4	47.7	0.91	6.1
405	110	33.9	71.8	1.1	44.4	54.7	1.00	6.1
405	110	42.1	62.7	1.0	33.3	55.8	1.13	6.1
405	180	41.8	69.9	1.1	66.7	61.6	1.35	5.0
425	60	45.7	65.8	1.2	55.6	46.5	0.85	5.3
425	160	56.6	66.8	2.0	55.6	66.3	1.70	3.6
433	110	55.5	64.9	2.1	44.4	59.3	1.55	3.7
Catalyst effect								
425 ^a	160	60.4	65.0	1.94	66.7	51.2	1.47	3.7
425 ^b	160	10.5	64.9	2.29	55.6	74.4	1.87	3.5
425 ^c	160	51.2	70.3	1.96	55.6	34.9	1.10	4.4

^a Co-Mo on alumina, Girdler G-51.

^b Pd on molecular sieve, Linde SK-120.

^c Pt on alumina, Girdler T3093.

TABLE 6. Two-stage hydroprocessing of SRC liquid

	SRC ^a blend	First-stage ^b hydroprocessed product	Second-stage ^c hydroprocessed product			
			Overall	IBP- 260°C	260°- 350°C	350°C+
Composition, wt %						
Oil	69.50	93.8	96.7			
Asphaltene	19.58	6.1	3.3			
Benzene insol	10.92	0.1	-			
Fraction, wt %						
IBP - 260°C	5.93	21.92	29.54			
260°C - 350°C	17.70	39.74	45.19			
350°C +	76.36	38.34	25.28			
Elemental analysis, wt %						
C	88.19	89.20	89.29	88.46	89.93	90.31
H	6.78	8.47	9.36	11.13	9.46	8.00
N	1.43	0.84	0.51	0.04	0.11	0.75
S	0.58	0.10	0.049	0.035	0.048	0.113
O	2.89	1.39	0.79	0.34	0.55	0.82
Ash	0.13	-	-	-	-	-
H/C atomic ratio	0.92	1.20	1.26	1.51	1.26	1.06
Specific gravity, 15/15°C	1.122	1.023	0.980			
Viscosity, cs at 60°C	450	39.8	5.0			

^a SRC blend contains 30 parts SRC solid and 70 parts SRC solvent.

^b Hydroprocessed at 1800 psi, 415°C and 4 hours with Ni-Mo.

^c Hydroprocessed at 1800 psi, 405°C and 3 hours with Ni-W.

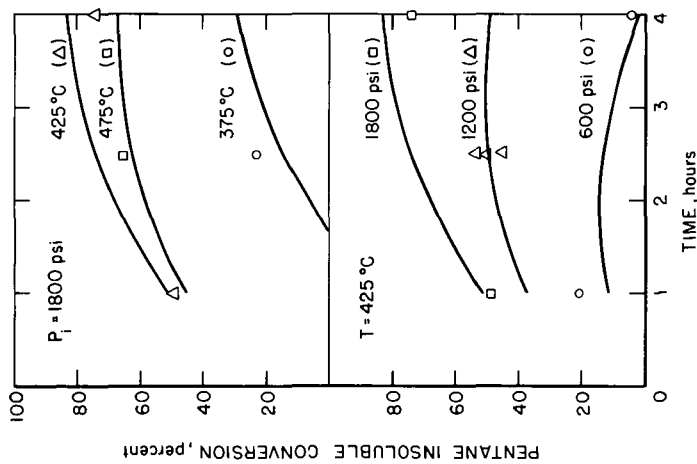


Figure 1—Effects of pressure and temperature on pentane insoluble conversion.

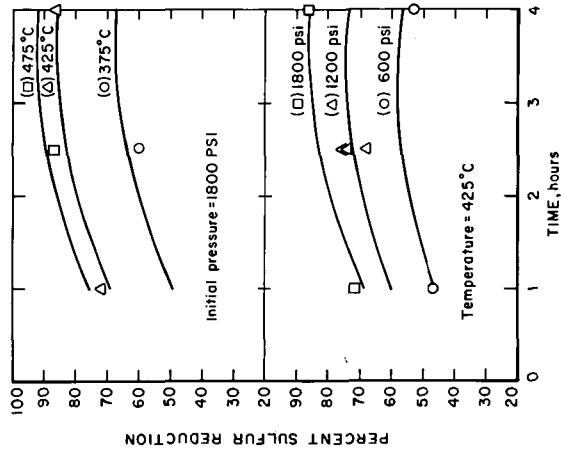


Figure 2—Effects of pressure and temperature on sulfur reduction.

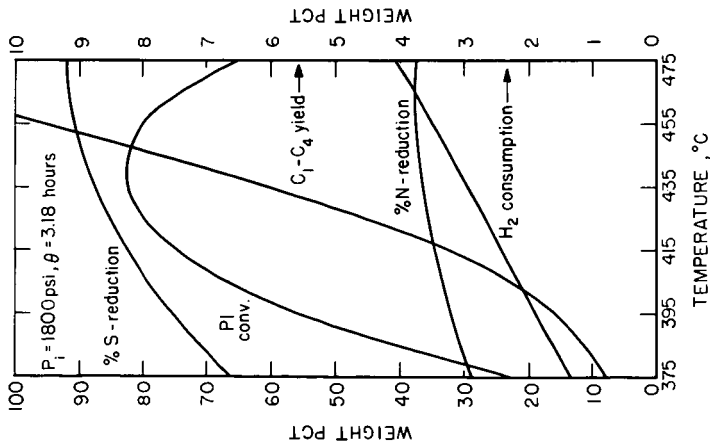


Figure 3--Change of characteristics with temperature.

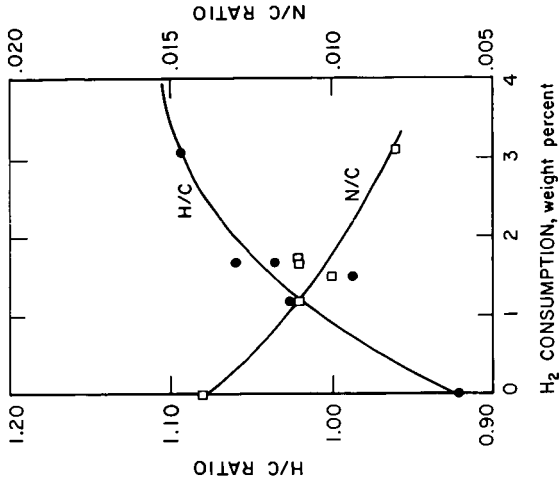


Figure 4--Change of H/C and N/C ratios with H₂ consumption.

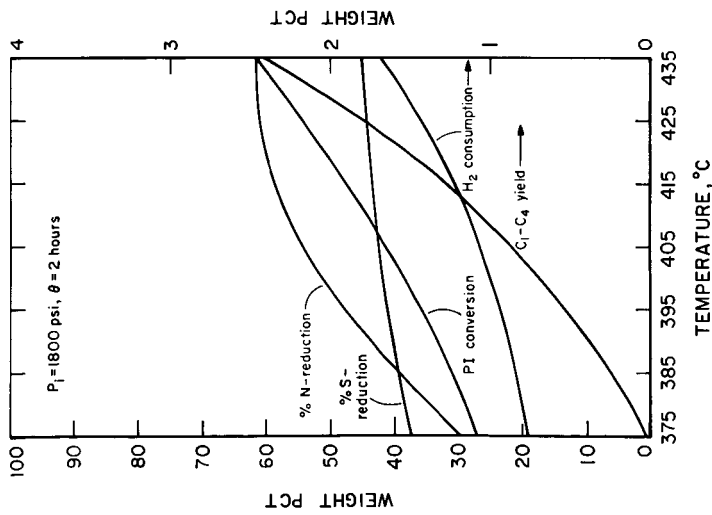


Figure 5—Change of characteristics with temperature for second-stage hydrocracking.

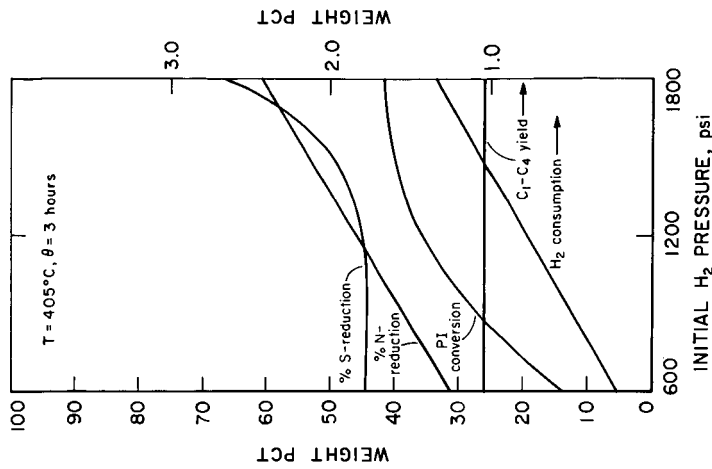


Figure 6—Effect of pressure in second-stage hydrocracking.

9-30-77 L-15633

The Sulfided Co-Mo/ γ -Al₂O₃ Catalyst: Evidence of Structural Changes During Hydrodesulfurization of Dibenzothiophene

D. H. Broderick, G. C. A. Schuit, and B. C. Gates

Center for Catalytic Science and Technology
Department of Chemical Engineering
University of Delaware
Newark, Delaware 19711

Introduction

The catalyst most often used for hydrodesulfurization (HDS) of petroleum fractions are derived from oxides of Co and Mo supported on γ -Al₂O₃, and their surfaces are sulfided prior to operation. Structures of the oxidic and sulfidic forms of the catalyst are incompletely understood and much debated (1-3), and since the available structural information has been derived from studies of catalysts at conditions far removed from those of commercial operation (about 50-200 atm and 350-320°C), it is not clear how operating variables influence the catalyst structure and activity in practice.

The hydrodesulfurization kinetics data reported here were measured to characterize the catalyst operating at about 100 atm and 300°C; the reactant stream contained dibenzothiophene (DBT) and hydrogen dissolved in n-hexadecane carrier oil. The results provide the first evidence of structural variations in the Co-Mo/ γ -Al₂O₃ catalyst brought about by changes in the reaction environment.

Experimental Methods

The catalyst used in all experiments was American Cyanamid HDS 16A having the following properties (prior to sulfiding): surface area, 176 m²/g; pore volume, 0.50 cm³/g; Co content, 4.4 wt%; and Mo content, 7.5 wt%. A sample of 10 mg of catalyst powder (80-100 mesh particles, demonstrated experimentally to be small enough to ensure the lack of intraparticle diffusion resistance) was charged to the reactor, and the catalyst was sulfided at 400°C for 2 h with a flow of about 40 cm³/min of 10% H₂S in H₂ at atmospheric pressure. Following the sulfiding, the flow of feed liquid was started. The feed contained 0.12 wt% DBT (Aldrich, 95% purity) in n-hexadecane [Humphrey Chemical Co. (redistilled)], and it was saturated with H₂ at 68 atm and room temperature. Occasionally, the feed was saturated with H₂S at various partial pressures before it was saturated with H₂. Experiments were carried out with a flow reactor described in detail elsewhere (4). The reactor operated at 300°C and 104 atm. Under all reaction conditions, the fractional conversion H₂ was < 5%, so the H₂ concentration could be considered to be virtually constant throughout the reactor.

Liquid product samples were collected periodically (without interrupting the reactant flow) and analyzed by glc (5). DBT and H_2 were converted into biphenyl and H_2S . To a first approximation, these were the only products formed; the detailed reaction network is considered separately (6).

Results

Some conversion data are plotted in Fig. 1. They show that the initial conversion at a relatively high inverse space velocity (proportional to reactant-catalyst contact time) increased about 10% over the first 10-20 h of operation, following by nearly constant conversion (referred to as "lined-out conversion") for 150 h or more. When the lined-out conversion was determined for various space velocities, the reaction was found to be pseudo-first-order in DBT (5).

Figure 1 shows the results of variations in the space velocity caused by changes in the feed flow rate. After the first step change in feed flow rate, there was a change in conversion characterized by a transient period of some 50 h before the catalyst achieved another time-invariant activity. After a second change in space velocity at 70 h onstream time, giving again the original value, there followed a transient period, as expected, but, surprisingly, the catalyst failed to return to its original lined-out activity.

In further experiments, each begun with a fresh catalyst charge, increasing concentrations of H_2S were added to the feed. The data of Fig. 2 show that at low H_2S concentrations [$(H_2S)/(H_2)$ in the feed liquid - 0.015], the qualitative pattern of changes mentioned above again occurred. The catalyst activity in the presence of added H_2S at each space velocity appeared to be less than that in the absence of added H_2S , corresponding to the well-known inhibition of reaction by H_2S (1, 6). When higher feed concentrations of H_2S were used, the transient periods of change in the catalyst activity became shorter; when the $(H_2S)/(H_2)$ ratio in the feed was as great as 0.2, the transients in catalyst activity were virtually eliminated.

In summary, these results show that H_2S does more than just inhibit the HDS reaction by adsorbing on catalytic sites in competition with DBT. We infer that when the space velocity was increased, reducing the concentration of H_2S produced in the reaction (Figs. 1 and 2), structural changes took place, reducing the number of catalytic sites. The presumed solid-state reactions were slow, in contrast to the adsorption of H_2S that caused the inhibition of reaction. The loss of catalytic sites was only partially reversed when the concentration of H_2S was again increased by decreasing the space velocity. But when H_2S was present in the feed in sufficient amounts that the H_2S concentration remained nearly constant throughout the reactor, then the catalyst activity (and structure) did not change with space velocity; the data then indicate only the simple competitive inhibition of reaction by H_2S , and there was no hysteresis.

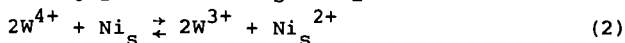
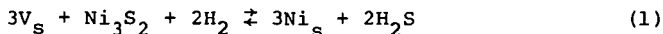
The foregoing results suggest that there is an optimum concentration of H₂S [or perhaps a (H₂S):(H₂) ratio] corresponding to a catalyst structure which has a maximum HDS activity. Experiments were carried out to test this suggestion. In one series, catalyst were brought on stream with initially low space velocities, producing initially high activities; the experiments were done with various feed H₂S concentrations. The pseudo-first-order rate constants (determined from linear semilogarithmic plots of fraction unconverted vs. inverse space velocity) are represented by curve B in Fig. 3; they indicate that in these experiments the H₂S was simply a reaction inhibitor.

In the complementary series of experiments, each new catalyst charge was brought on stream at a high space velocity and, correspondingly, with a relatively low conversion and a low H₂S concentration; H₂S concentration in the feed was varied systematically. The rate constants scatter around curve A in Fig. 3. These results confirm that increasing the H₂S concentration increased the activity of the catalyst when it was brought on stream in such a way that its initial activity was relatively low.

The important conclusion is that the catalyst achieves a lined-out activity which is dependent on the reactor startup procedure (and probably on the presulfiding procedure as well). This conclusion may be important to the technology of HDS, and we suggest that the industrial art may include the application of presulfiding and reactor startup procedures which maximize the catalyst activity; the optimum startup would ensure that some H₂S contacted the catalyst initially.

Discussion

The observed changes in catalytic activity and, by inference, catalyst structure, are suggestive of Farragher's (7) observations of the activity of Ni-W/γ-Al₂O₃ catalyst for benzene hydrogenation. Farragher presented evidence of hysteresis effects similar to those reported here, but caused by temperature variations; he explained the results in terms of solid-state reactions influencing catalyst structure and activity. The suggested reactions were the following:



The former reaction involves conversion of Ni from bulk Ni₃S₂ on the catalyst; it becomes intercalated in interstitial octahedral holes at the surface of WS₂ crystallites on the catalyst surface. The latter reaction is believed to produce W³⁺ ions at the surface, which Voorhoeve et al. (8,9) have characterized by esr and identified as the catalytic sites for benzene hydrogenation. Farragher showed that both the rate constant for benzene hydrogenation and the esr signal indicative of W³⁺ were dependent on the $\frac{P_{H_2S}}{P_{H_2}}$

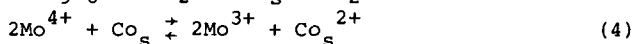
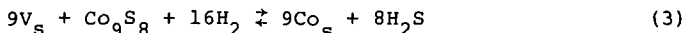
ratio in a way that is consistent with the catalyst stoichiometry suggested in Eqs. (1) and (2).

There is much evidence (1, 11) [but not a consensus (2, 3)] supporting the view that the Co-Mo/ γ -Al₂O₃ catalyst is similar to the Ni-W/ γ -Al₂O₃ catalyst, consisting of MoS₂ and Co₉S₈ on the Al₂O₃ surface, and esr evidence supports the idea that the catalytic sites are Mo³⁺ ions intercalated at the edges of the MoS₂ crystallites (1, 7, 12).

Following Farragher, and assuming the validity of the edge intercalation model for the Co-Mo catalyst, we suggest the following speculative interpretation of the structural changes in the catalyst brought about by changes in the reaction environment. The fully active catalyst is supposed to consist of MoS₂ crystallites intercalated with Co²⁺ ions, and H₂S can bond to the surface at anion vacancies in competition with DBT, causing inhibition of the HDS reaction. When only little H₂S is present, however, intercalated MoS₂ may be converted into a sulfur-deficient layer structure which may lack catalytic activity. We speculate that CoMo₂S₄ may be the sulfur-deficient structure, since it is known to lack HDS activity and to have the layer structure shown in Fig. 4 (10). Here both Co²⁺ and Mo³⁺ ions are octahedrally surrounded by S²⁻ ions, whereas in MoS₂ the surrounding is trigonal prismatic.

It is important that CoMo₂S₄ meets the criterion of having a lower sulfur content than the presumed catalyst, Co-intercalated MoS₂; to explain the observed intermediate activities, we suggest that the catalyst may consist of a range of intermediate structures which could be interconverted by local redistributions of Co and Mo ions accompanied by changes in the Mo-S surrounding.

An explicit suggestion is the epitaxial structure shown in Fig. 5. This structure accounts for the observed promotion by Co at higher Co/Mo ratios than can be accounted for by the edge intercalation model (11). It might be expected to undergo changes analogous to those postulated by Farragher for the Ni-W catalyst:



This model is consistent with the experimental evidence, but it is rough and speculative and in need of experimental evaluation.

Notation

- k pseudo-first-order rate constant, $\text{cm}^3/\text{h}\cdot\text{g}$ of catalyst
 P partial pressure
 V_s interstitial octahedral hole in a layer structure like MoS_2

Acknowledgment

This research was supported by ERDA

References

1. de Beer, V.H.J., and Schuit, G.C.A., Ann. New York Acad. Sci. **272**, 61 (1976).
2. Delmon, B., Preprints ACS Div. Petrol. Chem. **22** (2), 503 (1977).
3. Massoth, F. E., J. Catal. **50**, 190 (1977).
4. Eliezer, K. F., Bhinde, M., Houalla, M., Broderick, D., Gates, B. C., Katzer, J. R., and Olson, J. H., Ind. Eng. Chem. Fundam. **16**, 380 (1977).
5. Houalla, M., Broderick, D., de Beer, V.H.J., Gates, B. C., and Kwart, H., Preprints ACS Div. Petrol. Chem. **22**, 941 (1977).
6. Houalla, M., Nag, N. K., Sapre, A., Broderick, D. H., and Gates, B. C., to be published.
7. Farragher, A. L., paper presented at ACS meeting, New Orleans, March, 1977.
8. Voorhoeve, R.J.H., and Stuiiver, J.C.M., J. Catal. **23**, 228, 243 (1971).
9. Voorhoeve, R.J.H., J. Catal. **23**, 236 (1971).
10. van den Berg, J. M., Inorg. Chim. Acta. **2**, 216 (1968).
11. Furimsky, E., and Amberg, C. H., Can. J. Chem. **53**, 2542 (1975).
12. Konigsberger, D., comments accompanying paper B23, Sixth International Congress on Catalysis, London, 1976.

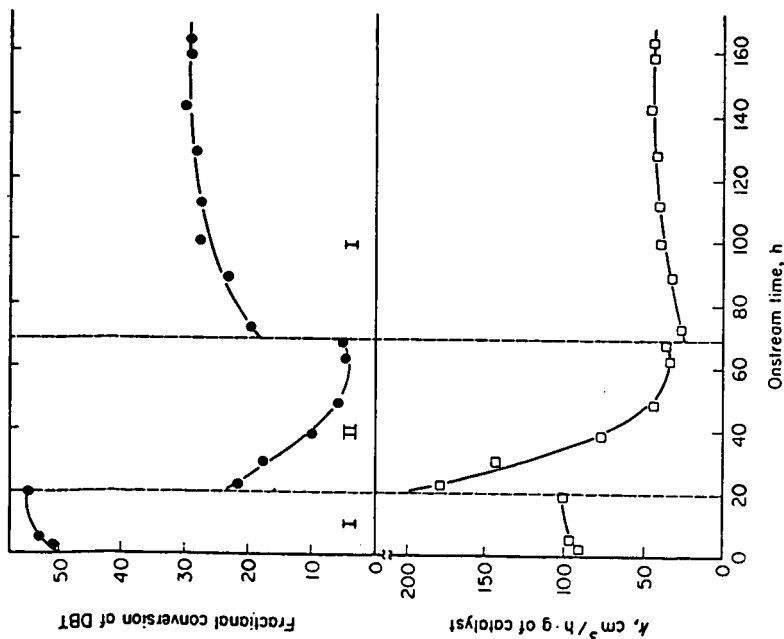


Figure 1. Conversion and pseudo-first-order rate constants for HDS of DBT. I: space velocity = 128 cm³/h·g of catalyst. II: space velocity = 7105 cm³/h·g of catalyst. Catalyst of DBT in n-hexadecane which had been saturated with H₂ at 25°C and 68 atm. The catalyst was American Cyanamid HDS 16A. Reaction conditions: 300°C and 104 atm.

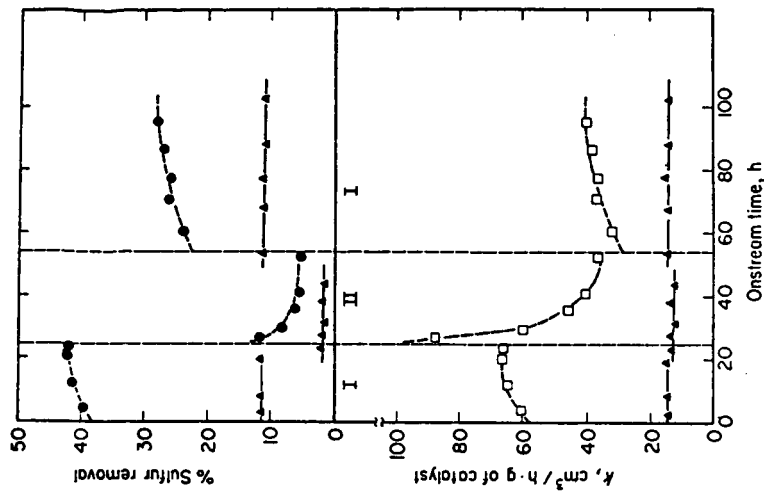


Figure 2. Conversion and pseudo-first-order rate constants for HDS of DBT. I: space velocity = 124 cm³/h·g of catalyst. II: space velocity = 705 cm³/h·g of catalyst. Concentration catalyst = 0.2 (-Δ-); 0.015 (-□-). The feed, catalyst, and reaction conditions were the same as those described in the caption of Fig. 1, except for the added H₂.

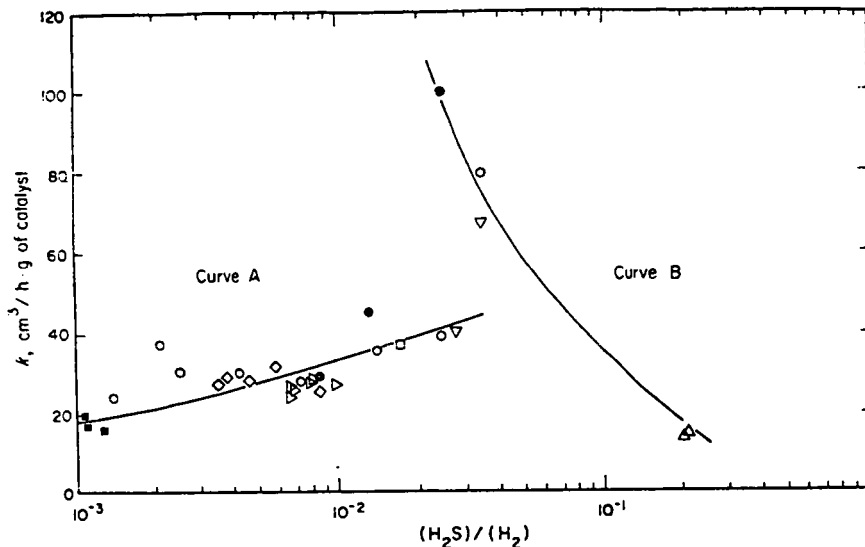


Figure 3. Effects of H_2S on catalyst activity for HDS of DBT at the reaction conditions given in the caption of Fig. 1.

The points on curve A represent conversion measured at various space velocities and with various feed $(H_2S)/(H_2)$ ratios for catalyst which had previously lined out at high space velocities (700^2750 $cm^3/h \cdot g$ of catalyst). These results show that the catalyst which lined out at high space velocities was sulfur deficient and relatively inactive, becoming more active on addition of H_2S , as discussed in the text.

The points on curve B represent conversion measured at various feed $(H_2S)/(H_2)$ ratios for catalyst which had previously lined out at low space velocities ($90-100$ $cm^3/h \cdot g$ of catalyst). These results indicate competitive inhibition of reaction by H_2S .

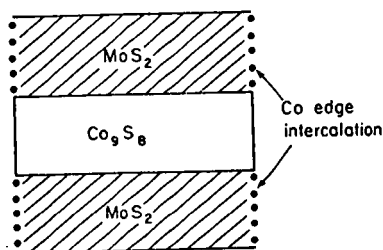


Figure 4. Model of the sulfided Co-Mo/ γ - Al_2O_3 catalyst, representing layers of Co_9S_8 and MoS_2 intercalated with Co^{2+} at the crystal edges.

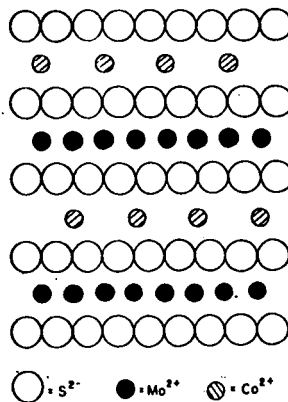


Figure 5. Representation of the layer structure of $CoMo_3S_4$. The actual structure is distorted, as shown by van den Berg (12).

EFFECT OF CATALYST COMPOSITION ON
QUINOLINE AND ACRIDINE HYDRODENITROGENATION

By

S. Shih,^a E. Reiff,^b R. Zawadzki^c and J. R. Katzer
Department of Chemical Engineering, University of Delaware
Newark, Delaware 19711

INTRODUCTION

Recently there has been increased interest in the hydrodenitrogenation of nitrogen-containing aromatic compounds typical of those found in petroleum, coal-derived liquids and shale oil. Because of the high nitrogen contents of coal-derived liquids and shale oil, hydrodenitrogenation will become increasingly important in the future. Mars and Coworkers (1-4) have clarified the reaction network and kinetics associated with the hydrodenitrogenation of pyridine. Their work was done on unsulfided Co-Mo/Al₂O₃ catalyst. Although several authors (5-9) have studied hydrodenitrogenation, neither the reaction network, nor the reaction kinetics have been adequately defined for anything but pyridine. We have recently established the reaction networks and reaction kinetics of the hydrodenitrogenation of quinoline (10, 11) and of acridine (12) over sulfided hydroprocessing catalysts under high-pressure liquid-phase conditions.

Both the prior literature and our work shows that hydrodenitrogenation of nitrogen-containing compounds occurs via a complex reaction network involving hydrogenation of the aromatic rings followed by carbon-nitrogen bond breaking. This is in contrast to hydrodesulfurization, in which sulfur removal occurs directly without hydrogenation of the associated aromatic rings (13). It is therefore important to understand how catalyst composition affects the relative rates of hydrogenation and of bond breaking in the complex nitrogen-removal reaction network. This bifunctional nature of the reaction network requires an appropriate balance between the catalyst hydrogenation and catalyst bond-breaking functions to provide the most active catalyst. A quantitative definition of the relative kinetic role of the two catalyst functions in hydrodenitrogenation is not available.

Generally Ni-Mo/Al₂O₃ or Ni-W/Al₂O₃ have been reported to be more active for hydrodenitrogenation than Co-Mo/Al₂O₃, the catalyst of choice for hydrodesulfurization, and the enhanced behavior is often assumed to be due to higher hydrogenation activity (9, 14, 15). This is not confirmed by

^aCurrently at Mobil Research and Development Corp., Paulsboro, N.J.
^bCurrently at Dept. Chem. Eng., Univ. of Mass., Amherst, Mass.
^cCurrently at American Cyanamid, Bound Brook, N.J.

quantitative experimental data, particularly under typical hydroprocessing conditions with multi-ring nitrogen-containing compounds. In this work we have evaluated the relative behavior of commercial hydroprocessing catalysts of differing metal composition and support under high-pressure liquid-phase conditions. The catalysts were examined in the oxidic form, the sulfided form and the sulfided form with H₂S in the system. First-order rate constants for all hydrogenation and bond breaking steps in the reaction networks were determined as a function of catalyst type and catalyst pretreatment. Our objectives were to determine how the catalyst type and pretreatment affected the rate of each individual step in the hydrodenitrogenation reaction network and thus to elucidate the fundamental differences in the catalysts.

EXPERIMENTAL

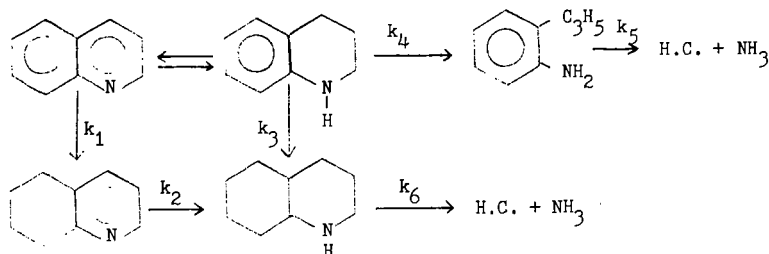
The experiments were carried out in a one-liter stirred autoclave (Autoclave Engineer) with glass liner; the autoclave was operated in batch mode. A special reactant-oil-catalyst injection system was attached to the autoclave to inject catalyst and reactant (nitrogen-containing compound) in carrier oil into the autoclave after it had been stabilized at the operating temperature and pressure. Consequently, the problems of reaction and catalyst deactivation during the long heat-up time frequently encountered in autoclave studies were eliminated, and zero time was precisely defined. The system has been described elsewhere (10, 11); operating conditions were:

Temperature: quinoline, 342 ±1°C; acridine, 367 ±1°C
Total pressure: quinoline, 34 atm; acridine, 136 atm
Reactant concentration: quinoline, 1.0 wt%; acridine 0.5 wt %
Catalyst: 0.5 wt % in carrier oil; 150-200 mesh;
 sulfided (quinoline, 2 hr at 325°C; acridine 2 hr at
 425°C) in 160 cc/min of 10% H₂S in H₂
Carrier Oil: 500 cc highly paraffinic White Oil;
 0.05 wt % CS₂ added to give 1.4 vol % H₂S in the
 gas phase
One-liter autoclave, stirred at 1700rpm

Analysis of reaction products was by G. C. using a 10' X 1/8' Chromosorb 103 glass column for quinoline, a 50m OV101 SCOT glass column for acridine and a nitrogen-specific detector so that individual nitrogen-containing compounds could be identified.

RESULTS

The reaction network for quinoline hydrodenitrogenation with specific rate constants identified, as established by Shih et al. (10, 11), is:



The behavior of different catalysts in quinoline hydrodenitrogenation is given in Table I. Ni-Mo/Al₂O₃ is a slightly better catalyst for the removal of nitrogen from quinoline than Co-Mo/Al₂O₃ or Ni-W/Al₂O₃ as shown by the pseudo first-order rate constants for total nitrogen removal. The Ni-containing catalysts appear to be more active for hydrogenating the benzenoid ring (k_1 and k_3); whereas the Mo-containing catalysts appear to be more active in hydrogenating the heteroaromatic ring (k_2). The pseudo first-order rate constants for the cracking steps (k_4 and k_6) are more dependent on the source of the alumina (catalyst) than on the metals present as demonstrated better by other studies not reported here.

TABLE I
HYDRODENITROGENATION OF QUINOLINE OVER DIFFERENT CATALYSTS

Rate constant, min ⁻¹	Ni-Mo/Al ₂ O ₃ (Cyanamid HDS-9A)	Co-Mo/Al ₂ O ₃ (Cyanamid HDS-16A)	Ni-W/Al ₂ O ₃ (Nalco NT-550)
k_1	3.10	1.49	2.17
k_2	1.11	1.51	0.52
k_3	0.63	0.26	0.33
k_4	0.077	0.067	0.073
k_5	0.61	1.51	0.36
k_6	2.54	3.56	1.11
$k_{\text{Total N-removal}}$	0.30	0.20	0.19

Operating conditions: Catalysts were presulfided, no CS₂ added to the system, T = 342°C, P = 34 atm.

Presulfiding has a marked effect on the total nitrogen removal rate (Table II); the rate constant for total nitrogen removal almost doubles. However there seems to be little or no gain in going from the oxidic form to the sulfided form of the catalyst in steps that involve carbon-nitrogen bond breaking. The rates for these steps remain basically the same, as can be seen upon comparing k_5 and k_6 for the oxidic and sulfided catalyst in Table II. Presulfiding has a marked influence on the rate of hydrogenation of the benzenoid and heteroaromatic ring (k_1 , k_2 and k_3). However, there seems to be a preference for hydrogenation of the benzenoid ring over the heteroaromatic ring in quinoline; there is a 4-fold increase in the value of k_1 and k_3 as compared to only a 1.5-fold increase in k_2 . The reaction path involving *o*-propylaniline is of negligible importance for the oxidic form.

TABLE II
EFFECT OF PRESULFIDING ON THE HYDRODENITROGENATION OF QUINOLINE

Rate constant, min ⁻¹	Ni-Mo/Al ₂ O ₃ (Cyanamid HDS-9A)	
	oxidic	presulfided
k_1	0.72	3.10 (4.3X)
k_2	0.75	1.11 (1.5X)
k_3	0.18	0.63 (3.5X)
k_4	0.0023 ^a	0.077
k_5	0.75	0.61
k_6	2.2	2.54
$k_{\text{Total N-removal}}$	0.17	0.3

Operating conditions: catalyst presulfided at 325°C for 2 hr in 10% H₂S/H₂, no CS₂ added, T = 342°C, P = 34 atm.

^aThis value was so small for the oxidic form that its value is uncertain.

The effect of CS₂ (H₂S) on the reaction system is shown in Table III. H₂S increases the rate of total nitrogen removal. The presence of H₂S enhances the carbon nitrogen bond breaking rates (i.e., k_6 and particularly k_4). However, k_5 is negatively affected since the transformation of *o*-propylaniline to a hydrocarbon and ammonia involves first a hydrogenation

step (10, 11); k_5 is a compound pseudo first-order rate constant. Little advantage of having H_2S present is seen in the hydrogenation rates (k_1 , k_2 and k_3). For the Co-Mo/ Al_2O_3 catalyst there is no enhancement of the hydrogenation of the heteroaromatic ring, but the benzenoid ring hydrogenation capacity is slightly enhanced. For the Ni-Mo/ Al_2O_3 and Ni-W/ Al_2O_3 catalysts the converse is true; they experience a decrease in their benzenoid ring hydrogenation activity and an increase in their heteroaromatic ring hydrogenation activity with gas-phase H_2S .

TABLE III

EFFECT OF H_2S ON THE HYDRODENITROGENATION OF QUINOLINE

Rate constant, min ⁻¹	Ni-Mo/ Al_2O_3 (Cyanamid HDS-9A)		Co-Mo/ Al_2O_3 (Cyanamid HDS-16A)		Ni-W/ Al_2O_3 (Nalco NT-550)	
	A	B	A	B	A	B
	k_1	3.10	3.09	1.49	1.51	2.17
k_2	1.11	1.57	1.51	1.51	0.52	1.24
k_3	0.63	0.32	0.26	0.24	0.33	0.21
k_4	0.077	0.13	0.067	0.18	0.073	0.15
k_5	0.61	0.13	1.51	0.78	0.36	0.38
k_6	2.54	3.89	3.56	3.64	1.11	2.94
$k_{total} N_2$ removal	0.30	0.57	0.20	0.41	0.19	0.60

Operating conditions: All catalysts were presulfided at 325°C in 10% H_2S/H_2 for 2 hrs, T = 342°C, P = 34 atm.

A: without CS_2 ; B: with 0.05 wt % of CS_2 in white oil to give gas phase H_2S .

The differences between Co-Mo/ Al_2O_3 and Ni-Mo/ Al_2O_3 increase with severity of operating conditions as shown in Table IV. Under the more severe operating conditions Ni-Mo/ Al_2O_3 is superior by a factor of about 2 for total nitrogen removal rate. The hydrogenation rates (k_1 , k_2 , k_3 and k_5) are all significantly higher over the Ni-Mo/ Al_2O_3 than over Co-Mo/ Al_2O_3 . The behavior for nitrogen-carbon bond rupture is consistent with the relative behavior observed for the less severe conditions.

TABLE IV

CATALYTIC HYDRODENITROGENATION OF QUINOLINE AT MORE SEVERE CONDITIONS

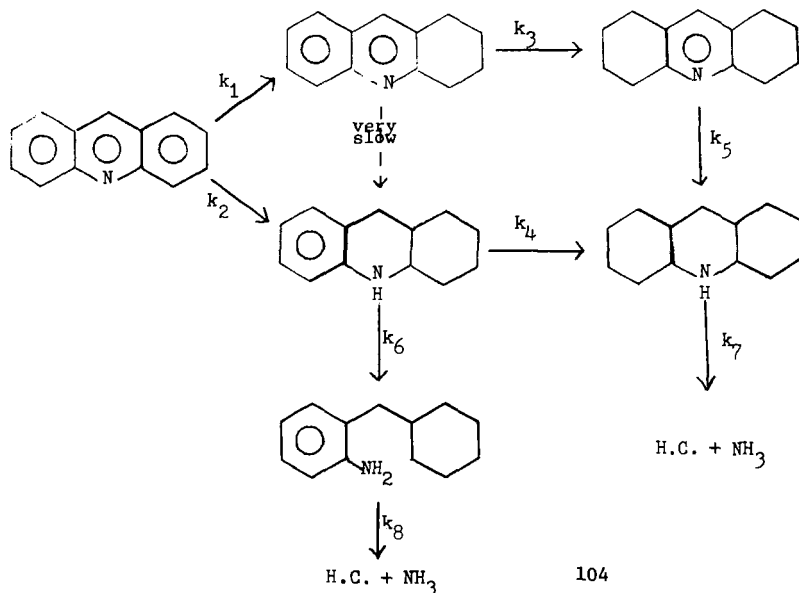
Rate constant, min^{-1}	Ni-Mo/Al ₂ O ₃ (Cyanamid HDS-9A)		Co-Mo/Al ₂ O ₃ (Cyanamid HDS-16A)	
	mild*	severe**	mild*	severe**
k_1	3.09	4.95	1.51	0.69
k_2	1.57	10.55	1.51	2.95
k_3	0.32	4.67	0.24	2.28
k_4	0.13	0.50	0.18	0.51
k_5	0.13	3.40	0.78	1.91
k_6	3.89	10.58	3.64	3.45
$k_{\text{total N-removal}}$	0.57	2.42	0.41	1.22

All catalysts presulfided at 325°C in 10% H₂S/H₂ for 2 hrs, 0.05 wt % CS₂ was added to all runs.

*mild operating conditions: temp., 342°C; total pressure, 34 atm.

**severe operating conditions: temp, 367°C; total pressure, 136 atm.

For acridine the hydrodenitrogenation reaction involves the following reaction network (12):



The effect of different catalysts on the hydrodenitrogenation of acridine is shown in Table V. Hydrogenation rates (k_1 , k_2 , k_3 , k_4 and k_5) are typically more rapid over the Ni-Mo/Al₂O₃ and Ni-W/Al₂O₃ catalysts than over the Co-Mo/Al₂O₃; the Ni-Mo/Al₂O₃ catalysts has a slight advantage over Ni-W/Al₂O₃. The Ni-Mo/Al₂O₃ catalyst shows distinctly higher activity for the carbon-nitrogen bond rupture steps and thus is overall the superior of the catalysts used in these studies.

TABLE V
EFFECT OF CATALYST TYPE ON THE HYDRODENITROGENATION OF ACRIDINE

Rate constant, min ⁻¹	Ni-Mo/Al ₂ O ₃ (Cyanamid HDS-9A)	Co-Mo/Al ₂ O ₃ (Cyanamid HDS-16A)	Ni-W/Al ₂ O ₃ (Nalco NT-550)
k_1	5.0	3.1	7.7
k_2	36.2	19.0	43.0
k_3	7.2	3.67	4.0
k_5	0.38	0.015	0.15
k_4	8.8	2.91	3.77
k_6	1.14	0.43	0.41
k_8	2.20	0.79	0.77
k_7	2.19	0.73	0.76
$k_{\text{total N-removal}}$	1.25	0.48	0.54

Operating conditions: T = 367°C; P = 136 atm; All catalysts presulfided at 425°C for 2 hr in 10% H₂S in H₂; 0.05 wt % of CS₂ in white oil was used in all runs.

Because of the complexity of the hydrodenitrogenation reaction network, involving hydrogenation and carbon-nitrogen bond rupture as distinct reaction steps, the evaluation and further development of hydrodenitrogenation catalysts can be greatly aided by knowledge of the rate of the various intermediate reaction steps in the reaction network. This work shows that Ni-Mo/Al₂O₃ is typically better for hydrodenitrogenation because it has higher hydrogenation activity than Co-Mo/Al₂O₃; Ni-W/Al₂O₃ appears to be slightly less active than Ni-Mo/Al₂O₃. The cracking activities appear to be more dependent on the source of the support and are also very important in determining the relative ranking of overall catalyst behavior. This aspect of catalyst behavior was not sufficiently investigated in this work to allow for firm conclusions.

LITERATURE CITED

- (1) Sonnemans, J., Neyens, W. J., and Mars, P., J. Catal. 34, 230 (1974).
- (2) Sonnemans, J., and Mars, P., J. Catal. 31, 209 (1973).
- (3) Sonnemans, J., Van Den Berg, G. H., and Mars, P., J. Catal. 31, 220 (1973).
- (4) Sonnemans, J., Goudrian, F., and Mars, P., in "Catalysis, Proceedings of the Fifth International Congress on Catalysis," ed. J. W. Hightower, p. 76-1085, North-Holland Publishing Co., Amsterdam, 1973.
- (5) McIlvried, H. G., Ind. Eng. Chem., Process Des. Develop. 10, 125 (1971).
- (6) Aboul-Gheit, A. K., and Abdou, I. K., J. Institute of Petroleum 59, 188 (1973).
- (7) Aboul-Gheit, A. K., Can. J. Chem. 53, 2575 (1975).
- (8) Doelman, J., and Vlugter, J. D., Proc. Sixth World Petroleum Congr. Section III, p. 247, The Hague, The Netherlands, 1963.
- (9) Flinn, R. A., Larson, O. A., and Beuther, H., Hydrocarbon Processing and Petrol. Refiner 42, No. 9, 129 (Sept., 1963).
- (10) Shih, S. S., Katzer, J. R., Kwart, H., and Stiles, A. B., "Quinoline Hydrodenitrogenation: Reaction Network and Kinetics," submitted to J. Catal.
- (11) Shih, S. S., Katzer, J. R., Kwart, H., and Stiles, A. B., Division of Petroleum Chemistry Preprints, Vol. 22, No. 3, p. 919 (1977).
- (12) Zawadzki, R., Shih, S. S., Katzer, J. R., and Kwart, H., "Kinetics of Acridine Hydrodenitrogenation," submitted to J. Catal.
- (13) Houalla, M., Broderick, D., de Beer, V. H. J., Gates, B. C., and Kwart, H., Division of Petroleum Chemistry Preprints, Vol. 22, No. 3, p. 941 (1977).
- (14) Rollmann, L. D., J. Catal. 46, 243 (1977).
- (15) Yarrington, R. M., Paper presented at 19th Canadian Chemical Engineering Conference and Third Symposium on Catalysis, Edmonton, 1969.

STERIC EFFECTS IN PHENANTHRENE AND PYRENE
HYDROGENATION CATALYZED BY SULFIDED Ni-W/Al₂O₃

J. Shabtai*, L. Veluswamy, and A.G. Oblad

Department of Mining and Fuels Engineering,
University of Utah, Salt Lake City, Utah 84112

The increased interest in coal liquefaction and catalytic upgrading of coal-derived liquids has recently led to a considerable amount of work on hydrodesulfurization and hydrodenitrogenation of model heterocyclic compounds in the presence of sulfided catalyst systems(1,2). In contrast, hydrogenation reactions of model polycyclic aromatic hydrocarbons in the presence of such catalysts have been studied to a limited extent (3-5). It is also noteworthy that in comparison with previous extensive studies on mechanistic and stereochemical aspects of metal-catalyzed hydrogenation of condensed aromatics, so far little attention has been paid to such aspects in hydrogenation studies with the structurally different class of sulfided catalysts.

In the present work the hydrogenation of phenanthrene (1) and pyrene (9) was systematically investigated as a function of sulfided catalyst type, reaction temperature, hydrogen pressure, and catalyst/feed ratio. Experiments were performed in a semi-batch reactor, and products obtained were identified and quantitatively analyzed by a combination of gas chromatography, PMR, and mass-spectral methods (see Experimental).

RESULTS AND DISCUSSION

Relative catalytic activities of sulfided Ni-Mo/Al₂O₃ (catalyst A), Ni-W/Al₂O₃ (catalyst B) and Co-Mo/Al₂O₃ (catalyst C) for hydrogenation of 1 were examined by comparative experiments under mild experimental conditions, i.e. pressure, 1500 psig; temperature, 341°C; reaction time, 2 hr. Under such conditions conversion of 1 into perhydrophenanthrene (8) is incomplete and the product contains, in addition to 8, a series of partially hydrogenated compounds expected from stepwise hydrogenation of phenanthrene (P), i.e. 9,10-dihydroP(2), 1,2,3,4-tetrahydroP(3), 1,2,3,4,9,10,11,12-octahydroP(4), 1,2,3,4,5,6,7,8-octahydroP(5), and isomeric mixtures of decahydroP(6) and dodecahydroP(7). With samples of the above indicated types of catalysts, having comparable concentrations of the active components and nearly identical surface areas and pore volumes, it was found that the decrease in H-aromaticity is 20-25% higher with A and B, as compared with C. Further, under conditions leading to complete saturation of 1 (2,900 psig; 341°C; 7 hr) the hydrogenation selectivity of B was found to be somewhat higher than that of A. Consequently, a catalyst of type B (containing 5.1% of NiO and 20.2% of WO₃; see Experimental) was selected for the hydrogenation study.

Figures 1 and 2 summarize the observed change in product composition from hydrogenation of 1 as a function of temperature in the range of 200-380°C. For the purpose of clarity the composition is plotted in two sets corresponding to anticipated consecutive stages of the hydrogenation process, i.e. an early stage (A) showing the change in concentration of phenanthrene derivatives with one or two hydrogenated rings (Fig. 1), and a later stage showing the change in concentration of derivatives with two or three hydrogenated rings (Fig. 2). Extrapolation of the curves in Fig. 1 to temperatures below 200°C, clearly indicates that 1,2,3,4-tetrahydroP(3) is the main primary product, while the other possible primary product, i.e., 9,10-dihydroP(2), is formed in considerably lower yield. The gradual decrease in the concentration of compound 3 with increase in temperature (Fig. 1) is accompanied by a corresponding increase in the yield of 1,2,3,4,5,6,7,8-octahydroP(5), a product which should be formed by hydrogenation of the residual aromatic end ring in 3. On the other hand, the gradual disappearance of 9,10-dihydroP(2) with temperature is not accompanied by

*Weizmann Institute of Science, Rehovot, Israel

any significant formation of the expected second-step hydrogenation product from 2, i.e., 1,2,3,4,9,10,11,12-octahydroP(4). Since conversion of 2 into 3 is a slow, indirect reaction (*vide infra*), these results indicate that 2 is not an important intermediate in the overall hydrogenation process leading to perhydrophenanthrene (8). After reaching a maximum of ~60% b.wt. near 300°C, the concentration of 1,2,3,4,5,6,7,8-octahydroP(5) decreases with further increase in temperature. Figure 2 indicates that hydrogenation of the residual inner aromatic ring in 5, leading to the final product 8, involves the formation of olefinic intermediates, i.e. isomeric mixtures of decahydroP(6) and of dodecahydroP(7). Patterns similar to those indicated in Figs. 1 and 2 are also observed in the study of product composition as a function of hydrogen pressure (between 500-2,900 psig), and of catalyst/phenanthrene ratio.

The results obtained can be rationalized by considering, among other factors, the stereochemistry of the intermediate compounds formed in the stepwise hydrogenation of 1 to 8:

Initiation of the process by hydrogenation of the inner ring in 1 at the 9,10-position produces a somewhat strained hydroaromatic ring. In forming this ring the two aromatic end rings are forced out of coplanarity, and the resulting 9,10-dihydroP(2) shows strong dehydrogenation tendency at temperatures $\geq 250^\circ\text{C}$ (*vide infra*). In contrast, hydrogenation of an end ring in 1, to yield 3, involves formation of a strainless hydroaromatic ring. Fast consecutive hydrogenation of the two end rings in 1 should produce 1,2,3,4,5,6,7,8-octahydroP(5), which is indeed observed as the main intermediate in the process. Examination of steric models of 5 indicates that flatwise adsorption of the residual inner aromatic ring B on the catalyst surface would be difficult as a result of steric interference by the two flexible hydroaromatic rings A and C (Fig. 3). The lower rate of hydrogenating the inner ring as compared to the end rings in 1 is reflected in the accumulation of compound 5 in reaction products formed under mild experimental conditions. Slow hydrogenation of B, however, may proceed by a stepwise doublet mechanism, involving slantwise or edgewise adsorption of 5 by means of the sterically unobstructed 9,10-position. Such mechanism would require formation of olefinic intermediates, e.g. 6 and 7, which are indeed found in the reaction products (Fig. 2).

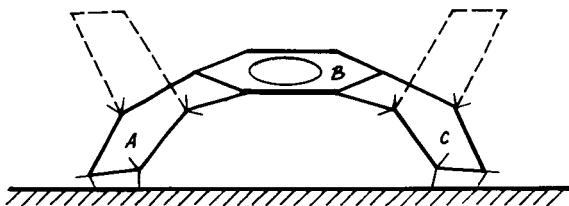


Fig. 3. Steric interference with flatwise adsorption of 1,2,3,4,5,6,7,8-octahydroP(5)

It should be noted that, depending on the surface structure and the strength of adsorption, steric interference of the type indicated in Fig. 3 may not necessarily be equally effective with different types of hydrogenation catalysts. For instance, hydrogenation of 1 using platinum group metals proceeds with strong preference (selectivity $\geq 75\%$) for formation of the *cis-syn-cis*-perhydrophenanthrene stereoisomer (6). This would require (a) preferential flatwise orientation of ring B on the surface; and (b) fast addition of hydrogen from the underside of the adsorbed system, so that all of the four hydrogen atoms found at the asymmetric bridge positions

appear on the same side of the produced hydroaromatic ring. No such selectivity is observed in the present study, viz. the perhydrophenanthrene fraction produced in the presence of sulfided Ni-W/ Al_2O_3 consists of a mixture of all six possible stereoisomers in maximal concentrations below 50% of the total fraction. This is in good agreement with the above proposal that in the presence of sulfided catalysts ring B is hydrogenated by a stepwise mechanism, which excludes any possibility of attaining cis-syn-cis stereoselectivity.

To confirm the proposed role of 1,2,3,4-tetrahydroP(3) rather than 9,10-dihydroP(2) as the main first-step intermediate in the process, comparative hydrogenation experiments using these two compounds as feeds were carried out under the following conditions: temperature, 250°C; hydrogen pressure, 1500 psig; and reaction time, 3 hr. It is found that 2 yields considerable amounts (17.2% b.wt.) of phenanthrene, which is then converted to perhydroP(8) via the usual intermediates, e.g. compounds 3 and 5. Significantly, the overall rate of conversion of 2 into 8 is lower compared to that observed in the conversion of phenanthrene into 8 under the same set of conditions. In contrast, 1,2,3,4-tetrahydroP(3) does not undergo any dehydrogenation to phenanthrene under identical conditions, and its relative rate of hydrogenation into 8 is markedly higher than that of phenanthrene proper.

The hydrogenation of pyrene (9) in the presence of sulfided Ni-W/ Al_2O_3 was investigated as a function of experimental variables, using an analogous procedure. Figures 4 and 5 summarize the change in product composition from 9 (at 341°C) as a function of hydrogen pressure in the range of 1,000-2,900 psig. As seen, only one type of product containing one hydrogenated ring, i.e. 4,5-dihydropyrene (10), is formed. The yield of this first intermediate decreases with increase in pressure, while that of the preferred second-step hydrogenation intermediate, viz. 1,2,3,3a,4,5-hexahydropyrene (12) passes through a maximum at \approx 1,500 psig and then gradually decreases at higher pressure (Fig. 4). It is found that the yield of the alternative second-step product, i.e. 4,5,9,10-tetrahydropyrene (11), is very low in the entire pressure range, indicating that this compound is not an important intermediate in the hydrogenation process. The strong preference for hydrogenation of 10 into 12 rather than into 11 apparently depends on a marked difference in the position of the respective aromatic saturation equilibria. Compound 11 contains two rather strained hydroaromatic rings which should be susceptible to easy dehydrogenation, whereas 12 contains two non-strained hydroaromatic rings in a skewed chair conformation which should be more resistant to dehydrogenation. Figure 5 indicates that hydrogenation of 12 to yield perhydropyrene (14) involves the intermediate formation of 1,2,3,3a,4,5,5a,6,7,8-decahydropyrene (13), followed by slow hydrogenation of the residual tetrasubstituted aromatic ring in 13. Examination of molecular models shows that flatwise adsorption of this residual aromatic ring on the catalyst surface would be difficult due to steric interference by the three surrounding hydroaromatic rings.

The observed slow rate of hydrogenating the inner ring in 1,2,3,4,5,6,7,8-octahydrophenanthrene (5), and the apparent slow rate of hydrogenating the residual tetrasubstituted ring in 1,2,3,3a,4,5,5a,6,7,8-decahydropyrene (13), to yield perhydropyrene (14), indicate that sterically blocked aromatic rings in polycyclic aromatic-naphthenic systems could be markedly resistant to hydrogenation in the presence of sulfided catalysts. This could provide a plausible explanation for the observed resistance of coal-derived liquids to complete hydrogenation, even in case the aromatic saturation equilibria are fully displaced in the direction of saturation (1).

EXPERIMENTAL

Apparatus - An autoclave of 300 ml capacity, rated at 4,000 psi (510°C), was adopted for use as a semi-batch reactor. The autoclave was equipped with a magnetic stirrer, a temperature-controlled heater, a pressure gage, and a water cooling system. It was connected to a high pressure hydrogen source through a check valve and a regulator permitting the maintenance of a constant pressure throughout the experiment.

Catalysts - A wide range of supported Ni-Mo, Ni-W, and Co-Mo systems, obtained

commercially or prepared in this Department, were used in a preliminary screening of hydrotreating catalysts. The selected catalyst had a surface area of 225 m²/g, and contained NiO, 5.1; WO₃, 20.2; Fe₂O₃, 0.03; and Al₂O₃, 74.1% b.wt. It was sulfided at 300°C and 250 psig with a mixture of hydrogen and carbon disulfide, using an appropriately designed pressure flow system (1).

Procedure - Highly purified samples (> 99%) of phenanthrene and pyrene were used as starting materials. In each experiment were used 13 g of the aromatic compound and 2.6 g of presulfided catalyst. After flushing, the charged autoclave was quickly brought to the desired temperature and hydrogen pressure, and kept under constant conditions for the selected length of time (2 hr in most experiments). At the end of each run, the reaction mixture was rapidly cooled to room temperature, and after releasing the pressure, dissolved in carbon tetrachloride, filtered to remove the catalyst, and analyzed.

Analysis - Products from the hydrogenation reactions were identified by mass spectrometry, PMR analysis, and measurement of gas chromatographic retention volumes. In most cases structures were confirmed by comparison with pure reference compounds. Quantitative analysis of product components was performed by temperature-programmed (60-270°C; 4°C/min) gas chromatography with a 9' x 1/8" column packed with 6% OV-17 on 100-120 mesh Chromosorb W.

REFERENCES

- (1) L.R. Veluswamy, Ph.D. Thesis, University of Utah, 1977, and references therein.
- (2) S.S. Shih, J.B. Katzer, H. Kwart, and A.B. Stiles, Preprints, Div. Petrol. Chem., A.C.S., 22, #3, 919 (1977), and references therein.
- (3) S. Singh, Ph.D. Thesis, University of Utah, 1972.
- (4) C.S. Huang, K.C. Wang, and H.W. Haynes, Jr., Preprints., Div. Fuel Chem., A.C.S., 21, #5, 228 (1976).
- (5) E.G. Prokopetz, G.E. Gavrilova, and L.A. Klimova, J. Appl. Chem. (U.S.S.R.) 11, 823 (1938), and subsequent papers.
- (6) R.P. Linstead, W.E. Doering, S.B. Davis, P. Levine, and R.R. Whetstone, J. Amer. Chem. Soc., 64, 1985 (1942).

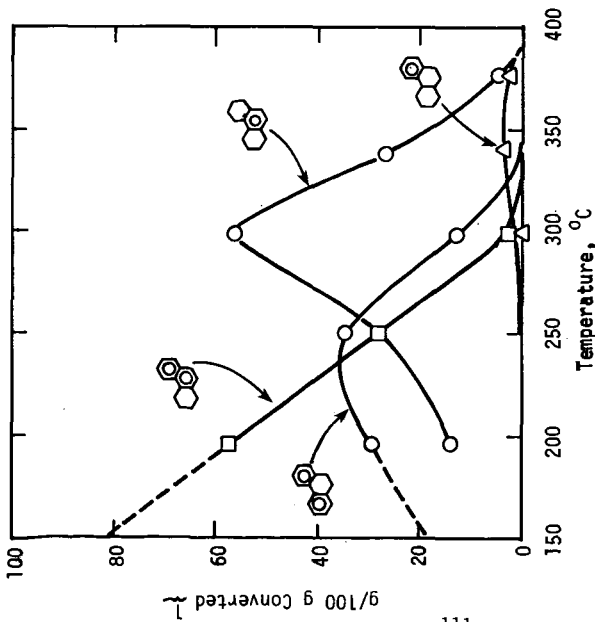


Fig. 1. Change in Product Composition from Hydrogenation of Phenanthrene (Stage A) as a Function of Temperature.

Catalyst: Sulfided Ni-W on Alumina

Pressure: 2900 PSIG

Reaction Time: 2 hr

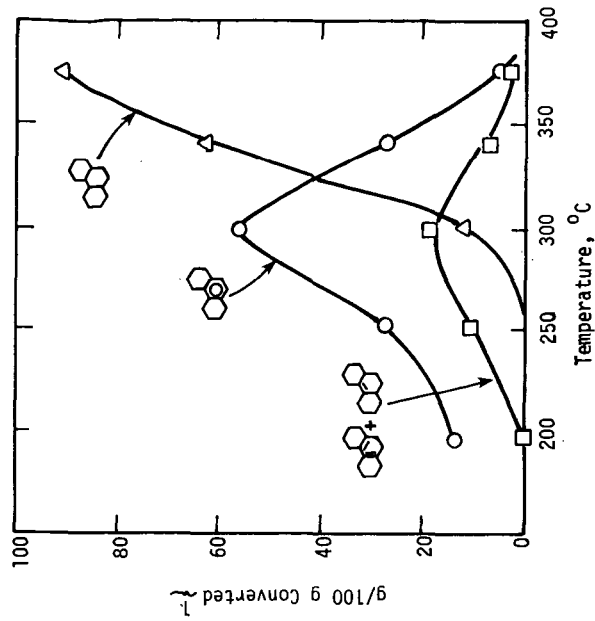


Fig. 2. Change in Product Composition from Hydrogenation of Phenanthrene (Stage B) as a Function of Temperature.

Catalyst: Sulfided Ni-W on Alumina

Pressure: 2900 PSIG

Reaction Time: 2 hr

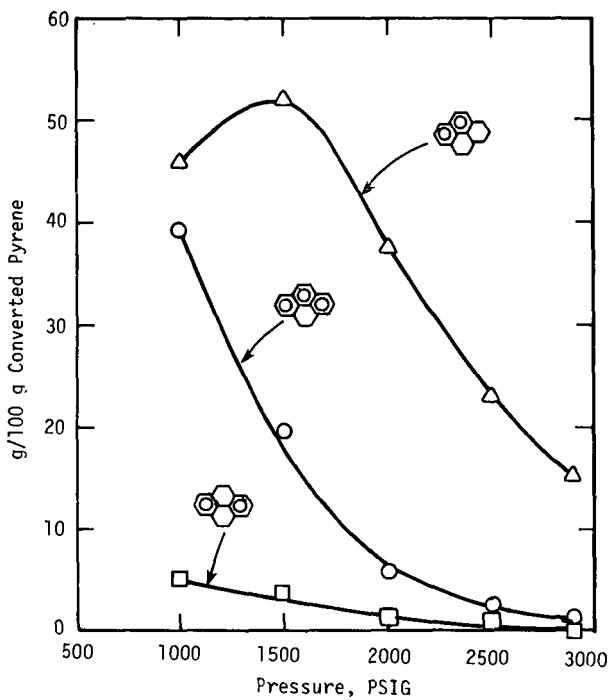


Fig. 4. Change in product composition from hydrogenation of pyrene as a function of pressure (Stage A).

Catalyst: Sulfided Ni-W on Alumina;

Reaction Temperature: 341°C;

Reaction Time: 3 hr.

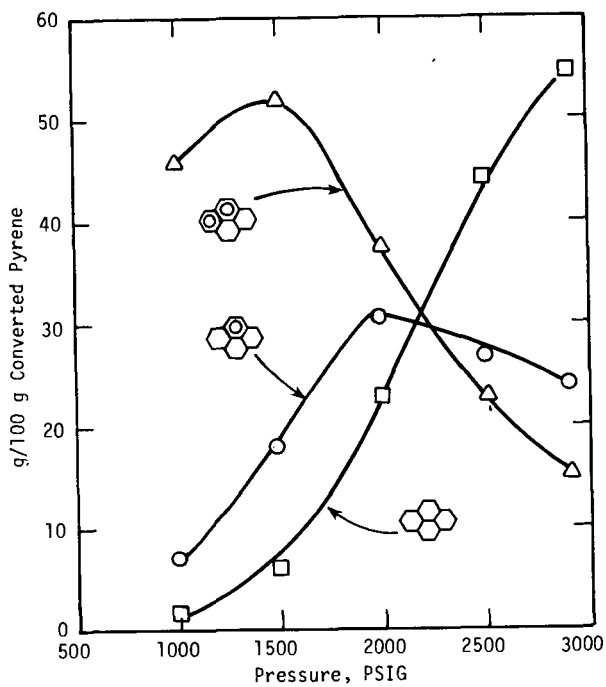


Fig. 5. Change in product composition from hydrogenation of pyrene as a function of pressure (Stage B).
Catalyst: Sulfided Ni-W on Alumina,

Reaction Temperature: 341°C;
Reaction Time: 3 hr.

STERIC EFFECTS IN THE HYDROGENATION-HYDRODENITROGENATION
OF ISOMERIC BENZOQUINOLINES CATALYZED BY SULFIDED
Ni-W/Al₂O₃

J. Shabtai*, L. Veluswamy, and A.G. Oblad

Department of Mining and Fuels Engineering,
University of Utah, Salt Lake City, Utah 84112

Mechanistic aspects of sulfide-catalyzed hydrodenitrogenation of N-heterocyclics, and in particular of condensed polycyclic systems, have been studied to a limited extent (1,2). Recently, this subject has attracted more interest and several significant kinetic studies have been reported (3,4). It is noteworthy, however, that so far very little attention has been paid to stereochemical aspects of hydrodenitrogenation processes. In order to obtain a first information on the possible importance of steric effects in such reactions, the hydrogenation-hydrodenitrogenation of two isomeric benzoquinolines, i.e. 5,6-benzoquinoline (1) and 7,8-benzoquinoline (2), was comparatively studied as a function of reaction temperature, hydrogen pressure, and sulfided catalyst type. Experiments were carried out in a semi-batch reactor, and products formed were identified and analyzed by a combination of gas chromatography, PMR, and mass spectrometry.

RESULTS AND DISCUSSION

Figures 1-4 summarize the change in product composition from hydrogenation of the two isomeric benzoquinolines as a function of reaction temperature in the range of 200-380°C, using a sulfided Ni-W/Al₂O₃ catalyst. As seen from Fig. 1, at temperatures below 250°C, the only product from 2 is 1,2,3,4-tetrahydro-7,8-benzoquinoline (3), derived by selective hydrogenation of the pyridine ring. With increase in temperature above 250°C, there is fast decrease in the yield of this intermediate compound, accompanied by formation of three other derivatives, i.e., 6-propyl-1,2,3,4-tetrahydronaphthalene(4), 2-propylnaphthalene(5), and 1,2,3,4,11,12,13,14-octahydro-7,8-benzoquinoline(6). The presence of compounds 5 and 6 indicates that hydrodenitrogenation of the primary product 3 could occur with or without preliminary hydrogenation of the end benzene ring. It is noted that the yield of 2-propylnaphthalene (5) reaches a maximum at ca 300°C and then decreases with increase in temperature, while the yield of 6-propyl-1,2,3,4-tetrahydronaphthalene(4) continues to increase up to 350°C and only then decreases with further increase in temperature (Fig. 1). This would indicate that 5 plays an important role as a precursor in the formation of 4. The latter could also be derived from 6, but the relatively low yield of this compound indicates that this alternative pathway is of lesser importance. At temperatures between 350-380° (Figure 2) the decrease in the concentration of 4 is accompanied by a corresponding increase in the yield of 2-propyldecalin(7), which is the final product of the hydrodenitrogenation process. At the relatively short contact time of 2 hr, at 341°C, the yield of 2-propyldecalin(7) is only 9%, and 6-propyl-1,2,3,4-tetrahydronaphthalene(4) is the major product (79%). However, at a contact time of 7 hr hydrogenation of 4 into 7 is essentially complete.

Patterns closely similar to those in Figs. 1 and 2 are found in the change of product composition as a function of hydrogen pressure.

Figures 3 and 4 summarize the change in product composition from hydrogenation of 5,6-benzoquinoline(1) as a function of reaction temperature. As seen, at temperatures around 200°C the single product observed is 1,2,3,4-tetrahydro-5,6-benzoquinoline (8), derived by fast, selective hydrogenation of the pyridine ring in 1. The indicated rate of this reaction is higher by at least one order of magnitude than that of the corresponding hydrogenation of 7,8-benzoquinoline(2) to 1,2,3,4-tetrahydro-7,8-benzoquinoline(3). At temperatures > 200°C there is gradual decrease in the

*Weizmann Institute of Science, Rehovot, Israel

concentration of 8, accompanied by formation of 1,2,3,4,11,12,13,14-octahydro-5,6-benzoquinoline(9). The yield of this second-step hydrogenation intermediate reaches a maximum around 300°C, and then decreases at higher temperature (Fig. 3). Further, this decrease in the yield of 9 (Fig. 4) is accompanied by a corresponding gradual increase in the yield of the hydrodenitrogenation product, 5-propyl-1,2,3,4-tetrahydronaphthalene(10), indicating that hydrodenitrogenation is mainly accomplished subsequent to the saturation of the end benzene ring. As seen from Fig. 4, at temperatures >300°C the product contains also small amounts (5-8%) of 1-propylnaphthalene (11), indicating that direct hydrodenitrogenation of the primary product 8 occurs to a minor extent. At reaction temperatures of ca 340-380° part of compound 10 is further hydrogenated to give 1-propyldecalin (12) which can be considered as the final product of the hydrodenitrogenation process. If the temperature is kept at ca 340°C and the reaction time is extended, or the pressure increased, compound 10 is converted largely into 12, without any significant extent of cracking. At ca 380°C, however, some cracking of compound 10 occurs to form 1,2,3,4-tetrahydrohaphthalene (Fig. 4).

The study of the reaction of 5,6-benzoquinoline(1) as a function of catalyst type indicates that there is no significant difference in the hydrogenation-hydrodenitrogenation activity of sulfided Ni-W/Al₂O₃ and Ni-Mo/Al₂O₃ catalysts.

The observed markedly slower hydrogenation of the pyridine ring in 7,8-benzoquinoline(1) can be ascribed to the steric hindrance effect of the 7,8-benzo group, which prevents edgewise adsorption of the pyridine ring to acidic sites on the catalyst surface by means of the nitrogen electron pair(5). In contrast, hindrance-free adsorption of this type, with consequent strong polarization and activation of the pyridine moiety is easily attained in the case of 5,6-benzoquinoline(1). Following the hydrogenation of the pyridine rings in 1 and 2 to give 1,2,3,4-tetrahydro-5,6-benzoquinoline(8) and 1,2,3,4-tetrahydro-7,8-benzoquinoline(3), respectively, there are marked differences in the subsequent reaction pathways leading to hydrodenitrogenation of these two isomeric intermediates, i.e. compound 3 undergoes direct hydrodenitrogenation to yield 2-propylnaphthalene(5), whereas 8 undergoes essentially complete hydrogenation of the end benzene ring, to form 1,2,3,4,11,12,13,14-octahydro-5,6-benzoquinoline(9), prior to the hydrogenolysis step (*vide supra*). This could be ascribed to differences in the steric characteristics of the intermediates involved. Examination of molecular models shows that in compound 3 the N-atom is in a *peri*-position relative to the aromatic H at C-14. This should cause some displacement of the nitrogen out of coplanarity with the aromatic system, and should facilitate the hydrogenolysis of the C-N bonds, leading to formation of 2-propylnaphthalene(5). In contrast, the 5,6-benzo group in 8 does not interact sterically with the hydrogenated pyridine ring, *viz.* in this case there is no destabilizing effect upon the C-N bonds. Consequently, 8 is hydrogenated to compound 9 prior to the hydrogenolysis step, which produces 5-propyl-1,2,3,4-tetrahydronaphthalene(10).

The results obtained indicate that the rate and depth of hydrodenitrogenation of coal-derived liquids may strongly depend on the steric characteristics of condensed N-heterocyclic-aromatic components, or of partially hydrogenated reaction intermediates formed during the process.

EXPERIMENTAL

The apparatus, as well as the experimental and analytical procedures were essentially the same as used in the preceding study of phenanthrene and pyrene hydrogenation.

REFERENCES

- (1) L.R. Veluswamy, Ph.D. Thesis, University of Utah, 1977.
- (2) D. Weisser and S. Landa, "Sulfide Catalysts, Their Properties and Applications", Pergamon Press, New York, 1973.
- (3) S.S. Shih, J.B. Katzer, H. Kwart, and A.B. Stiles, *Preprints*, Div. Petrol. Chem., A.C.S., 22, #3, 919 (1977), and references therein.

- (4) J.F. Coccheto, and C.N. Satterfield, *Ind. Eng. Chem., Proc. Des. Dev.* **15**, 272 (1976).
 (5) L.H. Klemm, J. Shabtai, and F.H.W. Lee, *J. Chromatog.*, **51**, 433 (1970).

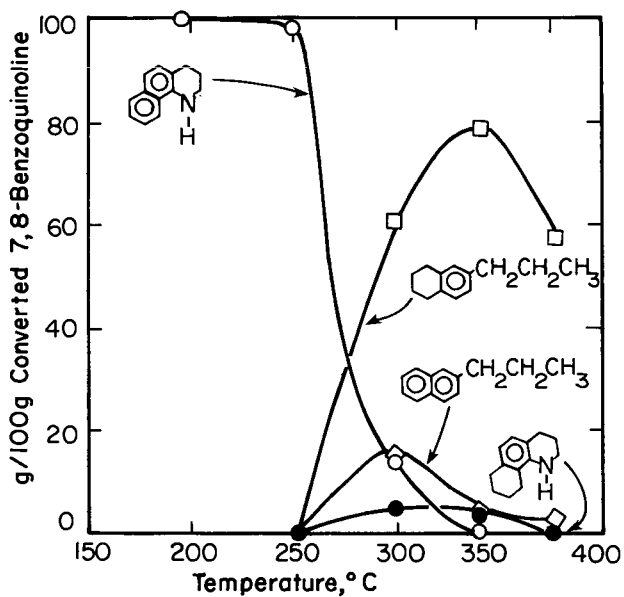


Fig. 1. Change in product composition from hydrodenitrogenation of 7,8-Benzoquinoline as a function of temperature (Stage A).

Catalyst: Sulfided Ni-W/Al₂O₃
 Pressure: 2900 psig;
 Reaction time: 2 hr.

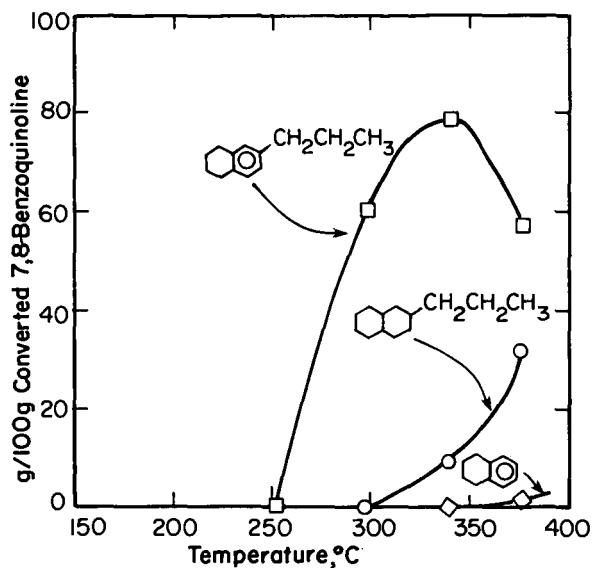


Fig. 2. Change in product composition from hydrodenitrogenation of 7,8-Benzoquinoline as a function of temperature (Stage B).

Catalyst: Sulfided Ni-W/Al₂O₃

Pressure: 2900 psig;

Reaction time: 2 hr.

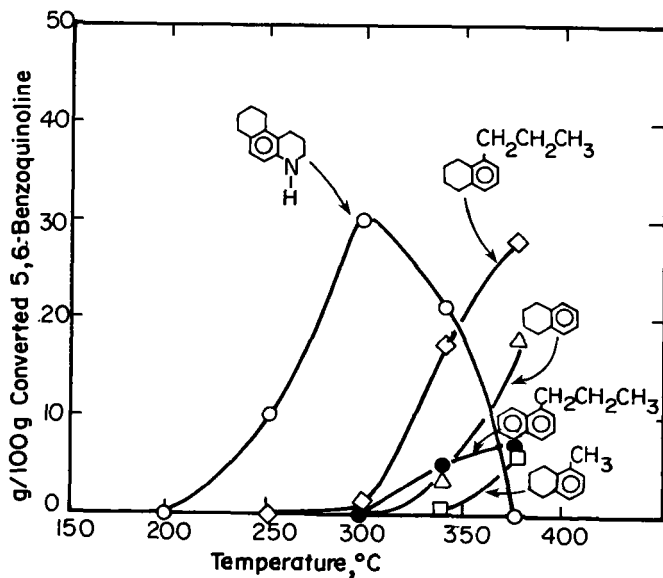


Fig. 4. Change in product composition from hydrodenitrogenation of 5,6-Benzoquinoline as a function of temperature (Stage B).

Catalyst: Sulfided Ni-W/Al₂O₃

Pressure: 2900 psig;

Reaction Time: 2 hrs.

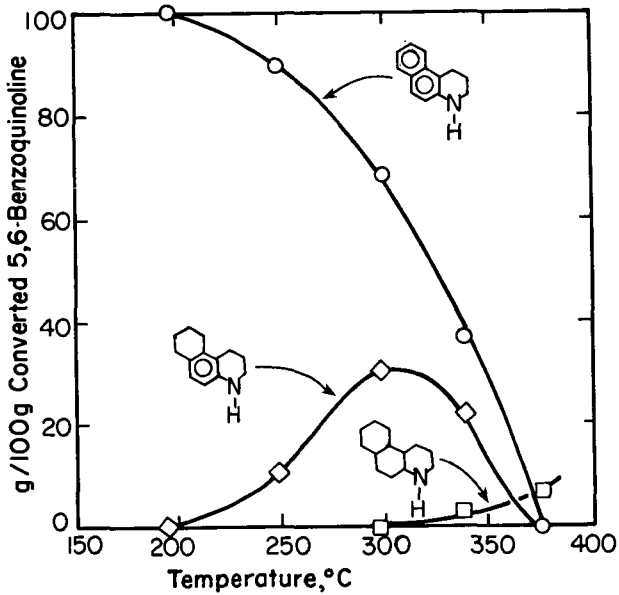


Fig. 3. Change in product composition from hydrodenitrogenation of 5,6-Benzoquinoline as a function of temperature (Stage A).

Catalyst: Sulfided Ni-W/Al₂O₃
 Pressure: 2900 psig;
 Reaction Time: 2 hrs.

UTILIZATION OF COAL-DERIVED LIQUID FUELS
IN A COMBUSTION TURBINE ENGINE

A. V. Cabal, M. J. Dabkowski, R. H. Heck, T. R. Stein
Mobil Research and Development Corporation, Paulsboro, New Jersey

R. M. Chamberlin, P. R. Mulik, P. P. Singh
Westinghouse Research Laboratories, Pittsburgh, Pennsylvania

W. C. Rovesti
Electric Power Research Institute, Palo Alto, California

1.0 INTRODUCTION

A number of processes are currently being developed on a large scale to produce liquid fuels from coal(1). It is anticipated that these coal liquids will supplement the ever decreasing supplies of petroleum crude now refined to produce gasoline, distillates, and residual fuel oil. However, detailed analysis of these coal liquids shows that they are more aromatic and contain more nitrogen and oxygen than do corresponding fractions from petroleum(2,3). In addition, coal liquids containing residual fractions high in asphaltenes, are incompatible when blended with typical petroleum fuels(4). Some preliminary results have been reported on the combustion of heavy coal liquids in residential boilers(5) and of synthetic jet fuel in aviation turbines(6).

The purpose of this work was to evaluate the use of raw and hydrotreated heavy distillate coal liquids from the Solvent Refined Coal (SRC) and H-Coal processes for use in heavy duty utility turbines. Presently, these turbines account for about nine percent of the installed power generation capacity in the U.S. Most of this capacity is dedicated to peak load generation where high reliability and the ability to put the capacity on-line rapidly are of critical importance. In the future, gas turbine capacity is expected to grow for intermediate and base load as high temperature combined cycle systems are introduced for power generation.

In considering fuels for use in these plants, certain fundamental combustion properties must be established in order to assure safe, efficient, and clean combustion of these fuels. Reliable utilization includes the determination of the operating limits of the combustion turbine with respect to corrosion, erosion, and deposition. Dependable operation of the combustor without the occurrence of flame-out, fouling or overheating of the combustor basket is also required for safe operation on coal-derived fuels. Furthermore, the time and power lost during shutdown to clean or repair hardware is an important factor to be considered. Finally, emissions from turbines burning coal-derived liquids must meet projected stringent EPA standards for oxides of sulfur and nitrogen.

Distillate coal liquids from the H-Coal and SRC processes were evaluated in a laboratory turbine combustor passage. The test fuels consisted of raw coal liquids and the same liquids hydroprocessed at several severity levels to produce additional test fuels of varying aromatic and nitrogen content. Each fuel was characterized by physical, chemical, and compositional analyses, and was evaluated in a small laboratory combustor at simulated commercial turbine

conditions. It should be noted here that due to the limited fuel quantity available, flows in this combustor were approximately 300 times smaller than those in full scale engines, so that caution should be exercised in interpreting the trends detected.

2.0 EXPERIMENTAL

2.1 HYDROPROCESSING OF COAL LIQUIDS

Samples of distillate coal liquids from the SRC pilot plant in Wilsonville, Alabama, and the H-Coal pilot plant in Trenton, New Jersey, were hydrotreated in a fixed-bed hydroprocessing pilot unit of the Mobil Research and Development Corporation. Commercial nickel-molybdenum and cobalt-molybdenum catalysts were employed for the H-Coal and SRC samples respectively. Each liquid was hydroprocessed at several sets of processing conditions. SRC recycle solvent processed at three different severities and H-Coal distillate processed at two different severities were selected for the tests. The entire liquid product was utilized for the SRC liquid, while the product from the H-Coal distillate was distilled to obtain a 350°F+ sample for the turbine tests.

Five gallons of each of the raw coal liquids, two gallons of each of the SRC hydrotreated liquids and three gallons each of the hydrotreated H-Coal liquids were sent to the Westinghouse Research Laboratories in Pittsburgh for testing in the small scale turbine combustor.

2.2 COMBUSTION TESTS

In order to evaluate the effect of burning coal-derived liquid fuels in commercial combustion turbines, it was necessary to reproduce as accurately as possible the gas residence time, temperature and aerodynamics of a combustor operating on conventional fuels. Because of the limited quantities of coal liquids available for these tests, a subscale combustor was designed and its performance evaluated on No. 2 distillate fuel to demonstrate combustion and emission characteristics representative of full scale combustors. Tests were performed at fuel flow rates of 1.6 gph with nominal operating conditions fixed as follows:

Combustion air pressure	3.0 atm
Combustion air temperature	500°F
Combustion air flow	0.1 lbs/sec
Fuel pressure	100 psig
Fuel flow	1.6 gph
Atomizing air pressure	70 psig
Atomizing air flow	3-5% of fuel flow
Reference velocity	7 ft/sec
Combustor exit temperature	1800°F
Primary zone residence time	~0.05 sec
Heat release rate	~1200 BTU/sec ft ³
Combustor cooling air flow	~40% total air
Diluent air flow	~20% total air
Combustor pressure drop	~3% of inlet pressure

The combustion test passage is shown in Figure 1. A bank of rotary compressors supplies compressed air, through an indirectly fired preheater, to the test passage. This system is designed to deliver 6.5 lb/sec of air at a pressure of 6 atm and a maximum temperature of 800°F. The desired quantity of combustion air is metered by a sharp edged orifice and forwarded to the combustor while the remaining air is bypassed and ultimately dumped near the end of the test passage. The test fuel is burned in a four-inch diameter combustor and the resultant hot gas flows through the passage past a back pressure valve which is partially closed to maintain a set pressure in the test passage. Thermocouples mounted on the combustor are used to measure and monitor the combustor wall temperature. Two thermocouples are placed directly after the combustor to measure the temperature of the hot combustion products. The exhaust products are then passed through a mixing device and an array of six thermocouples measures the mean bulk exhaust temperature of the gases. The temperatures of the thermocouples are recorded on a twenty-four point recorder. Further downstream, provisions exist for mounting test pins and for procuring samples of the exhaust gas for both emission analyses and smoke number determinations. A much larger sample flow rate than necessary is used to minimize sampling line interference and keep the residence time small. The sample gas is dried and filtered and passed to various analyzers.

In a typical run the combustion test passage was first fired with No. 2 fuel and allowed to run until the set standard test conditions were reached. The item with the longest time constant was the air preheater. It generally took about an hour before the combustion air temperature was up to the test design point. When the required combustion air temperature was reached the air flow through and the pressure in the combustion test passage was set at the desired level. The fuel flow was set to give an exhaust mixed temperature of approximately 1800°F. The combustion test passage was run until steady-state conditions were achieved and the base-line data for No. 2 fuel was obtained. Smoke Numbers, CO₂, CO, NO_x and unburned hydrocarbon levels in the exhaust were measured. A two color pyrometer was sighted through a view port to obtain the flame temperature in the primary zone.

By slowly turning off the No. 2 fuel oil needle valve and turning on the coal-derived liquid fuel valve a switchover with a negligible excursion from the set test condition was obtained. When the transition was complete, data were taken every fifteen minutes.

3.0 RESULTS AND DISCUSSION

3.1 HYDROPROCESSING RESULTS

The SRC recycle solvent was hydroprocessed over a commercial CoMo/Al₂O₃ catalyst (Cyanamid HDS-1441A) at three severity levels while the H-Coal distillate was hydroprocessed over a commercial NiMo/Al₂O₃ catalyst (Ketjen 153S) at two severity levels. Table I lists the properties of the feeds and hydroprocessed liquid products from these runs. Also shown in Table I are the processing conditions, yields of all products, and degree of heteroatom (O, N, S) removal. For the SRC recycle solvent, the pressure was held constant at 2500 psig for all three runs. The two highest severity runs were made at 715°F and space velocities of 0.8 and 0.4 consuming 2260 and 2800 SCF H₂/Bbl respectively. For the lowest severity run, the temperature was decreased to 678°F and the space

velocity increased to 2.9 LHSV. This resulted in a hydrogen consumption of 1140 SCF/Bbl. In all cases, the yield of C₆+ liquid product was greater than 98 %. The sulfur removal was greater than 85% for all three conditions while the oxygen and nitrogen removal varied from 30 to 95%.

The H-Coal distillate was processed at 1500 psig and 2.9 space velocity for the mild severity run and at 2500 psig and 0.5 space velocity for the high severity run resulting in chemical hydrogen consumptions of 570 and 1730 SCF/Bbl respectively. The temperature was approximately 700°F for both runs. Again, sulfur removal was greater than 95% while oxygen and nitrogen removal varied from 40 to 99%.

The raw and hydrotreated H-Coal distillate were distilled to remove the material boiling below 350°F. These, together with the as received raw and hydrotreated SRC recycle solvent, were used as the test fuels for the combustion tests. Table 2 lists the chemical and physical properties of the coal liquid fuels. Also shown are the properties of the No. 2 petroleum fuel used in the combustion tests. In general, the coal liquids have lower API gravities; are higher boiling; and contain less hydrogen (i.e., more aromatic) and more sulfur, nitrogen, and oxygen than the petroleum fuel. The trace metal elements are significant in the raw SRC recycle solvent and H-Coal distillate; hydroprocessing reduces these metals to levels equivalent to the No. 2 petroleum fuel. The raw SRC recycle solvent contains only 7.4 wt % hydrogen with 74 % of the carbon atoms in aromatic ring structures while the raw H-Coal distillate contains 9.1 wt % hydrogen and 55% aromatic carbon. The most severely hydroprocessed SRC recycle solvent and H-Coal distillate still contain 34 and 27% aromatic carbon respectively compared to 19% aromatic carbon in the No. 2 petroleum fuel. In addition, severe hydroprocessing increased the heat of combustion of the coal liquids equivalent to that of No. 2 fuel.

3.2 TURBINE ENGINE SIMULATION RESULTS

3.2a) Fuel Forwarding and Atomization

Due to the small quantities of fuel available, the constant pressure recirculating fuel system designed for use with the test passage could not be used. Instead a small tank pressurized with nitrogen was used as a source of constant pressure fuel. The fuel nozzle assembly chosen for these tests was the conventional air assist atomizing type used regularly with No. 2 fuel in the combustion test passage. This type nozzle consists of an orifice and a conical swirl element which produces a rapid rotation of the oil within the conical swirl chamber. The air to assist in atomization is brought close to the orifice by an air swirler where it mixes with the oil in a highly turbulent manner. The air swirler is kept in place by a cap that goes over the whole assembly. A second cap is used to keep the nozzle cool and to obtain an air flow pattern at the head of the combustor similar to that in a full scale combustor.

Studies were conducted to determine whether the regular fuel nozzle assembly designed for flow rates of ten to thirty gallons per hour would give good atomization in the one to two gallons per hour range if smaller fuel nozzles were employed. The small scale fuel nozzles were mounted in a suitable enclosure in the laboratory and No. 2 fuel was pumped into the nozzle at a pressure of 100 psi. The spray pattern was observed visually and photographs were taken.

It was found that the degree of atomization was better than that observed with the larger nozzles. No individual droplets or drippings could be seen and when the atomizing air was turned on the spray was effectively atomized. From this test, it was concluded that the hollow cone spray pattern produced by the small scale nozzle was suitable for the coal liquid combustion studies.

3.2b) Combustion and Emission Characteristics

The complete results of the combustion tests on the seven coal derived fuels are tabulated in Table 3. This table also presents data for the base No. 2 petroleum fuel. This fuel was run prior to the combustion of each coal-derived liquid and the values reported in Table 3 represent an average for all base line runs.

SRC Recycle Solvent:

SRC recycle solvent (7.4 wt % H) was the first coal liquid tested. The transition from No. 2 fuel to the SRC recycle solvent was fairly smooth and steady-state conditions were easily established in the combustion test passage. The most significant change observed was the sharp increase in NO_x emissions from the base line fuel. However, after about an hour of testing it became evident that the combustor walls were not maintaining a uniform temperature and were showing signs of erratic temperature fluctuations. Based on these observations, it was speculated that coke deposition and burning was taking place on the combustor walls. A small increase in smoke number at the time of fuel transition was observed but it eventually declined to values less than those observed for the No. 2 fuel. Apart from the difference cited above no other major observations were noted during the first one and one-half hours of testing with the recycle solvent. However, after about one and one-half hours of running it became evident that the combustor had burned out. The test passage housing the combustor developed a dull red hot spot and the test was terminated after 1.6 hours of running. On opening the test passage and observing the damage it was noted that a large portion of the combustor dome and a section of the combustor wall had burned through. Coke deposits were found both on the combustor wall and at the nozzle. The combustor can before and after this test is shown in Figures 2A and 2B.

The second fuel tested was the most severely hydrotreated recycle solvent (11.0 wt % H) using a new combustor can identical to the one that was destroyed. The base line test conducted with this combustor using No. 2 fuel produced higher NO_x and UHC readings. However, such variations in combustor emission characteristics are not unusual especially after replacing combustors. The transition from No. 2 fuel to the coal liquid was made smoothly and the test was conducted with no problems. After the test, the combustor was opened and no evidence of any coke deposits were found. The combustor wall showed no heat distress effects and this test also yielded fairly low smoke numbers.

A moderately hydroprocessed recycle solvent (10.3 wt % H) was the third fuel tested. The initial attempt to switch from No. 2 fuel to this hydroprocessed liquid was not very successful. It was found soon after the transition that the combustor wall temperature rose appreciably. This necessitated termination of the experiment and disassembly of the passage to check the fuel nozzle assembly and combustor can for coke formation. It was found that the nozzle was fouled by a small carbon deposit. The can was relatively clean except for two small spots where coke had deposited. Evidently, a disruption of the fuel spray pattern by the carbon deposited on the nozzle was responsible for the increase in wall temperature observed.

After cleaning the nozzle and can, a second attempt was made using this fuel. This time the transition from No. 2 fuel to the moderately hydro-processed recycle solvent (10.3 wt % H) was successful and the run was made without any difficulty. The wall temperatures as well as the NO_x emissions were substantially higher with this coal liquid compared to No. 2 fuel. On the other hand, smoke was satisfactory. After the run, the test passage was opened and examined for deposits. Evidence of coking on the can wall was noticed. A large piece of coke was found on the last step of the can and another attached to the dome. Other carbon deposits were also found on the wall of the test passage. In addition, the nozzle had moderate coke deposition.

The cleaned nozzle and can were put back in the test passage and the fourth fuel, a mildly hydrotreated recycle solvent, (8.9 wt % H), was tested. The transition from No. 2 fuel to the coal liquid was made and no major problems were encountered during this run. However, it was found that during the course of the run the combustor wall temperature continually increased from an initial level of 1265°F to 1810°F. Smoke levels as well as NO_x levels were higher than with No. 2 fuel. On termination of the run, the test passage was disassembled and a large coke piece was found lying in the passage. Further examination revealed that it had been attached to the nozzle and probably came off at the time the fuel was turned off. The coke piece remaining on the nozzle is shown in Figure 3.

H-Coal Distillate:

The first H-Coal fuel tested was the severely hydrotreated product (11.7 wt % H). The base line test data using No. 2 fuel oil indicated the same order of emissions as for the previous base line tests. The transition from No. 2 fuel to the severely hydrotreated H-Coal distillate was relatively smooth and the test was completed with no problems. After the run, the test passage was opened and the combustor examined. No evidence of any coke deposits on either the combustor can or on the nozzle were found. The fact that this fuel was clean-burning is also evidenced by the low smoke numbers measured (Table 3). The mildly hydrotreated H-Coal product (10.5 wt % H) was the second H-Coal fuel tested. Initially, the combustor was fired with No. 2 fuel and the base line operating characteristics obtained. The transition to the coal liquid was relatively smooth. It was found on transition that both the combustor wall temperatures and NO_x emissions increased slightly and then gradually decreased over the run. Otherwise, no significant changes were observed. After the run, the test passage was opened up and again examined. No evidence of any coke buildup either on the combustor can or on the nozzle was found.

The cleaned nozzle and the can were put back in the test passage and the third H-Coal fuel, raw H-Coal distillate (9.1 wt % H), was tested. The passage was started on No. 2 fuel and base line data were taken. The changeover from No. 2 fuel to raw H-Coal distillate was made without any problems. However, it was found that during the initial part of the test run the combustor wall temperature was much higher than with No. 2 fuel. Therefore, in order to prevent the likelihood of any damage to the combustor can the latter part of the test run was completed at a reduced exhaust gas temperature. The measured NO_x levels were higher in comparison to the No. 2 fuel. On termination of the test, the test passage was disassembled and, through the combustor can was found to be free of coke deposits, a buildup of coke around the nozzle was observed.

Data Analysis:

Raw coal liquid fuels differ from petroleum-derived fuels in that they are very aromatic and, as such, are hydrogen deficient. Hydrotreating of these fuels consists of catalytically adding chemical hydrogen to the fuel. Hydrogenation also decreases both the heteroatom and aromatic content of the liquid. Hence, the hydrogen content of the coal liquids is an important parameter and it is used as an index of fuel quality in the presentation of most of the emission and combustion results presented below.

In Figure 4, the emissions of CO₂, CO, UHC, NO_x and smoke are shown plotted against the weight percent hydrogen in the fuel. The CO₂ emissions (Figure 4A) in the exhaust do not show any appreciable trend with the hydrogen content of the fuel.

CO emissions, plotted in Figure 4B as a function of fuel hydrogen content, do not show any definite trend. However, the CO emissions are quite low and acceptable in spite of the small size of the combustor tested and the significant quenching effects observed under these conditions.

In Figure 4C, the unburned hydrocarbons are plotted as ppm of equivalent CH₄ in the dry exhaust gas. The emissions are again low and acceptable. The slight increase of UHC with increasing hydrogen content for the SRC derived fuels and not for the H-Coal derived fuels is probably due to the low boiling point constituents present in the former. These will tend to mix earlier and more rapidly with the can cooling air and subsequently be quenched out. The quenching effect is increased due to the combustor wall temperature being lower with the high hydrogen fuels.

In Figure 4D, the NO_x emissions are shown plotted against hydrogen in the fuel. These emissions decrease with increased hydrogen content of the fuel. This is as would be expected, for with increased hydrogenation of the coal liquids, the bound nitrogen content is decreased leading to reduced NO_x in the exhaust. An average value of NO_x emissions for No. 2 fuel for all the base line tests is 148 ppm as shown by the data point for this fuel. Thus, it is apparent that in order to meet the EPA proposed rules regarding NO_x emissions increased denitrogenation of coal liquids is desirable from the turbine designers point of view. However, even for No. 2 fuel (0.008 wt % Nitrogen) it is not easy to meet this EPA rule and turbine designers are looking for and working on alternative combustion systems. For example, if the premixed combustor concept is developed then other parameters, i.e., evaporation time, ignition delay, etc. will become of overriding importance rather than NO_x emissions.

The average smoke number measured is displayed in Figure 4E. Although low smoke numbers were indicated it is speculated that they were not really that low for all of the fuels tested. The reason for this thought is that when the raw SRC recycle solvent (7.4 wt % H) was tested the smoke increased immediately after the transfer to the coal-derived liquid and then started to decrease. Large carbon particles were found on the passage walls, etc., and the line connecting the smoke meter to the passage was found heavily laden with soot. The line, therefore, could be filtering out the smoke particles. A similar sudden increase in smoke and subsequent decrease was also observed on switching to the mildly hydrotreated SRC recycle solvent. Thus, the lined out readings listed in Table 3 are suspect for the SRC recycle solvent fuels.

For the H-Coal test series, the smoke sampling line was replaced with a short line avoiding sharp bends (to avoid carbon or moisture separation and subsequent carbon deposition) from the passage to the smoke meter and a much higher flow rate was used. It was observed during these series of tests that the smoke numbers observed varied from 0 to 1 for both the H-Coal fuels and No. 2 fuel; as such the maximum value of 1.0 was plotted on Figure 4E for H-Coal fuels.

The relative NO_x measured with coal-derived fuels divided by the base line NO_x measured with No. 2 fuel is plotted in Figure 5 as a function of the nitrogen content of the fuel. It should be noted that the NO_x values observed for the severely hydrotreated SRC recycle solvent (11.0 wt % H) and H-Coal distillates (10.5 and 11.7 wt % H) are lower than or equivalent to No. 2 fuel even though the coal liquids have a slightly higher nitrogen content. In these cases, the contribution due to fuel bound nitrogen is more than compensated for by the reduced thermal NO_x production rate. This is in agreement with the lower exhaust temperatures observed for these fuels (compared to No. 2 fuel). The average combustor wall temperature was always higher using the coal-derived fuels as compared to No. 2 fuel. This is due to the higher thermal radiation from these fuels. A possible exception, as shown below, to the previous comment on combustor wall temperatures is the most severely hydroprocessed H-Coal fuel (11.7 wt % H).

In Figure 6A, the average combustor wall temperature for SRC derived fuels is plotted from fifteen minutes before switchover to coal fuels to the time that either the wall temperature was unacceptable or the fuel was exhausted. Curve A is for the raw recycle solvent (7.4 wt % H) and as can be seen the wall temperature increased by almost 100°F after transfer to the coal liquid. Over the first part of the test the wall temperature increased by almost 200°F to 1680°F as compared with an average gas temperature of 1800°F. It is speculated that at this point the combustor was destroyed since the wall temperature began to behave in an erratic manner. Finally, after about ninety minutes of operation the destruction of the combustor became obvious due to the presence of a hot spot on the passage wall.

Curve B is for the least severely hydrotreated recycle solvent (8.9 wt % H). On switchover from No. 2 oil a similar increase to that observed for the raw recycle solvent was noted. This was possibly due to the onset of coking. A sharp increase in wall temperature at the termination of the test was also noted.

Curve C in Figure 6A is the data point observed with the aborted test using the moderately hydrotreated recycle solvent (10.3 wt % H). The sudden increase in wall temperature is hard to explain except to say that in the fuel transfer process the spray nozzle pattern was disturbed. On cleaning the nozzle and mounting it back in the passage a satisfactory run (Curve D) was obtained. However, the lined-out average combustor wall temperature for this coal liquid was about 250°F hotter than with the base No. 2 fuel.

Curve E was obtained using the severely hydrotreated recycle solvent (11.0 wt % H). It appeared to run slightly lower than No. 2 fuel on transfer but after fifteen minutes into the run the temperature increased by almost 200°F.

In Figure 6B, average combustor wall temperature data for the H-Coal fuels are presented in a manner similar to that utilized for the SRC fuels. Curve A is for the severely hydrotreated H-Coal distillate (11.7 wt % H). This curve indicates that no significant change in the can wall temperature occurred when utilizing this fuel as compared to the No. 2 fuel. Curve B is for the mildly hydrotreated H-Coal distillate (10.5 wt % H). It was found that a gradual increase in wall temperature occurred subsequent to the transfer from No. 2 oil. During the course of the experiment, the average wall temperature ran about 200°F hotter. Curve C is for the raw H-Coal distillate (9.1 wt % H). Subsequent to transfer from No. 2 fuel to the coal liquid the average can temperature rose from approximately 1180°F to 1675°F. To avoid possible damage to the combustor can if operation was continued at this condition, the fuel flow was reduced until the can temperature was in the safe operating regime.

3.2c) Corrosion, Erosion and Deposition

A test period of one-three hours is too short to obtain quantitative information on the long-term corrosion, erosion and deposition effects with these stocks. However, limited information was obtained by exposing two test specimens (pins) of turbine alloys (In 792 and X45) to the combustion products from the raw SRC recycle solvent. After running approximately two hours the test was terminated and the pins were examined with a scanning electron microscope. Figures 7A and 7B show general scans (500x) of the surfaces with arrows indicating possible deposits. Iron, silica, alumina, calcium, phosphorous, copper and chlorine were all detected in these scans. Longer runs are needed to quantify the ultimate effects of these deposits on turbine life. However, the analyses of the raw coal liquids (Table 2) and the depositions observed on the test pins during the two hour test indicate that trace metals may be a problem in the utilization of coal liquids. Although no test pins were used for the hydroprocessed liquids in this study, the analyses indicate a significant decrease in the level of trace contaminants after hydroprocessing. This should contribute to a longer turbine life.

4.0 CONCLUSION

Combustion tests on raw distillate coal liquids from the H-Coal and SRC processes resulted in significantly higher NO_x emissions and increased combustor wall temperatures than with a comparable boiling range No. 2 petroleum fuel. In addition, both of the raw coal liquid fuels were high in trace metal contents which could lead to excessive corrosion, erosion, and deposition of turbine blades in long-term service. Hydroprocessing was effective in producing fuels of lower fuel bound nitrogen content, higher hydrogen (i.e., lower aromaticity), and in eliminating most of the detrimental trace metals. The resulting hydroprocessed coal liquid fuels gave lower NO_x emissions in the turbine combustor. Combustor wall temperatures decreased with increasing hydrogen content (i.e., higher hydroprocessing severity). The most severely hydroprocessed H-Coal liquid showed no increase in NO_x nor increase in combustor wall temperature compared to a base No. 2 petroleum fuel. However, the most severely hydroprocessed SRC recycle solvent, requiring the addition of 2800 SCF H₂/Bbl, gave slightly higher NO_x and higher combustor wall temperatures than the base petroleum fuel.

Specific conclusions based on the results of this work are:

- H-Coal distillate and SRC recycle solvent can be readily forwarded and atomized.
- In general, the combustion wall temperature is higher when burning coal liquids than for a base No. 2 petroleum fuel. Combustor wall temperature decreases with increasing hydrogen content of hydroprocessed coal liquid. The most severely hydroprocessed H-Coal distillate showed no increase in wall temperature over the base petroleum fuel. On the other extreme, the raw SRC recycle solvent (7.4 wt % hydrogen) caused burn-out of the combustor can in less than two hours.
- NO_x emissions were 30% higher for the raw SRC recycle solvent (0.62 wt % fuel bound nitrogen) compared to the base petroleum fuel (0.008 wt % fuel bound nitrogen). Increasing hydroprocessing severity decreased the fuel bound nitrogen content and produced fuels with NO_x emissions equivalent to the petroleum fuel.
- Coke formation on the fuel nozzle used in the combustor is a major concern with raw and mildly hydroprocessed coal liquids. These deposits ranged from massive for the raw SRC recycle solvent to nil for the most severely hydroprocessed SRC and H-Coal liquids. The severity of deposits in full scale combustors may be less due to their higher flow rates.
- Unburned hydrocarbons emissions are acceptable, increasing slightly with increasing fuel hydrogen. CO emissions are acceptable.
- Smoke emissions were low for H-Coal liquids. Reliable smoke numbers could not be obtained for the SRC recycle solvent due to possible soot and coke formation in the sample line.
- Flame temperatures were not significantly different for any of the fuels tested as determined by optical pyrometry.

ACKNOWLEDGMENT

The work was performed under EPRI Project RP 361-2, jointly sponsored by Electric Power Research Institute and Mobil Research and Development Corporation.

REFERENCES

- (1) White, J. W., Sprague, R., McGrew, W., editors "Clean Fuels from Coal - Symposium II Papers", Institute of Gas Technology, June 23-27, 1975.
- (2) Callen, R. B., Bendoraitis, J. G., Simpson, C. A., Voltz, S. E., Ind. Eng. Chem., Prod. Res. Dev., 15, 223 (1976).
- (3) Schiller, J. E., Hydrocarbon Processing, 56 (1), 147 (1977).

- (4) Cabal, A. V., Voltz, S. E., Stein, T. R., Ind. Eng. Chem., Prod. Res. Dev., 16, 58 (1977).
- (5) Haebig, J. E., Davis, B. E., Dzuna, E. R., Preprint Div. Fuel Chemistry, Am. Chem. Soc., 20 (1), 203 (1975).
- (6) Nowack, C. J., Solash, J., Delfosse, R. J.; paper presented at 82nd National Meeting of American Institute of Chemical Engineers, Synthetic Liquid Fuels, Paper No. 19b, Atlantic City, N. J., August 29-September 1, 1976.

Table 1

Hydroprocessing Conditions and Yields for Upgrading SRC Recycle Solvent and H-Coal Distillate

Coal Liquid	SRC Recycle Solvent			H-Coal Distillate			
	Feed	Mild	Moderate	Severe	Feed	Mild	Severe
Hydroprocessing Conditions:*							
Pressure, psig	-	2500	2500	2500	-	1500	2500
LHSV	-	2.9	0.8	0.4	-	2.9	0.5
Temperature, °F	-	678	711	718	-	697	702
H ₂ Consumption, SCF/Bbl	-	1140	2260	2800	-	570	1730
Yields, wt %							
C ₁ -C ₃ Gas	-	0.16	0.11	0.42	-	0.04	0.20
C ₄	-	0.22	0.07	0.22	-	0.01	0.10
C ₅	-	0.11	0.05	0.12	-	0.03	0.06
C ₆ + Liquid	-	98.90	98.34	98.05	-	99.60	100.21
H ₂ S	-	0.34	0.38	0.39	-	0.13	0.14
NH ₃	-	0.22	0.62	0.73	-	0.18	0.46
H ₂ O	-	1.72	3.73	4.17	-	0.90	1.58
Heteroatom Removal, wt %							
Sulfur	-	85	97	98	-	95	99
Oxygen	-	39	85	95	-	54	93
Nitrogen	-	30	83	96	-	40	99
Total Liquid Product Properties							
Gravity, °API	5.3	13.0	19.5	23.4	17.1	21.3	28.0
Hydrogen, wt %	7.4	8.9	10.3	11.0	9.8	10.6	12.2
Sulfur, wt %	0.37	0.06	0.01	0.01	0.13	0.007	<0.002
Nitrogen, wt %	0.62	0.44	0.11	0.02	0.38	0.23	0.005
Oxygen, wt %	3.9	2.4	0.6	0.2	1.5	0.7	<0.1

*Catalysts: American Cyanamid HDS-1441A (CoMo) for SRC Recycle Solvent and Ketjen 153S (NiMo) for H-Coal Distillate.

Table 2
Properties of Combustor Test Fuels

Fuel	Petroleum No. 2 Fuel Oil	SRC Recycle Solvent			H-Coal Distillate		
		Raw	Mild	Hydrotreated Severe	Raw	Mild	Hydrotreated Severe
Sample No. Elemental Composition, wt %							
Hydrogen	12.9	7.4	8.9	10.3	11.0	10.5	11.7
Sulfur	0.093	0.37	0.06	0.01	0.01	<0.002	<0.002
Nitrogen	0.008	0.62	0.44	0.11	0.02	0.39	0.12
Oxygen	<0.1	3.9	2.4	0.6	0.2	1.5	0.3
Trace							
Contaminants, ppm wt							
Titanium	<1	20	1	1	1	<1	<1
Sodium	0.55	0.39	1.1	0.08	0.05	0.59	0.36
Potassium	0.37	0.19	0.22	0.03	0.01	0.08	0.04
Calcium	0.17	0.35	0.23	0.12	0.12	0.14	0.01
Vanadium	<0.1	0.9	<0.1	0.2	<0.1	0.1	0.1
Lead	-	0.9	0.9	0.6	0.3	< 1	< 1
Iron	0.2	61.0	2.3	1.5	3.4	10.3	5.7
Chloride	-	35.0	17.0	5.0	4.0	-	-
Properties							
Gravity, °API	33.6	5.3	13.0	19.5	23.4	14.7	18.8
Aromatic Carbon, %	19	74	66	46	34	55	42
Flash Point, °F	153	180	87	48	62	195	190
Heat of Combustion, BTU/lb	19500	16920	17730	18570	18900	18080	18630
KV, cs (at 100°F)	2.61	5.79	3.43	2.20	2.00	3.00	2.44
KV, cs (at 210°F)	1.09	1.48	1.10	0.93	0.90	-	-
Distillation, °F							
IBP	370	324	175	180	172	338	328
5%	412	375	303	216	207	366	357
10%	432	394	362	268	232	388	379
30%	474	446	413	402	387	406	402
50%	504	492	469	463	432	450	444
70%	540	564	534	525	495	503	493
90%	589	665	627	602	578	595	580
95%	611	709	681	649	630	659	632
EP	624	872	857	818	814	774	766

Table 3
Coal Liquids Combustion and Emission Results

Run No.	Fuel (wt % Hydrogen)		Air Flow, Lbs/Sec.	Fuel Flow, Lbs/Sec.	Atom. Air Flow, Lbs/Sec.	Comb. Press., Pslg.	Inlet Temp., °F	Exhaust Temp., °F	Flame Temp., °F	Emissions				
										CO, %	CO ₂ , Ppm	NO _x , Ppm	HC, Ppm	Smoke No.
	Petroleum No. 2 (12.9) *		0.12	0.0036	0.0054	52.6	512	1814	3543	5.3	33	148	18	1.5
1	Raw SRC Recycle Solvent (7.4)		0.088	0.0035	0.003	51.0	608	1783	3452	5.8	21	191	4.4	1.2
2	Severely Hydroprocessed SRC Rec. Solvent (11.0)		0.12	0.0037	0.006	51.5	502	1764	3207	5.7	33	149	30	2.0
3	Moderately Hydroprocessed SRC Rec. Solv. (10.3)		0.12	0.0036	0.006	53.0	503	1752	3564	5.3	28	166	12	1.5
4	Mildly Hydroprocessed SRC Rec. Solv. (8.9)		0.10	0.0040	0.005	51.0	493	1786	3422	5.9	13	194	0.5	3.5
5	Severely Hydroprocessed H-Coal Distillate (11.7)		0.13	0.0035	0.006	53.1	500	1781	3543	5.5	31	134	7	<1
6	Mildly Hydroprocessed H-Coal Distillate (10.5)		0.13	0.0037	0.006	53.0	527	1721	3614	5.7	41	150	7	<1
7	Raw H-Coal Distillate (9.1)		0.11	0.0037	0.006	52.4	520	1696	3577	6.1	39	181	10	<1

*Average value for all base line tests.

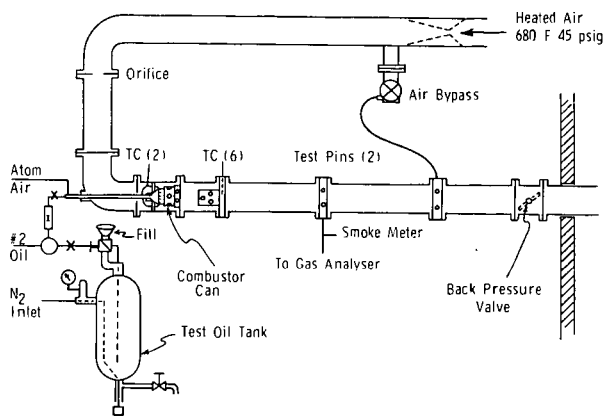


Figure 1. Combustor Test Passage



Figure 3. Coke Deposits on Fuel Nozzle Assembly After Test of Mildly Hydrotreated SRC Recycle Solvent (8.9 wt % Hydrogen)

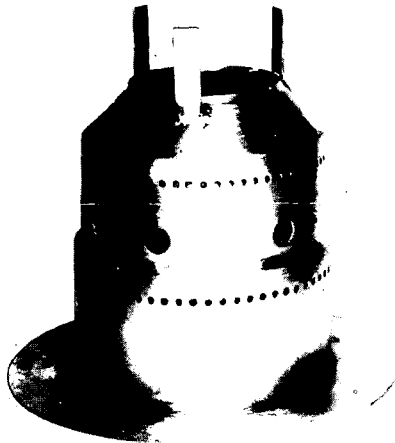


Figure 2a. Inconel X-750 Combustor Can Used for Combustion Tests

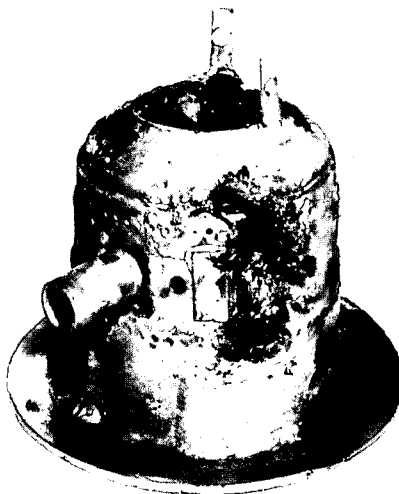
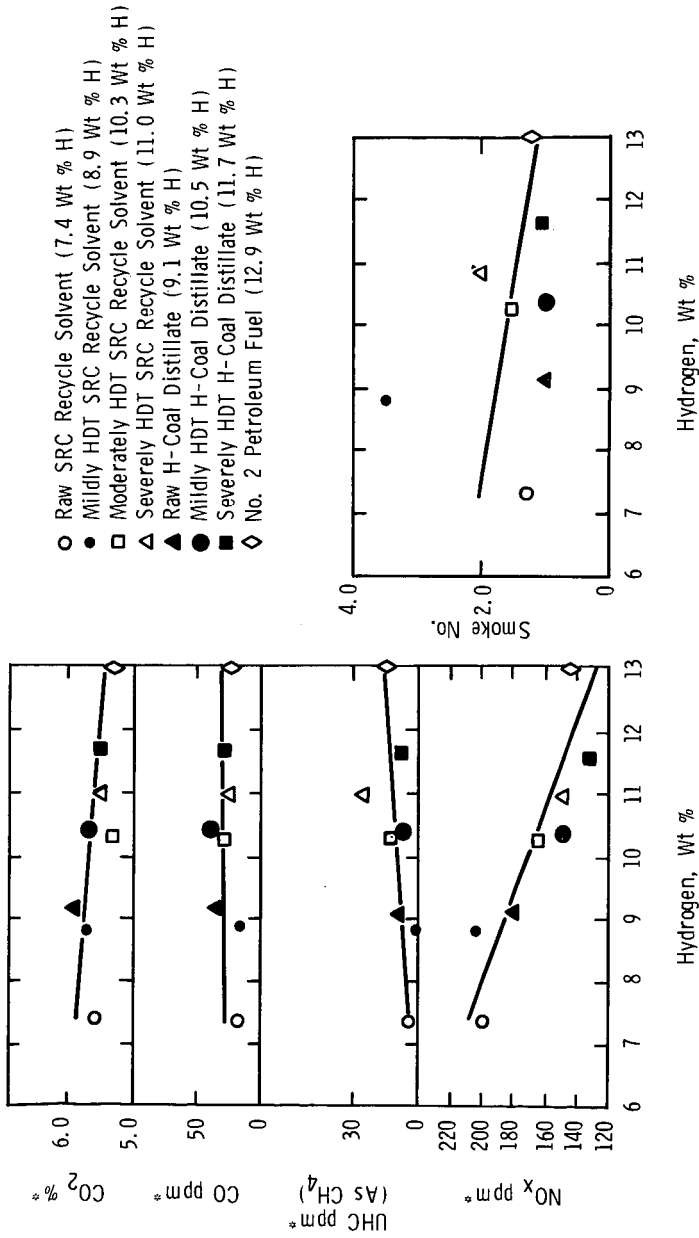


Figure 2b. Combustor Can (Side View) after Test of Raw SRC Recycle Solvent



* Based on Dry Volumetric Basis

Figure 4. Composition of Exhaust Gases as a Function of the Hydrogen Content of Fuels.

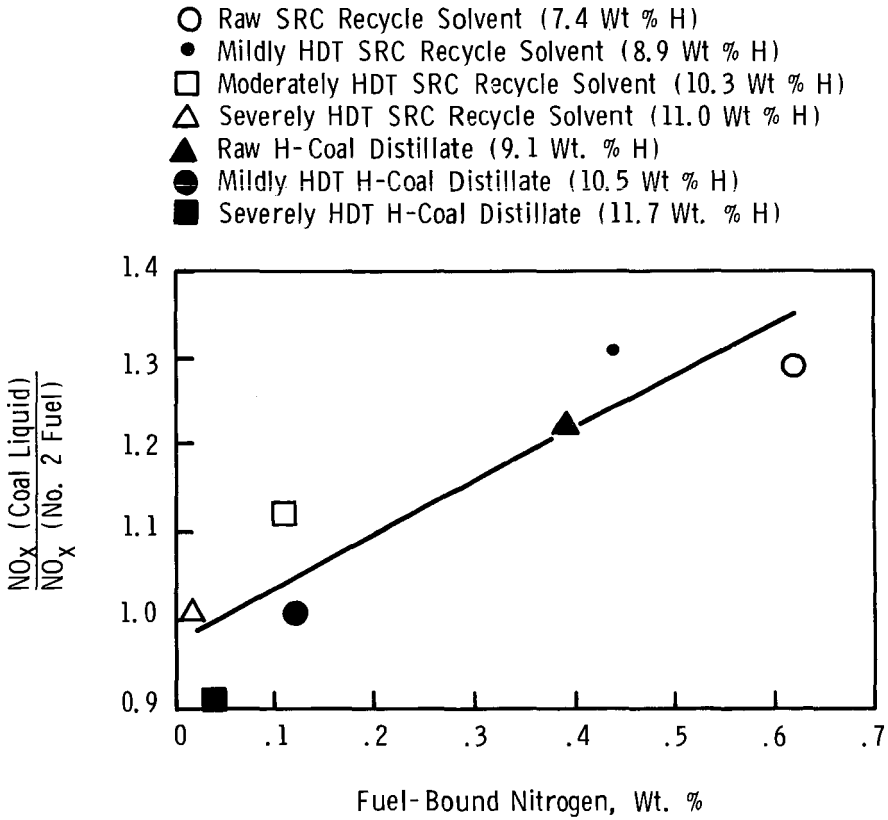


Figure 5. Relative NO_x Values as a Function of the Fuel-Bound Nitrogen Content of the Coal-Derived Fuels.

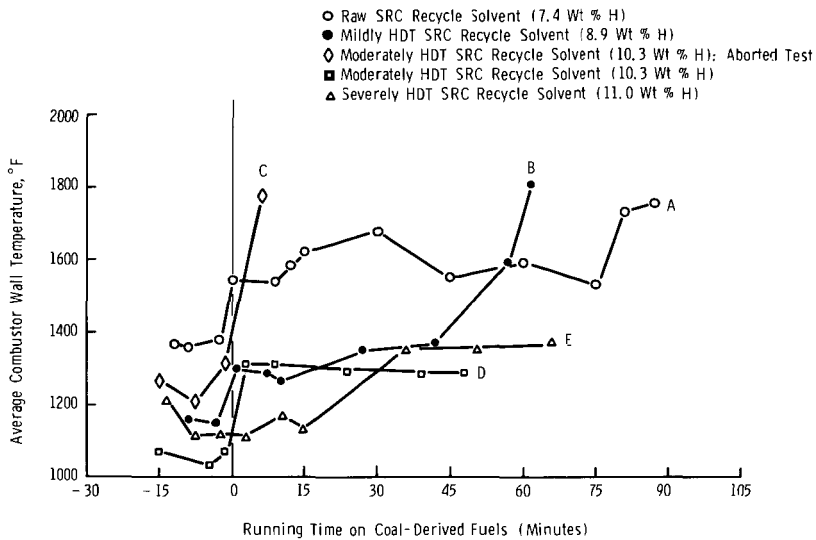


Figure 6A. Average Combustor Wall Temperature as a Function of Time for the SRC Recycle Solvent Fuels.

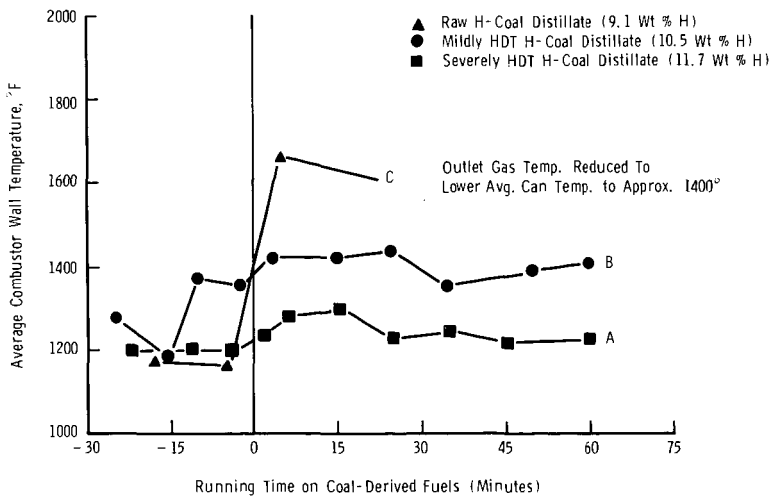


Figure 6B. Average Combustor Wall Temperature as a Function of Time for the H-Coal Fuels.

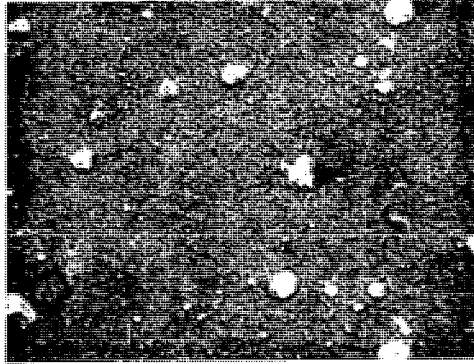


Figure 7a. General Scan of In 792 Surface (500X) Showing Surface Features and a Possible Deposit (Arrow)

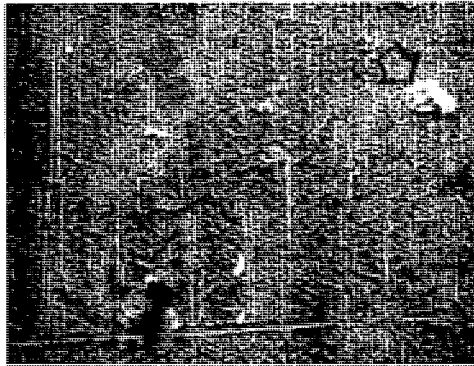


Figure 7b. General Scan of X45 Surface (500X) Showing Possible Deposit (Arrow)

COMBUSTION PROPERTIES OF COAL LIQUIDS FROM THE EXXON DONOR
SOLVENT PROCESS. C. W. Quinlan and C. W. Sigmund, Exxon
Research and Engineering Co., P. O. Box 4255, Baytown, Texas 77520

The Exxon Donor Solvent (EDS) Process converts bituminous, sub-bituminous and lignite coals into low sulfur liquid products. A brief description of the EDS process, the resulting liquid products and the flexibility of the EDS process to alter product distribution will be reviewed.

EDS liquid products produced from Illinois #6 bituminous coal were burned in a standard one gallon/hour home heating oil burner and a 50 HP industrial fuel oil boiler. Physical and chemical analyses and combustion emission data for both raw and hydrotreated coal liquids will be compared to conventional petroleum products.

Small Scale Evaluation of the Combustion
and Emission Characteristics of SRC Oil*

L. J. Muzio and J. K. Arand

KVB, Inc., 17332 Irvine Blvd., Tustin, CA 92680

INTRODUCTION

A potential alternate approach to the use of petroleum-based fuels in conventional combustion systems is liquid fuels derived from coal. In the present study, the combustion and emission characteristics of SRC fuel oil (a synthetic liquid fuel derived from coal) were evaluated in a laboratory boiler at a scale of 3 million Btu/hr. The facility was designed to simulate the combustion conditions found in large utility boilers. The synthetic liquid fuel was produced by the solvent refined coal process (1)** at the Department of Energy funded, and Gulf operated Solvent Refined Coal Pilot Plant.

The high nitrogen content (approximately 1% to 1.5% by weight) of the solvent refined coal oil (SRCO) is potentially a cause of high nitrogen oxides (NO_x) emissions from conventional combustion systems. It is known that in the combustion of fuels containing chemically bound nitrogen, a fraction of this nitrogen combines with oxygen in the air to form nitrogen oxides which are emitted as pollutants in the flue gases. One percent by weight of nitrogen in a typical fuel oil has a potential of producing about 1,300 ppm (dry) of nitrogen oxides in boiler flue gases at 3% excess oxygen if all nitrogen in the fuel is converted to nitrogen oxides. For conventional combustion configurations, approximately 20% to 50% of the fuel nitrogen is converted to NO_x with the percentage conversion decreasing as the nitrogen content of the fuel increases. Other variables such as excess air level and temperature play a lesser role (2,3). However, combustion modifications can be used to limit the conversion of fuel nitrogen to levels considerably less than the normally encountered 20% to 50%. These methods have been satisfactorily and repeatedly demonstrated on utility boilers. Additional nitrogen oxides are formed in high-temperature burner flame zones by oxidation of a small portion of the nitrogen in the combustion air.

The objective of this study was to document the combustion characteristics and the emissions of NO_x, SO_x, and particulates while burning SRC fuel oil in a boiler. In particular, the sensitivity of the emissions to load and excess air variations as well as air preheat, staged combustion, and flue gas recirculation were determined. These small scale test results can then be used to aid in assessing the performance of this fuel in a typical full scale utility boiler.

During the investigation, direct comparisons of the emission characteristics of the coal-derived fuel were made to those from a typical low-sulfur #6 fuel oil (0.24% nitrogen by weight) and a #2 oil with a nitrogen content of 0.024% by weight. Selected characteristics of the three fuel oils are shown in Table 1 along with the analysis of the western Kentucky coal from which the SRC oil was derived.

*Sponsored by Gulf Mineral Resources, Co., Denver, Colorado.

**Numbers in parentheses correspond to references at the end of the paper.

No attempt was made to explore the possible changes in storage and handling procedures which might be necessary to fire the coal-derived oil in a boiler originally equipped to fire residual, distillate oils or other fuels.

TABLE 1. TYPICAL FUEL CHARACTERISTICS

	Western Kentucky Coal	SRCO	#6 Oil	#2 Oil
C, wt %	72.2	86.6	86.61	86.82
H, wt %	5.0	8.38	12.25	12.69
N, wt %	1.4	1.12	0.24	0.024
S, wt %	3.6	0.26	0.28	0.11
Ash, wt %	10.5	0.008	0.016	0.003
O ₂ , wt % (by difference)	7.3	3.63	0.6	0.35
Gross Heat of Combustion, Btu/lb	13,150	17,040	19,150	19,190
API Gravity, 60 °F	--	8.3	2.3	32.3
Viscosity, SSU at 140 °F	--	35.6	324 (100°F)	34

APPARATUS

The basis of the combustion facility is a modified 80-HP firetube boiler which for these tests was fired at a rate of 3 million Btu/hr. The combustion modeling principles used in designing this facility to simulate combustion conditions in full scale utility boilers are discussed in Reference 4. The apparatus, shown in Figure 1, can be divided into five groups of components: (1) fuel supply, (2) air supply, (3) burner, (4) boiler furnace, and (5) instrumentation.

The oils were drawn from 55 gallon drums and delivered to the burner with a plunger type positive displacement metering pump. During tests with the #6 oil, the drums were heated to raise the oil to its pumping temperature and electrically heated to its firing temperature just upstream of the oil gun.

Air from an indirect-fired preheater passed through an insulated duct and a venturi meter to two valves which were then used to regulate the flow split between the burner air and second-stage air. For tests involving two-stage combustion, the second-stage air passed down an insulated duct, through another venturi meter, then to a perforated torus inside the combustion chamber. The secondary air was injected from this torus radially toward the axis of the combustion chamber through 32 orifices each 9/16" in diameter. Downstream of the burner air valve, the burner air flow was split into two ducts which enter the windbox from opposite sides. Recirculated flue gas, when used, was added to the combustion air upstream of the air preheater.

The burner used in this study was a scaled down version of a typical utility boiler oil burner. The burner utilizes a single 16-vane variable vane-angle air register for imparting swirl to the air flow. During these tests, the vanes were fixed at 20 deg. For the test results reported in this paper, a 30 deg. hollow cone mechanical type atomizer was used to deliver the oil to the combustion chamber. A more complete description of the burner can be found in Reference 5.

The boiler shell was an 80-HP Scotch dry-back type. At a firing rate of 3 million Btu/hr, the boiler's volumetric firing intensity was 38,500 Btu/hr-ft³, which is typical of oil-fired utility boilers. The steam produced by this boiler is vented at one atmosphere. Also, the laboratory boiler's combustion chamber was fitted with a stainless steel liner to give wall temperatures of about 800 °F, also typical of utility boilers.

The flue gas concentrations of NO, O₂, CO, and SO₂ were analyzed continuously using a Thermo Electron Corp. chemiluminescent nitric oxide analyzer, a Beckman Model 742 oxygen electrolytic analyzer, an Horiba Model PIR2000 nondispersive infrared carbon monoxide analyzer, and a Dupont 411 photometric analyzer for sulfur dioxide. Smoke levels were determined using a Bacharach smoke tester (ASTM D2156-65) and reported as Bacharach smoke spot numbers, the scale of which consists of a series of ten spots from 0 to 9. Total particulate loadings were determined using EPA Method 5.

TEST RESULTS

The combustion and emission characteristics of the SRC oil were evaluated over a range of operating parameters typical of large utility boilers. With the exception of the variable air preheat tests, the test results reported were obtained at a nominal condition of 550 °F combustion air temperature and a firing rate of 3 million Btu/hr. Results will be presented for the following methods of controlling NO:

reduced excess air	fuel blending
staged combustion	ammonia injection
flue gas recirculation	water injection for smoke suppression
reduced air preheat	fuel additives for smoke suppression

The methods listed in the left-hand column above were investigated early in the testing. It was found that while the combustion modifications were effective in controlling nitric oxide, they were limited in their degree of effectiveness due to a tendency of the SRCO to smoke when the control methods were fully implemented. This greater tendency of the SRC oil to smoke than the other fuels tested is thought to be due to the high aromatic content of the coal-derived liquid.

The effect of excess air and staged combustion on the nitric oxide emissions for the SRCO along with the #6 and #2 oil are shown in Figure 2. The open symbols are single stage combustion and the closed symbols are two-stage combustion tests. During the staged combustion tests, the overall excess air level was maintained at 16% (3% overall excess O₂). Figure 2 shows that for single-stage combustion of SRCO, the NO produced is very sensitive to the excess air level and significantly higher than the NO emissions from the #6 and #2 oil. For two-stage combustion, the NO produced reached a minimum at about 80% A_B (A_B is the theoretical air at the burner and A₀ is the overall theoretical air; for single stage combustion, A_B = A₀), with further reductions in burner air flow resulting in an increase in the NO emissions. This effect has been observed by other investigators (6-9) and is attributed to NO formation during combustion in the second stage region.

When flue gas recirculation, at rates up to 20%*, was utilized in conjunction with staged combustion, no further reductions in the nitric oxide emissions were observed. Gas recirculation could be expected to have greater effect in boilers in which the heat release per unit area is very high. These units would tend to have higher contribution of thermal NOx, and the use of recirculation would tend to reduce the thermal NO more noticeably.

The effect of the combustion air temperature on the NO emissions is shown in Figure 3 for the SRCO during single stage combustion. This data shows there is a strong effect of the combustion air temperature on the NO emissions (approximately 9 ppm/25 °F, at 120% excess air) and that the sensitivity of the NO emissions to combustion air temperature increases with an increase in the excess air level.

*Mass of recirculated flue gas/sum of combustion air and fuel flow.

Fuel blending was also investigated as a means of firing the SRCO while limiting the NO and particulate emissions. The NO emissions from blends of SRCO and #6 oil are shown in Figure 4 for both single and two stage combustion.

The homogeneous gas phase reduction of NO by ammonia injection into the SRCO combustion products was also investigated during this study. The reductions in NO which were achieved were in agreement with those obtained and reported with other fuels (10).

Fully implementing the nitric oxide control techniques with the SRC oil, in particular staged combustion, was limited by the tendency of the oil to form high levels of smoke and particulates. This effect is illustrated in Figure 5 where the Bacharach smoke numbers for single stage and two stage firing of the SRCO and #6 oil are compared. During the two stage tests the stack gas oxygen concentration was maintained at 3% (dry basis). For single stage firing, the data in Figure 5 show that the SRCO tends to smoke more than the #6, note that even at 40% excess air ($A_B = 140\%$), a No. 2 smoke spot is obtained. Although for excess air levels above about 10% to 15%, the performance is acceptable in this unit. A striking difference in the performance in the two fuels is seen for two stage combustion conditions. The #6 oil produced a gradual increase in the flue gas smoke level as the first stage was operated more fuel-rich. With the SRCO, large increases in the stack smoke levels were obtained even at moderate staging conditions; a smoke number of 9 was obtained when the burner was operated at $A_B = 102\%$. This smoking tendency is suspected to be a consequence of the high aromatic content of the SRCO which is on the order of about 60% based on the carbon-to-hydrogen ratio.

This trade-off in NO and particulate emissions is further illustrated in Figure 6. These results show that in this particular system, staged combustion cannot be used to reduce the NO emissions below the 1974 EPA New Source Performance Standards (NSPS) without exceeding the 1974 NSPS particulate standard. A similar situation will likely exist in a full size unit although, quantitatively, the trade-off may differ from the laboratory scale results.

A number of methods were tested to limit the smoke and particulate formation while implementing staged combustion with the SRCO. These included steam atomization instead of mechanical atomization, water injection into the combustion air, and the use of combustion improving fuel additives (alkali and manganese based).

In this unit the NO and smoke levels were similar for both steam atomization and mechanical atomization. Utilizing water injection into the combustion air (at a rate equal to 7% of the oil flow, volumetric basis) along with staged combustion, the nitric oxide emissions could be reduced to about 260 ppm prior to the onset of smoking. This is about 40 ppm lower than the levels previously obtained with staged combustion alone.

Fuel additives have been used with varying degrees of effectiveness to control smoke emissions from combustion systems. A recent study by Battelle (11) has shown certain additives to be effective in reducing smoke with single stage firing of #6 and #2 oil although the additives may result in an increase of total particulate loadings.

During the present study, various additives were used with the SRCO while firing in a staged combustion mode. The additives chosen for evaluation were: barium naphthenate, calcium naphthenate, and CI-2 (Ethyl Corp. proprietary, manganese based). The naphthenates produced the best results in the Battelle study (11), with CI-2 being less effective. In the present tests, the additive concentrations ranged from 50 to 350 ppm of the primary metal in the oil.

All three additives altered the smoking characteristics of the SRCO with both single stage and two stage combustion. However, the manganese-based additive was most effective in achieving low NO emissions (e.g., lower A_B at the burner). It was also found that the naphthenates altered the NO formation as well as the smoke formation. As a result, the NO emissions with staging were approximately 30 to 50 ppm higher than for the base condition without the naphthenate additive.

Particulate loadings were determined while operating under staged combustion conditions with the manganese-based additive (CI-2). The results of these tests are presented in Table 2.

TABLE 2. PARTICULATES AND NO EMISSIONS WITH SRCO AND CI-2 ADDITIVE

Test No.	1	2	3	4
Additive Concentration (ppm manganese)	0	0	0	345
A_0 Total Air, % Theor.	114.0	117.1	119.0	112.9
A_B Burner Air, % Theor.	114.0	103.0	83.0	77.0
Excess O_2 , % dry	2.7	3.2	3.5	2.5
CO, ppm dry	35	35	135	40
NO, ppm dry (corr to 3% O_2)	467	344	231	226
Smoke Number	0	3	< 9	8.5
Particulates, lb/MBtu	0.016	0.0168	0.344	0.068

As seen in Table 2, the additive was effective in limiting the particulate emissions during staged combustion. Also, the high particulate emission during Test No. 3 (staged combustion without the fuel additive) is due to carbon formation. Further, the amount of particulate contributed by the additive during Test No. 4 is apparently small. Based on the manganese content in the oil, the manganese would be expected to contribute to the particulates on the order of $0.014 \text{ lb}/10^6 \text{ Btu}$. The ash in the fuel contributes at most $0.004 \text{ lb}/\text{MBtu}$ to the flue gas particulate loading. It appears that the smoke emissions of the SRCO can be controlled on a larger unit with a fuel additive such as CI-2 when two stage or off-stoichiometric firing is used to reduce the nitric oxide emissions. It should be pointed out that tests were not conducted to determine the minimum additive concentration necessary to prevent smoke formation.

In general, the solvent refined coal oil appears to be a useful boiler fuel but its high nitrogen content dictates the need for applying NO control techniques to the system.

Since the SRCO is a very good solvent, compatibility of the oil with typical seals, O-rings, etc, used in boiler applications needs to be investigated.

The major problems encountered with the SRCO during this study were the high NOx emissions without NOx control methods coupled with the smoking tendency upon implementation of combustion modifications for NOx control. However, these small

scale tests show that control techniques are effective in reducing the NOx emissions. The carbon monoxide emissions were also found to be low during the tests and the SO₂ emissions were within the expected range based on the low-sulfur content of the SRCO.

In the laboratory tests, variables such as the location of second stage air addition, atomizer design, air swirl setting, etc. were not fully investigated. With a more extensive effort, lower NOx levels than demonstrated in this study may be possible on many large scale boilers. In addition, low NOx designs for boilers and burners may be expected to further aid in minimizing NO emissions from the combustion of the SRC oil.

CONCLUSIONS

The following specific conclusions can be drawn from the results of these small scale tests:

1. The combustion performance of the solvent refined coal oil is equivalent to that of typical utility type fuel oils. It is volatile (similar to #2 oil) and does not require preheating to achieve an acceptable viscosity for pumping or atomization.
2. Potential problems with furnace slagging and metal wastage occasionally encountered with coal combustion should be negligible with SRCO because of its low sulfur and ash contents.
3. Nitric oxide emissions could be maintained at about 0.4 lb/10⁶ Btu for the SRCO utilizing combustion conditions typical of many large utility boilers. This was accomplished with two-stage combustion and 3% excess oxygen in the flue gas. At this condition, low stack gas concentrations of carbon monoxide and particulates were maintained.
4. Nitric oxide emissions could be reduced below 0.3 lb/10⁶ Btu for the SRCO by
 - (1) blending the SRCO with other petroleum-based fuel oils having much lower fuel nitrogen and then firing with two stage combustion, or
 - (2) using a fuel additive containing manganese and then firing with two stage combustion.Acceptably low stack gas concentrations of carbon monoxide, smoke, and particulates were obtained.
5. Air preheat has a significant effect on the NOx emissions while firing SRCO.

REFERENCES

1. Schmid, D. K. and Jackson, D. M., "Recycle SRC Processing for Liquid and Solid Fuel," presented at the 4th Annual Interim Conference on Coal Gasification, Liquefaction, and Conversion to Electricity, University of Pittsburgh, Pittsburgh, PA, August 2-4, 1977.
2. Martin, G. B. and Berkau, E. E., "An Investigation of the Conversion of Various Fuel Nitrogen Compounds to Nitrogen Oxides in Oil Combustion," presented at the AIChE Meeting, Atlantic City, NJ, August 30, 1971.
3. Dzuna, G. R., "Combustion Tests on Shale Oil Fuels", presented at Central States Section/The Combustion Institute, April 1976.
4. Quan, V. et al., "Analytic Scaling of Flowfield and Nitric Oxide in Combustors," paper presented at EPA Pulverized Coal Combustion Seminar, June 1973.

5. Finney, C. S. and Sotter, J. G., "Pyrolytic Oil from Tree Bark: Its Production and Combustion Properties," AICHE Symposium Series No. 146, Vol. 71, June 1974.
6. Brown, R. A., Mason, H. B., Pershing, D. W., and Wendt, J.O.L., "Investigation of First and Second Stage Variables on Control of NO_x Emissions in a Pulverized Coal Furnace," presented at the 83rd National Meeting, AICHE, Houston, Texas, March 1977.
7. Pershing, D. W., Lee, J., and Wendt, J.O.L., "Fate of Coal Nitrogen Under Fuel Rich and Staged Combustion Conditions," presented at 70th Annual AICHE Meeting, New York, November 13-17, 1977.
8. Tenner, A. R., "Method and Apparatus for Reducing NO_x from Furnaces," United States Patent 4,021,186, May 3, 1977.
9. Arand, J. K., "Reduction of NO_x Through Staged Combustion in Combined Cycle Supplemental Boilers, Vol. II," EPRI Report 224, February 1975.
10. Muzio, L. J., Arand, J. K., and Teixeira, D. P., "Gas Phase Decomposition of Nitric Oxide in Combustion Products," Sixteenth Symposium (International) on Combustion, p. 199, The Combustion Institute, 1976.
11. Giammar, R. D. et al., "Experimental Evaluation of Fuel Oil Additives for Reducing Emissions and Increasing Efficiency of Boilers," FEA, PB 264 065, January 1977.

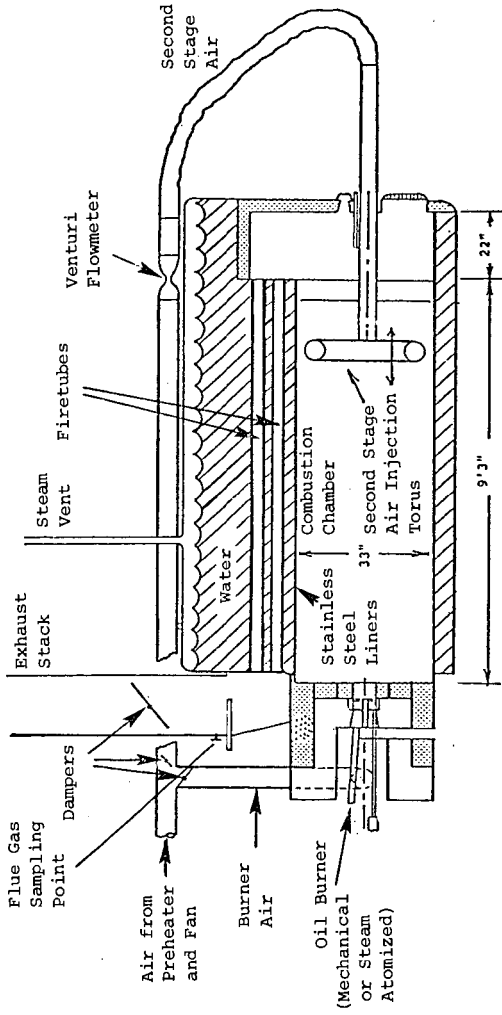


Figure 1. Schematic of 80 horsepower boiler.

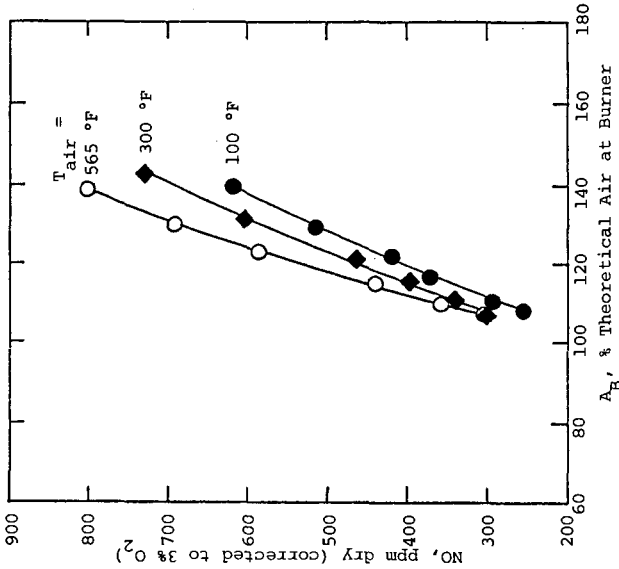


Figure 3. Effect of air preheat on NOx emissions from SRCO; single stage combustion.

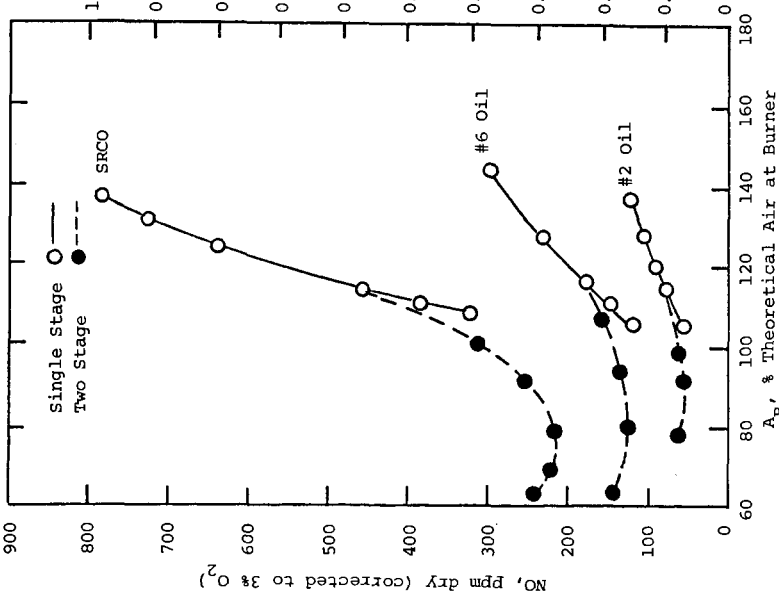


Figure 2. NOx emissions from SRCO, #6 oil, and #2 oil (single-stage and two-stage combustion).

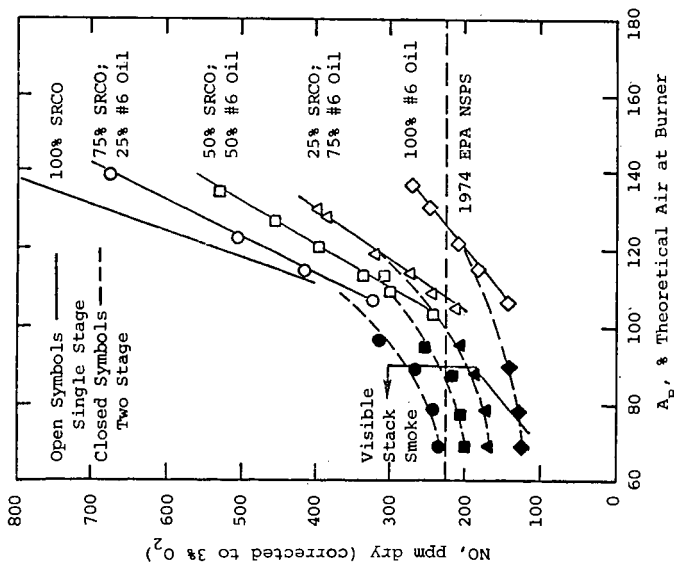


Figure 4. NO emissions from blends of SRCO and #6 oil.

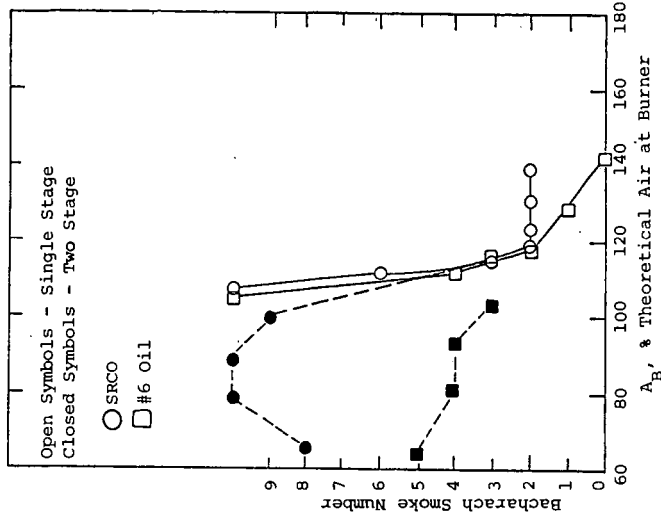


Figure 5. Smoke levels for SRCO and #6 oil.

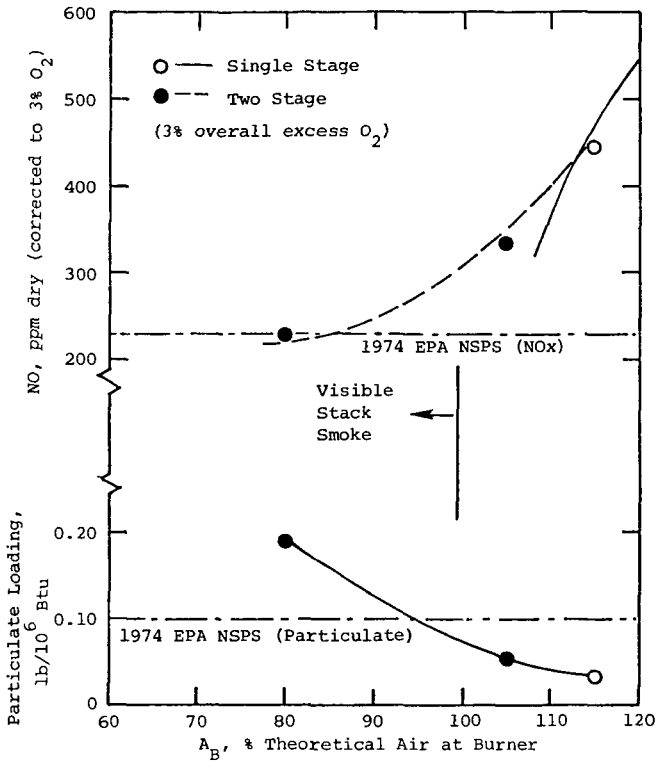


Figure 6. Particulate and NO emissions - SRCO.

Correlation of Fuel Nitrogen Conversion
to NOx During the Combustion of
Shale Oil Blends in a Utility Boiler

by

M. N. Mansour* and Melvin Gerstein**

In an oil fired utility boiler, nitric oxides are formed by two basic mechanisms; the thermal fixation of atmospheric nitrogen at elevated temperature within the flame zone, and the conversion of organically bound nitrogen in the fuel to NOx during the combustion process. NOx formation by thermal fixation, normally referred to as thermal NOx is essentially dependent upon flame temperature and concentration of oxygen and atmospheric nitrogen within the flame zone. The conversion of organically bound nitrogen to NOx, is directly related however, to the nitrogen content of the fuel.

Research on the reduction of nitrogen oxides produced from the reaction of atmospheric oxygen and nitrogen has been in progress for many years. More recently, attention has been given to the formation of nitrogen oxides from nitrogen compounds contained within the fuel. This source of nitrogen oxides becomes increasingly important as high nitrogen content fuels derived from shale and coal grow in use.

Recently, combustion tests have been conducted by Southern California Edison Company to evaluate NOx emission characteristics of shale oil (0.7% sulfur and 2% nitrogen) when burned in a utility boiler. The tests were conducted in a 45 MW Combustion Engineering boiler equipped with six

* Southern California Edison Company, P.O. Box 800, Rosemead, California 91770

** University of Southern California, School of Engineering, Mechanical Engineering Department, Los Angeles, California 90007.

face mounted oil burners each rated at 85 million Btu/hr. To comply with Air Quality Management District fuel sulfur content requirements shale oil was blended with low sulfur oil so that the average sulfur content of the fuel blend did not exceed 0.5%. Nitrogen content of the low sulfur fuel ranged between 0.2-0.25%. The NOx emission was evaluated when burning shale oil blends using both conventional and off-stoichiometric modes of combustion. The emission levels were determined for a developmental low NOx burner (LNB) and a conventional mechanical atomizing Peabody type burner.

As one might expect, NOx emission level increased as the quantity of shale derived oil in the blend was increased. The incremental increase in NOx emission level was proportional to the shale oil blending ratio which suggested that the increase in emissions was mainly caused by the high nitrogen concentration within the fuel. It was surprising to note, however, that the conversion efficiency of fuel nitrogen into NOx decreased, as shown in figure 1, as the fraction of shale oil (and fuel bound nitrogen) increased. It was also found that changing burner stoichiometry from fuel lean to rich achieved a substantial reduction in fuel nitrogen conversion rate, particularly in the case of the Peabody burner.

While a number of explanations can be offered to such result, it is felt that the reduction in nitrogen conversion efficiency illustrated in figure 1 appears to be the result of two competing processes. (a) The formation of NOx which increases as the nitrogen

containing shale oil content increases, and (b) the reduction of NOx by its reaction with high boiling hydrocarbons introduced with the shale oil and which is later released in the combustion process. The proposed model suggests that NOx is reduced after it is formed - a technique quite different from the classical approaches of slowing down NOx production by reducing the reaction temperature. The model assumes that the first process is a first order reaction with respect to fuel bound nitrogen and hence to the concentration of shale oil. The reduction process, however, is a second order reaction depending upon both NOx and the shale oil concentration, where the later term determines the residual hydrocarbon released late in the process. On this basis, the relative rate of NOx production would be given by:

$$\frac{1}{\text{NOx}} \frac{d(\text{NOx})}{dt} = k_1 (\text{shale oil}) - k_2 (\text{NOx}) (\text{shale oil})$$

or $\frac{d(\text{NOx})}{\text{NOx}(\text{shale oil})} = [k_1 - k_2 (\text{NOx})] dt$

A plot of $\frac{(\text{NOx})}{(\text{NOx})(\text{shale oil})}$ vs. (NOx) should be linear for equal residence times t. Such a plot is illustrated in figure 2 where a good correlation results.

The mechanism suggested here can lead to a general technique for reducing NOx formation by proper fuel blending. Burner design parameters could be also selected to enhance this delayed fuel vaporization while maintaining good burner flame stability. The

delayed vaporization of fuel, achieved through the use of high boiling temperature hydrocarbons or through optimization of burner design will then reduce NOx generated during the early phase of the combustion process. The concept is quite consistent with the general concept of staged combustion except that staging is accomplished by the natural separation processes occurring during fuel evaporation.

-
- * Southern California Edison Company
P. O. Box 800, Rosemead, California 91770
 - ** University of Southern California,
School of Engineering, Mechanical Engineering
Department, Los Angeles, California 90007

1d14b

R & D ON COMBUSTION OF SOLVENT REFINED COAL. W. Downs, C. L. Wagoner,
and R. C. Carr. Electric Power Research Institute, 3412 Hillview Ave.,
Palo Alto, Calif. 94305

The technical research for transportation, preparation, and combustion
of solvent refined coal that was performed by the Babcock and Wilcox Co.,
and Combustion Engineering to permit this new fuel to be utilized in a
utility boiler will be presented.

BURNING SOLVENT REFINED COAL. Richard D. McRanie, Southern Company Services, Inc.
Birmingham, Alabama 35202

Three thousand tons of solvent refined coal (SRC), manufactured at a Pittsburg & Midway plant in Tacoma, Washington, were successfully shipped to and burned in a Georgia Power Company 22.5 MW coal-fired utility boiler. The test demonstrated that SRC can be shipped in standard, open coal cars when treated with a commercially available coating spray to minimize blowing losses. Dust created in the conveyor system while loading and unloading the SRC can be controlled with a wetting agent spray. SRC was stored, pulverized, and burned with only minor modifications to existing power plant equipment. No modifications were necessary to the coal conveying equipment or the coal storage bunkers. The pulverizers were modified only to the extent that cold primary air was used and ball spring pressure was reduced. The only boiler modification was the installation of water-cooled, dual register burners. Emissions tests were performed while burning SRC and demonstrated that SRC is an acceptable fuel for meeting current EPA New Source Performance Standards for SO₂ and NO_x. The particulate emissions were greater than anticipated due largely to unburned carbon, a common problem with boilers of this vintage (1946). The particulate problem can be handled with a modern precipitator. Boiler efficiency tests were performed and indicate that efficiency when burning SRC is essentially the same as when burning coal. SRC was shown to be an exceptional boiler fuel from an operating standpoint. Soot-blowers, which normally have to be used 6-12 times a day, were not used at all during the 18-day test burn. The amount of flyash and bottom ash is significantly reduced. This will reduce ash system operating time and maintenance. The fact that SRC is brittle and easy to pulverize should reduce pulverizer maintenance.

ELECTRICITY INDUSTRY ASSESSMENT OF LOW BTU

GAS FOR POWER GENERATION

M. J. Gluckman and G. Quentin

Electric Power Research Institute

Prepared for presentation at the 175th National Meeting of the American Chemical Society, Division of Fuel Chemistry, Anaheim, California, March 1978.

Introduction

Gasification of coal with air or oxygen to produce low Btu (80-180 Btu/SCF) or intermediate Btu (200-350 Btu/SCF) gas represents a technology that is being given close scrutiny by the electric power utility industry. Recent legislation has precluded the use of natural gas as fuel for baseload power generation. Fuel oil is following closely on the heels of natural gas and will not be available to the electric utility industry for baseload applications in the near future. Coal, therefore, represents the last remaining fossil option available to the utility industry for baseload power generation in the last decade of the twentieth century and on, into the twenty first century.

Coincident with the fuel crunch, the utility industry is being confronted by an equally serious and difficult to handle environmental crunch. Coal gasification offers the potential for controlling SO_x, NO_x and particulate emissions in a far more efficient and less costly manner than can be achieved in pulverized coal boilers.

There are a variety of different ways in which the utility industry can employ the concept of coal gasification for electric power generation. Some of the more obvious options are shown in Table 1. It is important to realize that most of the cost and performance figures presented in Table 1 represent estimates generated by the authors. Specific engineering studies addressing each option in detail are currently underway or are in the process of being initiated. It must be pointed out, however, that the Electric Power Research Institute (EPRI) has been funding engineering and economic studies of gasification and combined cycle systems with Fluor Engineers and Constructors, Inc., Stone and Webster Engineering Corporation, R. M. Parsons, the Bechtel Corporation and C. F. Braun for many years. Therefore, the estimates presented in Table 1 are based on a substantial body of cost and performance information (1) (2) (3) (4) (5) (6) (7).

A cursory glance at Table 1 indicates that option 7 (methanol production) is too expensive to be considered for baseload fuel production. Considering the other six alternatives presented in Table 1, EPRI has identified options 5 and 6 (integrated gasification-combined cycle plants and integrated gasification-gas turbine power systems) as the most attractive options for baseload power generation. Table 2 presents cost and performance estimates for a variety of gasification-combined cycle power plants(3). It can be seen from this table that, in general, integrated gasification based power systems have the potential for more efficient operation and lower cost of electricity than conventional coal fired power plants with flue gas desulfurization. Keeping in mind the fact that integrated gasification based power plants have the potential to meet more stringent environmental control

TABLE 1
UTILITY OPTIONS FOR COAL GASIFICATION

<u>Option</u>	<u>Time Frame for Initial Introduction</u>	<u>Capital Requirements (a)</u>	<u>Heat Rate Btu/kWh</u>
1. Retrofitting existing gas/oil fired boilers	1982-1990	0.70 - 1.0	13,000 - 17,000
2. Retrofitting existing combined cycle equipment	1982-1990	0.60 - 0.9	12,500 - 15,000
3. Centralized gas production including distribution to a number of utility plants	1982-2000	(\$3.50/MMBtu - \$5.00/MMBtu) (b)	
4. Integrated gasification-steam boiler power plants	1982-2000	0.90 - 1.2	9,600 - 11,000
5. Integrated gasification-combined cycle power plants	1990-2000	0.85 - 1.1	8,400 - 9,500
6. Integrated gasification-gas turbine power plants	1995-2010	0.75 - 1.1	7,500 - 8,500
7. Syngas generation for methanol production	1982-2000	(\$5.00/MMBtu - \$7.00/MMBtu) (b)	

(a) A pulverized coal boiler with stack gas scrubbers costs 1.0.

(b) These selling prices based on utility financing, instantaneous 1976 dollars with no escalation, and coal costing \$1.00/MMBtu.

TABLE 2
COST ESTIMATES FOR GASIFICATION-COMBINED CYCLE POWER PLANTS

Gasifier	BGC Slagger		Lurgi (a)		Foster (b) wheeler		Texaco (b)		PC Boilers with Stack Gas Scrubbers (b)
	O ₂	CC (c)	Air	CC (c)	Air	CC (c)	O ₂	CC (c)	
Oxidant	O ₂		Air		Air		O ₂		Air
Power System	CC (c)		CC (c)		CC (c)		CC (c)		gas turbine (f)
Heat Rate, Btu/kWh	8,410		9,762		8,428		8,813		7,500 - 8,500
Make-up Water, gpm/1000MW	6,716		7,905		6,622		7,950		1,500 - 3,500
Total Capital Requirement, \$/kW (d)	711		906		705		816		650 - 900
Cost of Electricity, mills/kWh (e)	32.8		41.2		32.5		37.2		29 - 35

(a) Western coal

(b) Illinois #6 coal

(c) Combined cycles based on 2400°F gas turbine and 1450 p/900°F/1000°F steam turbine

(d) Mid-1976 dollars, no escalation, 1000MW, including construction loan interest, paid up royalties, initial catalyst and chemicals cost, preproduction costs, working capital, wet cooling towers, and emissions of < 1.2 lbs SO₂/MMBtu

(e) Coal costing \$1.00/MMBtu

(f) These estimates not included in Fluor report. Detailed performance and cost estimates for these systems are not yet available.

requirements as well as consuming substantially less water than conventional plants, it is evident why such systems represent a most attractive option for intermediate term baseload power generation.

It should be noted that gasification-combined cycle power systems have not yet been developed to the point where a utility company can order and install one with confidence. Such systems need to be demonstrated at sufficiently large scale (100MW - 200MW) such that the utility industry will have confidence that these plants can generate electricity reliably at the costs projected by the engineering studies.

Table 1 indicates that integrated baseload gasification-combined cycle power plants will only be available for utility use in the 1990's. A major question that must be addressed is: "Can coal gasification technology be utilized to alleviate utility needs for clean fuel prior to the 1990's?" The answer to this question has to be supplied in two parts i.e. a) an investigation of the development status of near term coal gasification technology and, b) identification of the technical possibilities and cost potential for rapid introduction of gasification systems for utility power generation.

Status of Near Term Gasifiers

Table 3 presents a summary of the development status of near term coal gasification options. It can be seen from this table that the suitability of the three commercially available gasifiers for combined cycle power generation is not good. Reasons for the lack of suitability range from low pressure operation to excessive by-product production - all of which result in an unacceptably high cost of electricity. It is the judgement of these authors that the gasifiers offering the greatest near term potential for combined cycle power generation at this time are the Texaco and Shell/Koppers partial oxidation units. This judgement is based on the extensive experience of the particular organizations in partial oxidation of oil, the simplicity of the gasifiers, their feedstock flexibility (ability to handle any coal as well as oil), absence of byproducts in the make gas, capability for high pressure operation, and the results of extensive engineering and economic studies. Information concerning the Shell/Koppers device is sparse. Texaco claims that based on successful operation of the 150 ton/day gasifier to be operated in Germany in 1978, they could scale-up to 1,000 tons coal/day capacity with confidence. Therefore, it appears that the Texaco gasification option could be available for utility use in the early 1980's.

Technical Possibilities for Near Term Introduction

It has already been mentioned that integrated gasification-combined cycle systems have not yet been demonstrated to the point where they would represent viable commercial options for the electric utility industry. Although all of the subsystems (i.e. gasifiers, gas clean-up modules, and combined cycles) have been operated at large scale independently, they have never been operated in an integrated mode for power production. Questions concerning the ability to control such integrated systems in a power plant environment can only be satisfactorily answered by building and operating an integrated test facility. One of the major control problems for these systems is posed by integrating the rapidly responding gas turbine and steam system with the more sluggish fuel production plant.

TABLE 3
DEVELOPMENT STATUS OF NEAR-TERM GASIFIERS

<u>Technology</u>	<u>Operational Mode</u>	<u>Suitability for Combined Cycle Operation</u>	<u>Current Status</u>	<u>Future</u>
Lurgi	Moving Bed	Intermediate	Commercial	---
Koppers Totzek	Entrained	Poor	Commercial	---
Winkler	Fluidized Bed	Poor	Commercial	---
Texaco	1 Stage Entrained	Good	15 ton/day running	150 ton/day 1978
Shell/Koppers	1 Stage Entrained	Good	5 ton/day running	160 ton/day 1978
BGC Slagger	Moving Bed	Intermediate - Good	360 ton/day running	1,000 ton/day 1983
Combustion Engineering	2 Stage Entrained	Intermediate	120 ton/day 1978	?

The influence of control problems on the operability of the system can be deemphasized by decoupling the fuel plant from the power equipment i.e. the gasification plant would operate independently of the power plant and would simply produce "over the fence" fuel gas to be consumed by the power system. The major penalty to be paid due to system decoupling is a significant decrease in power plant efficiency with a resultant increase in the cost of electricity (compare the heat rates of options 1 and 4 as well as options 2 and 5 from Table 1). The main advantage to be derived from decoupling the system is the fact that engineering for the first of such power plants could be started in 1978.

Non-integrated gasification based power systems of the type discussed above could most readily be achieved by retrofitting existing power plants which in the near future will have difficulty securing adequate fuel supplies i.e. gas and oil fired boilers as well as conventional combined cycle power plants. Such retrofitting can be accomplished in one of two different ways. Centralized gasification plants can be constructed to produce intermediate Btu fuel gas for limited distance pipeline distribution to one or more power plants. Alternatively, on-site retrofitting of individual power plants can be affected. The remainder of this paper will address the above two retrofit options and will attempt to highlight the advantages and disadvantages of each.

Centralized Gasification Plants

Large (10,000 tons/day coal - 30,000 tons/day coal) centralized gasification plants could be constructed to produce intermediate Btu gas for transmission to a number of power plants. Such gasification plants would have to produce 250 Btu/SCF to 300 Btu/SCF gas for two major reasons. First, the cost of pipeline distribution for low Btu gas is excessively high. Also, it has been shown by both Babcock and Wilcox (8) and Combustion Engineering (9) that retrofitting gas and oil fired boilers with fuel gas having a heating value much below 250 Btu/SCF will result in a rather serious derating of the existing boilers.

Some of the major advantages and disadvantages of large centralized gasification plants are shown in Table 4. Based on the high cost of fuel gas and the political and environmental problems associated with intermediate Btu gas transmission shown in Table 4, the option of large centralized gasification plants does not appear to offer sufficient economic incentive to be given major consideration by the electric utility industry at this time.

Gasification Plants For On-Site Retrofitting

There is an entire category of generic questions associated with on-site retrofitting of conventional steam electric power plants as well as combined cycle facilities with gasification systems that are site specific i.e. space availability, rail access, coal supply, environmental requirements (non degradation standards), etc. that need to be closely examined before any retrofit decision can be made. The purpose of this paper is to point out some of the technical opportunities and constraints associated with on-site retrofitting assuming that the answers to the above mentioned generic questions are all positive.

TABLE 4
ADVANTAGES AND DISADVANTAGES OF LARGE CENTRALIZED GASIFICATION PLANTS

ADVANTAGES

1. Fuel gas production decoupled from power plant operation.
2. Gasification plant can operate in steady state mode most of the time.
3. Transmission pipelines offer a minor form of fuel storage.
4. Ownership of the fuel production plant does not have to reside in the electric utility industry.
5. The gasification plant (and its emissions) can be remote from large population centers.

DISADVANTAGES

1. The cost of fuel will be high, i.e., \$3.50/MMBTU to \$5.00/MMBTU in 1976 dollars (see Table 1) and utility financing. If private financing is used, the gas cost will increase by approximately \$1.00/MMBTU.
2. Environmental and Right of Way problems associated with the installation of large underground pipelines.
3. Safety problems associated with the transmission of gases containing high concentrations of carbon monoxide.
4. Ownership If the electric utility industry does not own the gasification plant, the owner will require long term take-or-pay fuel contracts to insure the integrity of the large capital investment required.

A. Retrofitting Existing Gas and Oil Fired Boilers

In order to fire coal derived fuel gas in an existing boiler designed for natural gas or oil firing, Combustion Engineering (9) and Babcock and Wilcox (8) both claim that the heating value of the gas should be above 250 Btu/SCF in order not to derate the steaming capacity of the boiler. Summary results of the Combustion Engineering (9) study are shown in Table 5. The heating value requirement of the gas employed for this situation dictates that the gasifier be oxygen blown. As fuel gas for this application is not needed at high pressure, an atmospheric pressure gasifier could be utilized. Therefore, for boiler retrofitting, either an oxygen blown Texaco gasifier or an oxygen blown Combustion Engineering gasifier could be employed. EPRI has retained the Bechtel Power Corporation to study the cost of electricity from this type of retrofit.

It is the opinion of these authors that the electricity generated by this technique will be expensive due primarily to the excessively high heat rates anticipated for such systems (see Table 1, option 1). Such heat rates are unavoidable for decoupled systems as the efficiency of the conversion of coal to intermediate Btu gas ranges from 65% to 75%. These gasification efficiencies are somewhat lower than the much quoted cold gas efficiencies as they include the firing of up to 10% of the clean fuel gas produced to supplement superheated steam requirements for the air separation plant or to superheat steam generated in the gas coolers following the gasifier. Dividing the existing steam plant heat rates (ranging from 9,500 Btu/kWh to 11,000 Btu/kWh) by the fuel production efficiencies (65% to 75%) results in overall system heat rates in the range 13,000 Btu/kWh to 17,000 Btu/kWh. Not only are these high heat rates costly from a fuel consumption point of view, they will also require excessively high capital expenditures as the gasification plant needed to produce 1000 MW at a heat rate of 17,000 Btu/kWh will be twice the size of the same capacity system having a heat rate of 8,500 Btu/kWh (i.e. an integrated gasification-combined cycle power plant).

Notwithstanding the promise of substantial tax incentives by the current administration for this type of retrofit, the fuel and capital utilization efficiencies are sufficiently poor to render this option of low long term interest to the bulk of the electric utility industry.

B. Retrofitting Existing Oil Fired Combined Cycles

Most of the statements made concerning the retrofit of existing steam electric power plants apply to the decoupled retrofitting of oil fired combined cycle equipment with three differences:

- (i) For this application, a pressurized gasifier such as the Texaco unit would be preferred as fuel gas must be delivered to the gas turbine combustor inlet system at pressures ranging from 230 psia to 280 psia.
- (ii) Air or oxygen blowing of the gasifier would be acceptable as gas turbine combustors can be modified to fire either low Btu gas or intermediate Btu gas. This statement must be treated with extreme caution. If, for example, the gasifier is air blown and the air is not extracted from the gas turbine air compressor, the turbine would suffer a major derating due to the mismatch between compressor and expansion turbine sections resulting from the high mass flow rate of low Btu fuel gas. Modification of an existing gas turbine for air extraction is not simple and could result in a high capital cost.

TABLE 5

SUMMARY RESULTS OF COMBUSTION ENGINEERING BOILER RETROFIT STUDY (9)

With existing steam generating unit and auxiliary components, the approximate maximum rating that can be achieved firing low BTU gas with only minor modifications to the windbox and firing system equipment is:

Fuel Gas HHV	Original Design Fuel	
	Oil	Gas
396 BTU/SCF	100%	100%
292 BTU/SCF	100%	100%
179 BTU/SCF	70%	70%
128 BTU/SCF	65%	60%
105 BTU/SCF	50%	50%

(iii) The overall system heat rate would be approximately 10% better than that for the steam electric power plant due to the higher efficiency of the combined cycle system (see Table 1, Option 2).

Although the decoupled retrofit of existing combined cycle systems appears to be somewhat more attractive from a cost and heat rate point of view than the retrofit of existing steam electric power plants, the heat rates and capital requirement estimates shown in Table 1 are still too high to make this a high priority option for the electric utility industry.

To this point, the entire retrofiting discussion has been based on the premise that the power production plant (i.e. the steam boiler or the combined cycle system) has already been constructed and operated at a specific site. Based on the preceding discussions, none of the retrofit scenarios involving total decoupling of the gasification plant and the power system appears to offer an attractive baseload option to the electric utility industry.

There are, however, at least two additional possibilities for retrofiting combined cycle power plants with gasification systems that offer the potential for lower heat rates and lower costs than the decoupled retrofit discussed previously. These new situations will be termed integrated retrofits.

Potential for Integrated Retrofits

Two types of integrated retrofit possibilities will be discussed i.e.

- 1) Constructing the gasification plant first and firing the clean fuel gas in an existing boiler. When the gasification plant has been demonstrated to operate reliably and efficiently, it can be retrofit and integrated with a combined cycle power plant.
- 2) Constructing an oil fired combined cycle power plant initially to be retrofit and integrated with a gasification plant at some later date.

A) Integrated Retrofit - Gasification Plant Initially

The major attraction of this option is that it provides for the earliest possible introduction of coal gasification as a source of clean fuel for the utility industry without the disadvantage of having to suffer major thermal inefficiencies for the entire life of the gasification plant.

This could be achieved technically at an early time by constructing a self sufficient oxygen blown Texaco gasification plant at a utility site having the necessary space requirements as well as an oil or gas fired steam electric power plant. For the initial design, steam to power the air separation plant as well as the oxygen compressors would be generated in the gasifier gas coolers and could then be superheated in a furnace fired with clean fuel gas. The clean intermediate Btu fuel gas produced could be fired in the existing boiler for power production (at an overall system heat rate of 13,000 Btu/kWh to 17,000 Btu/kWh). The purpose of this phase of the project would be to demonstrate the operability of the gasification - gas clean-up system under utility operating conditions.

The second phase of the project would involve retrofitting and integrating the gasification plant with a combined cycle system. Major integration features would include:

- superheating steam produced in the gasification gas coolers in the new heat recovery steam generator (HRSG) for introduction into the new steam turbine.

- extraction of steam from the new steam turbine or HRSG to power the air separation plant, oxygen compressors and gas clean-up system.
- possibly reheating clean fuel gas in the new HRSG
- supplying hot boiler feed water from the new HRSG to the gasifier gas coolers.

The major purpose of this phase of the project would be to demonstrate the operability of an integrated gasification-combined cycle power plant (the major incentive for coal gasification) under utility operating conditions.

Some of the advantages and disadvantages associated with this option are shown in Table 6. In summary, this form of retrofit provides for the earliest low risk introduction of coal gasification for environmentally acceptable electric power generation. The penalties to be paid are high cost, limited capacity and a relatively short plant life.

B. Integrated Retrofit - Combined Cycle Plant First

The major attraction of this option is that it provides for extremely rapid introduction of new oil fired baseload capacity without any initial risk being taken concerning the integrability and operability of gasification-combined cycle power plants.

Initially, conventional oil fired combined cycle equipment would be installed. Salable electricity could be produced approximately three years after initiation of project engineering. At some later date, after demonstration of the viability of integrated gasification-combined cycle power plants, the existing combined cycle facility could be retrofit and integrated with a coal gasification plant. One of the major advantages of this scenario is based on the fact that knowing that the integrated retrofit is to take place some time in the future, the initially installed combined cycle plant could be designed to minimize the cost of the future retrofit. Some key technical questions concerning this type of retrofit are:

- can the gas turbine combustor cans be designed for dual fuel capability i.e. for firing oil initially and switching to low Btu or intermediate Btu gas at some later time? Such combustors are currently being designed by General Electric.
- If the gasification plant is to be air blown, can the gas turbine wrapper be designed to accommodate air extraction at some later date? If not, what would be the cost of changing the wrapper at the time of the retrofit?
- If the gasification plant is to be oxygen blown, will the compressor/turbine mismatch after retrofitting result in a significant derating of the gas turbine?
- A conventional combined cycle HRSG is balanced with respect to steam generation. For the integrated retrofit with a Texaco gasification plant, much interchange of boiler feed water and steam must take place between the gasification plant and the HRSG. Can the HRSG be designed initially to accommodate the retrofit? If not, what type of modifications will have to be made to the existing HRSG? Will it be cheaper to modify the existing HRSG than to scrap it and construct a new HRSG?

TABLE 6

ADVANTAGES AND DISADVANTAGES OF INTEGRATED RETROFIT - GASIFICATION PLANT FIRST

<u>Advantages</u>	<u>Disadvantages</u>
<p>1. Allows for the earliest possible introduction and demonstration of coal gasification technology for electric power production.</p> <p>2. The integrated retrofit provides an opportunity to dramatically improve the heat rate of the initially installed plant at an early date.</p> <p>3. Provides for the lowest risk demonstration of an integrated gasification-combined cycle power plant as the gasification plant will have been debugged prior to operation in an integrated mode.</p> <p>4. Project risk can be further minimized by designing the Texaco gasification plant to fire coal, coke and high sulfur heavy oil providing extreme fuel flexibility (risk is lowered as the Texaco gasifier has been commercially proven for oil firing).</p>	<p>1. Limited site availability as a site is required having an existing gas or oil fired boiler with sufficient space for the new project.</p> <p>2. Limited ultimate capacity of 100MW-150MW dictated by prudent engineering scale-up of gasification plant.</p> <p>3. Anticipated project cost will be higher than the cost of building an integrated system initially due to the two phase nature of the project.</p> <p>4. The resulting integrated plant will not be a commercial facility having a life of 20 years to 30 years due to the experimental nature of the project.</p>

- What is the incremental cost of initially sizing power plant auxiliaries (i.e. deaerator, water treatment, cooling towers, etc.) such that at the time of the retrofit only minor modifications would be required?

Answers to these and other technical questions should be developed as soon as possible if this form of retrofitting is to be given serious consideration by the electric utility industry.

Some of the advantages and disadvantages of this type of retrofit are shown in Table 7. In summary, this option provides the opportunity for rapid installation of new oil fired baseload capacity while awaiting the demonstration of the gasification-combined cycle power plant concept. The penalties to be paid are higher than normal costs associated with the original combined cycle equipment (which might be more than offset by the fact that the plant is being constructed at an early date, thereby eliminating inflation and escalation costs that would have been incurred if the entire plant had been constructed at some later date) as well as the possibility of owning a plant for which a guaranteed fuel supply cannot be assured if gasification-combined cycle power plants do not emerge as an economic option for electric power generation.

In conclusion, it can be stated that the information presented in Tables 6 and 7 indicates that the two forms of integrated retrofitting discussed in this paper have the potential for providing attractive options for the electric utility industry to replace oil and gas firing with coal gasification in a low risk and timely manner. A number of unanswered technical and economic questions have to be resolved before these options can be given serious consideration. During 1978, EPRI, in conjunction with a number of member utilities, will attempt to find answers to most of the major unresolved issues.

TABLE 7

ADVANTAGES AND DISADVANTAGES OF INTEGRATED RETROFIT - COMBINED CYCLE PLANT FIRST

<u>Advantages</u>	<u>Disadvantages</u>
1. Offers the opportunity to install new oil fired baseload capacity at an early date and an acceptable heat rate.	1. Higher than normal initial cost of combined cycle equipment due to the added flexibility required for the retrofit at a later time.
2. Provides maximum security for the initial investment as oil fired combined cycle plants can be considered to be minimum risk projects.	2. Possibility of having to make major modifications to or scrap the existing HRSG at the time of the retrofit.
3. Offers a low risk opportunity for the introduction of commercial scale coal gasification to the utility industry as the retrofit will only be attempted after large scale demonstration of the integrated concept has been achieved.	3. Space required for the ultimate retrofit of the gasification plant must be available at the beginning of the project i.e. eight to ten years before the retrofit is actually accomplished.
4. Provides the opportunity for rapid capacity expansion (500MW-1,000MW) as well as providing the potential for extending the time period in which oil is used for baseload generation.	4. If gasification-combined cycle power plants do not emerge as an economic option for electricity production the host utility company is stuck with a large investment in equipment for which a stable fuel supply cannot be guaranteed.
5. Project risk can be further minimized by designing the Texaco gasification plant to fire coal, coke and high sulfur heavy oil providing extreme fuel flexibility (risk is lowered, as the Texaco gasifier has been commercially proven for oil firing).	
6. The oil fired combined cycle plant can be operated over most of the construction period for the gasification plant. The down time required to accomplish the retrofit can be minimized.	

BIBLIOGRAPHY

- (1) "Economics of Current and Advanced Gasification Processes for Fuel Gas Production," Fluor Engineers and Constructors, Inc. EPRI AF-244, July 1976.
- (2) "Comparative Evaluation of High and Low Temperature Gas Cleaning for Coal Gasification-Combined Cycle Power Systems," Stone and Webster Engineering Corporation. EPRI AF-416, April 1977.
- (3) "Economic Studies of Coal Gasification Combined Cycle Systems for Electric Power Generation," Fluor Engineers and Constructors, Inc. EPRI AF-642, January 1978.
- (4) "Combined Cycle Power Plant Capital Cost Estimates," Bechtel Power Corporation. EPRI AF-610, September 1977.
- (5) "Coal-Fired Power Plant Capital Cost Estimates," Bechtel Power Corporation. EPRI AF-342, January 1977.
- (6) "Screening Evaluation: Synthetic Liquid Fuels Manufacture," R. M. Parsons Company. EPRI AF-523, August 1977.
- (7) "Production of Distillate Fuels and Methanol from Coal"--Interim Report, C. F. Braun and CO. EPRI RP832-1.7, October 1977.
- (8) "Low Btu Gas Study," Babcock and Wilcox. EPRI 265-2, January 1976.
- (9) "Retrofit of Gasified Coal Fuels to Steam Generators," Combustion Engineering, Inc. EPRI 265-1, December 1975.

Evaluation of Coal-Fired Fluid Bed Combined Cycle Power Plant

A. J. Giramonti*, J. W. Smith**, R. M. Costello***,
D. A. Huber***, and J. J. Horgan*

ABSTRACT

Recent studies and research indicate that fluidized-bed combustion systems, operating at atmospheric or elevated pressure in a combined cycle power plant, offer the potential for producing electrical energy from coal within present environmental restraints for clean flue gas emissions and at a cost less than for conventional steam power plants utilizing low-sulfur coal or flue gas cleanup equipment. The team of Burns and Roe Industrial Services Corporation, United Technologies Corporation, and Babcock & Wilcox Company is under contract to the Department of Energy to prepare a conceptual design for such a plant. The major objectives of this program are to identify the technology required to develop a coal-fired pressurized fluid bed combustor to drive an industrial gas turbine and to define the technical and economic characteristics of a nominal 600 MW base- or intermediate-load combined cycle power plant.

Several cycle configurations with variations of cycle parameters were investigated during the course of this study. These include the consideration of different pressure ratios, the use of an unfired and fired steam bottoming cycle, and reheating the gas stream before the power turbine. Efficiency estimates for these variations range from about 38 percent for the unfired waste heat system to over 43 percent for the reheat system. As a result of various trade-off studies, a commercial plant cycle arrangement has been selected which incorporates a coal-fired pressurized fluid bed combustor, operating at 10 atm and 1650 F, and supplementary firing of the gas turbine exhaust in a coal-fired atmospheric pressure fluid bed boiler which produces 2400 psig/1000 F/1000 F steam. Preliminary estimates for coal pile to bus bar efficiency for the selected system are around 41 percent (gross, HHV).

*United Technologies Corporation

**Babcock & Wilcox Company

***Burns and Roe Industrial Services Corporation

INTRODUCTION

Over the years, coal has become a major source of energy for power generation by electric utilities. However, it has become apparent that the use of coal requires control of the products of combustion to be compatible with the environment. This fact, coupled with the increased emphasis on coal usage has created an incentive to develop alternate methods of extracting energy from coal in an environmentally and economically acceptable way. In addition, it is highly desirable that these alternate methods result in more efficient coal utilization. Recent studies (1) indicate that the use of gas turbines in conjunction with fluidized bed combustion systems in a combined cycle power plant offer potential for satisfying these needs.

The feasibility of burning coal directly in an open cycle gas turbine was investigated by Bituminous Coal Research Inc., as early as 1944 when a coal-fired competitor to the diesel engine for railroad applications was being sought. In the intervening years, a number of organizations have attempted to design and test direct coal-fired gas turbines. However, problems with corrosion, erosion, and deposition on turbine blading due to the amount and nature of the ash passed through the high-temperature combustion zone have prevented the development of a commercially viable product. The low temperatures associated with fluidized bed combustion should alleviate the problems. Under Department of Energy (DOE) sponsorship (Contract EX-76-C-01-2371) the Burns and Roe Industrial Services Corporation, United Technologies Corporation, and the Babcock & Wilcox Company have formed a team to investigate the feasibility of a combined cycle plant utilizing a gas turbine with a pressurized fluid bed combustor. The purpose of this paper is to present important preliminary findings from the first year of effort on the DOE program. Because of the exploratory nature of this effort, some desired technical information is not yet available; indeed, more questions might be raised than are answered by this discussion. Nevertheless, it is deemed appropriate to present the preliminary findings to stimulate early discussion of this promising concept.

AIR-COOLED PRESSURIZED FLUID BED

Fluid bed combustion as currently discussed involves the combustion of coal in a fluid bed containing a crushed sulfur acceptor such as limestone or dolomite. Pressurized fluid bed (PFB) combustion is similar to atmospheric fluid bed (AFB) combustion except that the process takes place under a pressure of several atmospheres such as would exist at the exhaust of the compressor of a gas turbine unit. PFB combustion, therefore, offers the potential of serving as the gas turbine combustor (Figure 1). This use of a PFB as a gas turbine combustor has been studied by several investigators (2 through 7). Indeed, a 1-MW gas turbine has operated with a PFB combustor burning coal (8).

The temperature of the combustion process would be controlled by heat extraction from the bed and/or by controlling the fuel-air ratio in the bed. It would be necessary to maintain the PFB temperature at about 1650 F to minimize the release of

volatile alkaline metal compounds which would otherwise cause severe corrosion in the gas turbine and to assure an operating margin below the coal ash softening temperature to prevent agglomeration within the bed. The low combustion temperature also would result in NO_x emissions that are lower than the Federal EPA limits for coal fuel.

Higher PFB operating temperature would be beneficial to cycle performance and carbon utilization. It appears (9 through 13) that fluid beds could be satisfactorily operated up to 1750 F without incurring problems with sulfur retention or ash sintering, but deposits of elutriated material on the walls of the primary cyclone and in the turbine could be excessive. Considering the experience reported in the literature (9), a bed operating temperature of 1650 F was selected for the cycle analysis and PFB combustor design.

As the mechanical design of the PFB combustor developed it was determined that temperatures greater than 1650 F would not be practical. The heat exchange surface within the PFB must be designed for the bed temperature plus a margin for operating variations. Consequently, for the 1650 F bed temperature a 1700 F design temperature was used for the bed internals. At this temperature level the available materials exhibit little strength. The lower allowable stress levels that would result from using higher bed temperature would make such a design impractical, if not impossible. Also, while corrosion of the in-bed surface has not been quantified, it would be expected to be more severe at higher operating temperatures.

With the PFB process it should be possible to capture sufficient sulfur products to permit use of high-sulfur coals and still meet the current EPA limit of 1.2 lb SO₂/10⁶ Btu input. For a typical 3.4 percent sulfur, 12,000 Btu/lb HHV coal the required sulfur removal efficiency is about 80 percent. Dolomite appears to be an effective sulfur acceptor, and available data (9, 10) indicate that a calcium/sulfur ratio near 1.0 should be adequate to achieve the desired 80 percent sulfur retention at the selected bed operating conditions.

A low fluidizing (superficial) gas velocity is desirable to reduce elutriation from the bed, thereby reducing both the carbon loss and the required particulate cleanup duty. It should be noted that the size of both the coal and dolomite feed must be properly related to the fluidizing velocity, with increased velocity implying increased sizes. Low velocity also implies a larger bed area resulting in a shallower bed and, hence, lower bed pressure loss. A fluidizing velocity of 2.5 - 3.0 fps was selected for the PFB design reflecting previous work (9 through 11).

Even with low fluidizing velocity, a highly efficient particulate removal system would be required to prevent excessive turbine blade erosion. Since the cost of the particulate removal system is strongly influenced by the volume of gas passing through it, one method of reducing the system cost would be to limit the combustion air flow (and hence the dirty gas flow) to only as much as required for coal combustion within the PFB. This could be accomplished by splitting the compressor discharge flow with approximately 25 percent of the air being routed to the PFB combustion zone and the remainder of the air being routed through the bed cooling system consisting of tubes immersed within the fluid bed. The heat released during the combustion process would be transferred to the cooling air

less than one-quarter of the oxygen available in the air, the turbine exhaust gas could support considerable firing of additional coal. For this study, an AFB steam generator was considered as the means for capturing the SO_2 released during the final combustion process. The AFB could be steam cooled, as noted in Figure 4, or air cooled either by varying excess air to the bed or by using a split-flow arrangement similar to that described for the PFB in Figure 1. With either air-cooled approach, heat would be recovered from the air and combustion gases in a waste heat steam generator.

The performances of these various combined cycle configurations and of the simple cycle gas turbine are compared in Figure 5. Selected component efficiency, pressure loss, and temperature assumptions used in the calculations are summarized in Table I. As expected, the waste heat recovery system displays the lowest efficiency (about 38 percent, HHV) but, since it requires combustion at only one point in the cycle, it is a less complex configuration than the other cycles and has been utilized as a reference point in the economic analysis. The reheat system offers the highest potential efficiency (43 percent, HHV) but increases the complexity of the gas turbine design and requires a reheat fluid bed combustor with an associated particulate removal system. The PFB gas turbine topping of the AFB steam cycle has an attractive efficiency (approaching 41 percent, HHV) and shows promise for minimum equipment cost because of its relatively high specific work.

ECONOMIC ANALYSIS

The selection of the commercial plant configuration cannot be made on the basis of performance alone. The most important selection criterion is overall cost of electricity; therefore, an order of magnitude analysis was made to estimate the relative capital and operating costs of the alternative configurations. The operating cost differences due to fuel consumption were expressed in terms of equivalent capitalized costs where a one point difference in efficiency would give an equivalent fuel savings of \$10/kW.

The results of this economic screening analysis are given in Table II. All costs are given as incremental costs relative to the unfired waste heat recovery system which was taken as the base. The exhaust-fired, steam-cooled AFB with a gas turbine pressure ratio of 10 and the gas turbine system with reheat before the power turbine have the lowest evaluated net relative costs. The cost differential between these two systems is not statistically significant. The power turbine reheat cycle requires a more complex gas turbine design and additional hot particulate removal equipment. In addition, little data is available for design of a PFB combustor at the 2.5 atm pressure existing at the reheat point. Therefore, it was felt that the PFB cycle with an exhaust-fired steam-cooled AFB would offer less technical risk.

Capital costs were not estimated for all major pieces of equipment of systems required in the plant. Table III contains a list of those items which were considered. Obviously, some major systems (such as the coal and sorbent feed systems to the AFB and the low-pressure reheat PFB combustors) were omitted which would tend to decrease the advantage of the reheat and exhaust-fired cycles. However, it was

felt that the differences in the costs of these systems would not be large enough to offset the differences shown on Table II. Therefore, there is a strong probability that the trends shown in this study could be confirmed by more detailed design and cost estimates of the alternatives.

It should be recognized that the cost estimates did not consider some of the material, equipment, and other balance of plant costs normally associated with the items indicated on Table III. In addition, little more than conceptual outline drawings were available for many items that were considered. The basic intent of the effort was to provide a systematic approach for summarizing the relative pros and cons of each cycle on the basis of the preliminary design definition that was available. While each pro and con was, in effect, weighted on a cost basis, it would be misleading to consider the numbers shown as anything more than rough order of magnitude.

COMMERCIAL PLANT CONFIGURATION

On the basis of the preceding screening analysis, the PFB/AFB combined cycle power plant was selected for the commercial plant conceptual design study. During the course of the design study, further optimization of the selected configuration led to incorporation of three stages of regenerative feedwater heating and an adjustment in the relative power split between the gas and steam turbines. The resulting system, illustrated in Figure 6, utilizes two 63.5 MW gas turbines with two PFB combustors per gas turbine. The gas turbines would exhaust into a single exhaust-fired AFB steam generator and carbon burnup bed (CBB) which would generate steam at 2400 psig 1000 F/1000 F to drive a single 461.4 MW steam turbine. The resulting gross plant output would be 588.4 MW. Selected performance and cost data are summarized in the last column of Table II.

The gas turbine assumed for this study is a base load design which represents a modification of UTC's FT50 gas turbine or an engine of similar performance and physical characteristics. It would operate at 10:1 pressure ratio with 1600 F inlet temperature and have all necessary ducting to allow discharge of compressor air to the PFB combustor and return of hot gases to the turbine.

The PFB combustors, depicted in Figure 7, would heat the compressor discharge air from approximately 600 F to 1600 F. The compressor discharge air would enter the bottom of the refractory lined pressure vessel. The combustion air would flow through bubble caps in the distributor plate and into the fluidized bed. The cooling air would flow through supply pipes at the distributor plate to the inlet headers of the cooling circuits, through the tubes, and finally would be collected at the hot air outlet manifold. The flow split between cooling air and combustion air would be controlled by biasing valves in the hot air outlet piping and the hot gas outlet piping. The heat transfer from the bed to the cooling air would require a large surface area and a large bed volume. The desire to maintain a low bed superficial velocity (of the order of 3 ft/sec) is compatible with this large volume and would result in an expanded bed height of approximately 22 ft to submerge the cooling system within the bed.

Incoloy 800 alloy was selected for all material exposed to the fluid bed. This material has had greater usage than the other available high temperature alloys, and its physical properties (forming, welding, etc.) are better established. Also, currently available corrosion, creep, fatigue, and other data indicate that this alloy should give suitable life for the cooling system. However, ultimate material selection must eventually be based on the outcome of other more rigorous investigations of material characteristics within a PFB environment.

Operation at the elevated temperature of the PFB presents significant challenges in designing to accommodate the expected thermal expansion. The air in the bed cooling system would undergo nearly 1000 F temperature change from the inlet to the outlet in a total tube length of less than 26 ft. In addition, the cooling system from the distributor plate to the outlet header must be supported by the pressure vessel which operates at a temperature of 250 F. The design philosophy has been to support the outlet manifold and inlet and outlet headers of the cooling system from the same elevation on the vessel wall and to use U-shaped cooling tubes between the inlet and outlet headers. These U-shaped tubes would be designed with sufficient flexibility to accommodate the differential temperature along the length of the tube.

As previously noted, a particulate removal system would be required to limit the solid loading entering the turbine. Because of lack of actual operating experience with PFB exhaust gases in gas turbines, further testing is required to determine the acceptable level of particulate concentration in the gas entering the turbine. On the basis of limited data (14), an estimate of allowable gas turbine particulate loading was made showing that particles greater than 10 microns in size would give unsatisfactory turbine life, particles less than 2 microns in size would have negligible effect, and that some limited amount of particulate in the 2-10 micron size could be tolerated within the gas turbine. These estimates are compared in the top two lines of Table IV to the estimated particulate loading in the gas exiting from the PFB combustor.

Since the design requirements and characteristics of particulate removal systems are not fully known at this time, two different technologies were investigated in developing the overall plant design. The two concepts are a high-efficiency rotary flow cyclone and a granular bed filter, both of which are in the developmental stage at the temperature, pressure, and size required for the PFB combustion process. From a theoretical standpoint, both types of particulate collectors should meet the requirements of a commercial plant. The estimated effectiveness of the particle collectors is indicated in Table IV where the collector effluent is seen to satisfy the gas turbine requirement. Final dilution of the collector effluent with cooling air which bypassed the PFB combustion zone should reduce the particle concentration well below that required for the gas turbine. Only testing under actual operating conditions will ensure the suitability of these collectors.

The exhaust gases from the two gas turbines would be routed to the AFB steam generator system consisting of four AFB main beds in one structure (Figure 8) and a separate CBB. The main beds would combust coal using the exhaust of the gas turbines as combustion air. Unburned char elutriated from the AFB main beds would be captured and combusted in the CBB. The CBB would be in a separate enclosure, but the steam cooling system would be in parallel with that for the main beds. Most of

the superheater surface would be in three of the four beds, with the fourth containing only evaporator surface. The four main beds would each exhaust hot gas upward into a common convection section of the AFB steam generator. All of the reheater tubes and a portion of the primary superheater would be in the convection section. Gas from the convection section would flow into the economizer section. The CBB would consist of three beds, each with two compartments for load turn down control. All boiler surface would be above the beds in the convection zone.

The flue gas from the AFB boiler, after passing through high efficiency multi-clones, go through a high temperature electrostatic precipitator. The electrostatic precipitator would be designed for a maximum temperature of 750 F. The total volume of flue gas to be handled by the precipitator is 3.2×10^6 ACFM. The precipitator would have four electric fields in series. The total particulates emission would be less than 0.1 lb per million Btu of heat input. The gas stream from the precipitator would pass through the low level economizer to the induced draft fans and stack.

The hypothetical Middletown, USA site was selected for location of the PFB combined cycle power plant. An area site plan for the prospective power plant is shown in Figure 9. The plant island is centrally located with the cooling tower and switchyard to the east, coal and sorbent storage areas to the south, and wastewater treatment plant to the west.

CONCLUDING REMARKS

The air-cooled PFB offers the potential of using coal-fired gas turbines to top a more conventional coal-fired steam plant. The resulting combined cycle power plant has the capability of more efficient conversion of coal to electricity with the potential of yielding an overall lower cost of electricity than can be obtained with current technology. The PFB system requires development of high efficiency hot particulate removal systems and demonstration of material suitability. However, the technological challenges facing this type of system are less demanding than those for other advanced coal-fired conversion systems presently under study because of the lower temperatures and reduced degree of coal conversion and processing required. In closing, the prospective performance, economic, and environmental advantages of combined cycle power plants using PFB combustors suggest that development of this promising concept be energetically pursued.

ACKNOWLEDGMENT

This study was carried out under Contract EX-76-C-01-2371 for the U.S. Department of Energy. The authors gratefully acknowledge the assistance of Mr. George Weth of DOE in the publication of this paper.

REFERENCES

1. Evaluation of Phase 2 Conceptual Designs and Implementation Assessment Resulting From the Energy Conversion Alternatives Study (ECAS). NASA Lewis Research Center Report NASA TM X-73515, April 1977.
2. Hoy, H. R. and J. E. Stanton: Fluidized Combustion Under Pressure. Joint Meeting of Chemical Institute of Canada and Division of Fuel Chemistry, AlChE, May 1970.
3. Harboe, Henrik: Fluidized Bed Air Heater for Open and Open/Closed Gas Turbine Cycles. Proceedings of Third International Conference on Fluidized Bed Combustion, Heuston Woods, Ohio, November 1972.
4. Maude, C. W. and D. M. Jones: Practical Approaches to Power Generation from Low-Grade Fuels. The Chemical Engineer, May 1974.
5. Jones, D. and R. Hamm: Energy Conversion Alternatives Study-Investigations, Phase II Oral Report. February 18, 1976.
6. Fox, G. R. and J. C. Corman: Study of Advanced Energy Conversion Techniques for Utility Applications Using Coal or Coal Derived Fuels. General Electric Phase II Oral Report, February 17, 1976.
7. Kearns, D. L., et al.: Fluidized Bed Combustion Process Evaluation, Phase II, Pressurized Fluidized Bed Coal Combustion Development. National Environmental Research Center, Westinghouse Research Laboratories, Pittsburgh, Pa., September 1975, NTIS PB-246-116.
8. Energy Conversion from Coal Utilizing CPU-400 Technology - Combustion Power Company, Inc. Monthly Report FE-1536-M37, September 1976.
9. Pressurized Fluid Bed Combustion. National Research Development Corporation R&D Report No. 85, Interim No. 1, Prepared for the Office of Coal Research, Contract No. 14-32-0001-1511.
10. Vogel, G. J., et al.: Recent ANL Bench-Scale, Pressurized-Fluidized-Bed Studies. Proceedings of the Fourth International Conference on Fluidized-Bed Combustion, Mitre Corporation, May 1976.
11. Vogel, G. J., et al.: A Development Program on Pressurized Fluidized-Bed Combustion. Annual Report ANL/ES-CEN-1011 for period July 1, 1974-June 30, 1975.
12. Nutkis, M. S.: Operation and Performance of the Pressurized FBC Miniplant. Proceedings of the Fourth International Conference on Fluidized-Bed Combustion, Mitre Corporation, May 1976.
13. Hoke, R. C.: Emissions from Pressurized Fluidized-Bed Coal Combustion. Proceedings of the Fourth International Conference on Fluidized-Bed Combustion, Mitre Corporation, May 1976.
14. The Coal-Burning Gas Turbine Project. Report of the Interdepartmental Steering Committee, Department of Minerals and Energy, Department of Supply, Commonwealth of Australia, (1973).

TABLE I
SYSTEM ASSUMPTIONS FOR PERFORMANCE ANALYSIS

Combustion Efficiency, %		
PFB, main and reheat		99.0
AFB		98.5
Pressure Loss, % of local gas pressure		
	<u>Bed</u>	<u>Cooling Tubes</u>
PFB, main and reheat	10.0	10.0 (air)
AFB	9.2	- (steam)
Temperature, °F		
	<u>Bed</u>	<u>Cooling Tubes</u>
PFB, main	1650	1575 (air)
PFB, reheat	1550	1475 (air)
AFB	1550	- (steam)
Component Efficiency, %		
Electric generator (steam turbine)		98.4
Electric generator (gas turbine)		98.7
Electric motors		95.0
Boiler feed pump		82.0
Boiler feed pump drive turbine		75.0
Condensate pump		82.0
ID fan		70.0

TABLE II

PFB COMBINED CYCLE POWER PLANT COST SUMMARY

Cycle Type	Screening Analysis										Selected Cycle
	Waste Heat	Exhaust-Fired Air-Cooled AFB	Exhaust-Fired Steam-Cooled AFB	Exhaust-Fired Steam-Cooled AFB	Power Turbine Reheat	Exhaust-Fired Steam-Cooled AFB					
Gas Turbine Pressure Ratio	10	16	10	16	10	16	10	16	16	10	10
Number of Feedwater Heaters	0	0	0	0	0	0	0	0	0	3	3
Output per Gas Turbine, MW											
Gas Turbine	66.7	62.0	60.0	55.0	63.5	58.4	63.5	58.4	77.0	63.5	63.5
Steam Turbine	32.0	19.0	86.0	87.0	134.0	118.0	134.0	118.0	88.0	230.7	230.7
Total	98.7	81.0	146.0	142.0	197.5	176.4	197.5	176.4	157.0	294.2	294.2
Specific Work, kW-sec/lb-air	121	100	179	174	241	216	241	216	192	350	350
Gross Efficiency, % (HHV)	38.4	37.2	41.0	40.3	40.9	40.4	40.9	40.4	43.1	41.1	41.1
Relative Equipment Cost, \$/kW											
Combustion System	Base	+33	-8	-26	-16	-12	-16	-12	-42	-34	-34
Prime Movers & Electrical	Base	+55	-38	-17	-49	-32	-49	-32	-24	-61	-61
Miscellaneous	Base	-5	+76	+79	-10	-2	-10	-2	+20	-15	-15
Subtotal	Base	+83	+30	+36	-75	-46	-75	-46	-46	-120	-120
Equivalent Fuel Savings, \$/kW	Base	+12	-26	-19	-25	-20	-25	-20	-47	-25	-25
Net Relative Cost, \$/kW	Base	+95	+4	+17	-100	-66	-100	-66	-93	-145	-145

TABLE III

MAJOR EQUIPMENT INCLUDED IN COST SUMMARY

- . Main PFB Coal/Sorbent Feed System
- . Gas Turbines/Generators
- . PFB Main Combustors
- . PFB Reheat Combustors
- . AFB Combustors
(Excluding: Flues, Duct, Cyclones,
Fans, Coal/Limestone Feed System)
- . Electrical Equipment
- . Steam Turbine/Generators
- . Waste Heat Boilers
- . Electrostatic Precipitators

TABLE IV

PARTICLE SIZE DISTRIBUTION AND LOADINGS

<u>Size Range</u>	<u>Predicted Particle Concentration, gr/scf</u>		
	<u>Under 2μ</u>	<u>2-10μ</u>	<u>Over 10μ</u>
Gas Turbine Limit	unlimited	0.01	nil
PFB Effluent	0.3	2.0	6.4
Collector Effluent	0.06	0.01	0.00
Entering Turbine	0.02	0.003	0.000

Fig. 1

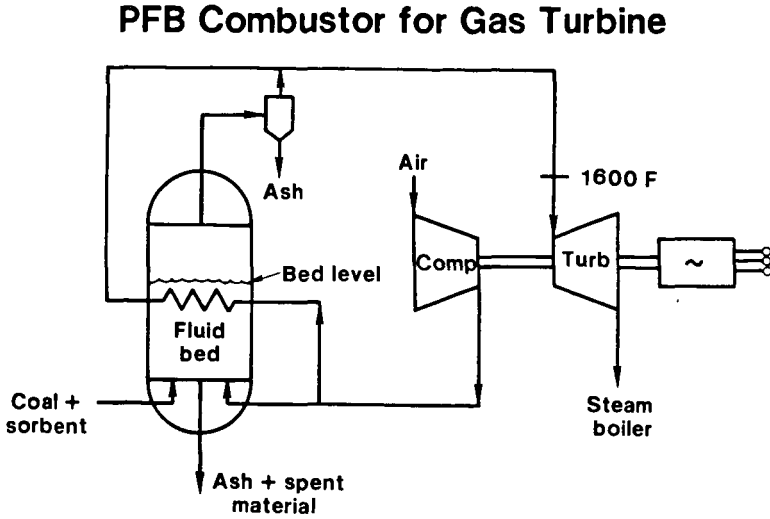


Fig. 2

Unfired Waste Heat Recovery Cycle

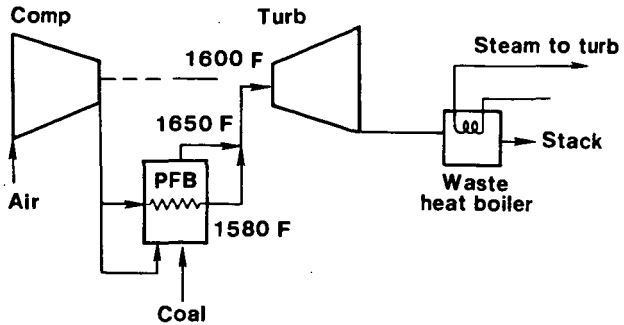


Fig. 3

Power Turbine Reheat Cycle

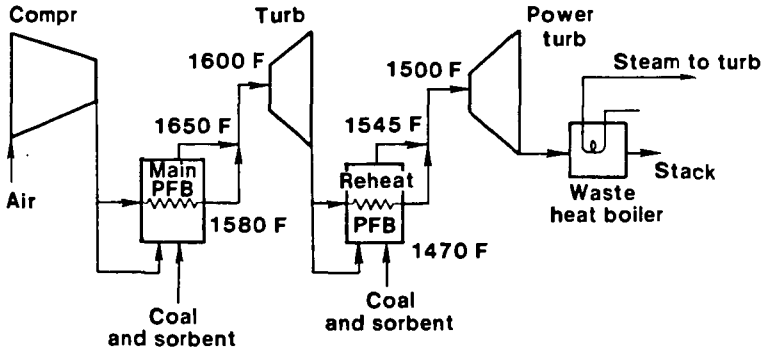


Fig. 4

Exhaust-Fired Steam-Cooled AFB Cycle

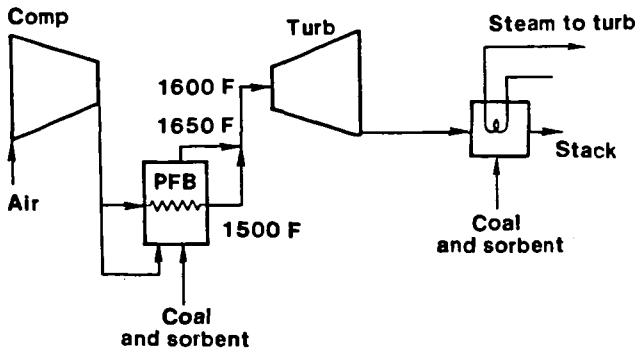
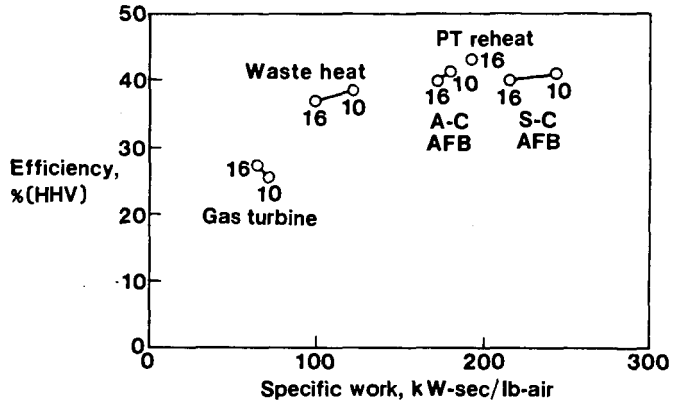


Fig. 5

PFB Cycle Performance Comparison



77-11-193-1

Fig. 6

PFB/AFB Combined Cycle Power Plant

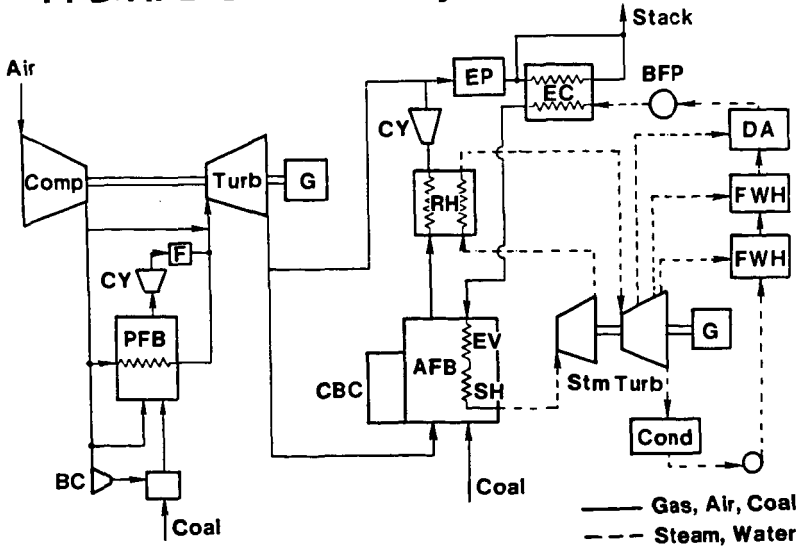


Fig. 7

Pressurized Fluid Bed Combustor

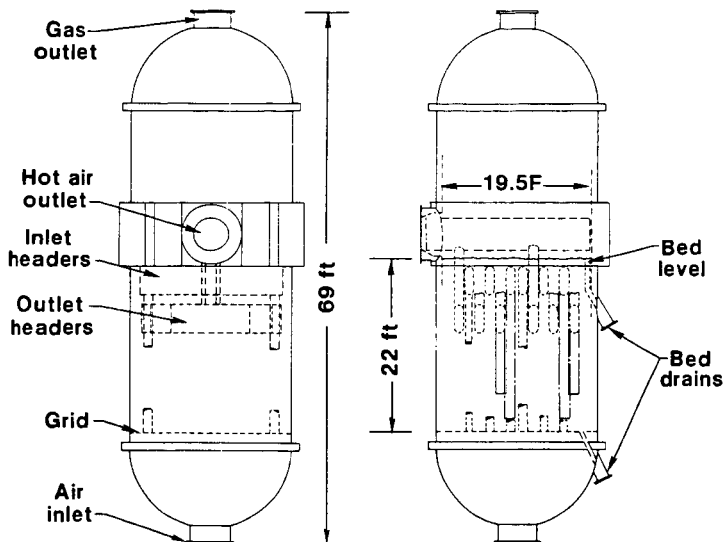


Fig. 8

Atmosphere Fluid Bed Boiler

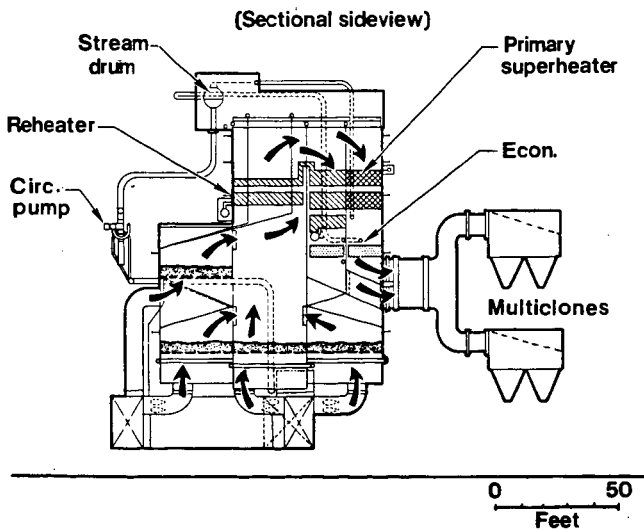
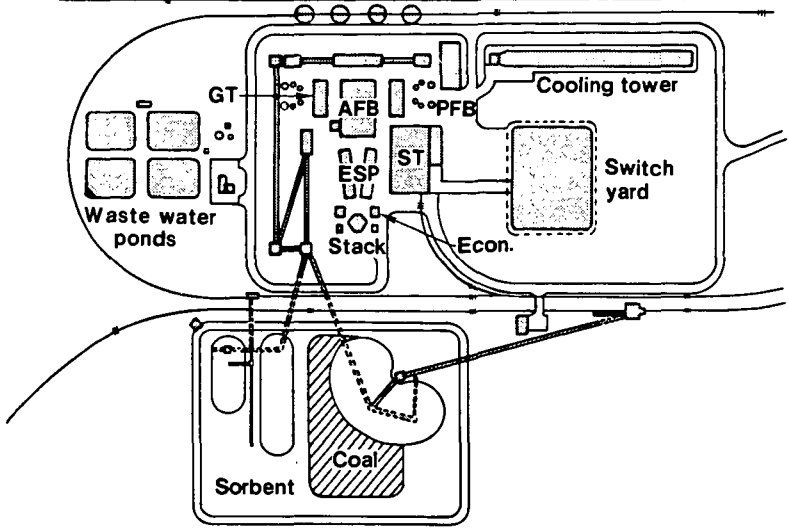


Fig. 9

Plot Plan for PFB Combined Cycle Power Plant



77-10-227-1

Assessment of Current and Advanced NOx Control Technology
for Coal-Fired Utility Boilers*

by

R. E. Thompson, T. W. Sonnichsen

KVB, Inc., Tustin, California 92680

and

Dr. H. Huang

Argonne National Laboratory, Argonne, Illinois 60439

INTRODUCTION

NOx is the remaining major or criteria pollutant that has not been effectively reduced to emission levels approaching 10% or less of those from an uncontrolled stationary combustion source. This is particularly true at the present in coal-fired utility boilers because of the conversion of fuel-bound nitrogen in the coal to NO during the combustion process. However, coal is our largest natural fossil fuel resource and DOE is responsible for developing methods of utilizing coal in an environmentally acceptable manner. An important factor in meeting future energy needs and achieving national energy independence is our ability to expand the use of coal in electrical power generation. Consistent with its responsibilities, EPA has established research goals for NOx emissions with coal of 200 ppm by 1980 and 100 ppm by 1985. If it is eventually shown that comparable levels are necessary to maintain air quality standards and cost-effective methods exist, then the likelihood of more stringent new source performance standards (NSPS) in the mid-1980's exists for coal-fired utility boilers.

For the reasons outlined above, a need existed to conduct a comprehensive state-of-the-art review of all potential combustion modification methods for NOx control on coal-fired units. Combustion modification has in the past been the most cost-effective approach to limiting NOx formation and emissions. With the emergence of selective gas-phase NOx decomposition methods, it was desirable to also conduct a review of the most recent developments in that field.

NOx FORMATION

Control of NOx formation during coal combustion is particularly difficult because nitrogen-bearing compounds in the coal are oxidized in the initial stages of the flame zone to produce "fuel nitrogen NOx". Important parameters in this process are local stoichiometry, temperature, and the residence time at these conditions plus the mixing conditions for supplemental air addition and carbon burnout.

Combustion modifications also influence the formation of "thermal NOx" at high combustion temperatures due to the thermal fixation of nitrogen and oxygen in the combustion air. Important parameters that affect peak flame temperature are local oxygen availability, fuel-air mixing patterns, the presence of heat absorbing inert combustion products, combustion air preheat, local heat transfer to adjacent cooled surfaces, etc. Both burner and furnace design are very important factors in total NOx emissions since they influence both thermal and fuel-related NOx.

*This study was conducted for Argonne National Laboratory under Contract 31-109-38-3726 as part of an ongoing program, Environmental Control Implications of Coal Utilization for Power Generation, being conducted in turn for DOE.

NOx CONTROL METHODS

One of the purposes of the study was to not only summarize the technical performance of various NOx control methods, but also to point out and quantify some of the more important operational constraints associated with these methods. The study was primarily concerned with the following control methods and operational concerns.

<u>Methods (or Factors)</u>	<u>Concerns</u>
Low excess air	Cost of combustion modifications
Staged combustion	Furnace wall corrosion
Flue gas recirculation	Tube wall erosion
Combination methods	Carbon carryover
Coal type - bituminous/ subbituminous	Combustion stability
Boiler design - wall fired, tangential, cyclone	Load restrictions
Burner design - conventional, low-NOx, advanced concepts	Secondary pollutants
	Energy penalties
	Retrofit applications
	Impact on auxiliary equipment
	Operation and maintenance

Available NOx emissions test program data was examined for the most prevalent boiler designs and the effectiveness of various combustion control measures is summarized in Table 1. The control method having the largest NOx reduction potential (short of reburnering with new low-NOx burners) was staged combustion, accomplished either by removing burners from service or by the use of overfire air (driving the remaining in-service burners fuel-rich). In the NOx Assessment Final Report (1) for Argonne National Laboratory, NOx reduction potential summary graphs were prepared for each of the various control methods. Although space limitations preclude showing all of this supporting data used in the preparation of Table 1, some examples for burner-out-of-service operation are shown in Figures 1, 2, and 3.

It should be emphasized that there are large unit-to-unit variations in coal-fired utility boiler NOx emissions, even within the same boiler design type. This is due to varied boiler geometry with size, age, and coal type. Boiler operating practice, maintenance, pulverizer settings, and coal characteristics often vary from plant to plant even within the same utility. Frequently a plant in the northeastern U.S. may obtain coal simultaneously from two or three sources. Therefore, it is not unusual to see baseline NOx emissions vary by as much as 500 ppm for a given boiler type (e.g., horizontally opposed fired). Because of this wide variation in baseline emissions, it frequently is more convenient to express the effectiveness of a given NOx control in terms of a potential percentage NOx reduction as in Table 1 and Figures 1 through 3. However, it is also recognized that many utility and government groups are interested in the lowest attainable "state-of-the-art" NOx emission levels as summarized in the table below.

STATUS OF COAL-FIRED UTILITY BOILER NOx CONTROL TECHNOLOGY
FOR NEW UNITS AND RETROFIT APPLICATIONS

	<u>Lowest Attainable NOx Emission Levels</u>			
	<u>New Units</u>		<u>Retrofit</u>	
	ppm at 3% O ₂	lb/MBtu	ppm at 3% O ₂	lb/MBtu
<u>Wall-Fired</u>				
Single Face Fired	300-350	0.45	400-500	0.6
Horizontally Opposed	300-350	0.45	400-600	0.6
<u>Tangential</u>	250-300	0.45	250-350	0.4

For new units, these emission levels are based on the most recent low-NOx burner designs (e.g., dual register configurations or overfire air on tangential units) frequently employed in combination with a compartmentalized windbox and liberal furnace volumes. Retrofit emission levels shown can be reached by reburnering or in some cases by carefully applied staged combustion firing modes. Although it is currently possible to attain these NOx levels with some consistency, this does not mean that all existing units can be modified to these levels regardless of boiler age, design, coal type, etc.

OPERATIONAL CONSIDERATIONS

Previous assessment studies have not properly evaluated the numerous operational factors that are of major importance to the user in selecting and implementing a combustion modification technique. Five major topic areas were examined as part of the current study:

1. Problems in design, installation, operation and maintenance of a NOx control technique
2. Applicability of a given technique for retrofit
3. Impact of low NOx modes on other pollutants
4. Effect of NOx control techniques on the performance of auxiliary equipment
5. Possible energy penalties associated with implementation of a given method

Some of the more important conclusions are outlined below by control method.

A. Operational Factors - Low Excess Air and Staged Combustion--

- Low excess air operation is possible with NOx reductions of up to 15% and a boiler efficiency improvement if careful attention is paid to combustion uniformity in the burner region. Reductions of 35% are possible with staged combustion.
- Close control of local and overall air/fuel ratio and rigorous combustion equipment maintenance is essential to the success of both methods.
- Overfire air port configurations or burner patterns resulting in flame impingement and potential tube wall corrosion must be avoided.
- New designs should incorporate adequate pulverizer and fan capacity to accommodate low NOx modes. Conservative windbox, furnace and convective section designs are recommended.
- Carbon carryover and particulate loadings are no greater than normal operation if the excess air is properly established and maintained (as required) for all loads, fuel types, and boiler conditions.
- No significant increase in secondary pollutants or impact on auxiliary equipment has been noted but more data is needed.

B. Operational Factors - Flue Gas Recirculation--

Flue gas recirculation was found to be a relatively unattractive NOx control method for some of the reasons listed below (2):

- NOx reductions of 15% or less do not compare favorably with reductions of 25% to 35% with staged combustion (20% of the burners out of service).
- A measurable efficiency penalty occurs (approximately 0.5%) with flue gas recirculation due to the auxiliary load of the fans.
- Potential problem areas include tube erosion, flame stability, fan vibration, and increased maintenance.

C. Operational Factors - Corrosion, Slagging and Fouling--

Staged combustion and low excess air operation are the most attractive techniques for NO_x control but the major unresolved issue concerns whether these operating modes with fuel-rich burner combustion zones tend to accelerate boiler tube wall corrosion. Because of the importance of this possible deterrent, a major subsection of the final report was devoted to this topic.

Since the more widespread application of low NO_x operating modes tends to hinge on this issue, the "facts" concerning corrosion tend to be in a state of dispute but some of the more important observations and recent findings are outlined below:

- High temperature fire-side corrosion of water walls in the radiant section of pulverized coal-fired boilers is generally confined to areas of flame impingement and/or slag buildup.
- The slag deposit on a relatively cold tube wall is usually coupled to a locally reducing atmosphere caused by flame impingement.
- Two types of corrosive attack have been identified in boilers firing coals with appreciable sulfur content; alkali iron bisulfate and iron sulfide modes of attack. The sulfate-type attack predominates over the sulfide type.
- Deposits found on corroded tubes often possess high alkali content, high SO₃ content, and high water solubility. Deposits frequently are pale, bluish white with a glossy "enamel" appearance.
- Slagging, fouling, and corrosion problems have frequently been solved in the past with maintenance or adjustments to the pulverizer, coal distribution pipes, and enforced replacement schedules for the burner impellers.
- Numerous corrosion measurements in low NO_x operating modes have been made in the past with air-cooled corrosion probes. These short term tests raise many questions concerning the validity of this technique. More extensive long-term tube-panel tests are necessary to resolve corrosion concerns.

COST OF COMBUSTION MODIFICATIONS

One of the most important factors in addition to NO_x reduction effectiveness and operational limitations from the utility operator's standpoint is the cost of combustion modifications. Numerous cost analyses have been conducted under EPA sponsorship for new units and retrofit applications including those by Combustion Engineering (3) and A. D. Little (4). Total costs have been broken down by annual capital, operational, and fuel costs. The relative cost effectiveness of NO_x emissions control on a 600 MW coal-fired unit is shown in Figure 4. With current technology, the cost effectiveness rapidly becomes unattractive at emission levels approaching 0.4 lb/MBtu.

ADVANCED NO_x CONTROL CONCEPTS

The two most promising advanced NO_x control concepts now undergoing research and development are the selective gas-phase NO_x reduction flue gas treatment systems and new advanced burner/boiler designs.

Studies by Exxon and KVB have demonstrated NO_x reductions up to 90% when ammonia is injected into flue gas streams in the vicinity of 1750 °F. Laboratory-scale feasibility tests with ammonia injection for coal applications has shown that 50% to 80% NO_x reductions are possible for the coals tested. Full scale commercialization studies are currently underway and the possibility of a full scale utility boiler demonstration test in the next two or three years is very likely.

Advanced burner/boiler design concepts have concentrated on combustion methods that will minimize the conversion of fuel-bound nitrogen to NO_x. Based on recent laboratory and subscale tests at EPA and EPRI contractor's facilities, the attainment of EPA's research goals of 200 ppm by 1980 and 100 ppm by 1985 are very likely.

This does not mean that all operational problems will be solved and production units will be available by that time. However, recent research programs at B&W, KVB, Aerotherm, and EER are establishing the proper stoichiometry, temperature, and residence times necessary to limit NOx formation to less than 200 ppm in these initial stages of direct coal combustion. Research is continuing into more complex problems of secondary air addition, carbon burnout, and containment of fuel-rich combustion conditions without extensive materials corrosion problems.

In conclusion, continued progress is being made to reduce NOx emissions from direct coal combustion through low NOx burner designs, currently capable of limiting emissions to 0.6 lb/MBtu and research designs expected to meet approximately 0.25 lb/MBtu emission goals by 1980.

REFERENCES

1. Thompson, R. E., Sonnichsen, T. W., Shiomoto, G. H., and Muzio, L. J., "Assessment of NOx Control Technology for Coal-Fired Utility Boilers," KVB Report 16400-709, September 23, 1977.
2. Thompson, R. E. and McElroy, M. W., "Effectiveness of Gas Recirculation and Staged Combustion in Reducing NOx on a 560 MW Coal-Fired Boiler," EPRI FP-257, September 1976.
3. Blakeslee, C. E. and Selker, A. P., "Program for Reduction of NOx from Tangentially Coal-Fired Boilers, Phase I," EPA 650/2-73-005, August 1973.
4. Standard Support (EIS Vol. 1), EPA 450/2-76-030a, 1977.

TABLE 1. COMBUSTION MODIFICATION ASSESSMENT SUMMARY

	Control Method					
	Low Excess Air	Biased Firing	Burners Out of Service	Overfire Air	Flue Gas Recirculation	New Burners
Basic Mechanism of Control	Increase fuel/air ratio at all burners	Increase fuel/air ratio to majority of burners	Increase fuel/air ratio to active burners	Increase fuel/air ratio to burners by diverting combustion air	Reduce peak flame temperature	Controlled diffusion flame
NOx Reduction Potential						
<u>Single Face Fired</u>						
Typical	0-15%	5%	30%	15%	--	--
Maximum	15%	7%	35%	30%	--	--
<u>Horizontally Opposed Fired</u>						
Typical	0-15%	5%	25%	30%	14%	30%
Maximum	15%	8%	35%	58%	17%	60%
<u>Tangentially Fired</u>						
Typical	0-10%	--	30%	30%	--	--
Maximum	10%	--	45%	35%	--	--
Modification Cost (\$/kW) New/Retrofit						
<u>Single Face Fired</u>	~ 0/0.64	--	--	0.2/0.75	--	--
<u>Horizontally Opposed Fired</u>	~ 0/0.64	--	--	0.2/0.75	--	--
<u>Tangentially Fired</u>	--	--	--	0.2/0.75	--	--
Primary Limitations	Slagging, smoke, flame instability	Degree of biasing, wall slagging and corrosion	Degree of staging, wall slagging and corrosion	Degree of staging, wall slagging and corrosion	Much less cost effective than staging	Cost
Limiting Factors in Effectiveness	Carbon carryover	Carbon carryover, flame stability, smoke	Carbon carryover, flame stability, smoke	Carbon carryover, flame stability, smoke	Flame stability	Windbox configurations, flame stability
Retrofit Limitations	Combustion controls and instrumentation	Pulverizer and fan capacity, flexibility in coal feed system	Pulverizer and fan capacity, flexibility of coal feed system	Furnace configuration, fan capacity	Unit layout, fan capacity	Furnace and windbox configuration, fan capacity
Energy Penalties	May increase slightly	None	None	None	0.5% due to auxiliary fan loadings	None
Secondary Pollutants	No effect*	No effect*	No effect*	No effect*	No effect*	No effect*
Operational and Maintenance Considerations	Additional combustion controls, increased maintenance	Additional combustion controls, increased maintenance	Additional combustion controls, increased maintenance	Additional combustion controls, increased maintenance	Tube erosion, fan vibration, increased maintenance	Minimal
Impact on Auxiliary Equipment	None	None	None	None	Increased fan loading	None reported

*Based on limited available data

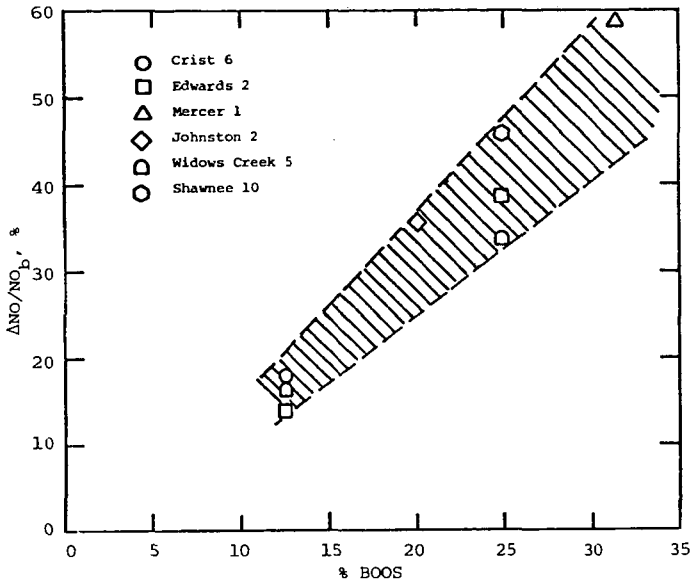


Figure 1. NOx reduction potential of BOOS for single face-fired units.

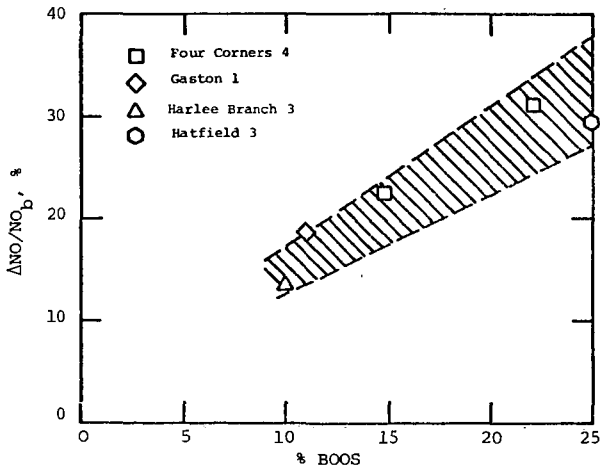


Figure 2. NOx reduction potential of BOOS for horizontally opposed units.

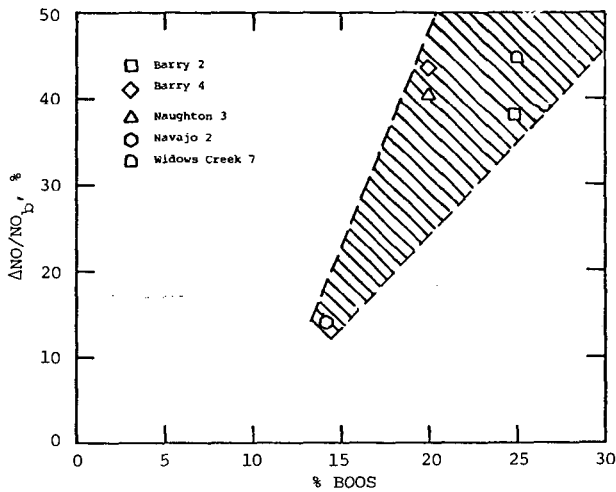


Figure 3. NOx reduction potential of BOOS for tangentially fired units.

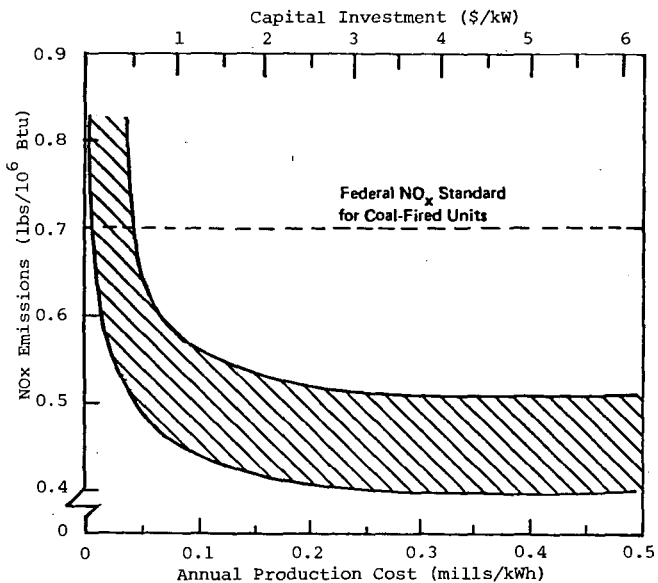


Figure 4. Cost effectiveness of NOx emissions control of a 600 MW steam electric generator (4).

MECHANISMS FOR TRACE ELEMENT ENRICHMENT IN FLY ASH DURING COAL COMBUSTION

Richard D. Smith, James A. Campbell and Kirk K. Nielson

Physical Sciences Department
Battelle, Pacific Northwest Laboratories
Richland, Washington 99352

INTRODUCTION

It is now well established that the smaller flyash particles formed during coal combustion show a significant enrichment of several volatile trace elements. The most widely accepted model for trace element enrichment in flyash formation involves the volatilization of these elements during combustion, followed by condensation or adsorption over the available matrix material (composed primarily of the nonvolatile oxides of Al, Mg, and Si) (1). The larger surface-to-volume ratio of the smaller particles leads to a trace element concentration in the free molecule regime(2) which is inversely related to the particle diameter. Indeed, flyash surfaces have been found to be enriched in several of the same trace elements showing enrichment in the smaller particles, supporting this mechanism(3-5). The smaller particles, which show the highest concentrations of several trace metals, are not efficiently collected by pollution control devices. These particles, enriched in potentially toxic trace metal, also have the highest atmospheric mobilities and are deposited preferentially in the pulmonary and bronchial regions of the respiratory system(1). A proper understanding of the trace element enrichment mechanism is a necessary prerequisite for the prediction of the environmental impact of coal-fired plants, as well as for improving the efficiency of pollution control devices.

Our goal is to determine the mechanism for flyash formation, the enrichment of certain elements in the smaller flyash particles, and the identity of the trace inorganic and organic products of coal combustion. In the initial phase of this study, our investigations have centered on the areas described below.

A. Surface Studies and Flyash Characterization

Studies of fly ash and flyash surfaces have been undertaken using photoelectron spectroscopy, proton induced X-ray emission, secondary ion mass spectrometry, Rutherford backscattering, and scanning electron microscopy. Several of these techniques were used in conjunction with sputtering to obtain concentration vs. sputtering depth profiles. Extensive studies have also examined the various types of flyash particles as a function of particle size and other characteristics. These studies have provided qualitative and semi-quantitative evidence showing the enrichment of several volatile trace elements on flyash surfaces.

B. Flyash Volatilization

On the assumption that species volatilized during combustion and condensed on flyash surfaces may be readily volatilized on heating, two experiments were designed to identify the volatile species. First, flyash samples were activated, and heated to temperatures up to 1400°C and the volatile components collected for neutron activation analysis. Volatilization vs. temperature profiles have been obtained for several elements including Se, Hg, Br, I and As. Second, flyash samples were heated up to 2000°C in a Knudsen cell and the volatile species analyzed by modulated molecular beam mass spectrometry; hence, obtaining information on the actual molecular species volatilized.

C. Extractions of Organic Matter

The organic fraction of the collected fly ash has been extracted from sized flyash fractions by both solvent extractions and a vacuum extraction of fly ash heated slowly to 400°C. These fractions have been analyzed by GC and GC/MS techniques.

D. Analysis of Sized Flyash Fractions

Flyash samples collected from the precipitators of two western coal-fired steam plants were separated into size fraction using a Bahco Microparticle Classifier. Separate aliquots of each size fraction were analyzed for 43 major, minor and trace elements by X-ray fluorescence (XRF), atomic absorption (AA), and instrumental neutron activation (INAA), to establish the concentration-particle size dependence for each element. Replicate analyzes of two separate size fractions have allowed us to assess the heterogeneity of the fly ash and sampling errors. Analytical results for the "best method" are collected in Tables 1 and 2; analytical results for the second coal-fired plant for a wider range of particle sizes (<0.2 μ to >150 μ) have also been obtained. These results provide information on trace element enrichment in submicron flyash particles.

RESULTS AND DISCUSSION

The analysis of well-defined flyash size fractions offers the most promising method for determining the controlling mechanisms in the volatilization-condensation processes. Surface-depth profiles from sputtering are semi-quantitative (at best), are not usually sensitive to trace elements, and are often dependent on the simultaneous examination of a "field" of particles (or of individual particles, with added problems resulting from low sensitivity and the heterogenous nature of fly ash). These studies also carry the implicit assumption that diffusion will not significantly disturb the surface-depth profile after condensation. The observation of crystal growth on flyash particles(6) makes this assumption dubious. On the other hand, the major requirements for concentration vs. particle size measurements are much more readily fulfilled; the major assumption being that after condensation interparticle diffusion is negligible.

Elemental analyses of fly ash have often shown an inverse concentration dependence upon particle size for many trace elements. This relationship has been rationalized in terms of a Volatilization-Condensation Model (VCM)(1). According to this model, trace elements volatilized during the combustion process condense upon the (mostly) spherical particles of unvolatilized material in the cooler post-combustion region. The larger surface-to-mass ratio of smaller particles results in an enrichment of the volatilized trace elements, having an inverse or an inverse squared dependence upon particle diameter, depending upon the flow regime [i.e., free molecule or continuum](1,2).

The VCM, as proposed by Natusch and coworkers(1,7), predicts an inverse dependence of the total concentration (C) upon particle diameter,

$$C = C_m + \frac{6C_s}{\rho D} \quad 1)$$

where C_m is the concentration in the matrix upon which the volatiles condense, C_s is the surface concentration, ρ is the density, and D is the particle diameter. Flagan and Friedlander, however, have recently suggested that a direct dependence of C on D^{-1} should exist only in the free molecule regime where the Knudsen number, Kn , is greater than 1(2). At lower values of Kn , in the continuum regime, they suggest that the total concentration will be proportional to D^{-2} . This corresponds to a

surface layer thickness which is greater for smaller particles (proportional to D^{-1}) and predicts a much greater increase in the concentration of volatilized elements for the smaller particle sizes.

To compare models we have obtained least squares fits of our experimental results to the models of Natusch and coworkers(1) and Flagan and Friedlander(2). The model of Natusch and coworkers(1), with only a few exceptions, provides a significantly better fit than the Flagan and Friedlander model(2) to the data. In the following discussion we implicitly assume a concentration dependence similar to the VCM of Natusch and coworkers.

In order to increase the flexibility of the VCM it is advantageous to generalize the model by assuming a discrete surface layer of thickness L to be deposited over all particles. The relationship between the bulk concentration (C), the concentration in the matrix (C_m), and the concentration in the surface layer (C_s) of thickness L is:

$$C = \frac{C_m d_m (D - 2L)^3 + C_s d_s D^3 - C_s d_s (D - 2L)^3}{d_m (D - 2L)^3 + d_s D^3 - d_s (D - 2L)^3} \quad 2)$$

where

D = particle diameter

d_m = density of matrix material

d_s = density of surface layer

Results of analyses of fly ash as a function of particle size indicate that the elements, Mn, Ba, V, Cr, Co, Ni, Cu, Ga, Nd, As, Sb, Sn, Br, Zn, Se, Pb, Hg and S, are mostly volatilized in the combustion process (Table 1). The elements, Ti, Al, Mg, Na, K, Mo, Ce, Rb, Cs and Nb, appear to have a smaller fraction volatilized during coal combustion. The remaining elements, Si, Fe, Ca, Sr, La, Sm, Eu, Tb, Dy, Yb, Y, Sc, Zr, Ta, Na, Th, Ag and In, are either not volatilized or show trends which are not readily rationalized in terms of the simple VCM (Table 2).

Figure 1 shows the concentration vs. particle size data plotted for As, Zn, Rb and Mn, which are typical of elements having behavior which may be attributed to volatilization during combustion. These data have been fitted to the VCM using Equation 2, indicated by the lines in Figure 1.

The elements listed in Table 2 show either very little enrichment in the smaller particles or unusual concentration profiles. The concentration of Si shows a definite direct dependence upon particle size, making it unique in this study (Figure 2). The VCM can be used to qualitatively rationalize the Si data; by assuming $L = 0.1\mu$, $C_m = 35.5\%$, and $C_s = 0$ (and $d_m = d_s$), one obtains the fit given by the line in Figure 2.

The most interesting trends with particle size are observed for a group of elements (Ca, Sr, La, Sm, Eu, Tb, Dy, Yb, Y, Sc and Th) which exhibit distinct maxima in concentration at an intermediate particle size (4-8 μ). These trends are most striking for Ca and Sr (Figure 3), where maxima at ~4 μ are observed, confirmed by analysis of different samples by AA, XRF and INAA. The similarity of Ca, Sc, Sr and Y, and the rare earth elements is not surprising; these elements are known to be chemically similar. Barium might also be expected to behave in a similar fashion, but its lower oxide boiling point apparently results in sufficient volatility to obscure these trends. Concentration profiles for several of the rare earth elements

are shown in Figure 5. In Figure 6 we have plotted the rare earth element (REE) abundances normalized to chondritic values: The REE pattern observed for fly ash is similar to that observed in apatite, a mineral containing high concentrations of the rare earth elements and present as an accessory mineral in rocks and soils. (Similar REE patterns are also commonly observed for coal, plant and soil samples.) There are two plausible explanations for the observation of a maximum at $\sim 5\mu$, one involving geochemical fractionation, and the second, a combined geochemical-volatilization mechanism. The first involves an introduction of a geochemical fractionation mechanism to explain a maximum in the concentration vs. particle size profile at $\sim 4\mu$. The second couples a more reasonable geochemical fractionation process with the VCM. By assuming a decreasing value of C_m with particle size, setting $C_s = 0$ and choosing a finite surface layer thickness (L), one can obtain maxima in the concentration profiles; a condensed layer 0.1μ thick can rationalize a maximum at $\sim 5\mu$. Since the concentration profile resulting from any geochemical fractionation mechanism is unknown, a precise estimate of L is impossible. However, values of $L > 0.05\mu$ would be required to explain the results. To determine the relative importance of possible geochemical fractionation mechanisms, samples of the mineral matter obtained by solvent cleaning and low temperature ashing of coal have been sized and subjected to chemical analysis.

Analysis of the results in Table 1 (and Figure 1) shows that many elements are only partially volatilized during combustion, whereas others are essentially completely volatilized. Attempts to rationalize the volatility of elements in terms of simple parameters, such as the boiling points or melting points of the elements, their oxides, or sulfides are only partially successful, the best being the correlation with oxide boiling points. This is reasonable since oxides are known to account for the bulk of the fly ash and the "inorganic" elements in coal often exist as oxides, or form the oxide upon heating. While a rough correlation with oxide boiling points does exist, there are several elements with oxide boiling points above 1600°C which show appreciable enrichment in fly ash, including Cu, B, Tl, Zn, Ba, Ga, Cr, Mn, U and Be. A similar lack of correlation is observed for elements with oxide boiling points of less than 1500°C , with several elements showing only limited volatility (e.g., Cs, Li, Rb and Na).

The reasons for the enhanced volatility of specific elements may be either physical or chemical. The amount of trace element volatilization which will occur during coal combustion will be dependent upon a number of physical parameters, the most important being the residence time in the furnace and the concentrations and temperature vs. time profiles for both the gas and particulate phases.

The "inorganic" elements (defined here as all elements other than C, H, S and N) usually account for between 2% and 40% of the coal by weight, with a range of 5% to 15% being most common. While inclusions of mineral matter account for the bulk of the inorganic elements in coal, specific trace elements may be primarily associated with the organic fraction of coal.

The trace elements associated with the organic fraction of coal will be especially important in determining the gaseous and particulate emissions from coal combustion. During combustion, trace elements which are trapped in an organic matrix, or bonded in organic compounds (organometallic species), may be volatilized, or form an aerosol of minute particles. These elements may have a much higher probability of being transferred to the vapor state than a similar compound associated with the mineral fraction. It should be noted, however, that a volatilization of the organically associated elements is unnecessary for trace element enrichment; a similar inverse dependence of concentration upon particle size will result as the coal is consumed, and nonvolatilized inorganic elements associated with the organic fraction ultimately deposit on the remaining mineral inclusions which

finally form the fly ash. Organically associated elements which are not volatilized (or atomized) will be agglomerated with the mineral inclusions as the coal particles shrink during the pyrolysis and combustion processes. The precise concentration vs. particle size dependence predicted by this model depends on the relationship between the initial coal particle size and the size of the mineral inclusion.

Since insufficient information is available to determine a reasonable model, and the fraction of organically associated elements volatilized [or existing in the gas phase as fine particles, which will heterogeneously condense on larger particles (2)] is unknown, we cannot predict the precise concentration dependence of organically associated elements. However, the concentration of organically associated elements will be inversely dependent upon particle size, and may be qualitatively described by the VCM. Thus, the organically associated elements (which account for more than 50% of several elements) must play an extremely important role in the trace element enrichment observed in emitted flyash particles. To examine this theory we have begun sink-float separations of coal samples to determine the organic affinity of various elements in the feed coal at a coal-fired plant. These results will be compared with flyash enrichment data in our presentation.

The relationship between the percent of ash volatilized during coal combustion and the surface layer thickness in the VCM may be explored if the particle size distribution is known. As an approximation we have used the size distribution data obtained by Schulz et al. (8), and fit their results to a log-normal distribution (Figure 4). Assuming surface layer thicknesses of 0.01μ and 0.1μ (and $d_s = d_m$), one can integrate over the size distribution and determine that 5% and 28%, respectively, of the total ash was volatilized during combustion.

In Figure 4 we have also plotted the cumulative volume of the surface layer (V_s) over the total volume of all particles (V_t), as a function of particle size for a surface layer thickness of 100\AA . This analysis shows that for elements completely volatilized (assuming $d_s = d_m$), half of their total mass will be in particles of 0.33μ or smaller, and that more than 50% will be in particles between 0.1μ and 1.0μ in diameter. This result is especially important since there is a minimum in the collection efficiencies of most emission control devices in the same size regime.

In general, and despite its simplicity and crude approximations, the VCM appears to predict the concentration vs. particle size dependence remarkably well. While the agreement may be fortuitous, as a result of the complex gas-particle and particle-particle interactions during combustion which are only partially understood (2), the VCM does provide a good empirical fit to the data, using parameters which may be rationalized in terms of the chemical nature of coal. Our analysis has shown the organically associated elements, which are a major fraction of many trace elements in coal, play an important role in the enrichment of the smaller size particles and, hence, the emissions from coal-fired plants.

ACKNOWLEDGMENTS

This paper is based on work performed under United States Energy Research and Development Administration Contract No. EY-76-C-06-1830. We gratefully acknowledge the assistance of M. R. Smith, R. W. Sanders, and J. C. Laul in obtaining the analytical results, and A. L. Roese of Battelle, Columbus Laboratories, for the particle size separations.

REFERENCES

1. Davison, R.L., Natusch, D.F.S., Wallace, J.R. and Evans, C.A., Jr., Environ. Sci. Technol. 8, 1107 (1974).

2. Flagan, R. C. and Friedlander, S. K., Presented at the Symposium on Aerosol Science and Technology at the Eighty-second National Meeting of the American Institute of Chemical Engineers, Atlantic City, New Jersey, August 29-Sept. 1, 1976.
3. Pueschel, R. F., Geophy. Res. Lett. 3, 651 (1976).
4. Cheng, R. J., Mohnen, V. A., Shen, T. T., Current, M. and Hudson, J. B., J. Air Pollut. Control Assoc. 26, 787 (1976).
5. Linton, R. W., Loh, A., Natusch, D.F.S., Evans, C. A., Jr., and Williams, P., Science 191, 852 (1976).
6. Fisher, G. L., Chang, D.P.Y. and Brummer, M., Science 192, 553 (1976).
7. Natusch, D.F.S., "Sampling Strategy on a Characterization of Potential Emissions from Synfuel Production", Symposium-Workshop Proceedings, Austin, Texas, available NTIS, CONF-760602.
8. Schulz, E. J., Engdahl, R. B. and Frankenberg, T. T., Atmos. Environ. 9, 111 (1975).

TABLE 1
 Concentrations as a Function of Particle Size for Elements Showing Enrichment in the Smaller Size Fractions^a

Diameter ^b	Element													
	Ti ^c (%)	Al ^d (%)	Mg ^e (%)	Na ^d (%)	K ^d (%)	Mn ^c	Ba ^c (%)	V ^d	Cr ^d	Co ^d	Ni ^d	Cu ^c	Ga ^c	Nd ^d
0.5	0.79	10.7	2.33	2.05	1.41	954	1.23	340	230	25.7	190	501	96	83
2.0	0.78	10.0	2.29	1.85	1.24	701	0.78	300	220	22.4	130	396	77	80
4	0.82	10.6		1.78	1.33	646	0.62	320	220	22.4	105	345	70	83
5	0.75	9.56	2.15	1.79	1.20	505	0.45	240	140	19.0	67	275	52	50
8.5	0.69	9.35	1.94	1.47	1.11	430	0.34	200	150	16.2	80	241	33	55
12.5	0.34	8.80	1.10	1.20	0.89	262	0.21	110	75	10.0	36	156	14	45
15.5	0.59	7.31	1.37	1.08	0.94	248	0.20	105	90	11.7	63	131		50
25	0.54	6.95	0.82	0.76	0.72	190	0.31	74	60	7.6	35	105	5.4	32
50	0.47		0.61			148						67	4.7	

Diameter ^b	Element													
	Mo ^c	Ce ^d	Rb ^d	Cs ^d	As ^c	Sb ^d	Sn ^c	Br ^c	Nb ^c	Zn ^c	Se ^d	Pb ^c	S ^c	
0.5	87	180	62.1	5.01	79	23.5	51	6.2	74	215	68	254	7920	
2.0	74	170	56.1	4.60	70	22.9	38	4.8	44	162	44	172	5060	
4	76	180	54.6	4.48	67	21.6	28	4.0	50	122	30	139	5120	
5	54	145	51.8	3.60	46	13.6	10	3.2	40	87	23	96	4160	
8.5	36	135	46.2	3.36	29	11.0	9	1.6	35	70	12	74	3100	
12.5	16	110	43.1	2.89	10.5	4.20		0.9	33	32	10	44	1440	
15.5	15	100	34.8	2.57	10.1	3.40	8	<0.7	30	30	8	21	<1500	
25	10	80	34.7	2.20	4.6	1.96		<0.6	27	20	5	42	<1500	
50	9				4.2			<0.6	16	10		17	<1500	

a. Concentrations given in PPM unless otherwise noted.
 b. Mass median diameter.
 c. By XRF.
 d. By INNA.
 e. By AA.

TABLE 2

Concentrations as a Function of Particle Size for Elements
Not Showing Enrichment in the Smaller Size Fractions^a

Diameter ^b	Element							
	Si ^c (%)	Fe ^e (%)	Ca ^d (%)	Sr ^e	La ^e	Sm ^e	Eu ^e	Tb ^e
0.5	21.9	3.47	5.14	1600	70.3	8.68	1.95	1.15
2	23.5	3.20	6.16	2080	73.7	10.9	2.14	1.5
4		3.22	6.71	2360	76.7	10.5	2.29	1.6
5	24.3	2.89	6.53	1720	72.8	10.1	2.17	1.4
8.5	26.7	2.66	5.99	1650	69.6	9.43	1.97	1.3
12.5	29.4	2.10	3.33	1270	53.4	5.92	1.49	1.1
15.5	29.4	2.20	3.16	1520	55.7	7.23	1.56	1.2
25	34.3	3.02	2.26	800	41.9	6.00	1.16	0.86
50	35.8		2.01	(600) ^d				

Diameter ^b	Dy ^e	Yb ^e	Y ^d	Sc ^e	Zr ^d	Ta ^e	Th ^e
0.5	7.3	4.26	48	24.6	280	3.2	32.6
2	8.7	4.69	54	26.8	290	3.0	35.2
4	9.6	4.79	61	28.7	306	2.9	37.6
5	8.8	4.96	55	26.9	330	2.7	58.2
8.5	7.8	5.00	49	24.7	320	2.8	32.8
12.5	6.6	3.47	37	17.7	350	2.1	25.6
15.5	7.1	3.49	36	18.5	440	2.1	28.4
25	4.7	3.33	32	13.7	624	1.8	22.8
50			28		374		

- a. Concentrations in PPM unless otherwise noted.
 b. Mass median diameter (microns).
 c. By AA.
 d. By XRF.
 e. By INAA.

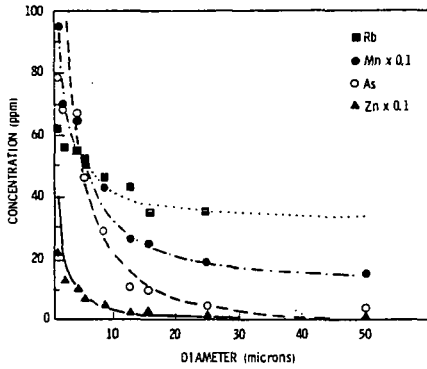


FIGURE 1. CONCENTRATION VERSUS PARTICLE SIZE DATA FOR Mn, Rb, As and Zn. ALSO GIVEN IS THE BEST FIT TO THE VOLATILIZATION-CONDENSATION MODEL

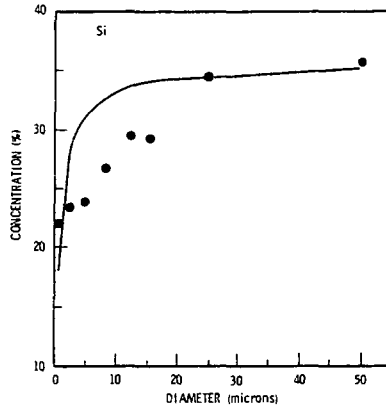


FIGURE 2. CONCENTRATION VERSUS PARTICLE SIZE DATA FOR SI WITH BEST FIT TO THE VCM ASSUMING A 0.1μ SURFACE LAYER THICKNESS

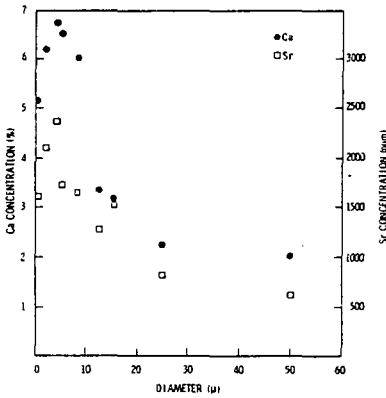


FIGURE 3. CONCENTRATION VERSUS PARTICLE SIZE DATA FOR Ca (●) AND Sr (□). A MAXIMUM WAS OBSERVED FOR BOTH ELEMENTS, AND MOST OF THE RARE EARTH ELEMENTS (TABLE 2), AT APPROXIMATELY 5μ . THE DATA FOR Ca AND Sr WERE CONFIRMED BY COMPARISONS OF ANALYSES BY AA, XRF, AND INAA TECHNIQUES

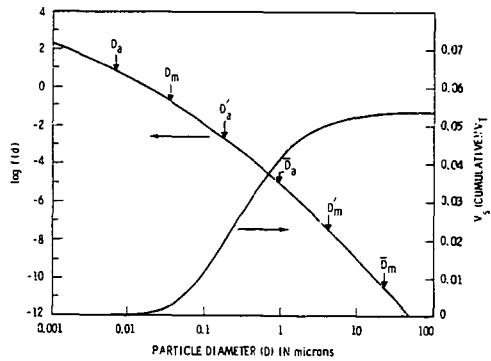


FIGURE 4. LOG-NORMAL DISTRIBUTION OF PARTICLE SIZES ASSUMED TO RESULT FROM COAL COMBUSTION (LEFT). D_a IS THE DIAMETER OF AVERAGE AREA, D_m IS THE DIAMETER OF AVERAGE MASS, D'_a IS THE AREA MEDIAN DIAMETER, D'_m IS THE AREA MEAN DIAMETER, D''_a IS THE MASS MEDIAN DIAMETER, AND D''_m IS THE MASS MEAN DIAMETER. ALSO GIVEN IS THE CUMULATIVE FRACTION OF THE TOTAL VOLUME OF THE FLYASH PARTICLES DUE TO A SURFACE LAYER 0.01μ THICK (RIGHT) FOR THIS LOG-NORMAL DISTRIBUTION

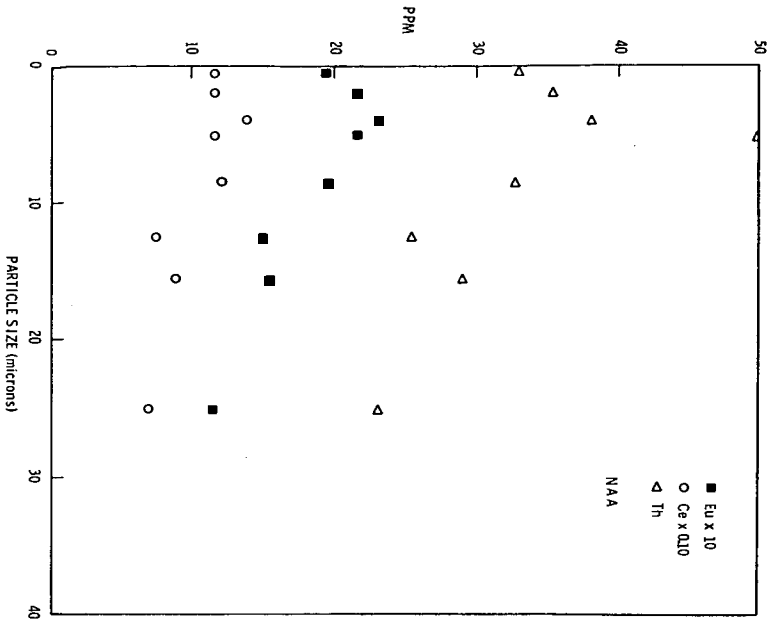
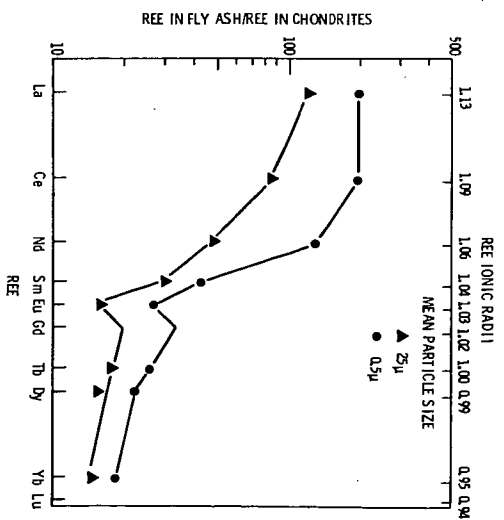


FIG. 5 (left) CONCENTRATION OF RARE EARTH ELEMENTS (REE) FROM NAA AS A FUNCTION OF PARTICLE SIZE
 FIG. 6 (above) RARE EARTH ELEMENT (REE) ABUNDANCES NORMALIZED TO CHONDRITES FOR TWO PARTICLE SIZES



Criteria for Selection of Coal Additives

Bruce L. Libutti and Rosanna L. Pall

Drew Chemical Corporation
One Drew Chemical Plaza
Boonton, New Jersey 07005

INTRODUCTION

Ash deposits are a major concern for coal users. They can reduce boiler availability, reliability, performance and efficiency.

The problems will become more acute in the near future. The energy crisis demands increased use of coal, and problems may be expected to grow at a faster rate than that of coal use. This is because disruption of normal coal supplies may be expected as increased demand puts a strain on the supply and transportation systems. Ash concentration will become less predictable. Cooperation will be needed among boiler manufacturers, coal users and coal suppliers.

Chemical treatment offers a means of alleviating the problems caused by coal ash deposits. Treatment of oil has been accepted for a number of years(1), but only occasional successes have been reported for coal (2-6).

This paper presents a rational approach to the choice of chemicals for treatment of ash from direct combustion of coal. It is hoped that application of the results of this study will advance the art, to the benefit of boiler owners and operators.

DEPOSIT PROBLEMS

There are two basic types of deposit problems, furnace slag and fouling of convection sections and superheaters. Corrosion of superheaters and supports is associated with the latter type of deposits. This study is addressed to alleviation of the fouling and corrosion of superheaters.

The key components in superheater corrosion by coal ash are the alkali iron sulfates. They are molten at superheater metal temperatures and participate in corrosive reactions, destroying the protective metal oxide coating and causing rapid corrosion. These compounds and their melting points are shown in Table 1.

TABLE 1. Alkali iron sulfates

<u>Compound</u>	<u>Melting points °F</u>
$\text{Na}_3\text{Fe}(\text{SO}_4)_3$	1155
$\text{NaFe}(\text{SO}_4)_2$	1274
$\text{K}_3\text{Fe}(\text{SO}_4)_3$	1145
$\text{KFe}(\text{SO}_4)_2$	1281

In addition to corrosion, the alkali iron sulfates may contribute significantly to the fouling of superheaters and the hotter parts of

convection sections. The molten sulfates can trap other ash particles and bond them.

CHEMICAL TREATMENT

There are two common mechanisms in direct chemical treatment of ash deposits. One is chemical reaction of the additive with the injurious deposit components or their precursors to form less harmful products. In the case of oil ash, for example, magnesium oxide reacts with vanadium pentoxide or sodium vanadyl vanadates to form magnesium vanadate, $3\text{MgO}\cdot\text{V}_2\text{O}_5$, which melts at 2179°F .

Treatment by chemical reaction has been suggested by Borio (7) and by Rahmel (8). Treatment with alkaline earth metal compounds was proposed to form compounds such as $\text{K}_2\text{Ca}_2(\text{SO}_4)_3$ and $\text{K}_2\text{Mg}_2(\text{SO}_4)_3$ at the expense of the alkali iron sulfates.

The second mechanism is physical. Dilution, formation of a barrier layer, or absorption of melts can prevent molten deposits from contacting tube surfaces, and hence prevent corrosion. All of these phenomena can also reduce the formation of bonded deposits. Certain types of successful oil additives are thought to work in this manner (1).

It appears from experience that the best method of application is to feed additives intermittently and to coordinate feed with the sootblower cycle. The treatment is fed immediately after the sootblowers have swept the target area, so as to allow maximum contact with inner deposit layers. Great care must be exercised in choosing the points and methods of addition to assure that the maximum amount of additive reaches the target surfaces. Success has been reported for intermittent feed (3, 6). To prevent corrosion and bonding, the alkali iron sulfates in the inner deposit layers must be affected. Attacking these compounds with additives is feasible, since they constitute a relatively small fraction of the total ash. Even with intermittent, directed feed, however, the major barrier to successful treatment is dilution or blocking of the additive by the bulk of the deposits. It is this effect of the matrix which chiefly distinguishes coal treatment from oil treatment.

Successful treatment with additives fed with the fuel is unlikely due to dilution by the bulk of the coal ash.

PRESENT INVESTIGATION

This paper reports a laboratory investigation of the effect of additives on synthetic superheater deposits which takes into account the effect of the matrix. The effect of additives on alkali iron sulfates was first determined. The experiments were then repeated with the addition of a third component: a matrix of bulk coal ash.

The criteria for success were the formation of solid, friable reaction products with the alkali iron trisulfates at 1100°F and maintenance of a solid, friable product with the addition of the ash matrix up to 1800°F , a representative gas temperature at superheater banks.

Friability of the mixture at the higher temperature was required since reaction of the additives with inner, sulfate-rich deposit layers will require periodic removal of outer layers by sootblowers. In

practice, if the additive and the outer parts of the deposit do not form friable products, attempts at treatment will simply powder the top of growing deposits.

EXPERIMENTAL

Additives were heated for two hours with alkali iron sulfates under a high-sulfur trioxide atmosphere to promote the stability of the sulfates. They were examined after heating at 1100°F and 1800°F. Appearance was noted visually and friability was tested with a spatula. It was noted whether the heated materials had wet the containers. Selected products were characterized by X-ray diffraction. The investigations were repeated with the addition of the ash matrix materials.

The equipment is shown in Figure 1. A commercial SO₂-air mixture was catalytically oxidized to SO₃ over a V₂O₅ catalyst.

ADDITIVES AND SYNTHETIC DEPOSITS

The alkali iron sulfates were prepared by the wet method of Corey and Sidhu (9). The synthesis and the stability of the materials at 1100°F under the experimental atmosphere were checked by X-ray diffraction. One simulated ash matrix had an elemental composition typical of Eastern coals. It was the following mixture: SiO₂ (40.1 weight %), Al₂O₃ (16.7), Fe₂O₃ (22.4), CaO (7.7), MgO (0.8), Na₂SO₄ (6.6), and K₂SO₄ (5.9). The other simulated Western coal ash and contained SiO₂ (25 weight %), Al₂O₃ (11), Fe₂O₃ (9), CaO (23), MgO (8) and Na₂SO₄ (25).

A mixture of K₃Fe(SO₄)₃ and Na₃Fe(SO₄)₃ by weight was used because the mixture melted below 1100°F. This allowed studies at 1100°F. Higher temperatures would have increased the instability of the sulfates and made the atmosphere more critical.

The additives in Table 2 are available in commercial grades. The rare earth oxide mixture contained 48% CeO₂ and 34% La₂O₃. The additives were applied at a ratio of 1:1 by weight to the alkali iron sulfate mixture. Matrix material was added as 1 part by weight to 1 part additive to 1 part sulfates.

RESULTS AND DISCUSSION

Without Matrix

Table 2 shows that effective deposit conditioning was achieved with a wide range of materials including both acidic and basic oxides. Mixtures contained the weight ratios shown.

TABLE 2. Additive evaluation, no matrix

Additive	Product at 1100°F	1800°F
Control	melt	melt
MgO	powder	melt
CaO	fusion, sticking	-
Rare earth oxide	powder	melt

TABLE 2. Additive evaluation, no matrix

Additive	Product at 1100°F	1800°F
TiO ₂	powder	melt
MnO	fusion, no sticking	fusion, melt
CuO	melt	
ZnO	melt	
Al ₂ O ₃	powder	fusion, slight melt
SiO ₂	powder	melt
MgO 66.7/Al ₂ O ₃ 33.3	powder	melt
MgO 28.3/Al ₂ O ₃ 71.7	powder	slight fusion
MgO 50.0/SiO ₂ 50.0	powder	melt
CaSiO ₃	slight fusion	melt

Of the transition and post-transition metals only titania, the rare earth oxides, and perhaps manganous oxide were satisfactory. Ti⁺⁴, La⁺³ and Ce⁺⁴ give a formal octet at the metal, as do the formal oxidation states in magnesia, alumina, and silica. The noble electronic configuration appears to be a favorable factor.

It is noteworthy that calcium and magnesium were not equivalent. A recent correlation of coal ash composition with melting behavior (10) distinguished elements on the basis of ionic radii and ionic potential. Magnesium fell with Si, Ti, and Al, while Ca fell with Na and K. The same trend appears to hold for reaction with alkali iron sulfates.

Another trend is that with the stability of the sulfate of the additive. Satisfactory additives with sulfates unstable at 1100°F were TiO₂, SiO₂ and Al₂O₃. Poor performers with stable sulfates at 1100°F included CuO, ZnO, CaO and MnO. MgSO₄ is stable, but less so than CaSO₄. Generally materials with unstable sulfates were more effective.

Since some of the heavier elements performed poorly, a study was conducted to assure that the results in Table 2 were not biased by unequal additive: sulfate mole ratios. It was determined that one mole of MgO per 0.23 moles of trisulfates was needed for a satisfactory product. All of the other oxides were then reacted with the sulfates at that mole ratio and their performance relative to MgO was not changed from that shown in Table 2.

The addition of a second component increased effectiveness in some cases. Calcium silicate performed better than CaO, and one MgO-Al₂O₃ mixture was superior to magnesia or alumina alone. The latter may have been due to spinel formation as shown in Table 3.

TABLE 3. Crystalline Reaction Products

<u>Additives</u>	<u>Temperature</u>	<u>Products</u>
MgO	1100°F	MgSO ₄ , K ₂ Mg ₂ (SO ₄) ₃ , (K, Na) ₃ Fe(SO ₄) ₃ *
MgO	1800°F	MgO, K ₂ Mg ₂ (SO ₄) ₃ , MgFe ₂ O ₄ *
Al ₂ O ₃	1100°F	Al ₂ O ₃ , (K, Na) ₃ Fe(SO ₄) ₃
Al ₂ O ₃	1800°F	Al ₂ O ₃ , Unidentified*
Al ₂ O ₃ 71.7 MgO 28.3	1100°F	K ₂ Mg ₂ (SO ₄) ₃ , Al ₂ O ₃ , Unidentified*
Al ₂ O ₃ 71.7 MgO 28.3	1800°F	MgAl ₂ O ₄ , K ₂ Mg ₂ (SO ₄) ₃ , Unidentified*

* Minor

The identification of the reaction products showed that magnesia reacted to form K₂Mg₂(SO₄)₃. No reaction was apparent for alumina. Its beneficial effects were due to dilution and absorption. At 1800°F magnesia and alumina reacted to form the spinel MgAl₂O₄. Alumina has been shown to be an effective adjunct to magnesia for conditioning oil ash deposits (11), and spinel has been identified in those deposits. The same beneficial effect is apparent here.

With Matrix

The results in Table 4 are cautionary and provide no simple trend to allow one to predict the relative performance of the additives.

TABLE 4. Additive Evaluation with Matrix

<u>Additive</u>	<u>Matrix</u>	<u>Product at 1800°F</u>
Control	Eastern or Western	melt
MgO	Eastern or Western	sl. fusion, sticking
Al ₂ O ₃	Eastern or Western	sl. fusion, sticking
SiO ₂	Eastern or Western	melt
MgO 28.3 Al ₂ O ₃ 71.7	Eastern or Western	powder, some sticking
MgO 50 SiO ₂ 50	Eastern or Western	powder, some sticking
CaSiO ₃	Eastern Western	melt powder, some sticking

Magnesia, alumina, their combination and the magnesia-silica combination showed satisfactory performance. Beneficial effects of mixtures were again seen for these materials, as the combinations were superior to MgO or Al₂O₃ alone.

However, silica, which performed well in the absence of the matrix, was unsatisfactory. The formation of the melt with the Eastern matrix was not predictable by standard composition-behavior correlations (12). The extreme difference for the two matrices with CaSiO_3 was also surprising. This unpredictability is a reflection of the complex chemical system involved. The complexity may be seen in mechanistic studies which have been reported (13). An empirical approach is suggested.

CONCLUSIONS

The corrosive components of superheater deposits may be chemically treated by a wide range of materials, both acidic and basic. They include magnesia, alumina, titania, silica and rare earth oxides and their combinations.

Only those additives which form high-melting friable products with the alkali iron sulfates in the presence of a matrix of bulk ash should be used. It is not possible to predict suitability from composition at this time.

Suitable additives may be selected empirically by studies such as the present one using samples of the appropriate deposits. The studies may be conducted by reputable chemical treatment suppliers.

Suppliers and boiler operators must then work in close cooperation to apply the additives in such a way that maximum benefits may be achieved. Only with such cooperation may the difficulties inherent in a high-ash fuel be overcome.

REFERENCES

1. W.T. Reid, External Corrosion and Deposits: Boilers and Gas Turbines, Elsevier, New York, 1971, Chapter 7.
2. A.D. Bailey, Trans. ASME, 60, 209 (1938).
3. H. Thompson, Proc. Amer. Power Conf., 18, 135 (1956).
4. Discussions in H.R. Johnson and D.J. Littler, editors, The Mechanism of Corrosion by Fuel Impurities, Proceedings of the Marchwood Conference, Butterworth's London, 1963, p. 526-528.
5. E. Raask, Mitt. VGB, 53, April, 248-54 (1973).
6. B.L. Libutti, Control of Coal Ash Corrosion by Additives, Paper 78e, 67th Annual AIChE Meeting, 1974.
7. R.W. Borio and R.P. Hensel, Trans. ASME, J. Eng. Power, 94, 142 (1972).
8. A. Rahmel, Johnson, op. cit. in H.R. Johnson and D.J. Littler, op.cit., p. 565ff
9. R.C. Corey and S. Sidhu, J. Amer. Chem. Soc., 67, 1490 (1945).
10. K.F. Vorres, Melting Behavior of Coal Ash Materials from Coal Ash Composition, ACS-CIC Fuel Chem. Symp. on Properties of Coal Ash, 1977.

11. G.K. Lee, E.R. Mitchell and R. Grimsey, Proc. Amer. Power Conf., 26, 531 (1964).
12. E.C. Winegartner, editor, Coal Fouling and Slagging Parameters, ASME, 1971.
13. P.H. Tufte and W. Beckering, Trans. ASME, J. Eng. Power, 97, 407 (1975).

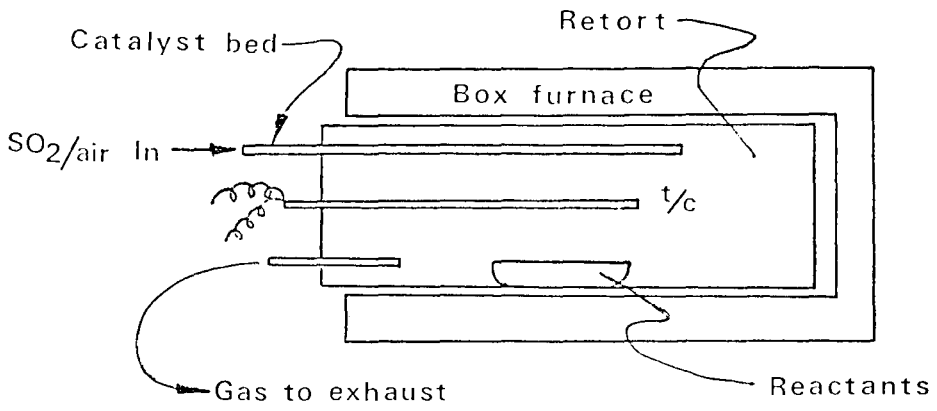


Figure 1 Furnace & Retort

THE RATE AND THE MECHANISM OF THE REACTIONS
OF HYDROGEN SULFIDE WITH THE BASIC MINERALS IN COAL

A. Attar and F. Dupuis

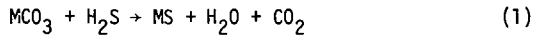
Department of Chemical Engineering
University of Houston

1.0 INTRODUCTION

The inorganic matter in coal can be classified into three groups of minerals according to their reactions with hydrogen sulfide (H_2S): (1) basic minerals, (2) minerals with catalytic activity, and (3) inert minerals. In the range of temperatures 200-900°C, most of the minerals are inert or have a slight catalytic activity on the rate of decomposition of H_2S . However, the basic minerals react with H_2S and the corresponding sulfides are formed. The most important minerals in this category are calcite (trigonal $CaCO_3$), aragonite (orthorhombic $CaCO_3$), dolomite ($CaCO_3 \cdot MgCO_3$), sidrite ($FeCO_3$), and to some extent montmorillonite (clay) (Attar, 1977).

The systems of reaction between H_2S and a metal carbonate MCO_3 involves four reactions (Glund *et al.*,²(1930), Stinnes (1930), Bertrand (1937), Parks (1961), and Squires (1972)).

1. Direct reaction of the carbonate with H_2S :



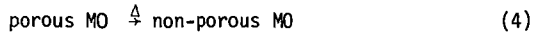
2. Decomposition of the carbonate to the oxide MO and CO_2 :



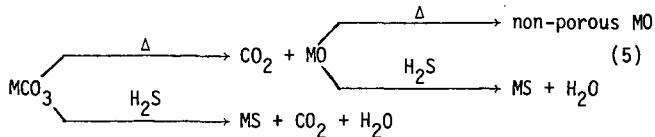
3. Reaction between the oxide and H_2S :



4. Sintering of the oxide and the formation of non-porous materials.



Reactions 1. and 2. are parallel, and reactions 3. and 4. are parallel. The last two reactions are in series with reaction 2.



H_2S is formed in coal by the reactions of FeS_2 with hydrocarbons and H_2 , (Powell, 1921) and by the decomposition of the organic sulfur compounds Thiessen (1945). In particular, H_2S is formed when the sulfidic functional groups decompose to H_2S and an olefin. The H_2S can react with the basic minerals and thus, the sulfur is trapped in the char in the form of the sulfide (Armstrong 1939). The kinetics of the reactions of H_2S with calcined dolomite and calcite were studied by Squires and co-workers (1970, 1972). In the present work, the mechanism of the reaction, their rate, and rate constants were derived for the reactions of H_2S with calcite, sidrite, dolomite, and montmorillonite.

Complete conversion of dolomite to CaS and MgCO₃ is obtainable at 570°C, but only 1.8-2.9 Wt. % of -200 mesh calcite reaction at these conditions (2.1 m²/gm surface area). At 700°C calcite and dolomite react at essentially identical rates. The rate of reaction of dolomite is however very sensitive to impurities.

Different rate controlling steps limit the apparent rate of consumption of H₂S at different temperatures. The rate controlling step depends also on the particular material and on its crystalline structure. At low temperatures, the rate is controlled by the rate of mass transfer and by the rate of diffusion of CO₂ in MS. At intermediate temperatures, the rate of consumption of H₂S is controlled by the availability of free surface of MO or MCO₃. In this range of temperature, the carbonates decompose according to reaction 2, a new surface is thus exposed which is not covered by MS, thus, the effective rate of consumption of H₂S increases. The available surface decreases by sintering when the temperature is too high, thus the rate of consumption of H₂S may decrease. When the rate of decomposition of MCO₃ becomes very large, the rate of consumption of H₂S may be limited by mass transfer in the gas.

The crystalline structure of calcite and dolomite is trigonal (Bragg *et al.* (1965) p. 127) and is basically identical, except that in dolomite alternate Ca⁺² ions are replaced by Mg⁺² ions. The spacial dimensions are different because the ionic radius of Mg⁺² is 0.65 Å and that of Ca⁺² is 0.99 Å (Greenwood, 1970). The mechanism of their reaction is however very different.

The rate of reaction of pure dolomite with H₂S is almost constant, and, does not vary with the conversion (up to 30 Wt. % conversion). Impure dolomite reacts initially at a much larger rate then after some of it had been converted. At 570°C the rate drops to about half the initial rate after about 4% of the material had been converted. At 570°C calcite reacts initially at about the same rate as pure dolomite, however, the rate of reaction drops to nil very rapidly. We estimate that when a layer of about 7.8 molecules of CaS, on the average, is formed on the surface of calcite, the diffusion of H₂S is blocked and the reaction stops. The layer of CaS breaks at around 635-650°C when the "pressure" of CO₂ inside the CaCO₃ crystal due to the decomposition reaction



becomes excessive. When the CaS layer breaks, a new surface is exposed and the reaction can proceed. Around 700°C no difference could have been detected between the rate of reaction of calcite and dolomite.

2.0 EXPERIMENTAL

Figure 1 is a schematic flow diagram which shows the relations among the various parts of the system.

The experimental system consists of four major components: (1) a differential reactor, (2) a pulse injector, (3) a gas chromatograph with a TC detector, and (4) an integrator with a data system.

Figure 2 shows the differential reactor. The shell (1), the tube (2), and the fillers (3) are made out of quartz. The gas inlet and outlet are through a SS connector. The quartz reactor is inserted through the wall of a high temperature furnace which temperature is controlled and monitored.

Pulses of the reactive gas, H_2S , are fed using a microprocessor controlled gas-chromatograph injector. The size of the injector loop determines the size of the pulse of H_2S which is introduced into the stream of helium. The helium passed through the reactor and into a chromatographic column and detector.

Each pulse of H_2S which is injected into the reactor resulted in a pulse which consists of the reaction products plus the unreacted H_2S . The mixture of gases is separated on the column and detected by the TC detector. The signal from the detector is integrated by a microprocessor which multiplies the areas by the proper calibration factors and prints the amounts of each component in the pulse of products of the reaction. The integrator and the injector are synchronized so that periodic operation is possible.

The repeatability of the injections was 0.05% or better. The overall accuracy of the analysis was at least 10% and usually better than 2% based on material balance.

Mixtures of H_2S , CO_2 , and H_2O were separated on a 6' X 1/8" column of chromosorb 103 80/100 mesh at 90°C. The helium flow was 75 ml/min.

The various minerals that were tested were NBS standard minerals,* except for the calcite which was purchased from Fisher Scientific.

*We wish to thank Dr. J. C. Butler, chairperson of the Department of Geology, University of Houston, who gave us the minerals.

3.0 MATHEMATICAL ANALYSIS

The rate of the reaction \bar{r} can be estimated using the relation:

$$\bar{r}_i = \frac{q(W_0 - W_i)}{W_s W_0} = \alpha \frac{q P_i}{W_s W_0} \quad (8)$$

where q is the carrier rate of flow, W_s the weight of material in the reactor, W_0 the number of moles that were injected in a pulse, W_i the number of moles of unreacted products, P_i the number of moles of products, and α a stoichiometric coefficient.

The rate of consumption of the solid in the reactor depends on the amount of solid, A , and on the instantaneous concentration of gas, C , around it; several cases deserve special attention and will be discussed in detail. Extension of the theory to other cases is straight forward.

3.1 Rate of Reaction Depends on n-Power of the Solid

When the rate of reaction depends on the n -th power of the weight of the solid in the reactor, A , then:*

$$-\frac{dA}{dt} = kA^n C \quad (9)$$

It is assumed for the moment that only one reaction takes place. If we multiply equation (9) by q , the volumetric rate of flow of the gas, and rearrange the equation we obtain:

$$-\frac{q}{1-n} d(A^{1-n}) = kqC \cdot dt \quad (10)$$

Integration of the equation for the i -th pulse yields

$$-\frac{q}{1-n} (A_i^{1-n} - A_{i-1}^{1-n}) = \int_{t_i}^{\infty} kqC_i dt \quad (11)$$

If the reaction is isothermal and only a small fraction of the pulse is consumed, thus the lower bound on k , k_1 , can be obtained by taking $c = c$ (feed)

$$\int_{t_i}^{\infty} k_1 q c dt = k_1 \int_{t_i}^{\infty} q c_i dt = k_1 W_i \quad (12)$$

where W_i is the number of moles of H_2S that were injected in the i -th pulse. Combining the last two equations yields:

$$\frac{A_i}{A_{i-1}} = \left[1 - \frac{(1-n)k_1 W_i}{q A_{i-1}^{1-n}} \right]^{\frac{1}{1-n}} \quad (13)$$

*This assumption is equivalent to saying that the rate of the reaction depends on a property of the solid which depends on the n -th power of its weight e.g., the surface area is roughly proportional to $A^2/3$.

If $A_i \approx A_{i-1} \approx A_0$ and $W_i = W = \text{constant}$ for all i -s then

$$\frac{A_i}{A_0} \approx \left[1 - \frac{B}{A_0^{1-n}} \right]^{\frac{i}{1-n}} \quad (14)$$

where $B = \frac{(1-n)k_1W}{q}$ (15)

Equation 14 can be used to evaluate B from which the rate constant k can be determined.

When a small fraction of the material is converted, $A_i \approx A_0$, a plot of $\log \frac{A_i}{A_0}$ vs. i yields a straight line with the slope $\frac{1}{1-n} \log \left(1 - \frac{B}{A_0^{1-n}} \right)$. To evaluate n , several experiments should be carried out with different initial amounts of the solid A_0 , or with pulses with a different size, W .

The upper bound on the rate constant k , k_u , can be estimated using the value of c at the outlet:

$$c = \frac{qC_0}{q + \alpha k A^n} \quad (16)$$

where C_0 denotes the concentration of the gas in the feed; and α is a coefficient to account for differences in the stoichiometry. Substitution of equation (16) in equation (9) yields:

$$\frac{q}{k_u(1-n)} (A_i^{1-n} - A_{i-1}^{1-n}) + \alpha (A_i - A_{i-1}) = -W_i \quad (18)$$

From stoichiometry:

$$\alpha (A_{i-1} - A_i) = (W_i - W_{iout}) \quad (19)$$

Therefore:

$$\frac{q}{k_u(1-n)} (A_i^{1-n} - A_{i-1}^{1-n}) = -W_{iout} \quad (20)$$

or

$$\frac{A_i}{A_{i-1}} = \left[1 - \frac{k_u(1-n)W_{iout}}{q A_{i-1}^{1-n}} \right]^{\frac{1}{1-n}} \quad (21)$$

A very important special case is when $n = \frac{2}{3}$. This occurs when the rate of reaction depends on the available surface area. When the solid is "infinitely porous" it may be 1. The case where $n \neq 1$ in the following section.

3.2 Rate of Reaction Proportional to the Weight of the Solid

If all the amount of the solid in the reactor is equally available for reaction, the rate may depend on the first power of the weight of the solid.

$$-\frac{dA}{dt} = kAC \quad (22)$$

The lower bound on the rate constant can be evaluated from the equation:

$$\ln \frac{A_i}{A_{i-1}} = -\frac{k_1}{q} W_i \quad (23)$$

Equation (23) can be simplified if the size of the pulses is equal, namely $W_i = W$ for all i . Then:

$$\frac{A_i}{A_0} = e^{-\frac{k_e W}{q} i} = e^{-\gamma i} \quad (24)$$

$$\gamma = \frac{k_e W}{q} \quad (25)$$

A plot of $\log \frac{A_i}{A_0}$ vs. i should yield a straight line with the slope γ , when such a model holds.

The upper bound on k , k_u , can be evaluated using the equation:

$$\frac{A_i}{A_{i-1}} = e^{-\frac{k_u W_i}{q}} \quad (26)$$

or

$$\frac{A_i}{A_0} = e^{-\frac{k_u}{q} \sum_0^i W_i} \quad (27)$$

3.3 Evaluation of the Rate Constants from Experimental Data

The data that are derived in each experiment include the initial condition of the sample, its weight, W_c , and its specific surface area, S_a . The length of the cycle, θ_c is usually determined by the difficulty of the separation of the products. The number of moles of reactive gas per injection, W , is determined by the fineness of the resolution which is required or by the sensitivity of the experimental system. The value of q can be used to modify B or γ , however it is usually dictated by the separation procedure.

The area of the pulse of gas when no reaction occurs is denoted by S_0 . The area of the peak of unreacted gas from the i -th pulse is denoted by S_i , and the area of the peak of the i -th product from the i -th pulse is denoted by K_i , where the response to the pulsed gas is taken as a unity. The total weight of solid in the reactor can react with the stoichiometric

amount of gas, W_g ; the equivalent area that a peak of magnitude W_g would have had it denoted by S_T . It is assumed that the detectors are linear, therefore, when all the weight of the solid is available for the reaction:

$$\phi_i = \frac{A_i}{A_0} = 1 - i \frac{S_0}{S_T} + \frac{\sum S_i}{S_T} \quad (28)$$

The average rate of consumption of gas per unit mass of solid is:

$$\bar{r}_i = \frac{q(S_0 - S_i)}{W_s S_0} \quad (29)$$

The rate of the single reaction which produces the j -th product is:

$$\bar{r}_i = \alpha \frac{q S_{ji}}{K_j S_0 W_s} \quad (30)$$

Note that if only part of solid, e.g. only a surface layer on the top of each crystal reacts, then S_T will have to be determined experimentally from the relation:

$$S_T = \sum_{i=1}^{\infty} (S_0 - S_i) \quad (31)$$

4.0 RESULTS

The most important variables that affect the rate of the consumption of H_2S are the temperature, the time-temperature history of the sample, the initial conditions of the sample, and the conversion.

Two types of kinetic experiments were conducted: (1) "isothermal," and (2) "temperature programmed." In each experiment, pulses of H_2S with a fixed size were injected, and the amounts of CO_2 , H_2O and unreacted H_2S were determined. In addition, the raw carbonates were tested by DTA and their specific surface area was determined by N_2 adsorption.

Arguments of material balance can be used to deduce the following conclusions: (1) The total number of moles of MS that are formed is equal to the total number of moles of H_2S that are consumed; and also to the number of moles of water that are produced. (2) The number of moles of H_2O and of CO_2 that are produced in reaction 1 as a result of a given pulse of H_2S , is equal to the number of moles of H_2S that are consumed in the reaction. The number of moles of H_2O , in excess to the number of moles of CO_2 , are formed by reaction 3. Figure 3 shows the isothermal rate of consumption of H_2S by calcite, pure dolomite, dolomite, montmorillonite, and sidrite at $570^\circ C$, as a function of the conversion of the solid. The rate of the reaction with H_2S behaves according to one of three modes: (1) rate independent of the conversion, (2) rate decreasing with the conversion, but complete conversion is obtainable, (3) rate decreasing very rapidly with the conversion, and complete conversion is not obtainable.

The rate of reaction of dolomite at 570°C as a function of the conversion is almost constant. However, at 700°C the rate decreases slowly with the conversion. The rate of reaction of calcite at 570°C decreases very sharply, and becomes essentially zero after about 2.8% of the material are converted. At 700°C the rates of conversion of dolomite and calcite to MS are the same.

Sidrite decomposes at much lower temperatures than CaCO_3 or dolomite, FeO and CO_2 are formed. The decomposition of sidrite is complete at 495°C, FeO sinters much more rapidly than CaO . Thus the available surface area of FeO decreases when the sidrite is heated for prolonged times above 500°C. Figure 4 shows the rate of consumption of H_2S by decomposed sidrite that was kept 2-1/4 and 5-1/4 hours at 635°C.

Figure 5 shows the rate of consumption of H_2S by calcite, dolomite, and sidrite which temperature was increased at about 3.3 °C/min. The data were not corrected for the conversion of the material; the effect of the correction is more important at the higher temperatures. The rate of consumption of H_2S by calcite and dolomite seems to be very similar above 650°C, however, different rates are observed below 650°C. Figure 6 shows the rate of evolution of CO_2 from calcite and dolomite as a result of reaction 1. The data show very clearly that the rate of evolution of CO_2 from calcite decreases with the temperature up to 635°C but then it increases very rapidly and at about 700°C it becomes identical to the rate of evolution of CO_2 from dolomite. The rate of evolution of CO_2 from dolomite increases monotonically with the temperature. It should however be noted that the apparent decrease in the rate is due to the coverage of the surface by CaS and the creation of resistance to mass transfer of CO_2 . (The plotted rate is not the initial rate of reaction of clean surfaces). The rate of evolution of CO_2 that results from the thermal decomposition of the carbonate, shows a continuous drift in the detector base line. The decomposition of calcite and dolomite to CaO were complete at 810°C and the decomposition of sidrite was complete at 495°C. Figure 7 shows the rate of formation of water by reaction 3. The data show that the rate of evolution of water becomes almost constant at temperatures above 685°C where no more CO_2 is formed by reaction 1.

5.0 DISCUSSION OF THE RESULTS

The discussion is divided into two parts: discussion of the mechanism of the reactions, and discussion of the rates of the reactions.

5.1 The Mechanism of the Reactions

The rate of consumption of H_2S is influenced by the rates of reactions 1-4, which takes place simultaneously, and by the rate of mass transfer of H_2S , H_2O , and CO_2 through the layer of product MS which is formed on the surface of the MCO_3 crystals. The rate of the chemical reactions is a strong function of the temperature, therefore, different reactions may dominate at different temperatures. In particular, the rate of decomposition of CaCO_3 and of dolomite (reaction 2) becomes very large at temperatures above 739°C. Therefore, large amounts of MO are produced

which competes with the MgCO_3 on the available H_2S . Since CaO reacts with H_2S more rapidly than CaCO_3 , the apparent rate of consumption of H_2S by the mixture of CaO-CaCO_3 at temperatures above 730°C is significantly larger than at lower temperatures. Mass transfer in the gas may also become the limiting step at very high temperatures.

The rate of mass transfer in the solid may limit the apparent rate of reaction by preventing the reagent H_2S from reaching the reaction metered, or by preventing the products CO_2 and H_2O from escaping out. The role that the product MS plays depends on the crystalline structure of MS and that of "host" crystal, the MO or the MCO_3 . If the crystalline structures of MS and the host are "compatible" so that the layer of MS can adhere to the surface of the host, (as a solid solution) then resistance to mass transport will be created as a result of the reaction.

Figure 3 shows that at 570°C calcite stops to react after about 2.8 Wt. % of the -200 mesh material was converted. Dolomite, which has the same crystalline configuration continues to react although the initial rate of the reaction depends on the impurities in the material. Dolomite and calcite have the same crystalline structure, except that in dolomite every alternate Ca^{+2} ion is replaced by a Mg^{+2} ion. Had all the components of dolomite been reactive, one would expect that MgS and CaS will be formed as a result of the reactions with H_2S . However, at 570°C only CaS is formed since MgCO_3 does not react with H_2S at 570°C . Therefore, a continuous layer of CaS can not be formed on the surface of dolomite but it can be formed on the surface of calcite. Therefore, once a layer of average thickness of about 7.8 molecules is formed on the surface of the calcite, at least one of the gases CO_2 , H_2O , or CO_2 can not diffuse through it anymore and reaction 1 stops.

It is plausible that the reaction between H_2S and calcite stops because CO_2 cannot diffuse through a layer of CaS . One evidence which supports this theory is that CaO reacts with H_2S according to reaction 3 and is completely converted to CaS . Had CaS been impermeable to H_2O or to H_2S , the reaction of CaO should have also stopped before complete conversion to CaS .

The latter theory is supported by the experimental evidence of CO_2 by retention 1 and of the absorption of H_2S by reactions 1 and 3 as a function of the temperature. The experiment was conducted as follows: first the surface of the calcite was reacted with H_2S at 590°C until the reaction stopped, and then the temperature was programmed up slowly while injecting small pulses of H_2S to study the reactivity of the material. The data shows clearly that around 640°C the layer of CaS breaks, new surfaces of $\text{CaO} + \text{CaCO}_3$ are exposed and reactions 1 and 3 can commence. The equilibrium pressure of CO_2 at 640°C is estimated to be about 0.02 atms. Such a pressure is apparently sufficiently large and can break the layer of CaS .

The crystalline structures of FeO and FeS are different and apparently FeS does not adhere to the surface of FeO . Indeed, even if it adheres,

FeS seems to permit diffusion of H₂S since reaction 3 can proceed at 570°C into completion. However, limited resistance to mass transfer is observed when 3-4 Wt. % of the material is converted.

FeO sinters at a much larger rate than CaO, and at high temperatures its available surface area decreases very rapidly with time. Figure 8 shows that at 570°C, equation (14) with $n = 2/3$ fits the data very adequately, but at 635°C or 700°C the description is inadequate. Equation (14) was derived from equation (9) in which the sintering effect which reduces the surface area was not taken into consideration. Note that an increase in the temperature results in an increase in the rate constant of reactions 3 and 4. The latter reaction reduces the surface area which is available for reaction with H₂S according to reactions 1 and 3.

5.2 Quantitative Rate Data

Rate data on some selected systems is presented in Table 2. The data were derived on samples of particles -200 mesh, of about 0.1-0.2 gm each. Unless otherwise specified, the material was permitted to equilibrate 2-1/4 hours at the reaction temperature. Equation (14) with $n = 2/3$ has been used to evaluate the lower bound on the rate constant.

The evaluation of the activation energies and their use should be done with caution, since they have greatly different values in different temperature regions. A summary of the data is given in Table 2.

TABLE 2
Activation Energies for the Rate of Consumption
of H₂S by Minerals

<u>Material</u>	<u>T°C Range</u>	<u>Controlling Mechanism</u>	<u>Ea kcal/mole</u> ±30%
Calcite	560	Diffusion of gas through CaS	0.0
Calcite (with CaO)	560-670	Rate of reaction	19.0
Calcite (with CaO)	670	Rate of gas-phase mass transfer	4.0
Dolomite	640	Rate of reaction	12.2-13.5
Dolomite (with CaO-MgCO ₃)	640	Rate of gas-phase mass transfer	2.4
Sidrite (with FeO)	460	Rate of reaction	15.2
FeO	460	Rate of gas-phase + mass transfer and sintering	0.0

In general, mass transfer controls when the reacting material is a carbonate, and the rate of reaction (2) or the rate of gas-phase mass transfer will control when the reacting solid is the oxide. Small activation energies (0-4 kcal/mole) are observed when the carbonate reacts and 30-45 kcal/mole are observed when the oxide reacts. Note should however be made of the decomposition reaction 2 in which the carbonate is transformed into an oxide. This reaction can not be controlled and it tends to activate the solid even when the carrier gas contains CO₂ (the rate of reaction 2 is suppressed in the latter case).

REFERENCES

- Armstrong, V. and Himms, G. W., Chem. and Ind., June 10, 543 (1939).
- Attar, A., "The Fundamental Chemistry and Modeling of the Reactions of Sulfur in Coal Pyrolysis," Paper presented in the AIChE Meeting, Houston, Texas, March 1977.
- Attar, A., "The Fundamental Chemistry and Modeling of the Reactions of Sulfur in Coal Pyrolysis and Hydrogenation," In print in a Chemical Engineering Progress technical manual.
- Bertrand, M. F., "Gas Purifying Materials," Brit. Pat., 462, 934 (1937). C.A. 31-6446.
- Bragg, L. and Claringbull, G. F., "Crystal Structures of Minerals," Cornell University Press, Ithaca, N. Y. (1965).
- Gluud, W., Keller, K., Klempt, W., and Berthorn, R., "Development and Operation of a New Process for Hydrogen and Hydrogen-Nitrogen Mixtures," Ber. Ges. Kohlentech., 3, 211 (1930).
- Greenwood, N. N., "Ionic Crystals, Lattice Defects and Nonstoichiometry," Butterworths, London (1970).
- Parks, G. D., "Mellons Modern Inorganic Chemistry," Longvans, London (1961).
- Powell, A. R., Ind. Eng. Chem., 13, 33 (1921).
- Ruth, L. A., Squires, A. M., and Graft, R. A., "Desulfurization of Fuels with Calcined Dolomite," Paper presented in the ACS Meeting, Los Angeles, California, March (1971).
- Squires, A. M., "New Systems for Clean Power," Int. J. Sulfur Chem., Part B, 7 (1), 85 (1972).
- Stinnes, G. M., "Gas Purifying Materials," Brit. Pat., 371, 117 (1930). C.A. 27-2565.
- Thiessen, G., "Forms of Sulfur in Coal," Chapt. 12, p. 475 in "Chemistry of Coal Utilization," Lowry, H. H., (ed.), Wiley, N. Y. (1945).

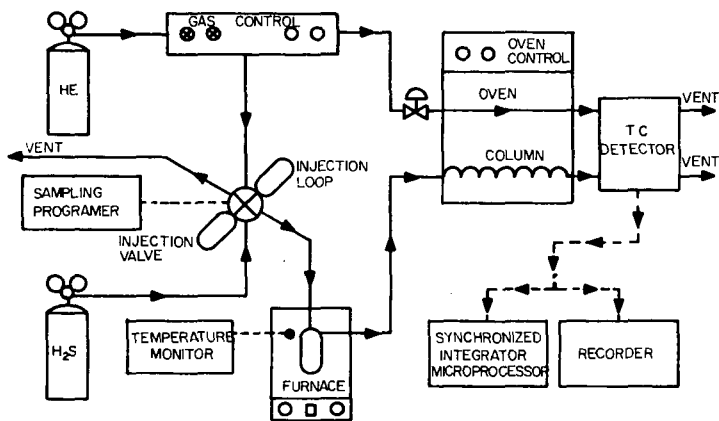


FIGURE 1: SCHEMATIC DIAGRAM OF EXPERIMENTAL SYSTEM

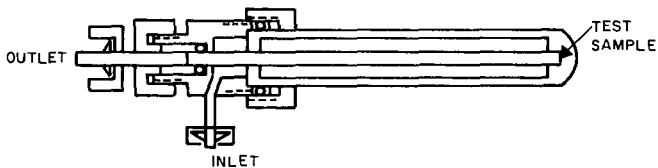


FIGURE 2: CROSS SECTION OF THE HIGH TEMPERATURES MICRO-DIFFERENTIAL REACTOR.

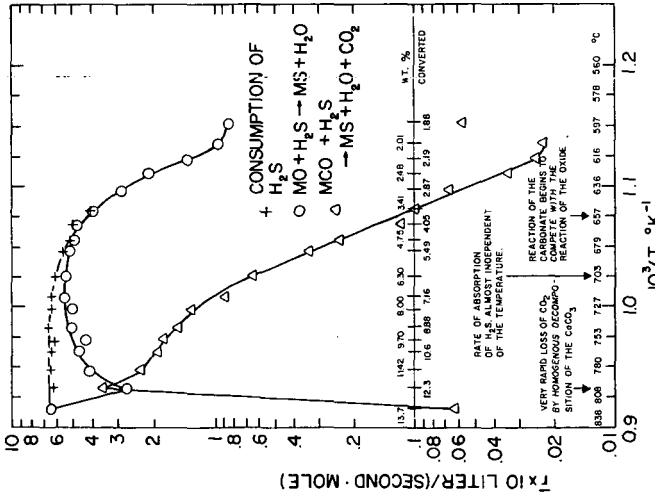


FIGURE 7: RATE OF CONSUMPTION OF H₂S AND THE RATES OF EVOLUTION OF H₂O AND CO₂ AT DIFFERENT TEMPERATURES. THE REACTION AT 590°C STOPPED. SEE TEXT.

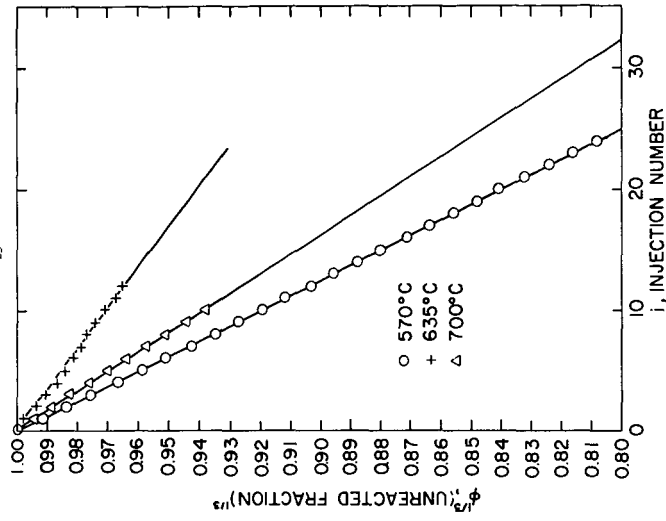


FIGURE 8: THE PROGRESS OF THE REACTION OF SIDRITE AT DIFFERENT TEMPERATURES.

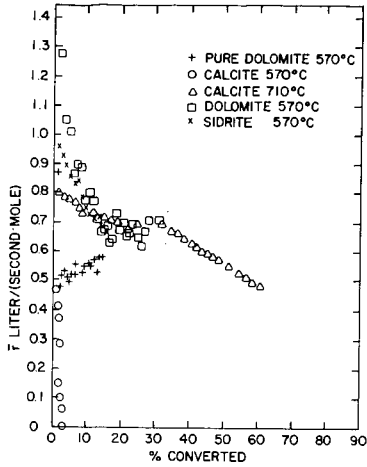


FIGURE 3: THE RATE OF CONSUMPTION OF H_2S BY BASIC MINERALS.

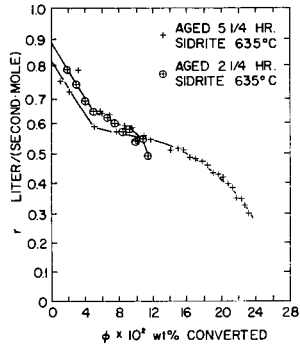


FIGURE 4: THE RATE OF CONSUMPTION OF H_2S BY DECOMPOSED -200 MESH SIDRITE AT $635^\circ C$

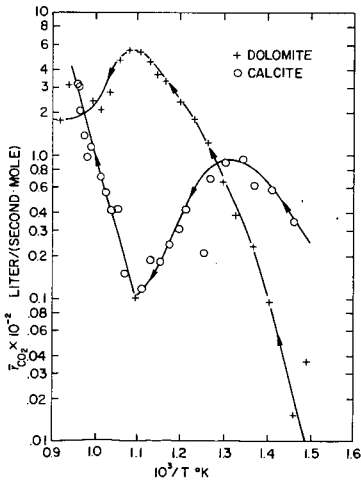


FIGURE 6: RATE OF EVOLUTION OF CO_2 FROM CALCITE AND DOLOMITE IN A TEMPERATURE-PROGRAMMED TEST.

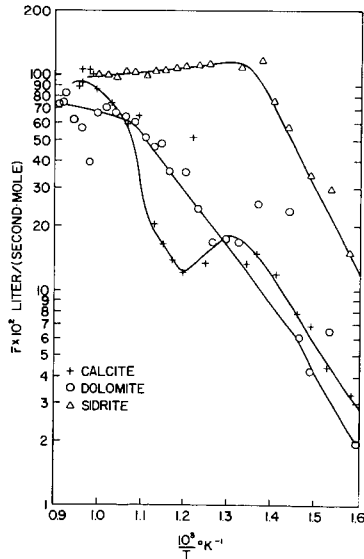


FIGURE 5: THE VARIATION IN THE RATE OF CONSUMPTION AT H_2S BY BASIC MINERALS IN TEMPERATURE PROGRAMMED EXPERIMENTS.

IDENTIFICATION OF ISOPRENOIDS, STERANES, AND TERPANES IN FISCHER ASSAY RETORTED SHALE OILS

J. Renzo Morandi and Frank Guffey

Department of Energy
Laramie Energy Research Center
P. O. Box 3395
Laramie, Wyoming 82071

INTRODUCTION

In the past 15 years much work has been done on the identification of individual compounds in the branched-plus-cyclic paraffin hydrocarbon fractions from Green River oil shale bitumens; i.e., on the small amount of material that can be solvent extracted from the shale. Cummins and Robinson (1) identified the C-16, C-18, C-19, and C-20 isoprenoid alkanes. Burlingame and coworkers (2) reported the presence of C-27, C-28, and C-29 steranes. Eglinton and coworkers (3) identified cholestane, ergostane, sitostane, and perhydro- β -carotene. Anders and Robinson (4) identified 52 cyclic alkanes, and Henderson (5) identified steranes and triterpanes. Gallegos (6) identified 36 individual components in the saturate fraction of an oil shale bitumen. Robinson and Cook (7) studied the bitumen from a Wyoming oil shale core with respect to the variations in the distribution of various alkanes with stratigraphy.

Most of the geochemical studies have been made on the unpyrolyzed bitumen because of the suspicion that pyrolysis of the kerogen would destroy or alter the biological markers and thus negate the results. However, recent studies suggest that some of these markers survive pyrolysis. Gallegos (8) reported the presence of gammacerane and the C-27, C-28, and C-29 steranes in a pyrolysis study of so-called "kerogen-shale"--shale residue after the extraction of solubles with a benzene-methanol mixture. Takeo (9) reported the presence of C-18 and C-20 alkane isoprenoids in an N.T.U. shale-oil distillate.

In this study, saturate fractions of Fischer assay oils from an earlier study (10) were examined in detail to see if the biological markers survive the retorting process. A study of these biological markers in the oils produced from a core might be used as an aid in the geochemical study of sediments. Although this core is not identical to that studied by Robinson and Cook, it is from the same area so that some comparisons can be made between the bitumen and the pyrolyzed product.

EXPERIMENTAL

A core was obtained from northern Green River Basin in T21N, R107W, Sweetwater County, near Rock Springs, Wyoming. Fischer assay (11) was carried out on the sections of the core containing kerogen. A lithographic description of the core was used to composite the Fischer assay oils into 11 composite oils comprising the oil produced from adjacent shale seams of similar appearance. The 11 composite oils are representative of the three principal members of the Green River oil shale formation in this basin. The first two composite oils, L-1 and L-2, are from the Laney member; the next eight composite oils, WP-1 to WP-8, are from the Wilkins Peak member; and the last oil, T-1, is from the Tipton member, which is the lowest stratum containing kerogen.

A saturate fraction of each composite oil was prepared by dissolving 3 g of oil in approximately 10 ml of cyclohexane. The nonsaturates were removed by sulfonation and centrifugation as described in ASTM method D-1019 (12). The resulting cyclohexane-saturates solution was chromatographed on a 1/2-in. i.d. by

6-in. column packed with 60-200 mesh silica gel and eluted with benzene. Organic material was recovered by rotary evaporation of solvent.

Each saturate fraction was separated into n-paraffins and branched-plus-cyclic paraffins (BCP) by molecular sieves. The n-paraffins were recovered by destroying the molecular sieves with hydrofluoric acid (13).

All the n-paraffins and BCP fractions were analyzed using a Hewlett-Packard* 5710A gas chromatograph equipped with a flame ionization detector. Paired 50-ft by 0.02-in. i.d. support coated open tubular (SCOT) columns coated with Dexsil 300 were used. The chromatograph was programmed from 100°C at 4° per minute up to 300°C, where the temperature was maintained for 16 minutes.

Combined gas chromatography-mass spectrometry (GC-MS) of selected samples were obtained using a Hewlett-Packard 5710A gas chromatograph and an AE IMS-12 mass spectrometer. A similar SCOT column was coupled directly to the source of the MS-12 without the benefit of a separator. All the mass spectra were obtained at 70 volts.

Data acquisition and processing were accomplished with a Finigan Incos 2300 series mass spectrometer data system. The magnet cycle time was 18 seconds.

RESULTS AND DISCUSSION

Geochemical investigations of biological markers are usually made on samples that have been carefully collected and preserved to prevent the formation of artifacts. However, recent work by Gallegos (8) suggests that some of the biological markers survive the retorting process, and Gallegos suggests that "The terpanes which have survived pyrolysis rather than those extracted reflect more faithfully the distribution and identity of the terpanoids originally laid down in the sediments." To investigate these possibilities, we examined the alkane hydrocarbons in oils produced by retorting oil shales from different geologic regimes. All the shales were retorted in identical fashions by Fischer assay which heats the shale at a controlled rate to 500°C.

Geology

A brief description of the geology of the area from which the subject core was obtained will set the stage for the discussions. The oil shales of the Green River Formation in Wyoming were formed in Gosiute Lake in early and middle Eocene age (14). This lake went through three major changes in size. During the first stage, in which the Tipton member was laid down, it was large and overflowing, and thus a fresh water lake. During the second, or Wilkins Peak stage, the lake shrank and became extremely saline. When the top, or Laney member, was laid down the lake had again expanded, overflowed, and become a fresh water lake.

General Characteristics

Table 1 shows the depth and length of the sections that were composited for Fischer assay, together with the oil yield, the percent of total saturates, and the percents of this saturate fraction that are normal and branched-plus-cyclic paraffins (BCP). The lengths of the core vary from 193 feet for WP-6 to 7 feet for T-1, showing considerable difference in the length of the homogeneous bands. The oil yield data show that the oil shale in this area is lean, ranging from 4.5 to 15.9 gallons per ton. The average yield for the core, excluding the barren sections, (most of which are in the top 300 feet) is 9.0 gallons per ton. The

*Mention of specific brand names or models of equipment is for information only and does not constitute an endorsement by the Department of Energy.

saturates represent 9 to 11 percent of all the oils except the Tipton, the single sample of which has a somewhat higher saturate content than the other oils. A previous study (10) showed that the Tipton oil had significantly smaller amounts of polar compounds than the other oils. Thus, its high content of paraffins may simply reflect a lack of dilution by the polar components.

TABLE 1. - Description of Wyoming core and percentages of saturates, normal, and branched-plus-cyclic hydrocarbons in the Fischer assay oils

Section ^{1/}	Depth ^{1/} ft.	Length ^{2/} ft.	Yield, gal/ton	Saturates, vol. % of oil	Vol % of saturates	
					n-paraffins	Branched-cyclic paraffins
L-1	771.5	38.1	5.3	9.7	63.9	36.1
L-2	870.5	59.6	10.3	11.1	60.4	39.6
WP-1	1064.7	44.3	13.5	8.9	39.3	60.7
WP-2	1109.0	48.6	15.1	9.7	46.4	53.6
WP-3	1157.6 ^{4/}	41.2	11.0	10.2	45.1	54.9
WP-4	1250.0 ^{4/}	26.4	8.0	9.8	48.0	52.0
WP-5	1276.4	45.6	15.9	9.7	51.5	48.5
WP-6	1322.0	193.0	6.1	9.9	39.4	60.6
WP-7	1515.0	101.0	8.9	9.8	51.0	49
WP-8	1616.0	94.0	7.3	10.0	56	44
T-1	1710.0	7.0	4.5	13.3	63.9	36.1

^{1/} L = Laney member, WP = Wilkins Peak member, T = Tipton member

^{2/} Top of section

^{3/} Excluding barren section

^{4/} 51.2 feet of core missing between WP-3 and WP-4

Normal Paraffins

Table 1 shows variations in the composition of the saturate fractions with regard to their content of n-paraffins. The Laney and Tipton saturates are 60 to 64 percent n-paraffin, while the Wilkins Peak saturates contain significantly lower amounts. Thus, the two freshwater deposits are higher in n-paraffins than the saline deposit. The high value of WP-8, which is adjacent to the Tipton core, may suggest an influence of the freshwater member on its adjacent saline member; i.e., a somewhat gradual transition from fresh to saline.

Gas chromatographic investigation of the n-paraffin fractions of the 11 oils shows n-paraffins from C-11 to C-34 with the greatest abundance at about C-17. The odd-to-even preference that was noted in n-paraffin fractions of bitumens from a similar core (7) is absent. This result was not unexpected in these oils, which had been heated at 500°C, because Cummins (15) showed disappearance of the odd-to-even preference when shales were degraded at temperatures of 150 to 350°C.

Branched-Plus-Cyclic Paraffins

Gas chromatograms of the BCP fraction of the oils suggested the presence of chain isoprenoids, steranes, and pentacyclic triterpanes. Chromatograms of samples from each of the members are shown in Figure 1. Combined GC-MS analyses were obtained on these three representative fractions to identify the major peaks. An example of the resulting reconstructed chromatograph for the Wilkins Peak sample is shown in Figure 2. Two of the peaks--26 and 31--contained two compounds, while each of the others contained one. Thirty-six compounds were identified in the GC

fractions and accounts for 55 percent of the BCP fraction. In several instances, as will be noted later, the MS identification was confirmed by coinjection of authentic samples. The qualitative data from the mass spectra may now be combined with the quantitative data from gas chromatography to examine the various types of compounds that are present in these oils.

Chain isoprenoids. - The larger peaks in the first part of the gas chromatograms (Figure 1) are chain isoprenoids. The GC peak number and the empirical formula of these compounds are listed in Table 2. The gas chromatographic data in Figure 1 show considerable variation in the amounts of the individual isoprenoids. Phytane (peak 14) increases from 2 percent in the Tipton to 5.5 in the Wilkins Peak and to 8.3 in the Laney. This increase in a compound usually thought to be a degradation product of chlorophyll (4) may suggest an increase in the amount of vegetative matter as the lake went from the Tipton to Wilkins Peak to Laney.

TABLE 2. - Chain isoprenoids (C_{n-2n+2}) identified

GC peak no.	Empirical formula	Molecular weight	Common name
1	$C_{13}H_{28}$	184	
2	$C_{14}H_{30}$	198	
4	$C_{15}H_{32}$	212	Farnasane
6	$C_{16}H_{34}$	226	
8	$C_{17}H_{36}$	240	
10	$C_{18}H_{38}$	254	
12	$C_{19}H_{40}$	268	Pristane
14	$C_{20}H_{42}$	282	Phytane
15	$C_{21}H_{44}$	296	
15A	$C_{22}H_{46}$	310	
16	$C_{23}H_{48}$	324	
17	$C_{24}H_{50}$	338	
18	$C_{25}H_{52}$	352	
19	$C_{30}H_{62}$	412	Squalane

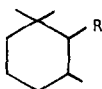
Inspection of Figure 1 reveals many differences in the ratios of the amounts of the chain isoprenoids. For example, the ratio of the heights of peaks 10, 12, and 14 changes from 1.2/1.0/2.4 to 1.2/1.0/1.3 to 0.8/1.0/1.0 as the depth increases.

Monocyclic Isoprenoids. - Eight monocyclic isoprenoids shown in Table 3 were identified, These are the small, odd-numbered peaks in the first part of the chro-

TABLE 3. - Monocyclic isoprenoids (C_nH_{2n}) identified

GC peak no.	Empirical formula	Molecular weight
3	C ₁₄ H ₂₈	196
5	C ₁₅ H ₃₀	210
7	C ₁₆ H ₃₂	224
9	C ₁₇ H ₃₄	238
11	C ₁₈ H ₃₆	252
13	C ₁₉ H ₃₈	266
18A	C ₂₉ H ₅₈	406
32	C ₄₀ H ₇₈	558

matograms (Figure 1) and 18A in the chromatogram of T-1. These compounds have the empirical formula C_nH_{2n}, and the general structure



where R is a saturated chain of varying length. The amounts of these compounds, which are thought to be derived from perhydro-β-carotene, are small so that quantitative differences are obscured except for the C-29 compound (peak 18A). This compound makes up 2.3 percent of the BCP fraction of the Tipton but is absent in the Wilkins Peak and the Laney. The mass spectrum of this compound shows fragments that are typical of monocyclic isoprenoids.

Dicyclic Isoprenoid--Perhydro-β-Carotene. - A dicyclic compound, peak 32 in Figure 1, was shown to be perhydro-β-carotene. The parent molecular ion observed in the mass spectrum of this component was at m/g = 558. Diagnostic fragment ions in the spectrum occurred at m/g = 125, 137, and 502. These ions have been noted in the mass spectrum of perhydro-β-carotene (6). The identity of component 32 was verified by coinjection of an authentic sample.

Steranes. - The steranes identified in the BCP fractions of the retorted oils are shown in Table 4. The compounds were identified by comparing mass spectra with published spectra and by coinjection in the case of the two cholestanes. All of these compounds have been identified in shale oil bitumen by Gallegos (6), Eglinton (3), Henderson (5), and others.

TABLE 4. - Sterane (C₂₇H₄₈) compounds identified

GC peak no.	Empirical formula	Molecular weight	Common name
20	C ₂₇ H ₄₈	372	5-β-cholestane
21	C ₂₇ H ₄₈	372	5-α-cholestane
22	C ₂₈ H ₅₀	386	5-β-ergostane
23	C ₂₈ H ₅₀	386	5-α-ergostane
24	C ₂₉ H ₅₂	400	5-β-stigmastane
25	C ₂₉ H ₅₂	400	5-α-stigmastane
26 ^{1/}	C ₃₀ H ₅₄	414	unknown

^{1/} Peak contains two compounds, one of which is a tetracyclic terpene, the other a pentacyclic triterpene of mass 398

The amounts of these compounds vary greatly, as shown in Figure 1. The Wilkins Peak samples contain more 5-α-ergostane (peak 23) and 5-β-stigmastane (peak 25) than either the Laney or the Tipton samples. A comparison of these peaks in the 11 samples shows three times as much α-ergostane and about four times as much α-stigmastane in the Wilkins Peak samples as in the Laney or Tipton samples. This, again, indicates that the sedimentary deposition during the Wilkins Peak time was different than during the Laney or the Tipton time.

The ratio of the abundance of the 5-α- to the 5-β- isomers of all three steranes--cholestane, ergostane, and stigmastane--was approximately 3 to 1, similar to that found by Gallegos (6) in oil shale bitumen. Thermodynamically, the more stable isomer is the alpha form, and the above results indicate that exposure to 500°C during the retorting step does not change the ratio of the alpha to beta isomers.

Pentacyclic Triterpanes. - The pentacyclic triterpanes identified are listed in Table 5. The structures of these compounds are shown in Figure 3. All of these compounds have been previously identified (4, 6, 7). Peak 26 contains two compounds. One is a pentacyclic triterpene with a molecular weight of 398; the mass spectrum of this compound is similar to the pentacyclic triterpene D reported by Whitehead (16) and by Gallegos (6) as compound 30. The peak labeled 27, Figure 3, is believed to be an isomeric form of the compound that emerged as part of peak 26. It was not possible to determine the position of the methyl group in the E ring of peak 27 from the fragmentation pattern. Peaks 28 and 29 are believed to be isomeric compounds with the structure shown in Figure 3. It was not possible to identify the position of the propyl group in these compounds, one of which may be hopane, as suggested by Henderson (5). Peaks 30 and 31 are apparently isomeric pentacyclic triterpanes, with the structures shown in Figure 3.

TABLE 5. - Pentacyclic triterpanes (C_nH₂₂₋₈) identified

GC peak no.	Empirical formula	Molecular weight
26 ^{1/}	C ₂₉ H ₅₀	398
27	C ₂₉ H ₅₀	398
28	C ₃₀ H ₅₂	412
29	C ₃₀ H ₅₂	412
30	C ₃₁ H ₅₄	426
31 ^{2/}	C ₃₁ H ₅₄	426

^{1/} Peak contains two compounds, one of which is a pentacyclic triterpane, the other a tetracyclic terpene with a molecular weight of 414.

^{2/} Peak contains two compounds, one of which is gammacerane, and an unidentified pentacyclic triterpane.

Semi-Quantitative Comparisons

Table 6 presents semi-quantitative data on some of the types of compounds in the BCP fraction. The data were obtained by integrating the areas under the chro-

TABLE 6. C-13 to C-20 chain isoprenoids, α -steranes, and perhydro- β -carotene in the branched-cyclic fraction of the retorted oils

Section	Vol % in branched-plus-cyclic fraction ^{1/}		
	Chain isoprenoids	α -Steranes	Perhydro- β -carotene
L-1	16.9	2.9	0.8
L-2	21.0	4.9	1.3
WP-1	17.7	8.8	1.4
WP-2	26.5	8.2	0.9
WP-3	25.2	5.2	1.0
WP-4	25.4	8.5	0.7
WP-5	23.6	6.0	1.4
WP-6	23.0	6.7	1.2
WP-7	20.4	8.3	1.4
WP-8	17.4	5.4	2.1
T-1	10.5	2.6	0.5
Oil average	20.7	6.1	1.1
Bitumen average ^{2/}	29.9	14.1	4.6

^{1/} Area percentages calculated from FID chromatogram

^{2/} Data from Cook and Robinson (7)

matographic peaks for perhydro- β -carotene and for the C-13 to C-20 compounds listed in Table 2 and the α -steranes in Table 4. The data are semi-quantitative because of the difficulty in establishing a baseline. No attempt was made to integrate the small peaks for monocyclic isoprenoids and β -steranes. In general the table shows lower amounts of chain isoprenoids, α -steranes, and perhydro- β -carotene in the samples from the Laney and the Tipton member than in the Wilkins Peak samples. This suggests that the sedimentary deposition during the Laney and the Tipton time was different than during the highly saline period of the Wilkins Peak time.

Table 6 also shows the average of chain isoprenoids, α -steranes, and perhydro- β -carotene for the 11 oils and a similar calculation on the bitumen samples studied by Robinson and Cook (7). The BCP fraction of the bitumen contains 1.4 times more chain isoprenoids, about twice the amount of α -steranes, and about 4 times more perhydro- β -carotene than the retorted samples.

CONCLUSIONS

Biological markers have been identified in shale oil produced by Fischer-*asay* retorting of oil shale. The biological markers identified include isoprenoid alkanes, monocyclic terpanes, steranes, and pentacyclic triterpanes. These are the same classes of compounds that have been identified in extracted bitumen and pyrolyzed oil shale. The results from this study do not indicate the source of these compounds in oil shale. These compounds probably represent material from both the bitumen and kerogen.

The distribution of these compounds in the different sedimentary layers varies considerably. The data show little if any influence of depth-related factors, a conclusion similar to that drawn from a study (7) of the bitumen from a Wyoming core. Although the phytane appears to decrease with increasing depth, this may be due to an increase in the amount of vegetative (chlorophyll-bearing) matter as the lake went from the Tipton to the Laney era. In agreement with the bitumen data of Robinson and Cook, we found that the Laney (top) and the Tipton (bottom) member samples were usually similar and had a somewhat lower quantity of isoprenoids, steranes, etc., than the Wilkins Peak (middle) member samples. This difference is probably due to the differences in environment, that is, fresh water lake during the Laney and Tipton eras and a salt water lake during the Wilkins Peak era.

The chain isoprenoid content in the BCP fractions from the 11 retorted oils average approximately 21 percent, and Robinson and Cook's results for the bitumen on their core were about 30 percent. Although direct comparisons cannot be made because their work was on a different core and on the extracts of the oil shale from the core, our results appear to indicate that the chain isoprenoids are stable to the retorting process. The chain isoprenoids averaged approximately 19 percent for the Laney, 23 percent for the Wilkins Peak, and 10 percent for the Tipton samples. This difference in the amount of these isoprenoids in the three member samples points out again the difference in the environment in the Gosiute Lake during the formation of these three members.

For the most part, previous studies of the biological markers in oil shale have dealt with the material extracted from bitumen. Gallegos had indicated that the material produced from the pyrolysis of oil shale may be more indicative of the biological source material than extracted bitumen (6). We feel that both the material from extracted bitumen and the product oil should be investigated for a more complete geochemical picture of oil shale formation.

REFERENCES

1. J. J. Cummins and W. E. Robinson, *J. Chem. Eng. Data*, 9, 304 (1964).
2. A. L. Burlingame, P. Haug, T. Belsky, and M. Calvin, *Proc. Nat. Acad. Sci.*, 54, 1406 (1965).
3. Sister Mary, T. J. Murphy, A. McCormick, and G. Eglinton, *Science*, 157, 1040 (1967).
4. D. E. Anders and W. E. Robinson, *Geochim. et Cosmochim. Acta*, 35, 661, (1971).
5. W. Henderson, Wojtech Wollrab, and G. Eglinton, *Advances in Org. Geochem.*, 1968, 181.
6. E. J. Gallegos, *Anal. Chem.*, 43, 1151, (1971).
7. W. E. Robinson and G. L. Cook, U.S. BuMines, Rept. of Inv. 7820 (1973).
8. E. J. Gallegos, *Anal. Chem.*, 47, 1524, (1975).
9. Iida Takeo, *Yakugaku Zasshi*, 96, 796, (1976).
10. L. P. Jackson, J. R. Morandi, and R. E. Poulson, Preprints, Div. Fuel Chem., ACS, 22 (3), 66, (1977).
11. K. E. Stanfield and I. C. Frost, U.S. BuMines, Rept. of Inv. 4477 (1949).
12. ASTM Book of Standards, 1975, Part 23, Method D-1019-68, p. 477.
13. J. V. Brunnock, *Anal. Chem.*, 38, 1649, (1966).
14. W. H. Bradley and H. P. Euster, U.S. Geol. Survey Prof. Papers, 496-B, 71 pp. (1969).
15. J. J. Cummins, F. G. Doolittle, and W. E. Robinson, U.S. BuMines Rept. of Inv. 7024 (1974).
16. I. R. Hills and E. V. Whitehead, *Nature*, 209, 977 (1966).

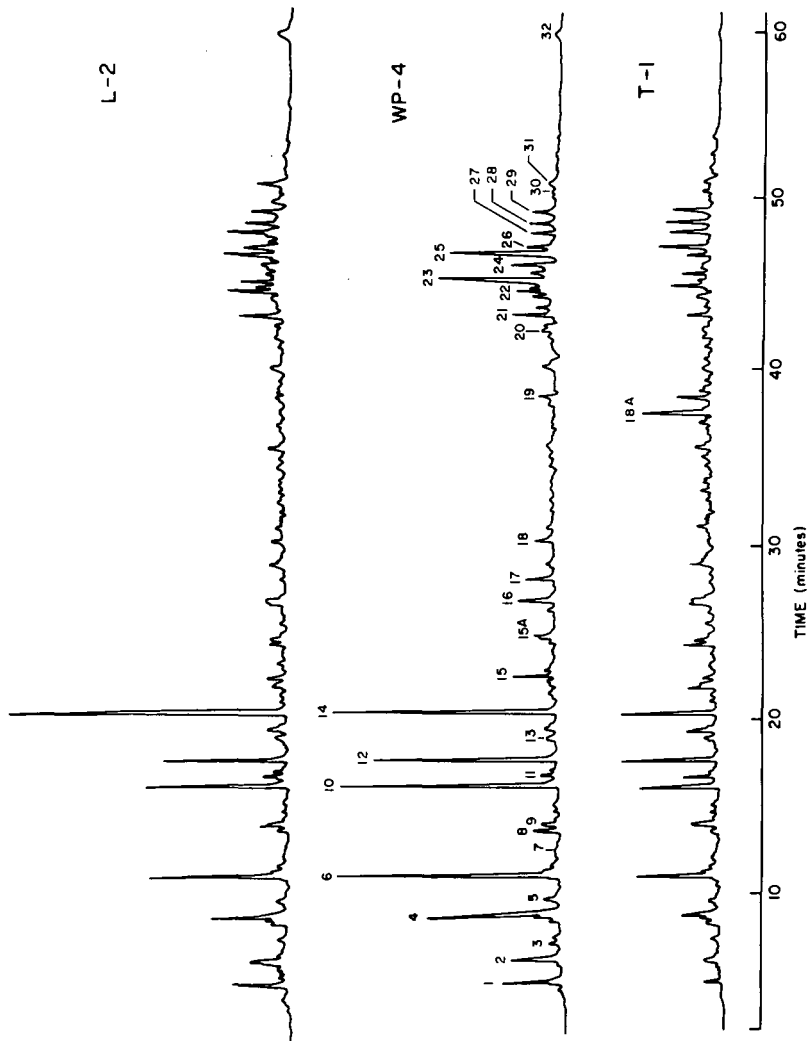


FIG. 1. GAS CHROMATOGRAPHS (FID) OF THE BRANCHED-CYCLE HYDROCARBON FRACTION FROM RETORTED WYOMING SHALE OIL.

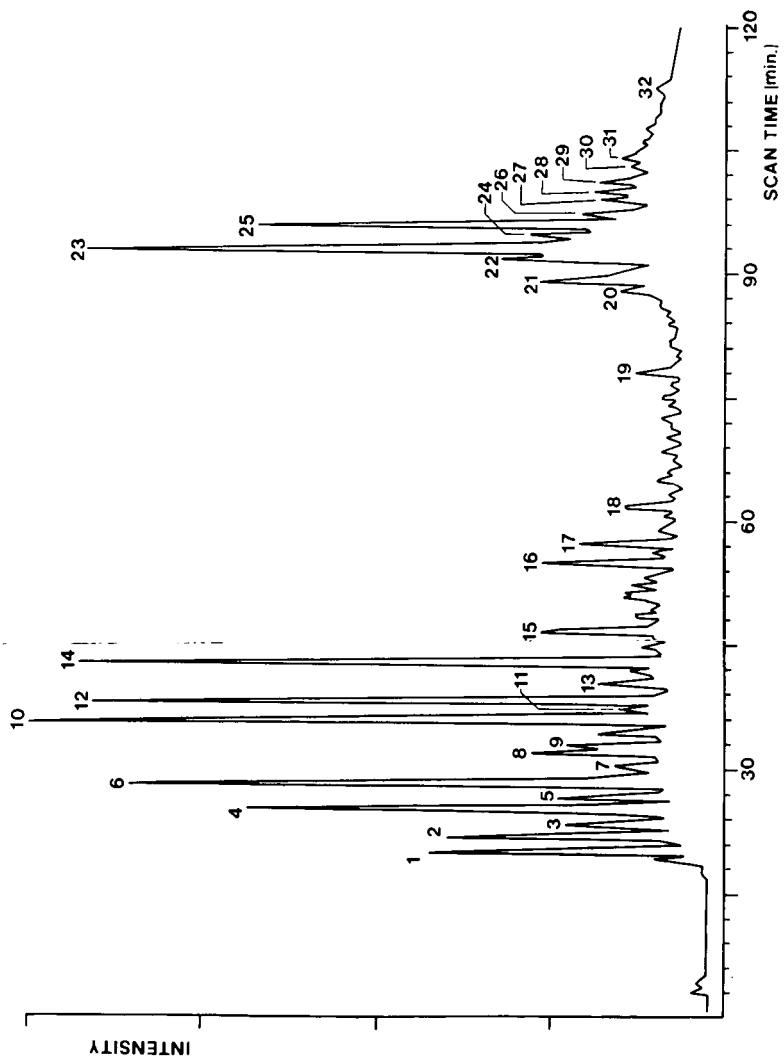
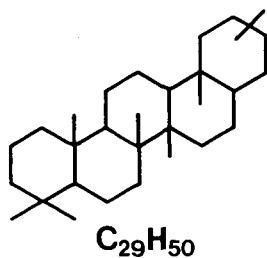
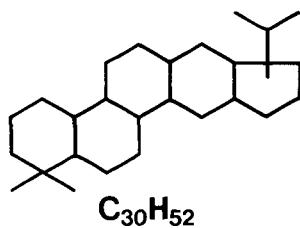


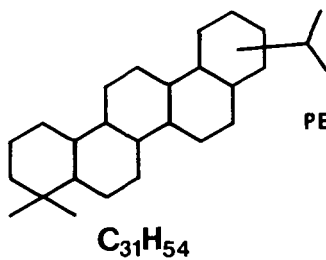
FIG. 2. RECONSTRUCTED GAS CHROMATOGRAPH OF BRANCHED-CYCLE HYDROCARBON FRACTION FROM WP-4 RETORTED WYOMING SHALE OIL.



PEAK NO. 26 & 27



PEAK NO. 28 & 29



PEAK NO. 30 & 31

FIG. 3. PENTACYCLIC TRITERPANES IN GREEN RIVER RETORTED SHALE OIL

GAS COMPOSITION CALCULATION FOR THE IN SITU
GASIFICATION OF THIN SEAMS AND THE APPROACH TO MODELING

S. Debrand and O. J. Hahn

Institute for Mining and Minerals Research
University of Kentucky
Lexington, Kentucky 40506

INTRODUCTION

The Appalachian region contains numerous coal seams which are under 60 inches in thickness. A portion of this coal is usually recovered by Auger mining techniques after contour stripping. At least fifty percent of the remaining coal may be gasified to produce a low Btu fuel. The application of underground gasification to very thin seams (below 40 inches in thickness) is limited by the reduction of the heating value of the gas. This reduction is caused by an excessive heat loss to the surrounding strata. The purpose of this work was to evaluate the pertinent factors affecting the gas composition and the limitations of modeling calculations. The logical sequences leading to a gas composition model and the estimation of the temperature profile in the gasification zone were presented. The available literature data related to the various calculation techniques were also quoted.

PARAMETERS AFFECTING THE GAS COMPOSITION

The total heat losses during the in situ gasification affect significantly the gas composition and its heating value. A heat balance results in a temperature profile of the gasification zone. One modeling approach is to calculate the gas composition and compare this composition to the data obtained from the experimental tests. A second approach involves a prediction of the temperature profile of the gasification zone. The gasification of coal seams having a thickness from one or more meters is considered here. The combustible gases formed during the underground forward gasification mode are obtained by pyrolytic coal decomposition superimposed upon the gasification products. As far as the gasification is concerned, the reaction of coal with the steam and/or hydrogen is of paramount importance because this is the main reaction which produces a gaseous burnable product of heating value above 100 Btu/SCF. The ratio of the total amount of water (in the form of coal moisture plus inflow of water or steam) to the supplied amount of oxygen seems to be a predominant factor in maximizing gas heating value for the defined level of total heat losses.

In general, the gas composition of the underground gasified coal depends on the volatile content, the seam moisture, the blast air moisture content, and the chemical reactivity of the coke. The gasification efficiency and combustion stability are sensitive [Stewart et al. (24)] to the optimum combination of the coal seam moisture and of blast air moisture.

The reactivity of a particular coal is a function of the chemical properties of its organic and mineral constituents and of the physical structure of the coal; generally, it is observed that the coal reactivity in gasification increases with decreasing coal rank and is proportional to the internal surface area [Schora, F. (23)]. When experimental values for the relative low-rate gasification reactivity factors (f_o) are not available; values for many coal [Johnson, S. L. (15)] may be estimated from the following equation: $f_o = 6.2 y (1-y)$ where y is the mass fraction of total carbon in the original coal on a dry ash-free basis. The conditions during a pyrolysis of the coal affect the physical nature of the char and

its reactivity. In the temperature range 600-700° C, where the apparent activation energy is high (80-70 kcal/mole), the reaction rate is low and the composition of gas is limited by the kinetic reaction rate; in the temperature range 700-750° C the diffusion process through the pore structure is a limiting factor. However, [Limears et al. (19)] have shown that for some coal types the particle size has nearly no effect upon the char reaction rate.

In general, the rate of the steam-hydrogen reaction with the coal depends on many variables such as: temperature, pressure, character of the coal solid surface and the amount of volatile matter in coal. The first stage of the reaction is rapid and is related to the gasification of the carbon portion included in the volatile matter. The low reactivity coal portion is the residual, carbonaceous coke. This stage is usually denoted as (1) $C^* + H_2O \rightarrow CO + H_2$ and (2) $H_2 + H_2O + 2C \rightleftharpoons CO + CH_4$ where C^* is the reactive carbon in the volatile matter. Most coals are made up of a number of macerals which differ in their reactivity. [Davis et al. (19)] found a reactivity order fusian < durain < vitrain.

The endothermic reaction of steam with carbon is of primary importance. These endothermic reactions are maintained by the endothermic oxidation reaction of carbon and oxygen.

The higher activation energy observed for the carbon reaction with the steam-hydrogen mixture indicated an inhibiting effect of hydrogen (and/or methane) on the char-steam reaction. The reactivity of such a mixture was proportional to the steam pressure raised to the 0.93 power [Johnson (15)].

[Young et al. (30)] reported on the effect of the steam upon the methane production and the shift reaction under conditions that are similar to those of underground gasification. Wyodak and Hanna char was used. No carbon monoxide was detected for the steam-char gasification process to indicate that the water shift reaction $CO + H_2O \rightarrow CO_2 + H_2$ had taken place. The gas shift reaction was probably catalyzed by the ash content in the char. Introduction of steam during the pyrolysis period doubled the rate of methane production. The rate of methane production was 20 percent of that of carbon dioxide. Russian investigators have reported similar data.

Experimental kinetic data indicate that we will not be able to use equilibrium compositions in making our modeling calculations.

We compare below the equilibrium composition of wet water gas at 900° C and 1000° C and the kinetic data of the reaction between the flowing gas (0.7 - 0.9 m/sec) and the carbon particles 2-3 mm. in the reactor (data according to [Kaftawov et al. (17)]).

TEMPERATURE	EQUILIBRIUM COMPOSITION DATA		COMPOSITION ACCORDING TO KINETIC DATA			
	%CO	%H ₂	%CO ₂	%CO	%H ₂	%CH ₄
900° C (1652° F)	45	50	10.1	34.6	55.2	0.1
1000° C (1832° F)	50	50	8.8	38.1	52.9	0.2

The equilibrium constant may be calculated from the Gibbs free energy (G): $\Delta G = R T \ln K$ where $\Delta G = \Delta H - T \Delta S$. The correlation between the equilibrium constant and the temperature is expressed usually by the equation ($p = \text{const}$):

$$\ln k = \frac{1}{R} \int \frac{\Delta H}{T^2} dT + a \text{ (where } a \text{ is an integration constant).}$$

Several difficulties are encountered in a discussion of the kinetics of coal gasification. Since the effects of coal devolatilization on the product gas rates are important up to temperatures between 600-700° C, usually only the data above 700°C are analyzed to obtain the kinetic constant. Laboratory experiments show that during the coal burn-off versus time studies a gradual induction period is followed by a region in which burn-off increased with a time. Instantaneous reactivity (R) may be calculated from the equation:

$$R_t = \left(\frac{1}{W_E} \right) \left(\frac{dw}{dt} \right)$$

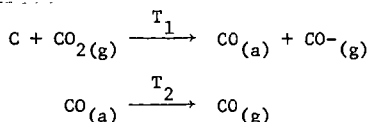
where W_E is the weight of the unreacted char on a dry-ash free basis and $\frac{dw}{dt}$ is the slope of the burn-off versus time. For the reaction in the air R_t increases and often W_E is replaced by W_0 (starting weight) and $\frac{dw}{dt}$ is taken for the maximum rate of weight loss.

The first principal reaction which occurs during the underground coal gasification process is the pyrolysis. The rate of pyrolysis as well as the amount and composition of the volatile products from a given sample of coal or char depends on the rate of heating, the final decomposition temperature, the vapor residence time and the environmental conditions such as applied pressure, particle size, coal type, etc. under which the pyrolysis takes place.

Normally pyrolysis starts at about 350°-400° C and is completed at about 1000° C. The reactivity with steam, oxygen, hydrogen or carbon dioxide during the pyrolysis of coal is mainly a function of the volatile matter and the rate of heating.

GASIFICATION RATE OF CHAR IN THE CARBON DIOXIDE ATMOSPHERE

The reaction between the char and carbon dioxide is hardly detectable below the temperature 800-900° C. According to Wen, C. Y. et al. (4) the activation energy is about 59.26 kcal/mole which indicates chemical-reaction control. The following mechanism was proposed by Walker (28):



Experimental data indicated that the order of reaction with respect to CO_2 can be assumed to be unity up to about one atmosphere pressure. However, at higher temperatures, the diffusion resistance within the solid particle may become significant and therefore an effectiveness factor must be introduced for such cases.

According to Wen et al. (4) the rate of the char-carbon dioxide reaction is found to depend on the coal origin more than on the gasification scheme used. The various rate characteristics of coals and chars are apparently due to the difference in their pore characteristics.

GASIFICATION RATE OF CHAR ON OXYGEN-ATMOSPHERE

The reaction rate in the temperature range 424-576° C using air was determined recently by C. Y. Wen et al. (4). The rate of reaction showed a maximum at a conversion of 10-50 percent; the maximum depended on the sample used. The observed

maximum reaction rate, dx/dt , was $1.67 \times 10^{-3} \text{ sec}^{-1}$. Under these conditions the reactivity of the char is determined by chemical kinetics and depends more on the extent of the gasification of the char rather than on the parent coal.

In the temperature range 834-1106° C, the reaction rates appear to correspond to a film-diffusion control regime. The rates do not change significantly with conversion degree until about 80 percent conversion is reached. Assuming a spherical particle shape, the average rate at 1000° C was $1.8 \times 10^{-6} \text{ g/cm}^2 \text{ s atm}$. A nitrogen-air mixture was used as the low oxygen concentration source.

THE GASIFICATION RATE OF CHAR IN THE HYDROGEN-ATMOSPHERE

A. Tomite et al. (26) investigated the reactivity of a char which was prepared at 1000° C. Usually the reactivity profile of a majority of the chars shows some slow induction period followed by a rate increase. The reaction rate generally increases as the rank of the parent coal decreases. Removal of mineral matter profoundly affects the reactivity profile of chars. In most cases the reaction rate decreases with mineral-matter removal.

The pseudo-activation energy changes from 150 kcal/mole to about 213 kcal/mole with increased conversion of the char.

According to Feistel et al. (6) the kinetic constant of hydrogasification is strongly affected by the hydrogen pressure and was expressed by the equation:

$$K_{H_2} = \frac{0.00402 \exp. (-5200/T) P^2_{H_2}}{1 + 0.000648 \exp. (4100/T) P_{H_2}}$$

The gasification rate with steam-hydrogen, resulted in the experimental equation, which shows a significant effect of the temperature upon the gasification rate.

The activation energy for the kinetic equation rate was 33,600 cal/ mole and the frequency factor was $2.51 \times 10^4 \text{ l/min}$.

THE REACTION RATE OF CHAR IN STEAM ATMOSPHERE

Linares et al. (19) found that in general the char reactivity was related to the steam reaction and decreased with an increase in the rank of the parent coal. However, a considerable spread in reactivities of char produced from coals of similar rank was observed. Removal of mineral matter diminished the char reactivity but the removal of mineral matter also resulted in a profound change in the surface area and porosity. The influence of each of these variables is difficult to access. Below 890° C the reaction is chemically controlled with an apparent activation energy of 42 kcal/mole. Above 890° C, the reaction is diffusion controlled and has an activation energy of 18 kcal/mole. The reaction rate was found to be proportional to steam pressure raised to the 0.60 power.

The rate of gasification of bituminous coal in the ($H_2O - H_2$) mixture in the temperature range 700-1100° C was investigated by Feistel et al. (6). The kinetic constant for steam decomposition was a function of steam pressure and temperature. The rate of reaction for a pressure higher than 10 atm. was described as:

$$\frac{dx_B}{dt} = K (1-x_B)$$

where x_B is base carbon conversion degree; t-time; k-kinetic constant

$$k_{H_2O} = \frac{1.88 \times 10^6 \exp(-2.24 \times 10^4/T) P_{H_2O}}{(1 + 1.56 \times 10^5 \exp(-1.65 \times 10^4/T) P_{H_2O}}$$

$$x_B = \frac{\text{base carbon gasified}}{\text{base carbon in feed coal char}} \quad (\text{according to Johnson})$$

THE CHAR REACTIONS IN THE CONDITIONS OF UNDERGROUND GASIFICATION

One possible approach is to calculate the residence time of the char in the high temperature zone of 1500-1800° F. The thickness of the coke zone (coal with 10 percent seam moisture) would be about 0.5 m; for the brown coal at 50 percent moisture this is about 15 cm assuming the advance rate of burning zone about 0.1×10^{-3} m/sec. The obtained residence time (40-130 hour range) implies that the seam moisture and volatile content are more significant factors than that of char reactivity upon the overall reaction rate.

THE EFFECT OF THE BLAST INTENSITY AND GASIFICATION ZONE ADVANCEMENT RATE ON THE HEATING VALUE OF PRODUCED GAS

A Russian investigation [Ludin *et al.* (20)] has shown that the optimum blast rate depends on the thickness of the coal seams. It was explained that the thicker seams have a larger water intrusion rate than the thinner seams. If air is used as the blast; there is an optimum water to air ratio that gives a maximum heating value of produced gas. On the other hand, it was observed the gasification front advancement increased with the higher blast rate. Therefore a certain gasification front advancement rate will correspond to the optimum gas heating value.

THE EFFECT OF THE PEAK GASIFICATION TEMPERATURE UPON THE HEATING VALUE OF THE GAS PRODUCED

The lower concentration of hydrogen caused by the lower temperature gasification does not necessarily lead to a low Btu product gas since a higher methane yield may be obtained in some cases. For example, Gregg *et al.* (10) found, during some underground tests, 6.3 percent of methane in the gas produced. Fisher *et al.* (7) made the observation that the presence of steam resulted in a higher concentration of methane in the produced gas. It could be explained that either the steam promotes the reaction of hydrogen and char or the following methanation reaction $CO + 3H_2 \rightleftharpoons CH_4$ occurs. This methanation reaction could be catalyzed by the mineral matter in the char.

INSTABILITY AND UNCERTAINTY FACTORS IN THE UNDERGROUND GASIFICATION MODELING

The following factors would lead to instability of the gasification process and may result in a large modeling error:

1. Change in coal and strata permeability.
2. Rapid water influx. The water may intrude upstream and go through the combustion zone or it may intrude downstream of the combustion zone. In theory an optimum water intrusion exists for any air blast injection. In practice of the gasification usually has a higher water intrusion rate than desirable and operates on the water rich side of optimum.
3. Rapid channeling of gasification process.
4. Rapid gas or air leakage to the strata.

The purpose of this study is to formulate a specific theoretical description of the forward combustion process of thin coal seams (one to several meters thick-

ness) and to establish the base which would allow to compare the model prediction to the eventual results of the field tests. It seems to be worthwhile to mention a few recent publications relating to the in situ gasification modeling. Different methods of gasification and various geological formation lead to different mathematical models. For example modeling were presented by Kotowski (18) and by Gunn and Whitman (12) in the study of reverse and forward combustion. Thorsnes described the evaluation of thermal front measurements and pressure drop versus flow rate. The longwall generator modeling was reported by Sawyer and Shuck (22). Some preliminary analysis was given by Gidaspow (9). The practical purpose of underground gasification modeling is to be able to predict the gas composition and permit the development of improved gasification control strategies. The experimental data [Yauagimoto (29)] have shown a significant effect of the gasification zone temperature upon the gas composition. It seems to be difficult to perform an adequate heat balance and to calculate the resulting temperature of the gasification zone considering such phenomena as: thermoplastic behavior as the coal is heated through a certain temperature; porous coke structure, contact area between the flowing gas and gassified coal etc. Therefore the measurements of the gasification zone temperature of the thin seams has been proposed. The equilibrium data calculated for the system volatile - gases from carbon reacting with oxygen, carbon dioxide etc. at the determined temperature, superimposed by the gas composition resulting from the kinetic of char burn out and shift reaction would give the resulting composition of produced gas.

MODELING OF GAS COMPOSITION FOR THE IN SITU GASIFICATION

The logical objectives of fitting equations to experimental data are twofold: to estimate the effect for each of the independent variables and to be able to predict the responses. The preliminary examination of experimental data should lead to:

1. Ordering (in the space or time)
 - a. List and magnitude of independent variables
 - b. Locate the clusters for estimation of error
2. Plotting
 - a. Factor or variable space
 - b. Time sequences

The next stage is the construction of specific equations according to the experimental data.

The calculation of gas composition requires a listing of independent experimental variables, as below:

1. Rate of air blast (and the oxygen concentration in the case of air enrichment). This factor is interrelated to the rate of gas production; temperature profile and flame front velocity.
2. Total rate of water moisture supply consisting of coal moisture; blast air moisture and water influx. This is obtained from the total mass balance and measurements.
3. Composition and rate of gas production.
4. Rate of carbon combustion (calculated from point 3.)
5. Coal properties such as moisture, ash, content of volatile, caloric value, conductivity.

6. Coal combustion characterization such as char reactivity, rate of pyrolysis reaction.
7. Temperature profile of the gasification zone with velocity flame front. The temperature profile follows from the total energy balance. Yanagimoto *et al.* (29) observed that the calorific value of the gas produced is sensitive to the combustion temperature of underground gasification.

The calculation program is presented below:

- 100 Mass balance of oxygen and total water. Water influx and air leakage (from material balance). Estimated cluster of errors.
- 200 The reaction rate and resulting gas composition at the equivalent average temperature of the gasification zone.
- 201 Pyrolysis of coal and the tar and gas composition derivated from Kinetic equations.
- 202 Rapid reaction (oxygen, hydrogen, steam) with volatile carbon. Gas composition derivated from equilibrium data.
- 203 Char reaction with gas phase (oxygen, carbon dioxide, steam). Gas composition derivated from kinetic data. The conversion reaction.
- 204 Calculation the resulting carbon monoxide, hydrogen and carbon dioxide concentration.
- 300 Energy balance and the temperature profile.
- 301 The general energy balance of the solid phase.
- 302 Heat sink by conduction for surrounding materials.
- 303 Heat sink by convection to the flowing gases.
- 304 Heat losses to the ash.
- 305 Heat used for the water-steam system.
- 306 Dependent factor: rate of combustion.
- 307 Problems related to the boundary conditions.

100 The conservation of mass equations for oxygen and total water would be as follows:

$$[\text{Rate of oxygen (water) mass in}]_1 - [\text{Rate of oxygen (Water) mass out}]_2 + [\text{Rate of generation of oxygen (water mass)}]_3 - [\text{Rate of accumulation of oxygen (water mass)}]_4 = 0$$

Due considerations have to be given for the moisture content of the air; the gasified coal; soil or rock; the strata of the roof in the area of gasified coal; and gravity influx of water respectively as well as the moisture dissociated in the heterogeneous reaction zone and the undissociated moisture in the heterogeneous reaction zone). The formula to calculate these water types has been summarized by Kalashinitkov *et al.* (16). The mass balance of water (being in a form of coal moisture; the water influx and blast moisture) and its discrepancy would show the magnitude of seam water influx and the rate of steam decomposition rate. The continuity equation for these mass balances could be presented as follows:

$$\frac{\partial}{\partial X} (\Delta \text{ mass}) + \phi_m \cdot r + \frac{\partial}{\partial \text{time}} (\phi_m \cdot \Delta \text{ mass}) = \text{const.}$$

where Δm can be calculated as the weight fraction of the component in the injected air and $\phi_m \cdot r$ is an oxygen (water) reaction rate function. The mass balance of

oxygen and its discrepancy would indicate the gas (air) leakage rate and the rate of steam decomposition due to the reactions, e.g.,



200 The kinetic data concerning the coal devolatilization (pyrolysis) and the combustion of the matter devolatilized from coal should be applied if reliable prediction is to be obtained.

201 The kinetic rate (r) of coal pyrolysis under non-isothermal conditions can be described by two functions:

$r = \frac{d\alpha}{dt} = K(T) \phi(\alpha)$ where $a = \frac{Vt}{V^\infty}$, Vt is the volume of the product in time t and V^∞ is the final product volume attained at the end of the reaction. The function $K(T)$ is only temperature dependent, while $\phi(\alpha)$ is a function of the instantaneous phase composition. Using the Arrhenius equation one may obtain the final equation in which the rate of gas production is expressed as follows:

$$\frac{dv}{dt} = \frac{Av^\infty}{c} \exp \left(\frac{-E}{RT} - \frac{A}{C} \frac{RT^2}{E} \right) e^{-E/RT}$$

The heating rate is denoted here as $c = \frac{dT}{dt}$. As an example we use the following experimentally determined kinetic parameters (according to Campbell (2) for subbituminous coal types).

GAS	PEAK AREA %	KINETIC PARAMETERS	
		A (min ⁻¹)	E ^b (Kcal/mole)
H ₂	100	1.2 x 10 ³	22.3
CH ₄	32.3	1.0 x 10 ⁷	31.0
CO ₂	53.6	3.3 x 10 ⁴	19.5
CO	30	3.3 x 10 ³	18.0

Pyrolysis of the larger coal particles was described by Forrester (8).

202 The devolatilized compounds, resulting from the coal pyrolysis, burn with oxygen. The reaction rate of volatile compound is very high in the range of 0.5-2 sec. depending on the temperature of the gasification zone. Therefore, the assumption that the equilibrium composition is formed in this zone, seems to be justified. When the state of the system is such that $\Delta G = 0$ no process will occur and the system is at equilibrium. For a system consisting of n -species $\Delta G = \sum N_i \Delta g_i$ where N_i is the number of moles of i and Δg_i is the molar specific Gibbs function for species i .

If the Gibbs function has the minimum value then for any complete set of independent reaction

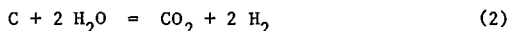
$$\frac{\partial \Delta G}{\partial \epsilon_i} = \sum_{j=1}^n \frac{\partial \Delta G}{\partial N_j} \frac{\partial N_j}{\partial \epsilon_i} = \sum_{j=1}^n (\beta_{ij} - \alpha_{ij}) \frac{\partial \Delta G}{\partial N_j} = 0$$

A procedure described in the literature as the Newton or Newton-Raphson method may be applied in order to solve the equations and to obtain numerical values. The computer calculations for the equilibrium data were described in the report of Combustion Engineering, Inc. (21).

203 The reaction of coal-char with the gases. The rate constant for the char reactions can generally be written in the Arrhenius form: $K = A \exp(E/RT)$ where E is the activation energy and the parameter A is the frequency factor and does depend on the number of molecules covering unit surface area. These values vary depending on the type of reaction and the carbon sample; for example, for the carbon-oxygen reaction it is from 20-80 Kcal/mole, for the carbon-steam reaction it is from 55-83 Kcal/mole [Isley *et al.* (14)] and for the carbon-carbon dioxide reaction it is from 26-84 Kcal/mole. Johnson (15) reported the kinetics of bituminous coal char gasification with gases containing steam and hydrogen.

The petrographic type and coal rank affects the char reactivity during gasification [Davis *et al.* (1)] so that the velocity constant for the coal type subjected to underground gasification should be determined experimentally. The manual of coal conversion fundamentals recently prepared by the Institute of Gas Technology presents a calculation procedure (using a char of a known reactivity factor) for the produced gas composition from a fluidized bed gasifier. However, for an average flame front velocity of about 0.1 cm per hr. in the underground gasification and for the resulting long residence time of char in a high temperature gasification zone, (30-130 hours) the char reactivity does not play a significant role.

The reaction of coal with steam and the resulting gas composition is defined by the kinetic of the two primary and two secondary reactions:



By denoting Z_i as the participation coefficient of the i reaction in the mixture, we would obtain [according to B. M. Derman (3)]:

$$Z_i = \frac{d(C_x) V_i}{\sum d(C_x)} \quad \text{and (e.g.)} \quad \frac{dc^1}{dc^{111}} = \frac{2 Z_3 + Z_1 - Z_4}{Z_1 + 2 Z_2 + Z_1}$$

Experimental data [Ludin *et al.* (26)] show that the conversion reaction occurs downstream from gasification zone is catalyzed by the inorganic matter in the coal. Therefore, the modification of the gas composition due to this reaction should be included in the last stage of a computation.

204 A hybrid computer program was prepared by NASA (TMx-3403) that can solve chemical kinetic systems with many chemical species for either a flow or static reactor.

300 Energy balance and temperature profile calculation approach.

301 The general solid phase (coal-char) energy balance may be presented as follows:

[Thermochemical heat from reactions] + [heat input (output) by conduction] - [convective loss to flowing gas] + [Extended loss e.g. ash] = [Net heat accumulated in solid phase].

Analysing the mass balance, the change in an accumulation of solid phase may be obtained from the equation:

[Carbon used by oxygen] + [Carbon used by carbon dioxide] + [Carbon used by the reaction with steam] = - [Change of solid accumulation].

The primary combustion reaction rate is controlled by the oxygen supply. One dimensional peak temperature and temperature profile are a function of the following parameters: the total heat generated by carbon combustion reactions, the total heat losses and dissipated energy resulted by the coal conductivity, water heating and evaporation, convective heat transfer from solid to flowing gases, and heat losses in the leftover ash. The endothermic reactions, e.g., between the steam and char, are usually considered as a portion of the carbon combustion reactions. The approximated results may be obtained using the calorific value of coal instead of the heat reaction.

In the one dimensional energy balance the total heat of the various reactions would be expressed:

$$\sum_{i=1}^n \Delta H_i \frac{\partial x_i}{\partial \text{time}} \mu = \text{total heat} \quad (1)$$

where x_i is stoichiometric coefficient of reaction and μ is a function of the solid phase which reacts with oxygen (carbon dioxide; steam).

320 We can now combine the heat transfer sink by conduction (solid) and the heat reaction representing uniformly distributed heat source and express it by the equation:

$$\frac{\partial}{\partial x} \left(K \frac{\partial t}{\partial x} \right) + \frac{\partial}{\partial y} \left(K \frac{\partial t}{\partial y} \right) + \frac{\partial}{\partial z} \left(K \frac{\partial t}{\partial z} \right) + \sum_{i=1}^{i=n} \Delta H_i \frac{\partial x_i}{\partial \text{time}} \mu = \rho c \frac{\partial t}{\partial \text{time}} \quad (2)$$

(t = temperature) This equation can be easily converted to the form containing the property $\left(\frac{k}{\rho c}\right) = \alpha$ which is the thermal diffusivity coefficient. Several authors (American and Russian) have confirmed that the temperature peak of coal combustion depends on this coefficient. However, the porous-capillary property of coal-char material requires further modification of the equation due to the convective transport associated with forced air and the gas flowing through the body. This should include the coolant mass flow (G_c) and the porosity of the material $\left(\frac{G_c}{K_e}\right)$. For one dimensional conduction equation (2) becomes:

$$\frac{\partial^2 t}{\partial x^2} + \frac{G_c \cdot C_c}{K_e} \frac{dt}{dx} + \frac{\sum \Delta H_i \frac{\partial x_i}{\partial t} \mu}{K} = \frac{1}{\alpha} \frac{\partial t}{\partial \text{time}} \quad (3)$$

Depending on the boundary conditions various types of solution of this type of equation may be obtained. If we assume that the high temperature gasification zone may be represented as a porous plate cooled on our side, then the general solution of the equation (3) becomes:

$$\frac{t - t_x}{t_a - t_x} = \frac{Bi}{Bi + F} e^{-p (\alpha/s)} \quad (4)$$

where Bi is the Biot number and F is a Fourier number.

303 Further steps should include the heat losses by convection from the solid to the flowing gases. The significant portion of this type of heat loss is related to heating of the nitrogen and the water vapors.

The heat transfer from solid surfaces to the flowing gases and water vapor can be conveniently expressed in terms of a nondimensional Nusselt number, $Nu = \frac{hD}{K}$, where

h is the heat transfer coefficient, K is the thermal conductivity of the gas and D is a characteristic dimension. For turbulent flow, $Nu = f(Re)$ where Re is a Reynolds number.

A significant difference of opinion exists as to whether or not a turbulent flow type occurs during the gasification in situ [Hahn & Debrand (13)]. It probably depends on the local circumstances of gasification such as cracks size, channeling, surface area of the channels, etc. Therefore a practical solution would include an estimation of this loss by the equation:

$$\frac{Q \text{ convective}}{V \text{ nitrogen}} = h (T \text{ average} - T \text{ inlet}) \quad (5)$$

where V nitrogen is the flow rate of nitrogen in the blast air; T inlet gas temperature, T average - temperature of gasification zone.

304 A significant effect of the ash content upon the peak temperature of gasification zone was observed experimentally. Some experimental data has shown that the exothermic reaction of ash formation does not compensate for the latent heat of the ash left in the gasification zone. The estimated heat losses would be proportional to the ash content in the coal and the rate of the coal combustion ($\frac{\Delta m}{\text{time}}$):

$$Q_{\text{ash}} = K_1 \cdot \Delta \text{ Ash content} \cdot \frac{\Delta m \text{ carbon}}{\text{time}} \quad (6)$$

305 Based on the water heat balance, the heat use for the water evaporation and the water vapor latent heat, should be included. This heat would be proportional to the moisture content of the coal and the rate of the coal combustion:

$$Q_{\text{water}} = K_2 \Delta \text{ water content} \frac{\Delta m \text{ carbon}}{\text{time}}$$

306 The width and the rate of advancement of the gasification zone are proportional to the rate of the blast air. The coal combustion rate is also controlled by the supply of oxygen and in this context, the oxygen supply rate is the only independent factor.

~~In the circumstances in which the water supply (influx) can be controlled, the ratio of total moisture/oxygen supply effects the following parameters:~~

- a) The equilibrium and the kinetics of the combustion reaction as well as changes in the balance of the thermochemical heat of the gasification reaction.
- b) The change of the temperature in the gasification zones due to the endothermic reaction of steam decomposition and the heat sink is determined by the heat related to the water evaporation, latent heat of steam and heat losses to the strata.

The total solid phase energy balance would include the above mentioned inter-related expressions for the nonsteady heat transfer and the definition of the boundary conditions. The limitation of these calculations lie in the assumed boundary conditions. Further study is needed in this area.

REFERENCES

1. Davis Alan, William Spackman; Peter Given, Energy Sources, page 55, Vol. 3 No. 1 (1976).
2. Cambell, J. H., Lawrence Livermore Laboratory, Report No. UCRL-52035, March 1976.

3. Derman, B. M. Academia Nauk CCCP, Trudy Institute Gorutchih Iskopaemyh XIII, page 19 (in Russian).
4. Dutta, S., Wen, C. Y., Ind. Eng. Chem. Proc. Des. Dev., Vol. 16, No. 1 p. 20 and p. 31, 1977.
5. Daniel Cuthberg and Fred Wood; Fitting Equations to Data, Wiley-Interscience, Inc., New York, 1971.
6. Feistel, P. P., Van Hook, R. R. Juntgen, 173rd ACS Meeting March 21-25, 1977, Vol. 22, No. 1, page 53.
7. Fischer, J., et al., Argonne National Laboratory, Report No. ANL-77-7, December, 1976.
8. Forrester, III, R. C., ERA, Vol. 1, No. 4, pos. 4501, Conf., 750870-1.
9. Gidaspow, D., Paper No. 4D, Presented at the 83rd ASCE National Meeting, Houston, Texas, March, 1977.
10. Gregg, D. W., Hill, R. W., Olness, D. U., Lawrence Livermore Laboratory, Report No. UCRL-52004, January, 1976.
11. Gregg, D. W., Olness, D. U., ERDA Report No. UCRL - 52107, August, 1976.
12. Gunn, R. D., and Whitman, D. L., Laramie Energy Research Center, Report No. L ERC/RI-76/2, Feb., 1976.
13. Hahn, O. J., and Debrand, S., Heat Transfer Limitation for Underground Gasification of Thin Coal Seams., Paper presented at the 83rd National Meeting of the American Institute of Chemical Engineers, Houston, Texas, March 20, 1977.
14. Ilsley, J. M., et al., Principles of Gasification Reactions Department of Fuel Tech. University of Sheffield, Page 1.
15. Johnson, J. L., Coal Gasification ACS Advances in Chemistry Series No. 131 p. 145-78 (1974).
16. Kaleshnikov, P. J. et al., UCRI, Trans. 10899. Tr. Vsesoy, Nauch, Inst. Ispol. Gas. No. 2, p. 97, 1967.
17. Kaftanov, S. V., Fedosev: Khimia Tverdogo Topliva, Vol. 10, No. 4, p. 83, 1976.
18. Kotowski, M. D., and Gunn, R. D., ERDA Report No. LERC-RI/76/4, March, 1976.
19. Linares, A., Mahajan, O., Walker, P. L., 1973rd Meeting ACS, March 21-25, 1977, Vol. 22, No. 1, p. 1.
20. Ludin, J. D., Krugov, O. W., Makerova, M. J., and Birukov, W. F., Laboratory of the Coal Gasification, Page 19 (in Russian).
21. Mathematical Modeling of Chem. Processes for Low Btu Gasification Combustion Engineering Inc., Windsor, Conn., August, 1976.
22. Sawyer, W. K., Shuck, L. Z., Society of Petr. Eng. of ASME, Paper No. SPE 5743.
23. Schora, F. C., Sixth Synthetic Pipeline Gas Symposium, Chicago, Ill, October, 1974, page 27.
24. Stewart, T. and Wall, T. E., Sixteenth International Symposium on Combustion (1977)
25. Stephens, D. R., and Miller, D. G., Lawrence Livermore Laboratory, Report No. UCJD-17245, August, 1976.
26. Tomite, A. et al. 1973rd ASC Meeting, March 21-25, 1977, Vol. 22, No. 1, p. 4, Fuel Vol. 56, p. 137, 1977.
27. Thorsness, C. B., Lawrence Livermore Laboratory, Report No. UCID-17007, Jan. 19, 1976.
28. Walker, P. L. et al., 173rd ACS Meeting March 21-25, 1977, Vol. 22, No. 1, Page 7
29. Yanagimoto, et al., ERDA Energy Research Abstracts, ERA, Vol. 1, No. 8, pos. 12397.
30. Yang, R. et al., 173rd ACS Meeting, March 21-25, 1977, Vol. 22, No. 1, p. 19.

METALLURGICAL COKES FROM OXIDIZED HIGHLY CAKING COALS

B. Ignasiak, D. Carson, P. Jadernik, and N. Berkowitz

Alberta Research Council, Fuel Sciences Division
Edmonton, Alberta, Canada T6G 2C2

ABSTRACT

Laboratory studies suggest that improvements of coke strength brought about by preheating caking coals before carbonization accrue from inadvertent oxidation rather than from physical changes in the coal mass due to removal of moisture. Controlled oxidation of highly caking coal, followed by carbonization, produces cokes which, in terms of strength, are equivalent to those obtained from prime metallurgical blends. Appropriately formulated blends of exhaustively oxidized and fresh caking coal similarly yield cokes whose properties are comparable to those cokes made from the same coal after oxidation under optimum conditions.

In exercising quality control over the manufacture of metallurgical cokes, it is frequently found useful to preheat the oven-charge in an inert atmosphere at some temperature between 150° and 350°C. The principal benefit of such treatment is a substantially shortened carbonization cycle (1,2) and, hence, greater oven productivity; but in some instances, it has also been observed to result in somewhat greater strength of the finished cokes, and this has been attributed to higher bulk density and better thermal conductivity of the charge after removal of moisture (2).

Bearing in mind that even very slight oxidation affects the rheological properties of caking coals (3), and that preheating tends to reduce their maximum dilatation (4), it appears, however, just as likely that greater coke strength accrues from inadvertent oxidation of the coal during preheating, and the study reported below does, in fact, indicate this to be the more correct view.

EXPERIMENTAL

For the purposes of this investigation, three Appalachian hvAb coals (see Table 1), all characterized by high (Gieseler) fluidity and very pronounced (maximum) dilatation (see Table 2), were used.

In one set of experiments, samples of these coals were preheated for varying periods of time in a sand bath at $180 \pm 3^\circ\text{C}$ while commercial "pure" nitrogen or helium (from Canadian Liquid Air Ltd. and Union Carbide Canada Ltd., respectively) was passed through them at $\sim 10 \text{ ml min}^{-1}$. In a second, the same procedure was used, but the inert gas was thoroughly purified by passing it through a fixed bed of metallic nickel on lamp black at 800°C (5) before admitting it to the coal samples.

After cooling to room temperature in the protective atmosphere, portions of the preheated samples were then tested for their dilatometric and fluidity characteristics, and others were carbonized as previously described (6) and submitted to coke strength tests. Strength was expressed in terms of the F_{5-45} Index (6) which, over a wide range of values, is directly proportional to the ASTM coke stability factor.

To avoid a basis for comparison with oxidized coal, one of the test coals (No. 3) was also exposed to oxygen (at 200°C) and to air (at 100°C and 150°C) for varying periods of time, and then examined like the preheated samples.

RESULTS AND DISCUSSION

After preheating under thoroughly purified nitrogen or helium for 24 hours, the rheological properties of all three coals were found to be entirely unchanged. But preheating under commercial "pure" nitrogen or helium caused rapid loss of fluidity and progressive decrease of the (maximum) dilatation - although at the same time very significantly raising the strength of the coke obtainable from the preheated coal. Figure 1, in which the bracketed numbers refer to coke strength, illustrate these effects for preheating in nitrogen. (Preheating in helium yielded very similar results, except that fluidities then decreased even faster, possibly due to a higher residual oxygen content of this gas.)

The enhanced coke strengths shown in Figure 1 are qualitatively paralleled by the variation of the strengths of cokes made from variously oxidized coal No. 3 (see Figure 2). As anticipated, the oxidation period to optimum oxidation depended on the severity of the treatment, and thus ranged from 15 minutes (for oxygen at 200°C) to 60 hours (for air at 100°C). But in all three cases, a limited oxidation of the coal before carbonization is seen to result in quite dramatic improvements of coke quality. The total oxygen contents of the coal samples after optimum pre-oxidation and oxidation to total loss of caking properties are shown in Table 3.

Verification of the conclusion that slight "accidental" oxidation of the coal during preheating increases coke strength was obtained from semi-technical-scale tests in a 500 lb movable wall oven*. In one test, fresh No. 3 coal was charged, and in a second, preheated No. 3 (96 hours at 170-190°C) was carbonized. Preheating was done in an externally gas-heated hopper through which commercial "pure" nitrogen was passed at 900 ml min⁻¹ (see Figure 3).

The data obtained from evaluation of the two coke lots made in the experimental oven are shown in Table 4 and established a 10 point improvement in the ASTM stability factor when the preheated charge was used. But perhaps even more interesting, in the control of this study, is the variability of coke strengths observed when smaller (20 lb) samples, withdrawn from different locations in the hopper, were carbonized in the laboratory. This variation is graphically presented in Figure 4 in which the bracketed numbers at the sampling points show the maximum dilatation of the preheated coal before carbonization. Comparison of Figures 3 and 4 shows that the point of nitrogen entry into the hopper charge - which is presumably also the point at which the highest concentration of contaminant oxygen would be encountered - lies in a zone from which maximum coke strengths and minimum dilatation were recorded.

Since Figure 4 shows the preheated hopper charge to have been almost as heterogeneous as a coal blend, one further series of laboratory carbonization experiments was carried out with variously formulated blends of fresh and "exhaustively" oxidized coal No. 3. ("Exhaustive" oxidation here means oxidation to total loss of caking properties.) The results of these tests are summarized in Figure 5 and show that, irrespective of the manner of oxidation, addition of oxidized coal can be an effective means for maximizing coke strength. Scanning electron micrographs (see Figure 6) underscore this conclusion by showing that the microscopic structure of cokes made from optimally composed blends of fresh and exhaustively oxidized coal No. 3 compares very favorably with that of coke made from a prime mvb caking coal alone.

*These tests were conducted in collaboration with the Energy Research Laboratories, Department of Energy, Mines and Resources, Ottawa. Fuller details of this program will be published elsewhere.

ACKNOWLEDGEMENTS

We are indebted to Professor T. H. Patching, Department of Mineral Engineering, University of Alberta, for the micrographs, and to Mr. J. C. Botham and his staff for assistance in conducting tests in the movable-wall coke oven.

REFERENCES

1. Beck, K. B., 25th Canadian Conference on Coal, Victoria, B.C., Sept. 16-19, 1973.
Jackman, H. W. and Helfinstine, R. J., Illinois State Geological Survey, Circular 423, 1968; Circular 434, 1968; Circular 449, 1970, Circular 453, 1970.
Dukham, V. N. and Gryaznov, N. S., Koks Khim., 1967, (7) 6.
Yoshida, S. and Sato, H., Nenryo Kyokaishi, 1966, 45 (472), 563.
Yoshida, Y., Nenryo Kyokaishi, 1966, 45 (476), 898.
Dietrich, W., Engschuber, M., and Fritzsche, E., Energietechnik, 1969, L9 (4) 168.
Holub, Y., Sb. Pr. UVP, 1969 (13) 5.
2. Rohde, W. and Beck, K. G., Gluckauf, 1973, 103 (6) 1.
3. Ignasiak, B., Nandi, B. N., and Montgomery, D. S., Fuel (Lond.) 1970, 43, 214.
Ignasiak, B., Clugston, D. M., Montgomery, D. S., *ibid.*, 1972, 51, 76.
Ignasiak, B., Szladow, A. J., and Montgomery, D. S., *ibid.*, 1974, 53, 12.
Ignasiak, B., Szladow, A. J., and Berkowitz, N., *ibid.*, 1974, 53, 229.
4. Beck, K. G., personal communication.
5. Ignasiak, B., Nandi, B. N., and Montgomery, D. S., Analytical Chemistry, 1969, 41, 1676.
6. Ignasiak, B., and Berkowitz, N., Bull. Canada Inst. Min. Metall., 1974, 67, No. 747, 72.
Carson, D., Ignasiak, B., and Berkowitz, N., *ibid.*, 1976, 69, No. 766, 100.

Table 1. Composition of Test Coals

Coal	Rank	Proximate analysis, %				Fixed Carbon (d.a.f.)	Calorific Value (Gross) BTU/lb.	Ultimate analysis, % (d.a.f.)			
		(Capacity) Moisture	Ash (dry basis)	V.M. (d.a.f.)				C	H	N	S
1	hVAb	2.1	4.2	32.3	67.7	14,510	87.6	5.4	1.6	0.8	4.6
2	hVAb	1.7	6.3	34.2	65.8	14,290	87.3	5.5	1.6	1.5	4.1
3	hVAb	2.0	5.3	36.9	63.1	14,270	86.0	5.5	0.9	0.7	6.9

* by difference

Table 2. Rheological Properties of Test Coals

Coal	FSI	(Gieseler) plasticity				Ruhr-dilatation				
		Soft. temp., °C	Max. fluid. temp., °C	Solid. temp., °C	Max. fluid. temp., °C	Soft. temp., °C	Max. contr. temp., °C	Max. dilat. temp., °C	Max. dilat. %	
1	8	403	455	491	3600	365	423	519	27	182
2	8	400	443	476	13100	355	401	611	23	394
3	8	400	443	475	8200	369	412	487	29	122

Table 3. Oxygen Contents of Oxidized No. 3 Coal.
(Initial [O] = 6.2%)

Oxidation method	Oxygen contents, (% w/w)	
	after "Optimum" Oxidation	after Oxidation to Total Loss of Caking Properties
Air at 100°C	6.7 (60)*	7.4 (410)
Air at 150°C	7.1 (6)	7.8 (22)
Oxygen at 200°C	6.4 (0.25)	10.1 (0.75)

* Bracketed numbers show time of oxidation (hrs) to oxygen contents.

Table 4. Evaluation of Cokes from Tests in 500 lb Movable-Wall Oven

	ASTM Stability Factor, (%)	Factor, (%)	Breeze, (% of ½ in fraction)
1. Fresh Coal	35.2	64.5	3.9
2. Preheated Coal (Nitrogen; 170-190°C, 96 hrs)	45.8	64.5	3.6

FIGURE 1. VARIATION OF MAXIMUM DILATATION (---) AND MAXIMUM (GIESELER) FLUIDITY (---) WITH DURATION OF PREHEATING IN COMMERCIAL "P URE" NITROGEN. (BRACKETED NUMBERS SHOW THE STRENGTH INDICES OF COKES.)

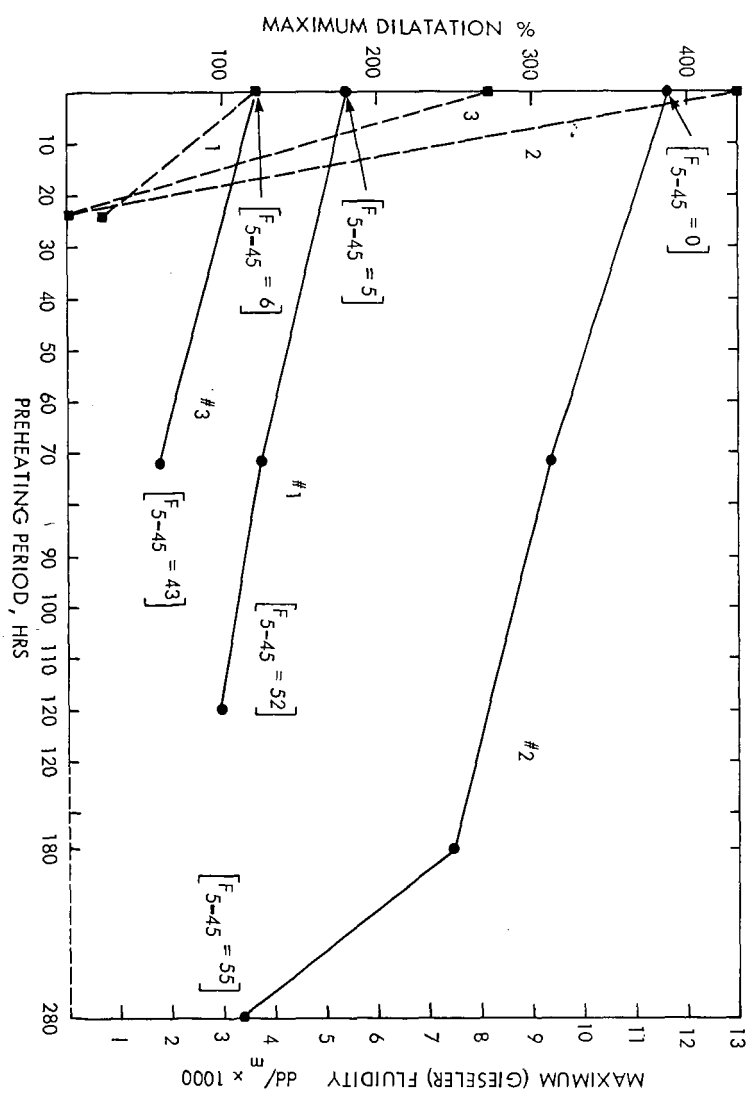


FIGURE 2. EFFECT OF OXIDATION ON STRENGTH OF COKES FROM COAL NO. 3

- A. OXYGEN AT 200°C
- B. AIR AT 150°C
- C. AIR AT 100°C

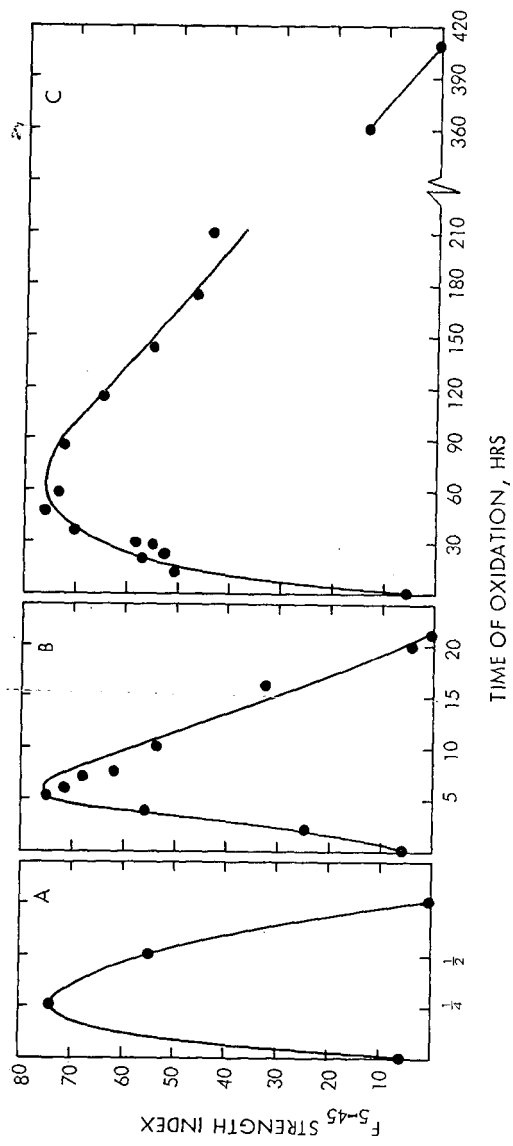


FIGURE 3. PREHEAT HOPPER FOR 500-LB

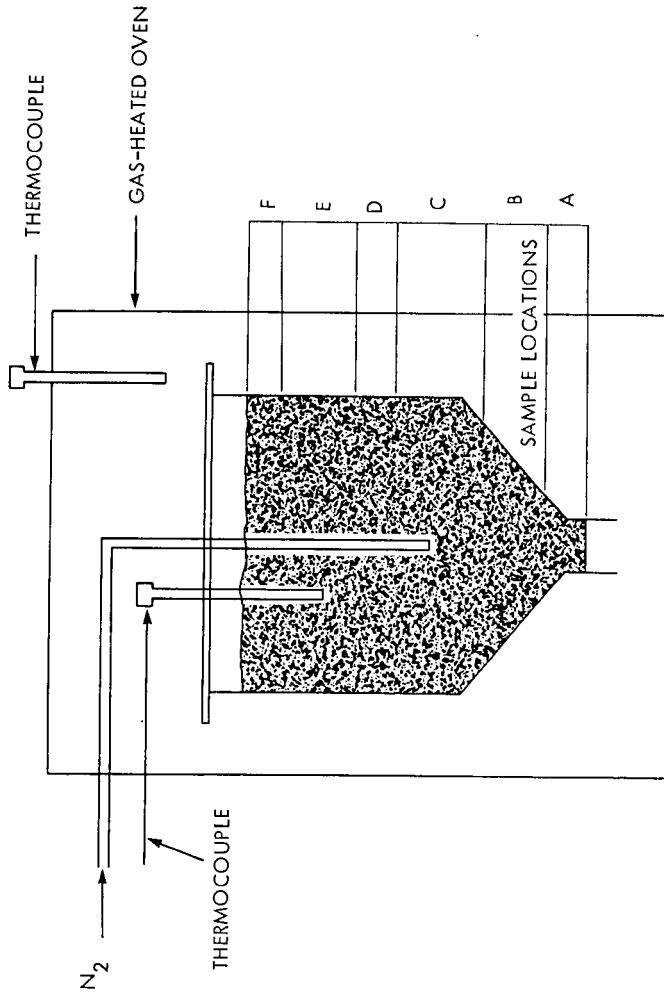


FIGURE 4. MAXIMUM DILATION OF PREHEATED NO. 3 COAL SAMPLES AND STRENGTH OF COKES AS FUNCTIONS OF LOCATION IN PREHEAT HOPPER.

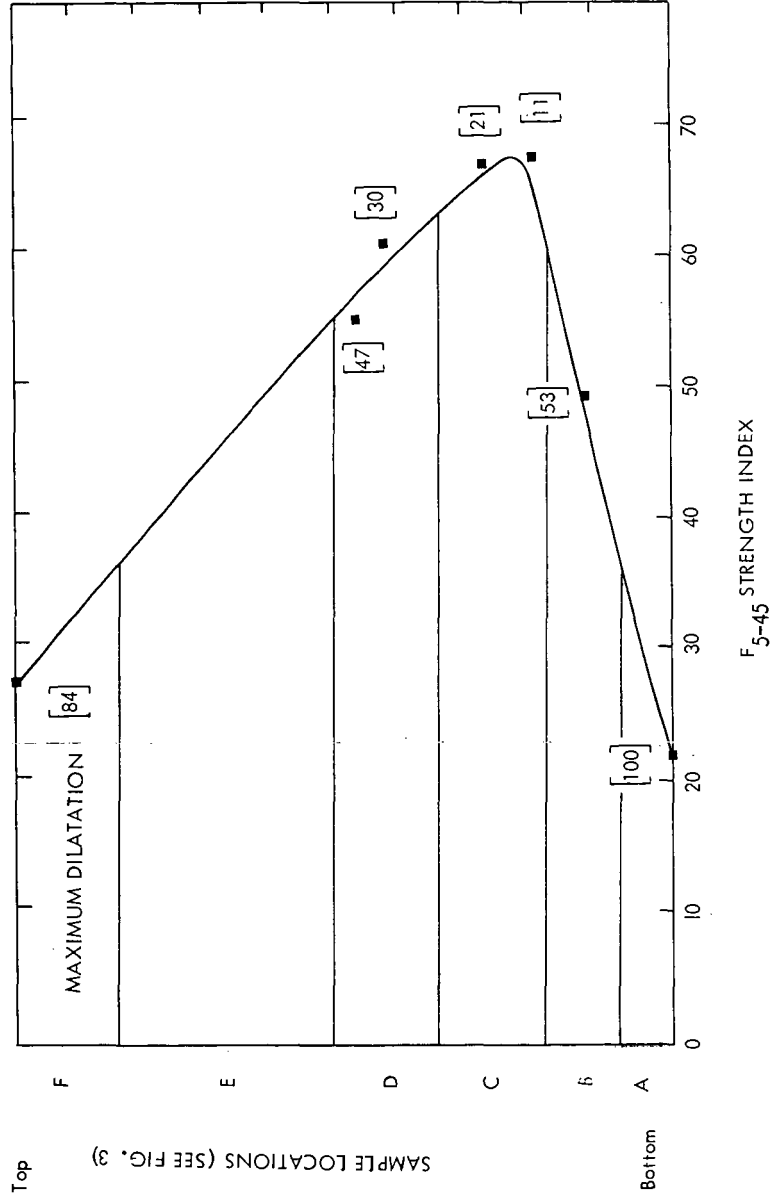


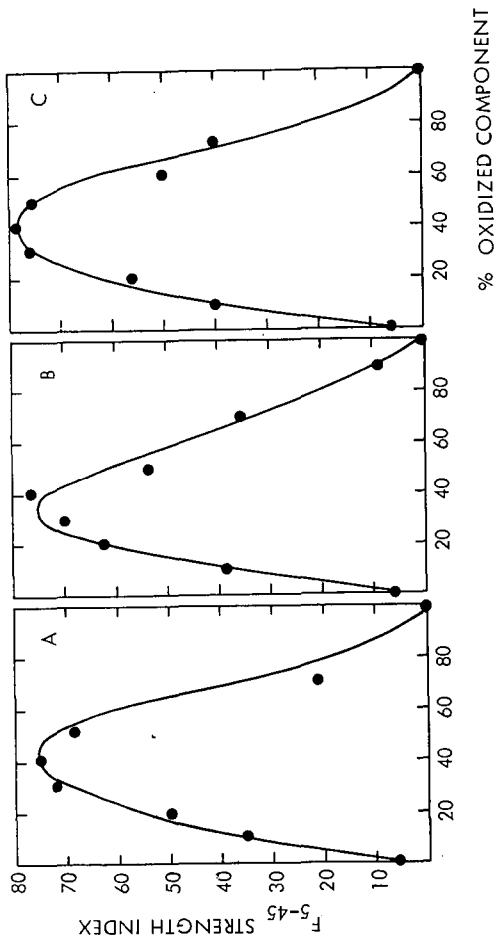
FIGURE 5. STRENGTH OF COKES FROM BLENDS OF FRESH AND "EXHAUSTIVELY"
OXIDIZED COAL NO. 3.

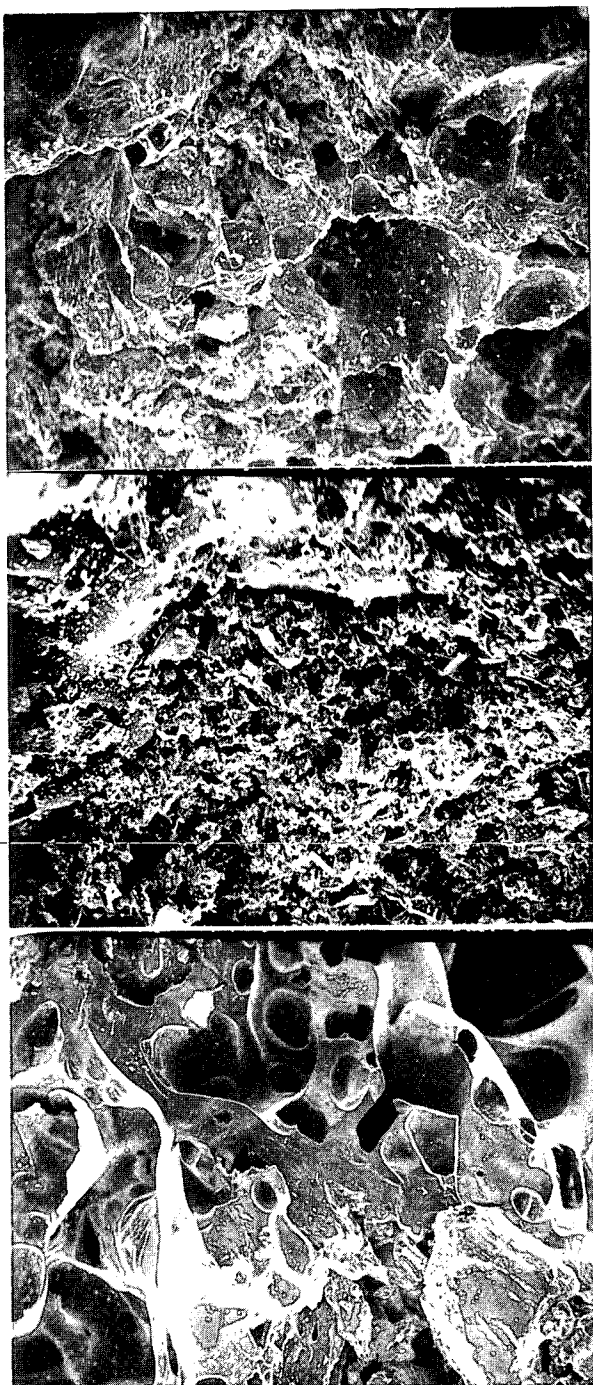
(OXIDIZED COMPONENT PREP. BY TREATMENT WITH)

A. OXYGEN AT 200°C, 2.5 HRS

B. AIR AT 150°C, 22 HRS

C. AIR AT 100°C, 407 HRS





A.

B.

C.

Figure 7. Scanning Electron Micrographs ($\times 100$) of cokes

A. - coke from a blend containing fresh (60 parts) and "totally" oxidized (40 parts) No. 3 coal

B. - the same as A but in the 80:20 ratio

C. - coke from mvb prime coking coal from Cardinal River

MOSSBAUER SPECTROSCOPY OF IRON IN COAL AND COAL HYDROGENATION PRODUCTS

Bernard Keisch,^{1/} Gerst A. Gibbon^{2/} and Sayeed Akhtar^{2/}

^{1/} Carnegie-Mellon Institute of Research
4400 Fifth Avenue, Pittsburgh, PA 15213

^{2/} U. S. Department of Energy
Pittsburgh Energy Research Center
4800 Forbes Avenue, Pittsburgh, PA 15213

ABSTRACT

The chemical states of iron in a Kentucky coal and in the products of its hydrogenation were determined by Mössbauer spectroscopy. The iron in the coal was present chiefly as pyrite, FeS_2 . There was, however, evidence for some non-pyritic iron, most likely present as szomolnokite ($\text{FeSO}_4 \cdot \text{H}_2\text{O}$). The products from hydrogenation of this coal by the SYNTHOIL process at 723 K and 28 MPa contained all the iron as FeS_x where $x = 1.0$ to 1.14. There was no evidence for unreduced FeS_2 or FeSO_4 . There was also no evidence for elemental iron. At the experimental conditions for hydrogenation of coal in this work, the reactor gas contained 0.32 percent H_2S . Evidently, FeS_x is not reduced to elemental iron in the presence of this concentration of H_2S in the reducing gas.

INTRODUCTION

Iron is a major constituent of the mineral matter in many U. S. Coals (1). The metal occurs principally as iron pyrite, FeS_2 , in coal although small quantities of the element may be present as sulfate, oxide, carbonate or silicate (2, 3). In several Australian brown coals, significant quantities of iron occur as salts of carboxylic acids (4, 5, 6). An investigation of iron in coal by Mössbauer spectroscopy was first reported by Lefelhocz *et al.* (7). From an examination of seven U. S. coals ranging in rank from lignite to anthracite, they concluded that, in some coals, iron occurs exclusively as FeS_2 , and non-pyrite iron, when present, occurs as Fe(II) in a high-spin configuration.

The purpose of the present investigation was to determine, by Mössbauer spectroscopy, the iron compounds in a coal utilized in the SYNTHOIL process and in the process products. In this process, a feed paste consisting of pulverized coal in recycle oil is reacted with hydrogen at 723K (450°C) and 14-28 MPa (2000-4000 psi) in a turbulent-flow reactor packed with pellets of Co-Mo/SiO₂-Al₂O₃ catalyst. The product stream is cooled and the gross liquid product, after separation from gases, is centrifuged to remove the unreacted solids. The centrifuged liquid product is a low-sulfur, low-ash fuel oil a portion of which is used as recycle oil to prepare more feed paste for continuous process operation (8, 9).

"By acceptance of this article, the publisher and/or recipient acknowledges the U. S. Government's right to retain a nonexclusive, royalty-free license in and to any copyright covering this paper."

EXPERIMENTAL

Samples of feed coal, feed paste, gross liquid product, centrifuged liquid product and centrifuged residue were drawn from a 1/2 ton per day SYNTHOIL plant currently in operation at the Pittsburgh Energy Research Center. The basics of the plant and the sampling points are shown in figure 1. A detailed description of the procedure and precautions required for obtaining representative samples has been published by Schultz *et al.* (10). The origin and analysis of the coal are given in table 1. The hydrogenation was conducted at 723K and 28MPa.

Samples were placed in circular plastic containers, 25 mm in diameter and 3 mm deep, for Mössbauer analysis. The containers were covered with plastic discs and mounted horizontally in the spectrometer so that any settling of the solids from the liquid samples was uniform with respect to the gamma ray beam. The source was ^{57}Co diffused in Cr. The Mössbauer spectrometer used was of conventional design (Nuclear Science Instruments, Inc.*) and the spectra were obtained by transmission. Iron foil was used for velocity calibration and also provided the reference for isomer shifts. All spectra were recorded at room temperature ($\sim 300\text{K}$).

RESULT AND DISCUSSION

The weights of samples, the results of chemical analyses for iron in each of them and the spectrometer run times are given in table 2. Isomer shifts, quadrupole splittings, ΔS 's and approximate strengths of the internal magnetic fields are given in table 3. The literature values of the Mössbauer parameters for a number of pertinent iron compounds are presented in table 4.

The Mössbauer spectrum of the feed coal showed two strong peaks with an isomer shift of 0.32 mms^{-1} and a quadrupole splitting of 0.64 mms^{-1} . These values agree well with the isomer shift and quadrupole splitting values reported in literature for pyrite and marcasite, two naturally occurring minerals of composition FeS_2 (7, 13). The Mössbauer parameters for the two minerals are so similar that their spectra cannot be resolved if both are present. Although Mössbauer analysis is unable to distinguish pyrite from marcasite, petrographic and X-ray diffraction studies have shown that FeS_2 in coals is generally pyrite (20, 21). Specifically, the FeS_2 in the present coal has been shown by Ruch, *et al.* to be iron pyrite (22).

The spectrum of the coal also showed a single, very weak peak with a velocity of 2.83 mms^{-1} relative to the source. This, no doubt, corresponds to one peak of the doublet for non-pyrite iron reported by Lefelhocz *et al.* in several coals (7). They determined an isomer shift of about 1.1 mms^{-1} (recalculated with reference to iron) and a quadrupole splitting of about 2.6 mms^{-1} . Unfortunately, the second peak for non-pyrite iron in our spectrum is completely obscured by one of the strong pyrite peaks, probably that with a velocity of 0.22 mms^{-1} relative to the source. Lefelhocz *et al.* concluded that the non-pyrite iron may be organic iron or inorganic iron as a silicate (7). Montano (27), however, observing similar

*Use of brand name facilitates understanding and does not necessarily imply endorsement by the U. S. Department of Energy.

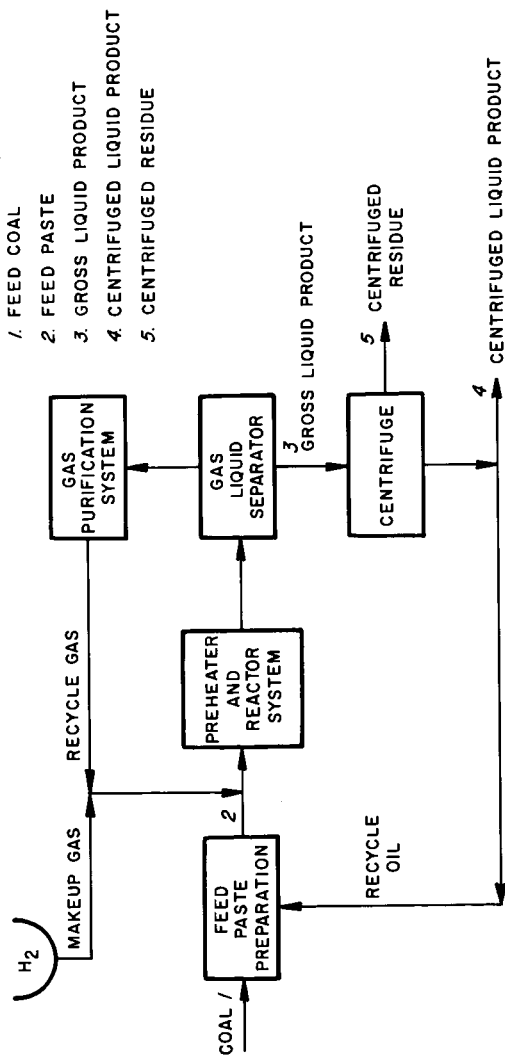


Figure 1 - Sampling points in the SYNTHOIL 1/2 ton per day unit

Table 1. - Analysis of the as-received feed coal¹

Proximate analysis, (wt. pct.)

Moisture	6.1
Volatile matter	36.3
Fixed carbon	42.1
Ash	15.5

Ultimate analysis, (wt. pct.)

Hydrogen	4.9
Carbon	60.3
Nitrogen	1.2
Oxygen (By difference)	12.8
Ash	15.5
Sulfur	5.3
as sulfate	0.58
as pyrite	2.69
as organic	2.03

Rank: hvBb

¹A blend from Kentucky seams No. 9, 11, 12 and 13 which are mined together; Homestead mine, Western Kentucky. The coal was pulverized to a fineness of 70 percent through 200 mesh, U. S. Standard Sieve, and 100 percent through 100 mesh.

Table 2. - Samples analyzed by Mossbauer spectrometry

Material	Weight (g)	Iron content (wt. pct.)	Spectrometer run time (hr.)
Feed coal	1.24	3.58	113
Feed paste	2.60	1.47	160
Gross liquid product	2.40	1.84	139
Centrifuged liquid product	2.16	0.55	189
Centrifuged residue	3.20	10.1	~100

Table 3. Results of Mössbauer Analysis

Material	Isomer shift ^{1/} (mms ⁻¹)	Quadrupole splitting (mms ⁻¹)	ΔS^2 / (mms ⁻¹)	Approximate interval magnetic field ^{2/} H_I , (kOe)
Feed coal	0.32 ^{4/}	0.64	--	--
Feed paste	0.32 ^{5/}	0.63	--	--
Gross liquid product ^{6/}	0.59	--	0.55	280
Centrifuged liquid product	0.70, 0.74	--	0.00, 0.15	310, 270
Centrifuged residue ^{6/}	0.72	--	0.28	280
	0.69, 0.72	--	0.05, 0.69	310, 270

^{1/} Relative to iron

^{2/} Calculated from the 4 outer peaks of a 6-peak pattern as follows: $\Delta S = (S_6 - S_5) - (S_2 - S_1)$.

^{3/} $H_I = (S_6 - S_1) * 31$ where S_1 and S_6 are the outermost peaks of a six-peak pattern.

^{4/} An additional low intensity (5%) peak was observed at a velocity of 2.83 mms⁻¹ with respect to the source; see text for discussion.

^{5/} Calculated from the predominant doublet of the 6-peak spectrum.

^{6/} Discussion of multiple values given in text.

Table 4. Literature Values of Mössbauer Parameters for Some Pertinent Fe Compounds.

Compound	Isomer shift ^{1/} δ (mms ⁻¹)	Quadrupole splitting (mms ⁻¹)	ΔS (mms ⁻¹)	Internal Magnetic field H_i (kOe)	Reference ^{2/}
FeS (troilite)	0.77	0.28		310	(11)
FeS _{1.14} (pyrrhotite)	0.64		0.16	307	(11)
	0.69		0.31	225	
FeS _{1.00}	0.71		-0.32	308	(12)
FeS _{1.05}	0.82		-0.40	276	(12)
FeS _{1.07}	0.77		-0.52	275	(12)
FeS ₂ (pyrite)	0.28	0.60			(7)
	0.29	0.61			(13)
FeS ₂ (marcasite)	0.25	0.50			(7)
	0.23	0.51			(13)
FeSO ₄ ·H ₂ O (szomolnokite)	1.2	2.62			(26)
Fe (metal)	0.00		0.00	330	(14)
α Fe ₂ O ₃	0.43	0.17		515	(17)
Fe ₃ O ₄	0.30			492	(16)
	0.63			455	
FeO	1.08	0.55			(18)
α FeOOH	0.35		0.6	384	(15)
FeSO ₄	1.25	2.94			(17)
FeSO ₄ ·4H ₂ O	1.32	3.17			(18)
FeSO ₄ ·7H ₂ O	1.31	3.20			(18)
Fe ₂ (SO ₄) ₃ × H ₂ O	0.45	0.28			(19)
FeCO ₃	1.25	1.80			(16)
Fe(HCO ₂) ₂ (formate)		1.86			(16)

Table 4. Literature Values of Mössbauer Parameters for Some Pertinent Fe Compounds (Continued).

Compound	Isomer shift ^{1/} δ (mms)	Quadrupole splitting (mms ⁻¹)	ΔS_{-1} (mms ⁻¹)	Internal Magnetic field H_i (kO _e)	Reference ^{2/}
Fe(C ₂ H ₃ O ₂) ₂ (acetate)	0.42	0.50			(14)
Fe ₂ (CO) ₉	0.08	0.37			(17)
Fe ₃ (CO) ₁₂ (-85°C)	0.10 0.15	1.09			(19)

^{1/} Relative to iron. The following correction values were used: Stainless steel to iron -0.90 mms⁻¹, sodium nitroprusside to iron -0.26 mms⁻¹.

^{2/} The numbers refer to the bibliography at the end of the text.

spectra concluded that the non-pyrite fraction is anhydrous iron (II) sulfate FeSO_4 . But the literature values (28) he quotes for isomer shift and quadrupole splitting are inaccurate, as the experiment was probably inadvertently performed on $\text{FeSO}_4 \cdot \text{H}_2\text{O}$. More recent work, using carefully prepared materials, gave values for FeSO_4 and $\text{FeSO}_4 \cdot \text{H}_2\text{O}$ as shown in table 4. Assuming that, in our spectrum, the hidden peak of the high spin doublet is directly under the low velocity peak of the pyrite spectrum our values for the isomer shift and quadrupole splitting would be $\sim 1.3 \text{ mms}^{-1}$ and $\sim 2.6 \text{ mms}^{-1}$, respectively, which are in excellent agreement with $\text{FeSO}_4 \cdot \text{H}_2\text{O}$ as are Montana's and Lefelhocz's.

The spectrum of the feed paste was a composite of the spectra of its components, namely the feed coal and the recycle oil. The latter, as explained above, is a portion of the centrifuged liquid product from a previous batch. For convenience, therefore, the spectrum of the feed paste will be discussed after discussing the spectrum of the centrifuged liquid product.

The spectra of the gross liquid product, the centrifuged liquid product and the centrifuged residue were similar and may be discussed together. Each of the spectra showed a six-peak pattern with isomer shifts in the range of 0.69 to 0.74 mms^{-1} , ΔS 's in the range of 0.00 to 0.69 mms^{-1} and the strengths of the internal magnetic fields in the range of 310 to 270 kOe . The outermost peaks in the spectra of the gross liquid product and the centrifuged residue showed partial resolution into two subpeaks. The values of the isomer shifts, the ΔS 's and the strengths of the internal magnetic fields given in table 3 for these two materials are the values obtained by using the positions of the outer and inner subpeaks respectively to calculate the parameters. Hafner and Klavins observed similar fine structures in the Mössbauer spectra of two pyrrhotites and used a comparable technique for data reduction (11). A comparison of the Mössbauer parameters in tables 3 and 4 shows that the gross liquid product, the centrifuged liquid product and the centrifuged residue contain Fe_x where $x = 1.0$ to 1.14 .

In agreement with our findings, Ruch *et al.* found pyrrhotite in the centrifuged residue by X-ray diffraction analysis of aliquots drawn from the samples used in this work (22).

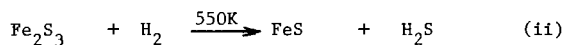
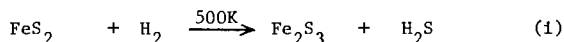
The spectrum of the feed paste had six peaks: two strong peaks corresponding to the pyrite peaks in the spectrum of the feed coal, and four weak peaks, two on each side of the strong doublet. The four weak peaks correspond to the outer four peaks in the size-peak spectrum of the centrifuged liquid product. The two middle peaks of the centrifuged liquid product are obscured by the two strong peaks of the pyrite. Clearly the spectrum of the feed paste is a composite of the spectra of coal and centrifuged liquid product, the components of the feed paste.

None of the spectra obtained in this work showed any absorptions other than those discussed above. We estimate the precision of our measurements is such that other compounds (for example, those shown in table 4 starting with iron) would have been detected had they been present in significant

amounts. Elemental iron, Fe_2O_3 , Fe_3O_4 , or $\alpha\text{-FeOOH}$ would have been detectable in any of the materials analyzed if present in quantities as small as 5% of the total iron present. In the case of the feed coal, the detection limits for iron and above oxides would have been even lower and, in addition, the presence of many of the other compounds in the lower portion of Table 4 would have also been detectable at the 5% level. Possible exceptions are the iron (III) sulfates, iron (III) acetate and $\text{Fe}_2(\text{CO})_9$ with detectability limits of the order of 10-20%.

Although the feed coal does contain a small amount of $\text{FeSO}_4 \cdot \text{H}_2\text{O}$, the quantity of it is too small to account for all the sulfate the coal is known to contain by conventional analysis (see Table 1). Some of the sulfate is presumably combined with Ca or some other cation.

The spectra of the gross liquid product, the centrifuged liquid product and the centrifuged residue showed no evidence for elemental iron. The absence of iron is significant since Gallo has reported the reduction of FeS_2 to elemental iron by the following successive reactions (23):



These results were obtained with gavorranto, a natural pyrite, containing 97.12 percent FeS_2 . It should be noted that reaction (iii) is reversible and, therefore, the reduction of FeS to Fe will not be feasible if the partial pressure of H_2S in the reducing gas is above some critical value. Rosenquist has measured K_p for reaction (iii) at 723K (24). At 28 MPa hydrogen pressure, the equilibrium H_2S pressure is 0.008 percent of the hydrogen pressure. In the present study, the reactor gas contained approximately 0.32 percent H_2S and, evidently, FeS_2 was not reduced to iron in the presence of this concentration of H_2S .

In the qualitative agreement with our results, J. T. Richardson has reported that FeS_2 is reduced to Fe_7S_8 ($\text{FeS}_{1.14}$) during coal hydrogenation (25). By thermomagnetic analysis of a char from a coal liquefaction plant he concluded that the iron in char was present as a mixture of Fe_7S_8 and FeS_2 . The exact composition of the mixture varied with the process conditions.

CONCLUSIONS

Mössbauer analysis of a Kentucky coal showed that iron in the coal was present mainly as FeS_2 . There was some non-pyritic iron, most likely present as szomolnokite ($\text{FeSO}_4 \cdot \text{H}_2\text{O}$). Products from hydrogenation of the coal at 723K and 28 MPa contained FeS_x where $x = 1.0$ to 1.14. There was no evidence of elemental iron in the products.

ACKNOWLEDGEMENTS

We thank Andrew G. Sharkey, Jr., Robert A. Friedel and Paul M. Yavorsky of Pittsburgh Energy Research Center for their interest in this work. A. G. Sharkey, Jr. and R. A. Friedel also participated in several technical discussions.

REFERENCES

1. Abernethy, R. F., Peterson, M. J., and Gibson, F. H., 1969. Major Ash Constituents in U. S. Coals, USBM/RI-7240. U. S. Bureau of Mines, Pittsburgh, PA, pp. 4-9.
2. Thiessen, G., 1945. Composition and Origin of Mineral Matter in Coal. In: H. H. Lowry (Editor), Chemistry of Coal Utilization John Wiley & Sons, New York, p. 487.
3. Dutcher, R. R., White, E. W., and Spackman, W., 1964. Elemental Ash Distribution in Coal Components - Use of Electron Probe. In: Proceedings of the 22nd Ironmaking Conference, Iron and Steel Division, Metallurgical Society of A.I.M.M.E., pp. 463-483.
4. Shaffer, H. N. S., 1977. Organically Bound Iron in Brown Coal. Fuel, 56:45.
5. Brooks, J. D., Durie, R. A. and Sternhell, S., 1958. Chemistry of Brown Coal II. Infrared Spectroscopic Studies. Australian Journal of Applied Science, 9:63.
6. Brooks, J. D. and Sternhell, S., 1957. Brown Coals I. Oxygen-Containing Functional Groups in Victorian Brown coals. Australian Journal of Applied Science, 8:206.
7. Leflhocz, J. F., Friedel, R. A., and Kohman, T. P., 1967. Mössbauer Spectroscopy of Iron in Coal. Geochimica et Cosmochimica. Acta, 31:2261.
8. Akhtar, S., Mazzocco, N. J., Weintraub, M., and Yavorsky, P. M., 1975. SYNTHOIL Process for Converting Coal to Nonpolluting Fuel Oil. Energy Communications, 1:21.
9. Yavorsky, P. M., Akhtar, S., Lacey, J. J., Weintraub, M., and Reznik, A. A., 1975. The SYNTHOIL Process. Chemical Engineering Progress, 71:79.
10. Schultz, H., Gibbon, G. A., Hattman, E. H., Booker, H. B., and Adkins, J. W., 1977. The Distribution of Some Trace Elements in the 1/2 Ton Per Day SYNTHOIL Process Development Unit. PERC/RI-77/2. Pittsburgh Energy Research Center, Pittsburgh, PA, pp. 2-6.
11. Hafner, S. and Klavius, M., 1966. The Mössbauer Resonance of Fe⁵⁷ in Troilite (FeS) and Pyrrhotite (Fe_{0.88}S). Zeitschrift für Kristallographie, 123:443.
12. Ono, K., Ito, A., and Hirahara, E., Mössbauer Study of Hyperfine Field, Quadrupole Interactions and Isomeric Shift of Fe⁵⁷ in FeS_{1.00}, FeS_{1.05} and FeS_{1.07}. Journal of the Physical Society of Japan, 17:1615.
13. Temperley, A. A. and Leferve, H. W., 1966. The Mössbauer Effect in Marcasite-Structure Iron Compounds. Journal of the Physical Chemistry of Solids, 27:85.

14. Muir, A. H., Ando, K. J., and Coogan, H. M., 1966. Mössbauer Effect Data Index, Interscience, New York, 351 pp.
15. Forsyth, J. B., Hedley, I. G., and Johnsen, C. E., 1968. The Magnetic Structure and Hyperfine Field of Graphite (αFeOOH). *Journal of Physics C* (Proceedings of the Physical Society, Ser. 2, 1:179).
16. Stevens, J. G. and Stevens, V. E., 1972. Mössbauer Data Index (covering 1971 literature), Plenum, New York, 430 pp.
17. Stevens, J. G. and Stevens, V. E., 1972. Mössbauer Data Index (covering 1970 literature), Plenum, New York, 369 pp.
18. Stevens, J. G. and Stevens, V. E., 1970. Mössbauer Data Index (covering 1969 literature), Plenum, New York, 281 pp.
19. Fluck, E., Kerler, W., and Neuwirth, W., 1963. The Mössbauer Effect and Its Application for Chemistry. *Angewandte Chemie*, 75:461. (In German).
20. Thiessen, G., Ball, C. G., and Grohs, P. E., 1936. Coal Ash and Coal Mineral Matter. *Industrial and Engineering Chemistry*, 28:355.
21. Mitra, B. G., 1954. Identification of Inorganic Impurities in Coal by the X-Ray Diffraction Method. *Fuel*, 33:316.
22. Ruch, R. R., Gluskoter, H. J., Dreher, G. B., Russel, S. J., Cahill, R. A., Frost, J. K., Kuhn, J. K., Steele, J. D., Thomas, J. and Malhotra, R., 1977. Determination of Valuable Metals in Liquefaction Process Residues. Quarterly Technical Progress Report No. 18 to U. S. ERDA, under contract (E46-1)-8004 20 pp.
23. Gallo, G., 1927. The Reduction of Iron Ores With Hydrogen. *Annalen Chemie Applicata*. 17:39. (Chemical Abstracts, 1927, 21:1243).
24. Rosenquist, T., A Thermodynamic Study of the Iron, Cobalt, and Nickel Sulphides., *Journal of the Iron and Steel Institute*, 176:37.
25. Richardson, J. T., 1972. Thermomagnetic Studies of Iron Compounds in Coal Char. *Fuel*, 51:150.
26. Gallagher, P. K., Johnson, D. W. and Schrey, F., 1970. Thermal Decomposition of Iron (II) Sulfates. *Journal of the American Ceramic Society*, 53:660.
27. Montano, P. A., 1977. Mössbauer Spectroscopy of Iron Compounds in West Virginia Coals. *Fuel*, 56:397.
28. Grant, R. W., Widersick, H., Muir, A. H., Gonser, U. and Delgass, W. N., 1966. Sign of the Nuclear Quadrupole Coupling Constant in Some Ionic Ferrous Compounds. *Journal of Chemical Physics*, 45:1015.

An Infrared Absorption Study of Coal-Metal Salt Catalyst Interactions

J. M. Lee*, R. E. Wood and W. H. Wiser, Mining and Fuels Engineering Department, University of Utah, Salt Lake City, Utah 84112. *Present address, Department of Chemical Engineering, Auburn University, Auburn Alabama.

Introduction

A thorough study of the infrared absorption patterns produced by coal samples conducted by Friedel, et. al., (1) resulted in the assignment of absorption bands to specific structures or components of coal. Those assignments of importance to this study are listed in Table I.

Although some uncertainty exists with respect to these assignments the 3030 cm^{-1} band is considered to represent the aromatic C-H and the 2920 cm^{-1} and 2850 cm^{-1} bands represent aliphatic C-H. CH_3 , CH_2 , and CH (aliphatic) configurations all contribute to these absorption bands but the dominant effect is that from CH_2 because of its relative abundance. However, the IR differentiation does not discriminate between aliphatic C-H bonds in aliphatic side chains, in hydroaromatic structures, in cycloparaffins or in aliphatic connecting bridges. The 1610 cm^{-1} band is assigned to double bond carbon and/or carbon only bonds. In coal this is taken to be aromatic carbon (2,3). The 1450 cm^{-1} band is assigned to aliphatic H bending and/or aromatic carbon stretching. The 1260 cm^{-1} band is assigned to phenoxy and ether structures. Figure 1 shows these band assignments as derived by Friedel (1) and applied to the IR pattern of a thin section of vitranite.

Temperature effects on functional groups in coal have been studied by several authors (1,3,4,5,6). These reports indicate that the IR band assigned to the OH structures in bituminous coals disappears near 500°C. The band attributable to phenoxy structures (1260 cm^{-1}) decreases in intensity at 300°C but does not completely disappear even at 550°C. The C-H stretching band intensities decrease and the aromatic C-C and C-O band (1610 cm^{-1}) is unchanged at temperatures approaching 600°C. Oelert (4) has published an extensive interpretation of thermally induced structural changes in coal as a result of IR measurements.

The present study is an attempt to use the IR absorption procedure to measure change in coal structure under nitrogen and hydrogen (one atmosphere pressure) and in the presence of metal salt catalysts.

Experimental

A Beckman IR-20 Infrared Spectrophotometer was used to measure infrared spectra of KBr pellets containing finely dispersed coal and char samples. Kapaiowitz, Utah coal sized to 44-53 microns (-270 +325 mesh) was used. Proximate and ultimate analyses of this coal are given in Table II.

Coal samples were impregnated with metal salt catalysts (ZnCl_2 , CdCl_2 , $\text{SnCl}_2 \cdot 2\text{H}_2\text{O}$, $\text{CoCl}_2 \cdot 6\text{H}_2\text{O}$ and $\text{FeSO}_4 \cdot 7\text{H}_2\text{O}$) by mixing the coal with a water

solution of the salt and drying the slurry under vacuum at 110°C. The catalyst application rate was 0.112 moles of catalyst per 100 grams of MAF coal. The prepared sample (50 mg) was heated to various temperatures (250, 350 or 450°C) for 30 minutes in the presence of either H₂ or N₂ gas (99.98 % purity). Figure 2 shows a schematic drawing of the equipment used for heat treatment.

Following reaction, the chars were weighed to permit a correction for loss of volatile matter and KBr pellets were prepared. Twenty mg of each sample were ground in a Wig-L-Bug vibrator for 1 hour. Then, 0.5 to 2.0 mg of the coal or char were mixed with 250 mg of IR grade KBr for 10 minutes in the same device. Two hundred mg of the mixture were briquetted in a hot die (110 C) after evacuation. The result was a clear pellet 13 mm in diameter and 0.6 mm thick. Each sample was measured 4 times, not as duplicates, but at 0.2, 0.4, 0.6, and 0.8 weight percent of the KBr disc.

Results and Discussion

Figure 3 shows the IR pattern to be expected from different amounts of coal dispersed through a KBr pellet. Because the grinding and mixing were done in polystyrene vials there is an obvious contamination of this polymer in the sample as measured by the spectrometer. In fact, because the polystyrene contains similar bonding to that found in coal, the spectra of KBr with no coal present (but with polystyrene contamination) is very similar to the pattern obtained when coal is present. The effect of this contamination becomes constant at 10 minutes grinding or mixing time and hence is a constant which can be subtracted from the KBr plus polystyrene plus coal pattern.

Beer's law for absorption states that:

$$A = km/S + A_0 = k M/100S + A_0 = Kc + A_0$$

where A = sample absorbance at a specific absorption band

A₀ = constant absorbance due to the polystyrene

k = specific extinction coefficient (cm²/mg)

m = weight of coal in the disc (mg)

S = area of disc (cm²)

M = weight of the disc (mg)

c = weight percent of coal in the disc

K = slope of the line A vs c

The values of k, K and A₀ as measured for this study are shown in Table III for the 2920 cm⁻¹ absorption peak. Some literature values of k are included for comparison. Because the data obtained using the conventional base line (3120-2780 cm⁻¹) did not yield a straight line of A vs c for either the 2920 or 3030 cm⁻¹ bands, a second base line (3740-2200 cm⁻¹) was used. This base line provided the desired straight line function and also gave larger values of k and K without significantly changing A₀. Slopes were calculated for each of the A vs c lines (K values in the Beer law relationship). Correlation coefficients (r²) were calculated for

all the lines and data points generated. Statistically, all data points gave r^2 values in excess of the 90 percent confidence level and most cases were in excess of the 95 percent level.

Subsequent calculations have included data for N_2 and H_2 atmosphere, 350 and 450°C and no catalyst, plus the metal salts listed above. The data obtained on samples treated at 250°C were not included because of overlap of lines caused by water absorption with lines used in the calculations. For statistical purposes, the data provide two levels of atmosphere, two levels of temperature and two levels of catalyst application for each of the 5 metal salts used. The total data (K values) accumulated are included in Table IV. Changes in K values from one condition to another indicate an increase or a decrease in the type of bonding that gives rise to that particular absorption band. Therefore, changes in K values can be related to changes in aromatic hydrogen, aliphatic hydrogen, aliphatic carbon, etc., in the coal or char structure.

The infrared absorbance data were analyzed by means of a multivariable linear regression analysis procedure to discover which absorbances were statistically related. The percent volatile matter from each trial was included as the dependent variable in the computation. The correlation coefficients shown in Table V are the result of this calculation. The following comments can be made with respect to these correlation values.

1. The 3030 cm^{-1} absorbance peak (aromatic hydrogen) has a negative correlation with all other peaks, but a positive correlation with volatile matter. Although the correlation is not high in any case it means that the concentration of aromatic bonding in the char increases with increase in volatile matter production. This supports the concept that aromatic bonds are produced in the char as more volatile matter is produced.

2. All the absorbance bands, except 3030 cm^{-1} , have a negative correlation with respect to volatile matter. This indicates that the bonds represented by the absorbance bands, aliphatic or naphthenic hydrogen, aromatic carbon, carbonyl, carboxylates, phenoxy structures, etc., are destroyed or removed to produce volatile material.

3. A very good correlation coefficient (+0.785) is found for the 2920 and 2850 cm^{-1} bands. This supports the concept that these two bands measure the same thing, in this case aliphatic or naphthenic hydrogen.

4. Good positive correlation coefficients between 1610, (aromatic C and/or C=O), 1450 (CH_2 , CH_3 , C-C) and 1260 (C=O in phenoxy structures) indicate that they are also a measure of the same thing, or at least that the bonds they measure are affected simultaneously by the various sample treatment procedures.

5. The fairly good inverse correlation between the 2920 and 2850 cm^{-1} absorbance bands and the percent volatile matter is in agreement with published ideas on the origin of volatile components. The changes found in aliphatic hydrogen bonding indicate a decrease with increased volatile matter. This can be explained as abstraction of hydrogen from hydroaromatic structures by thermally produced free radicals, a second order reaction, (8,9) or by a first order pyrolytic breaking of aliphatic bonds (10,11).

6. The positive, but low, correlation between 2920 and 2850 cm^{-1} with 1610, 1450 and 1260 cm^{-1} indicates that the bonds responsible for these

absorbances are again treated similarly by the various sample treatment procedures. Although the bonds involved may not be the same, the various peaks do increase or decrease together.

The significance of the numerical (K) data of Table V was tested with the conventional F ratio, using three variables, each at two levels. The results of this study are shown in Table VI. In this table, the significance is noted by a number which is the statistical probability of error. The number 0.20 indicates a 1 in 5 probability that the statement is in error, 0.05 indicates a 1 in 20 probability that the statement is in error, 0.01 indicates a 1 in 100 and 0.001 indicates a probability of 1 in 1000 that the statement is in error.

Analysis of Table VI tells us that little difference is realized by virtue of hydrogen pressure at one atmosphere. FeSO_4 affects both the 3030 and the 2850 cm^{-1} absorption bands when hydrogen is present. Since both are increased, the Ar/Al ratio as represented by 3030/2920 is not affected. ZnCl_2 depresses volatile matter evolution at low temperature but increases it at high temperatures when hydrogen is present. CdCl_2 does act to increase volatile matter evolution when hydrogen is present. The 1610 cm^{-1} band is not affected by hydrogen presence with any of the metal salts.

Temperature acts to increase volatile matter evolution with all of the salts present. However, this volatile matter is obtained at the expense of different bonds in the presence of different salts. SnCl_2 and CdCl_2 act to increase aromatic hydrogen while FeSO_4 acts to decrease the aliphatic hydrogen at higher temperatures. CdCl_2 is the only salt of the five tested which does not decrease the aromatic carbon at the higher temperature.

The catalytic effect, as opposed to hydrogen or temperature, is shown in the final section of Table VI. ZnCl_2 acts to decrease the absolute amount of aromatic hydrogen in the char while SnCl_2 acts to cause an increase. This would appear to be an anomaly but can be explained if we assume that these salts influence different bonds. ZnCl_2 may influence hydrogen release from aromatic structures with consequent polymerization of the residual groups. SnCl_2 may influence hydrogen abstraction from hydroaromatic structures yielding aromatic structures in the residue which are less condensed than with ZnCl_2 . ZnCl_2 increases the aliphatic hydrogen as does FeSO_4 . For ZnCl_2 this indicates a transfer of hydrogen from some aromatic to form some aliphatic structures. ZnCl_2 , CdCl_2 and CoCl_2 decrease the ratio of aromatic hydrogen to aliphatic hydrogen while SnCl_2 increases it. SnCl_2 , CdCl_2 and FeSO_4 decrease the absolute content of aromatic carbon. SnCl_2 acts to increase volatile matter evolution while FeSO_4 has a slight tendency to repress the evolution. Other salts seem to have no effect on the final quantity of volatile matter evolved.

As a summary we can say that infrared absorption technique is capable of differentiating some types of bonds affected by coal pyrolysis in the presence of metal salts. Further, these salts do not act uniformly with respect to specific bonds. This is especially apparent in the cases of ZnCl_2 and SnCl_2 , both of which are effective as coal hydro-generation-liquefaction catalysts. ZnCl_2 acts to decrease the absolute content of aromatic hydrogen bonding while SnCl_2 acts to increase the absolute quantity of aromatic hydrogen in the char.

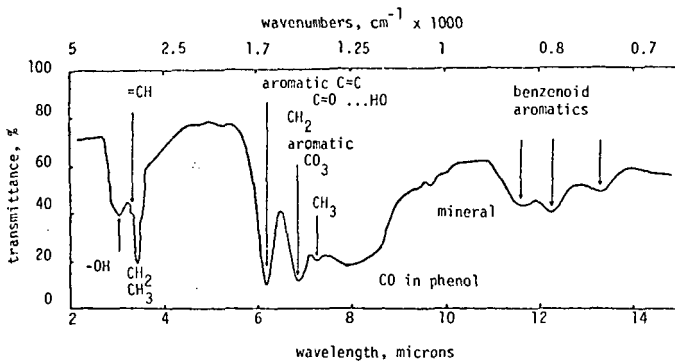


Figure 1. Infrared Spectrum of Vitrain Thin Section

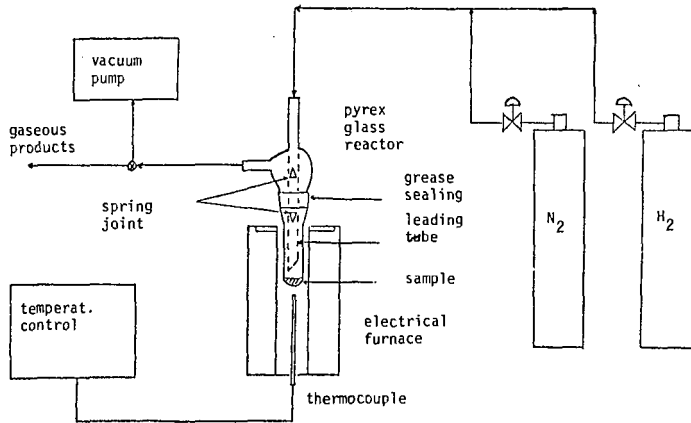


Figure 2. Flow Scheme of Reactions with N₂ and H₂

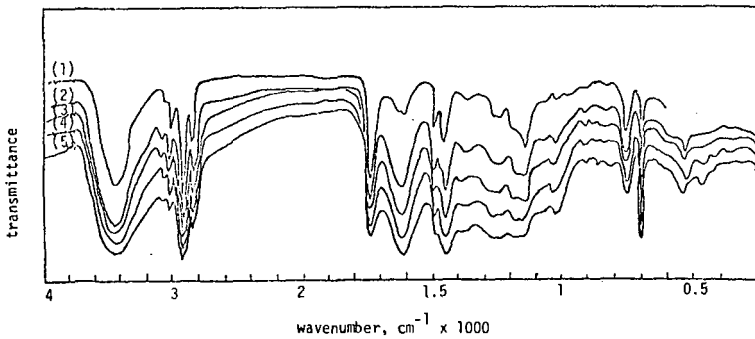


Figure 3. Spectra by Varying the Hiawatha Coal Concentration in the KBr Pellet; (1) KBr alone, (2) 0.218%, (3) 0.420%, (4) 0.600%, (5) 0.807%

TABLE I
Selected Infrared Absorption
Absorption Assignments in the Coal Structure (1)

Absorption Band, cm^{-1}	Assignment
2920	Naphthenic and/or aliphatic C-H
3030	Unsaturated CH, probably aromatic
1610	Aromatic C-C and/or C-O...HO-; carboxilates
2850	Naphthenic and/or aliphatic C-H
1450	CH_2 and CH_3 ; aromatic C-C or ionic carbonates
1260	C=O in phenoxy structures

TABLE II
Proximate and Ultimate Analysis
of Kaiparowitz, Utah Coal

Dry Basis		MAF Basis				
% Ash	% V.M.	% C	% H	% N	% S	% O
10.8	51.4	73.4	6.17	1.91	0.55	18.00

TABLE III
Constants Obtained From Beer's Law, 2920 cm^{-1}

Coal Sample	k	K	A_0
This work 3120-2780 base	0.27	0.401	0.245
3740-2200 base	0.40	0.599	0.264
Freidel (1) 3120-2780 base vitrain (84% C)	0.17		
Fujii (7) 3210-2780 base vitrain (83.4% C) vitrain (84% C)	0.38 0.42		

TABLE IV
K Values Obtained from IR Spectra

A	T	C	3030	2850	2920	1610	1450	1260	V.M.%
N ₂	350	None	0.184	0.263	0.268	0.835	0.636	0.547	6.9
N ₂	450	"	0.214	0.234	0.207	0.751	0.611	0.537	21.8
H ₂	350	"	0.223	0.307	0.388	0.787	0.648	0.474	6.2
H ₂	450	"	0.258	0.267	0.247	0.789	0.711	0.497	24.7
N ₂	350	ZnCl ₂	0.200	0.245	0.382	0.819	0.587	0.478	7.1
N ₂	450	" ²	0.159	0.367	0.426	0.654	0.524	0.523	21.4
H ₂	350	"	0.155	0.335	0.466	0.819	0.675	0.548	6.4
H ₂	450	"	0.171	0.286	0.401	0.789	0.692	0.512	25.4
N ₂	350	SnCl ₂	0.227	0.341	0.404	0.734	0.460	0.434	12.5
N ₂	450	" ²	0.330	0.258	0.118	0.419	0.267	0.387	29.0
H ₂	350	"	0.219	0.197	0.287	0.665	0.470	0.438	17.3
H ₂	450	"	0.290	0.168	0.199	0.464	0.334	0.323	28.8
N ₂	350	CdCl ₂	0.209	0.290	0.383	0.744	0.610	0.469	3.4
N ₂	450	" ²	0.236	0.323	0.312	0.595	0.581	0.529	19.4
H ₂	350	"	0.171	0.332	0.518	0.676	0.582	0.401	13.4
H ₂	450	"	0.246	0.242	0.372	0.750	0.632	0.464	34.7
N ₂	350	CoCl ₂	0.280	0.407	0.539	0.858	0.708	0.536	2.4
N ₂	450	" ²	0.240	0.231	0.335	0.773	0.592	0.488	17.5
H ₂	350	"	0.244	0.396	0.525	0.888	0.703	0.591	2.4
H ₂	450	"	0.269	0.324	0.415	0.735	0.630	0.571	26.7
N ₂	350	FeSO ₄	0.228	0.338	0.443	0.693	0.536	0.488	0.0
N ₂	450	"	0.189	0.283	0.462	0.653	0.447	0.404	12.1
H ₂	350	"	0.238	0.331	0.497	0.657	0.512	0.449	0.0
H ₂	450	"	0.258	0.315	0.318	0.664	0.512	0.449	23.9

TABLE V
Multilinear Regression Analysis Correlation Coefficients

Correlation	Coefficient	Correlation	Coefficient
3030-2920	-0.225	2850-1260	+0.478
3030-2850	-0.098	1610-1450	+0.841
3030-1610	-0.167	1610-1260	+0.709
3030-1450	-0.120	1450-1260	+0.779
3030-1260	-0.129	3030-V.M.	+0.289
2920-2850	+0.785	2920-V.M.	-0.594
2920-1610	+0.327	2850-V.M.	-0.557
2920-1450	+0.234	1650-V.M.	-0.322
2920-1260	+0.182	1450-V.M.	-0.119
2850-1610	+0.353	1260-V.M.	-0.190
2850-1450	+0.371		

TABLE VI
Statistical Significance of I.R. Absorbance Data

ATMOSPHERE

N ₂ or H ₂	3030		2850		3030/2920		1610		% V.M.	
	S	E	S	E	S	E	S	E	S	E
ZnCl ₂	---	---	---	---	---	---	---	---	0.01	I Hi T D Lo T
SnCl ₂	---	---	---	---	---	---	---	---	---	---
CdCl ₂	---	---	---	---	---	---	---	---	0.05	I
CoCl ₂	---	---	---	---	0.20	D	---	---	---	---
FeSO ₄	0.05	I	0.05	I	---	---	---	---	---	---

TEMPERATURE

350 or 450°C

ZnCl ₂	---	---	---	---	0.05	I	0.05	D	0.001	I
SnCl ₂	0.01	I	---	---	---	---	0.001	D	0.001	I
CdCl ₂	0.05	I	---	---	0.01	I	---	---	0.01	I
CoCl ₂	---	---	---	---	0.01	I	0.05	D	0.001	I
FeSO ₄	---	---	0.05	D	---	---	0.05	D	0.01	I

CATALYST EFFECT

ZnCl ₂	0.05	D	0.20	I	0.01	D	---	---	---	---
SnCl ₂	0.05	I	---	---	0.20	I	0.001	D	0.05	I
CdCl ₂	---	---	---	---	0.05	D	0.05	D	---	---
CoCl ₂	---	---	---	---	0.01	D	---	---	---	---
FeSO ₄	---	---	0.01	I	---	---	0.01	D	0.20	D

S = Significance
E = Effect

I = Increase in measured absorbance
D = Decrease in measured absorbance

REFERENCES

1. R. A. Friedel, H. L. Retcofsky and J. A. Queiser, Advances in Coal Spectrometry-Absorbance Spectrometry, U.S. Bu. Min. Bul. 640, 1967.
2. R. A. Friedel and G. L. Carlson, "Difficult Carbonaceous Materials and Their Infrared and Raman Spectra, Reassignments for Coal Spectra," Fuel, 51, 194, (1972).
3. J. H. Shih, Y. Osawa and S. Fujii, "Infrared Spectra of Heat Treated Coal," Fuel, 51, 153, (1972).
4. H. H. Oelert, "Chemical Characteristics of the Thermal Decomposition of Bituminous Coals," Fuel, 47, 433 (1968).
5. J. K. Brown, "The Infrared Spectra of Coals" J. Chem. Soc., 744, 1955.
6. J. K. Brown, "Infrared Studies of Carbonized Coals," J. Chem. Soc., 752, 1955.
7. S. Fujii, Y. Osawa and H. Sugimura, "Infrared Spectra of Japanese Coal: The Absorption Bands at 3030, 2920 and 1600 cm^{-1} " Fuel, 48, 161, (1969).
8. W. H. Wiser, "A Kinetic Comparison of Coal Pyrolysis and Coal Dissolution," Fuel, 47, 475, (1968).
9. W. H. Wiser, L. L. Anderson, S. A. Qader and G. R. Hill, "Kinetic Relationship of Coal Hydrogenation, Pyrolysis and Dissolution," J. Appl. Chem., 21, 82 (March 1971).
10. B. K. Mazumdar, S. K. Chakrabartty and A. Lahiri, "Dehydrogenation of Coal and Tar Formation," Fuel, 38, 112 (1959).
11. B. K. Mazumdar, S. K. Chakrabartty and A. Lahiri, "Further Studies on the Dehydrogenation of Coals by Sulfur," Fuel, 41, 121 (1962).

CHARGE TRANSFER COMPLEXES OF COAL-DERIVED ASPHALTENES

I. Schwager, J.T. Kwan, J.G. Miller and T.F. Yen

University of Southern California
Chemical Engineering Department
University Park
Los Angeles, California 90007

INTRODUCTION

Coal-derived asphaltene are thought to be key intermediates in the conversion of coal to oil (1). A model, based on x-ray diffraction studies (2), has been proposed to describe the macrostructure of associated asphaltene in the solid state (3). The state of association of these species in benzene and tetrahydrofuran solution has been studied by vapor pressure osmometry, and molecular weights have been reported as a function of concentration (4). Evidence has been presented recently in the literature supporting a hydrogen-bonding donor-acceptor association in solution (5-7). Previously the mechanism of association of petroleum asphaltene (8-10), and coal and chars (11) was described in terms of charge transfer donor-acceptor forces. A study of the properties of iodine-petroleum asphaltene complexes was carried out, and led to useful information on the structure of petroleum asphaltene (12). It was therefore decided to synthesize charge transfer complexes of coal-derived asphaltene, and to study their properties by a variety of physical and analytical techniques.

EXPERIMENTAL

Coal-derived asphaltene were separated by solvent fractionation (13, 14) from coal liquids produced in five major demonstration liquefaction processes: Synthoil, HRI H-Coal, FMC-COED, Catalytic Inc. SRC, and PAMCO SRC. The asphaltene were further separated into three fractions by exhaustive solvent elution chromatography on silica gel using the solvents: benzene, diethyl ether, and tetrahydrofuran. The benzene and diethyl ether eluted fractions, known to contain a higher and lower proportion of basic asphaltene molecules (13), were used in addition to starting asphaltene to form some of the complexes.

Complexes were formed by mixing benzene solutions of the asphaltene (-50 g/l) with benzene solutions of either iodine or tetracyanoethylene (freshly sublimed reagent grade) in the approximate mole ratios, asphaltene/acceptor = 0.7 - 1.0/1. A precipitate forms rapidly. It was filtered, washed with benzene and dried overnight at 40°C/2mm Hg.

The dark brown to black I₂-asphaltene complexes are relatively insoluble in benzene, carbon disulfide, and pentane, and slightly to moderately soluble in chloroform and tetrahydrofuran. The brown-black TCNE-asphaltene complexes are only moderately soluble in THF.

Analyses were performed by the ELEK Microanalytical Laboratories, Torrance, California. Iodine was determined gravimetrically after nitric acid oxidation in the presence of silver nitrate; nitrogen was determined by the Dumas procedure. Molecular weights were measured in THF with a Mechrolab Model 301A Vapor Pressure Osmometer. Infrared spectra were determined as KBr disks on a Beckman Acculab 6 IR. Ultraviolet-visible spectra were run in either chloroform or tetra-

hydrofuran solution on a Beckman Model 25 Spectrophotometer. X-ray diffraction measurements were made with a General Electric XRD-6 x-ray diffractometer with a $\text{CuK}\alpha$ radiation source (15). Electron spin resonance spectra were taken with a Varian E-12 x-band spectrometer. Resistivity measurements were carried out at 25°C over the pressure range 10-3000 atmospheres by use of a cell and procedure described by Hadek (16).

RESULTS AND DISCUSSION

Composition of Complexes

Analytical data for I_2 -asphaltene and TCNE-asphaltene complexes are presented in Tables I and II. The mole ratios of asphaltene to iodine are approximately 1 to 1 with the exception of the FMC-COED - I_2 complex which afforded a tar-like material initially instead of a precipitate. The mole ratios of asphaltene to TCNE are more widespread, but are closer to 2 to 1. The mole ratio calculations are based on the assumption that the molecular weight of the asphaltene portion of the complex is the same as the molecular weight of the starting asphaltene, which may not be strictly correct.

Ultraviolet-Visible Spectra of Complexes

Measurement of the UV-Visible spectrum of I_2 -asphaltene complexes in THF or CHCl_3 (Fig. 1) leads to the observation of a new band at ≈ 295 nm and new shoulder at ≈ 355 nm. Neither of these absorptions is observed in the free components. These bands are presumed to be charge-transfer absorption bands of the iodine-asphaltene complex. The nature of the donor interaction of the asphaltene may be either via the electrons of the π -orbitals, or via the non-bonded, lone pair electrons in atomic orbitals of n donors such as nitrogen or oxygen bases.

Measurement of the UV-Visible spectrum of TCNE-asphaltene complexes in THF (Fig. 2) leads to the observation of new bands at 406 and 425 nm not found in the free components. These bands are presumed to be charge-transfer absorption bands of the donor asphaltene molecules and the π -acceptor TCNE.

Infrared Spectra

Asphaltene-iodine samples were run as KBr disks, and infrared spectra were obtained directly, and differentially of asphaltene-iodine complexes versus reference asphaltene. No C-I stretching frequencies were observed in the 400-600 cm^{-1} region, and no aromatic- I_2 bands in the 992 cm^{-1} to 1200 cm^{-1} region (17, 18).

Asphaltene-TCNE complexes were run in KBr disks and the infrared spectra compared with those of the free components, and physical mixtures of the free components. The most obvious changes are in the TCNE doublet at 2200 cm^{-1} which changes to a singlet, and in the appearance of a prominent new band at 1500 cm^{-1} .

X-Ray Diffraction

The x-ray diffraction patterns of asphaltenes show diffuse bands typical of mesomorphic or semicrystalline substances (2): the (002) band is attributed to the interplanar spacing between condensed aromatic rings of ≈ 3.5 Å; the gamma band is attributed to the spacing between disordered aliphatic chains or alicyclic rings of ≈ 4.6 Å (Fig. 3).

X-ray analysis of petroleum asphaltene-iodine complexes indicates a low degree of order exists within these complexes (12). The (002) band disappears on forming a petroleum asphaltene-iodine complex, and a new band at 8.7 Å appears. These observations were rationalized by assuming that the layered structure of the asphaltene was expanded from 3.5 Å to 8.7 Å by intercalation of a molecule of iodine between the aromatic layers of the asphaltene.

In the case of coal-derived asphaltene-iodine complexes, the x-ray results show the loss of both the (002) and the (γ) bands, but no new peak is formed at ≈ 8.7 Å (Fig. 3). This result may be interpreted by assuming that iodine molecules are not sandwiched between the aromatic layers, and that the asphaltene-iodine complexes are no longer ordered in the solid state but have become amorphous.

The x-ray diffraction patterns of asphaltene-TCNE complexes have been measured. The diffraction patterns show a large increase in the intensity of the 002-Band of the TCNE complex, which is associated with the interplanar spacing between condensed aromatic rings, and the appearance of a new band for Synthoil-TCNE, which corresponds to a larger distance of ≈ 11 to 14 Å. The x-ray diffraction patterns were analyzed, and aromaticity and x-ray crystallite parameters determined (Table III). The results indicate structural differences between the asphaltene base fractions (Et₂O eluted from silica gel) and their TCNE complexes. The aromaticity, f_a , increases from asphaltene base fractions to complexed products. The distance through the aromatic sheets, L_a , and the number of layers per cluster M are increased after complexing. However, the diameter of the aromatic sheet, L_a , shows a decrease or no change. The spacing between aliphatic chains or sheets, d_y , and the spacing between the aromatic sheets, d_m , do not show much change. These results, and the appearance of the new bands at 11-14 Å, may be rationalized in terms of asphaltene-TCNE complex clusters such as the ones shown in Fig. 4. If the TCNE molecules are complexed on top and below the asphaltene sheets, instead of intercalated between the asphaltene sheets, then an increase of L_c would be observed, but an increase in d_m or d_y would not be required. L_c , the average diameter of the aromatic sheet would be expected to be lower if a smaller TCNE molecule in the complex represented a pseudo-aromatic sheet. M , the effective number of aromatic sheets would be expected to be larger. The new bands corresponding to an 11-14 Å separation in Synthoil-TCNE could represent the distance between TCNE molecules in the complexes. The aromaticity, f_a , would be expected to increase in the complexes due to the pseudo-aromatic character of the TCNE π -system.

ESR Spectra

ESR parameters of Synthoil asphaltenes and their I₂ and TCNE complexes are presented in Table IV. The spin intensity is seen to be significantly larger in the complexes than in the uncomplexed asphaltenes. This may be indicative of low lying triplet states in the complexes which can be populated at room temperature.

Conductivity

The resistivities of a series of asphaltenes and their I₂ and TCNE complexes have been measured, and range between about 3×10^9 - 3×10^{10} ohm-cm at 25°C and 10 atm. pressure. In each case the resistivity of the complex is lower than that of the parent asphaltene, but not by more than an order of magnitude. These resistivities may be contrasted with those obtained for petroleum asphaltenes which exhibit higher values, in the insulator range, of 10^{16} - 10^{17} ohm-cm at 25°C, but upon addition of iodine, the resistivities of the complexes formed decrease by about one million-fold (12).

The effect of pressure, over the range 10-3000 ATM., on resistivity is shown in Fig. 5. The resistivity of the uncomplexed asphaltenes is seen to remain essentially constant, however, two of the asphaltene-I₂ complexes afford a decrease in resistivity over the same pressure range. This is consistent with electronic conduction.

ACKNOWLEDGMENT

This work was sponsored by the U.S. Department of Energy under contract no. E(49-18) 2031.

LITERATURE CITED

1. S. Weller, M.G. Pelpetz, S. Friedman, *Ind. Eng. Chem.* **43**, 1572 (1951); *ibid.*, p. 1575.
2. T.F. Yen, J.G. Erdman, and S.S. Pollack, *Anal. Chem.*, **33**, 1578 (1961).
3. T.F. Yen, Workshop on Coal Chemistry Preprint, Stanford Research Institute, 1976, pp. 144-164.
4. I. Schwager, W.C. Lee, and T.F. Yen, *Anal. Chem.*, **49**, in press, Nov. 1977.
5. H.N. Sternberg, R. Raymond and F.K. Schweighardt, *Science*, **188**, 49 (1975).
6. F.K. Scheighardt, R.A. Friedel, and H.L. Retcofsky, *Applied Spectroscopy*, **30**, 291 (1976).
7. S.R. Taylor, L.G. Galyla, B.J. Brown, and N.C. Li, *Spectroscopy Letters*, **9**, 733 (1976).
8. T.F. Yen, *Fuel*, **52** 93 (1973).
9. T.F. Yen and D.K. Young, *Carbon*, **11**, 33 (1973).
10. R.M. Elofson, K.F. Schulz, and B. Hitchon, *Geochimica et Cosmochimica Acta*, **41**, 567 (1977).
11. R.M. Elofson and K.F. Schulz, *Am. Chem. Soc., Div. Fuel Chem., Preprints*, **11**(2), 513 (1967).
12. G.A. Sill and T.F. Yen, *Fuel*, **48**, 61 (1969).
13. I. Schwager and T.F. Yen, *Am. Chem. Soc., Div. Fuel Chem., Preprints*, **21** (5), 199 (1976).
14. I. Schwager and T.F. Yen, Liquid Fuels from Coal, (R.T. Ellington, ed.), Academic Press, New York, 1977, pp. 233-248.
15. J.T. Kwan and T.F. Yen, *Am. Chem. Soc., Div. Fuel Chem., Preprints*, **21**(7), 67 (1976).
16. V. Hadek, *Rev. Sci. Instr.*, **42**, 393 (1971).
17. W. Haller, G. Jura, and G.C. Pimetel, *J. Chem. Phys.*, **22**, 720 (1954).
18. E.E. Ferguson, *Spectrochim. Acta*, **10**, 123 (1957).

Table I. Analytical Data for I₂-Asphaltene Complexes

Asphaltene	VPO ^a MW	% Iodine	Asphaltene ^b /I ₂
Synthoil	560	35.02	0.84
HRI H-Coal	492	28.13	1.33
FMC-COED ^c	375	22.00	2.38
PAMCO SRC ^d	363	38.36	1.12
CAT. INC. SRC	483	32.72	1.08
CAT. INC. Benzene Eluted 511		30.34	1.15
CAT. INC. Et ₂ O Eluted ^e	459	34.03	1.08

^aAverage of infinite dilution MW's in benzene and tetrahydrofuran of starting asphaltenes. ^bMole ratios calculated assuming MW of asphaltene portion of complex is the same as the MW of the starting asphaltene. ^cA tar formed on mixing the asphaltene/I₂ solutions. ^dFrom Filter Feed. ^eEluted from Silica Gel.

Table II. Analytical Data for TCNE-Asphaltene Complexes

Asphaltene ^a	VPO ^b MW	ZN Complex - ZN Starting Asphaltene	Asphaltene ^c /TCNE
Synthoil	522	5.08 ^d , 5.21	1.87, 1.82
HRI H-Coal	496	5.13	1.95
FMC-COED	383	5.48	2.34
PAMCO SRC	532	3.76	2.56
CAT. INC. SRC	459	7.61	1.33

^aAsphaltene eluted from Silica Gel with Et₂O after exhaustive elution of asphaltene with benzene. ^bAverage of infinite dilution MW's in benzene and tetrahydrofuran of starting asphaltenes. ^cMole ratios calculated assuming MW of asphaltene portion of complex is the same as the MW of the starting asphaltene. ^dTwo different preparations.

Table III. X-Ray Analysis of Synthoil Asphaltene Basic Fraction and Synthoil Asphaltene-TCNE Complex

	Synthoil Asphaltene Et ₂ O Eluted	Synthoil Asphaltene Et ₂ O Eluted-TCNE Complex
f _a ¹	0.64	0.72
d _a ²	3.47	3.46
d _y ²	4.52	4.52
l _c ²	12.1	13.8
L _a ³ (11) band	10.0	10.1
L _a ⁴ (11) band	11.4	11.9
M ⁵	4	5

¹f_a = C_A/C_{total} = A₀₀₂/A₀₀₂ + A_y, ²d_a = interlayer distance, d_y = interchain distance, l_c = diameter of the aromatic clusters perpendicular to the plane of the sheets, L_a³ = diameter of the aromatic sheets from Diamond's Curve, L_a⁴ = diameter of the aromatic sheets from Scherrer's Eq., all values in Å. ⁵Effective number of aromatic sheets associated in a stacked cluster.

Table IV. ESR Parameters of Asphaltenes and Asphaltene Complexes^a

Sample	g-Value ^b	Intensity, N (x10 ¹⁸) Spins/g	Line Width ΔH, Gauss
Synthoil Asphaltene	2.0030	1.4	6.4
Synthoil Asph. Et ₂ O Eluted	2.0031	0.8	6.8
Synthoil Asph.-I ₂ Complex	2.0032	28.8	9.8
Synthoil Asph. Et ₂ O Eluted-TCNE Complex	2.0029	5.5	8.2

^aSolid samples. ^bMeasured relative to DPPH.

A Review of Fuel Science and Engineering Courses at
MIT, the University of Sheffield and the University of Leeds, England.

Malcolm T. Jacques and J. M. Beer

The Energy Laboratory and Department of Chemical Engineering,
MIT, Cambridge, Ma. 02139

Introduction

Traditionally Fuel Science and Engineering has been regarded, from an educational viewpoint, as something of a hybrid subject which cannot be easily accommodated within the accepted framework of separate academic disciplines. In general faculties of science tend to treat the subject as an extension of Physical and Organic Chemistry with considerable emphasis on basic fuel properties and the chemistry of combustion. Engineering faculties on the other hand often provide courses in both Mechanical and Chemical Engineering Departments which concentrate on specific areas of fuel utilization and processing. Courses in Mechanical Engineering Departments deal mainly with only the physical and thermodynamic aspects of the combustion of fuels in F. C. engines and gas turbines. Chemical Engineering Departments in general do not provide specific courses on Fuels but do include a considerable amount of basic material relevant to the Fuel Processing area in several standard Chemical Engineering courses. Consequently it is the exception rather than the rule to find well-balanced schemes of study in the areas of Fuel Science and Engineering. Very few academic institutions provide a broad-based education in all aspects of fuels ranging from resources and recovery through to utilization and pollution control.

The current wave of interest and concern in all matters relating to the national energy situation provides sufficient justification for closely examining the educational programs of the scientists and engineers who will be needed to meet the demands in this area. It would be somewhat ironic if the new technologies and industries proposed to overcome the nations fuel supply problems were themselves subjected to a supply problem of adequately trained personnel. The question of whether or not our educational institutions currently provide appropriate programs for the number of personnel required in this area, still remains open. It is perhaps worth noting that several large American companies are currently recruiting graduate-level fuel scientists and engineers directly from U.K. Universities. Also it appears inevitable that as we turn to progressively more difficult fuels, the environmentally acceptable extraction, processing and utilization will lead to an increased requirement for professionals at all levels in the fuel and energy sector. A satisfactory answer to the questions raised here can of course only be obtained by conducting a detailed market survey of both the sources of supply of and demand for fuel scientists and engineers at both graduate and undergraduate levels. It is in this area that the professional societies could play an important role.

It is not the objective of this paper to provide answers to these questions of supply and demand, nor to address the more fundamental questions relating to the role of universities in regulating or controlling the supply in the interests of particular professions. Based on the premise that some changes may be desirable to improve either or both the quality and quantity of Fuel Science and Engineering courses, three examples of University Departments currently offering schemes of study in this area are presented which represent three alternative levels of commitment to education in this subject area. At MIT the Department of Chemical Engineering has traditionally maintained a strong graduate program in Fuel Engineering which represents only one specialist subject area in a comprehensive Chemical Engineering curriculum. The Department of Chemical Engineering and Fuel Technology at the University of Sheffield has maintained a very strong commitment to both

subjects at graduate and undergraduate levels. The Department of Fuel and Combustion Science at the University of Leeds offers both graduate and undergraduate degree schemes devoted exclusively to the subject of Fuels.

Fuel Engineering Courses at MIT

In common with many Engineering Schools in Departments of Mechanical and Nuclear Engineering at MIT offer specialized graduate courses which are related to certain areas of Fuel Engineering. Courses in Combustion, Thermal Power System, Energy Conversion and Nuclear Fuels fall into this category. The Department of Chemical Engineering is one of the few departments in the country to offer a coordinated scheme of study at the graduate level in Fuel Engineering. This scheme of study is completely optional and represents only one possible area of graduate specialization amongst a total of twelve Chemical Engineering topics. An integrated program in this area, leading to an M.Sc, requires a total of 66 credit hours at least 42 of which must normally be obtained from the following list of courses subjects:

<u>Subject</u>	<u>Credit hours</u>
Energy Technology	9
Chemical Engineering Thermodynamics	12
Mechanics of Fluids	9
Catalysis and Catalytic Processes	9
Absorption and Catalysis	9
Chemical Reaction Engineering	9
Principles of Combustion	9
Seminar in Air Pollution Control	9
Seminar in Fuel Conversion and Utilization	9
Radiative Transfer	9
Nuclear Chemical Engineering	12

In addition, a research thesis is required and the Department Fuels Research Laboratory together with the MIT Energy Laboratory provide excellent facilities for research on a wide range of fuel processing and combustion topics. Normally the general requirements for an M.Sc. degree can be met within one academic year.

The general philosophy in respect to education in Fuel Engineering is to treat the subject as a specialized area of Chemical Engineering. Courses are presented only at graduate level and require a firm background in the general principles of Chemical Engineering. However, the courses are available to undergraduate students in their senior year as restricted electives. This approach to graduate education in Fuel Engineering inevitably leads to a considerable degree of specialization. The very nature of graduate-course work usually precludes much of the less intellectually demanding qualitative material associated with some of the more pragmatic aspects of Fuel Engineering. At MIT the areas of specialization reflect the department's strong interest in Chemical Engineering aspects of Fuel Processing, Combustion and Air Pollution. Several other engineering schools offer graduate courses which cover other important aspects of Fuel Engineering such as Resource Recovery, Thermal Power Engineering and Energy Management. In general, it is felt that even though very few graduates obtain degrees specifically in Fuel Science and Engineering, there is a sufficient pool of specialist graduates to meet the demands of the upper level managerial, research and development areas of the fuel and energy sector.

The Department of Chemical Engineering and Fuel Technology, University of Sheffield, England.

Before discussing the structure of the graduate and undergraduate courses offered by the Department of Chemical Engineering and Fuel Technology at the University of Sheffield, it is worthwhile to point out the general differences, particularly in respect of entrance requirements, between U.K. and American Universities. In general U.K. students are a year older than their American counterparts on entering a university. They will have spent two years studying three or four subjects appropriate to the area of university study they wish to pursue. For instance, most students wishing to enter Chemical Engineering Schools will have studied Maths, Physics and Chemistry. Each university and university department is then free to set whatever entrance requirements it feels necessary for specific degree courses. Eligibility for entrance is then judged on the basis of individual students performance in national examinations conducted by independent examining bodies. Entrance requirements are consequently somewhat more stringent in the U.K., and the students are equipped to commence their undergraduate degree courses at a higher academic level than freshmen in American Universities. As a result most undergraduate courses are only three years in duration, leading to the Bachelors degree. By the time of entrance, students have already chosen their subject areas, and specialists courses in the appropriate subjects are given during the first year.

The scheme of study at undergraduate level, offered by the Department of Chemical Engineering and Fuel Technology at the University of Sheffield, consists of courses during the first two years with optional subjects in the final undergraduate year. Students are required to obtain satisfactory results in all prescribed subjects at the end of the second year before being allowed to proceed to the final year. Progress is monitored essentially by formal written examination at the end of each year. The results of these examinations determine whether or not the student is considered for an Ordinary or Honours degree.

First year subjects are mostly extension of Maths, Physics and Chemistry, general engineering courses and introductory courses to Fuel Technology and Chemical Engineering which represent about 20% of the total course load. These courses are designed to equip the student for the more advanced courses in the second and final year's scheme of study. Laboratory classes in the first year introduce students to many of the practical aspects of Fuel Technology including properties and testing of solid, liquid and gaseous fuels. During the second year the prescribed scheme of study consists of courses in,

Fuel Technology	Mechanical Engineering	Maths
Chemical Engineering	Electro-Technology	Chemistry

The Fuel Technology and Chemical Engineering courses occupy approximately 50% of the course work. At this stage, Chemical Engineering courses deal essentially with the fundamentals of Heat, Mass and Momentum Transfer at quite an advanced level. The Fuel Technology courses deal with some of the general aspects of Fuels including handling and processing, and introduction to some of the more practical problems associated with the combustion of different types of fuels. After successfully completing the first two years of prescribed undergraduate courses, students then have the option of choosing between final year schemes of study in either Chemical Engineering and Fuel Technology or Environmental Chemical Engineering. The prescribed courses of study for these two options are given below;

Either (i) Chemical Engineering and Fuel Technology

Chemical Engineering Operations	Fuel Processing
Control and Instrumentation	Direct Electricity Generation
Nuclear Reactor Engineering	Combustion Theory
Business Economics	Refractions Technology

or (ii) Environmental Chemical Engineering

Chemical Engineering Operations	Project Evaluation with respect to
Control and Instrumentation	Pollution Control
Environmental Chemical Engineering	Medical and Legal aspects of Pollution

together with any three of the following advanced topics:

- Fluid Dynamics
- Advanced Combustion Theory with Gas Dynamics
- Heat Exchanges
- High Temperature Chemical Engineering
- Process and Project Engineering
- Advanced Topics

In addition during the final year students are required to undertake either an experimental investigation or a design study of some problem of Chemical Engineering or Fuel Technology.

These course details clearly show that the subject of Fuel Technology can be included as a major element in a Chemical Engineering curriculum at undergraduate level. However, it should be realized that much of the course material on fuels is contained in the final year of study, and as such, the overall effect is to provide basic core of Chemical Engineering courses around which the subjects of Fuel Technology, and in particular, Combustion are handled primarily from a Chemical Engineering and Processing point of view.

In common with most other U.K. University Departments, the Department of Chemical Engineering and Fuel Technology offers both Master's and Doctorate research programs requiring no formal course work. However an advanced course on Combustion Science and Pollution Control is also offered, which leads to the award of a Diploma or Master's Degree by examination. The course consists of two full terms of lectures, seminars and experimental work on topics which include:

- Physical Chemistry of Combustion
- Connective Heat Transfer
- Radiative Heat Transfer
- Theory and Technology of Combustion Process
- Minor Constituents of Flames and Combustion Gases
- Combustion Noise and Oscillations
- Flame and Plasma Reactors
- Open Flames, Flares and Incinerators, Plume Dispersion
- Furnace Refractories
- Measurement and Control in Flames (Experimental Techniques)
- Mathematical Models of Combustion Systems.

In addition, students prepare a dissertation in either a design study or a research project, which is completed after the course work and can serve as an introduction to a Ph.D. course.

This Master's course is open to graduates in engineering, physics, chemistry and mathematics.

The Department of Fuel and Combustion Science at the University of Leeds.

Instruction and research in fuel science have been provided by the University of Leeds since 1906, and courses are currently offered at the undergraduate level in Fuel and Energy Engineering and in Fuel and Combustion Science. The courses are offered by the Department of Fuel and Combustion Science which is the only University Department in the U.K. to offer undergraduate schemes of study devoted exclusively to the subject of fuels. The department providing these schemes of study is the founding member of the Houldsworth School of Applied Science. The school itself consists of five departments which, although independent in themselves, have so much in common that they have elected to work together as a group. These departments are Fuel and Combustion Science, Chemical Engineering, Metallurgy, Ceramics and Mining, and Mineral Sciences. The school organization allows the various departments to share lecture rooms, the library, common rooms, workshops and many items of costly equipment which could not easily be provided separately. In addition, the departments provide carefully tailored service courses in specific subject areas for students from other departments within the school.

The Department currently offers four undergraduate degree programs,

- B. Sc. Fuel and Combustion Science
- B. Sc. Fuel and Energy Engineering
- B. Sc. Chemistry/Fuel and Combustion Science
- B. Sc. Fuel and Energy/Management Studies

The first two of these schemes involve only the Fuel and Combustion Science Department. Both are essentially three year courses and have a basic theme in common but are varied to cater to the individual ability and intentions of the student. The Fuel and Combustion Science course contains rather more basic science than the Fuel and Energy Engineering course, which as its name implies, is biased more towards engineering and technological aspects. Broadly, but not exclusively, the former is intended to equip graduates for entry into the research and development sectors of the industries supplying and using fuels and the latter is intended for future designers and builders of plant and equipment for the large-scale processing or use of fuels.

The last two undergraduate degree schemes are combined courses offered jointly with the Departments of Chemistry and Management Studies. The Chemistry/Fuel and Combustion Science scheme of study allows the chemistry-minded student to carry this subject further while at the same time receiving sound training in the science of fuel and combustion. The combined course in Fuel and Energy/Management studies is aimed at providing both a firm technological and engineering appreciation of fuels and energy for students wishing to follow conventional courses in Management Studies. This combination of courses is hoped to provide the correct blend of technological and managerial knowledge required for the new generation of fuel and energy managers.

The Honour's degree schemes of study for both Fuel and Combustion Science and Fuel and Energy Engineering are given below.

First Year- courses are essentially common for both degree schemes.

Fuel and Energy Sources	Maths
Fuel and Energy Utilization	Physics
Materials Science	Physical Chemistry
Computational Techniques	

Second Year- again the majority of fuel courses are common, the only differences being in the subsidiary subjects.

Fuel and Combustion Science

Fuel and Energy Engineering

Combustion Technology *
Fuel Processing and Flow of Materials *
Power Generation I *
Instrumentation and Control *
Fuel and Energy Economics *
Applied Physical Chemistry *
Heat Transfer I *
Chemical Engineering (Unit Operations) *

Physics
Chemistry (Organic)

Mathematics
Engineering (Mechanical
and Electrical).

(* Common Courses)

Third Year- all courses are given by the Department.

Fuel and Combustion Science

Fuel and Energy Engineering

Combustion Aerodynamics and Heat Transfer *
The Efficient Use of Energy *
Management and Organization of the Energy Industries *

Combustion and Explosion
Petroleum and National Gas Science
Coal and Carbon Science

Petroleum and National Gas Engineering
Fuel and Combustion Plant Design
Power Generation II

(* Common Courses) In addition to the above courses, students are required to conduct an experimental research project on some aspect of fuel and combustion science or energy engineering.

Courses for the combined degree schemes in Chemistry/Fuel and Combustion Science and Fuel and Energy/Management Studies consist of combinations of some of the above courses with selections of standard courses in the Departments of Chemistry and Management Studies, respectively.

Schemes of study are also offered at graduate level leading to

- M. Sc. Combustion and Energy
- M. Sc. Environmental Pollution Control.

The latter course is run in conjunction with several other university departments, though combustion and fuels-related pollution aspects are covered by the department. The former course is offered by the Center for Combustion and Energy Studies which draws upon the expertise of the Departments of Fuel and Combustion Science, Mechanical Engineering and Physical Chemistry. Both of these graduate programs take one complete academic year and include both course work and a research exercise.

Discussion

The major differences in approach to education in Fuel Science and Engineering in the three Departments discussed here are ones of scope and breadth of coverage. Treatment at graduate level without any prior introduction to the subject of Fuels leads inevitably to a considerable degree of specialization, usually in some area amenable to a qualitative and analytical approach, such as combustion. The inclusion of Fuel Science and Engineering courses at undergraduate level can readily be integrated into 9 Chemical Engineering curriculum without seriously affecting the basic elements essential for education in Chemical Engineering. This approach can eliminate the need for specialization in one particular area and can lead to a well-rounded appreciation of the engineering significance of fuels. Undergraduate schemes of study devoted exclusively to the study of fuels provide an extremely broad training in all aspects of Fuel Science and Engineering. The major advantage of this approach is that it provides sufficient coverage of many important qualitative, practical and technological aspects in all areas

of Fuel Science and Engineering. Hence not only are the more academically inclined students able to pursue careers in research and development, but the more practically-minded students are well prepared to enter the operational side of many industries making or using fuels. It is often at this level where many important decisions affecting fuel and energy usage are made particularly in the small to medium size industries.

It is always easier and usually safer to alter the superstructure rather than the foundation of any particular institution. Consequently it is felt that any changes deemed necessary in the education of Fuel Science and Engineering in the U.S.A. will take place predominately in graduate schools by alteration of existing courses or implementation of new courses. However, it is felt that many of the important subjects, particularly fuel and energy utilization, can best be included at undergraduate level.

Fuel Science and Engineering courses can easily be integrated into a Chemical Engineering curriculum and the provision of such courses could certainly help to provide the technological background so often missing in graduate level courses.

FUEL CHEMISTRY
Undergraduate and Graduate Fuel Science and Engineering
Education at West Virginia University

Duane R. Skidmore

College of Mineral and Energy Resources
West Virginia University
213 White Hall
Morgantown, WV 26506

Introduction

Fuels science and engineering at West Virginia University refers to those educational activities in engineering and science programs whose subjects deal with the extraction and utilization of fossil fuels. In this broader sense, fuels science and engineering are involved with all aspects of fossil fuels. In particular, they deal with combustion, conversion, coking and the utilization of coal, oil shale and tar sands. In a narrower sense, the subject covers chemical and physical changes involved in fuel utilization. The purpose of an educational endeavor in this subject area is to develop the potential in able and interested people for solving complex problems of fuel utilization. The need for such educational programs is expected to intensify in the near term.

West Virginia University is a land-grant university and the comprehensive state university for West Virginia. Tuition is one of the lowest in the nation and admissions are open. Self-selection by students provides an academically oriented student body as described by college-bound test scores and high school grades. As the comprehensive state university, WVU offers programs in professional schools and graduate departments. Agriculture, dental, engineering, law, forestry, medicine, minerals, nursing, and pharmacy schools are supported by graduate programs in basic sciences.

The university is in Morgantown, Monongalia County; a county which customarily ranks first or second among the counties in the state in coal production. West Virginia has ranked first or second in coal production among the states for many years. Other energy resources are also recovered commercially.

Need

The need for fuels-oriented programs is variously viewed. In the scientific and engineering disciplines, the state, regional, and national dependence on imported fuels are considered important reasons for study; faculty have acquired appropriate interests and skills over the years, and student demand has remarkably strengthened over a five year period. Personnel in the science and engineering programs are additionally motivated by their interest in new and improved understanding of nature; a desire to publish, and the increased availability of university, state, and federal support.

Jobs are available in industry, government, and academia. Pressure from recruiters has been strong and effective. Students and faculty alike have received offers of high salary and optimum working conditions. An important co-effect has been the disruption of traditional ivory tower inclinations and reduction of leisure to ruminate among ideas and over problems.

History of Co - Going Effort

Different programs throughout the university have a different historical pattern of response to the perceived educational needs in fuels. Programs vary greatly in their longevity, levels of sophistication, and orientation toward a specific fuel. Some stress science and some are engineering oriented.

As an example of a science department, geology is of special interest. The faculty offer three courses in which coal is of primary concern. Two of these courses - Coal Geology and Coal Petrography - were approved formally within the last two years. Considerable jurisdictional discussion had ensued between faculty in geology and those in the College of Mineral and Energy Resources. A single geology course is offered in Petroleum Geology. Geological research on fuels is centered on characterization and on resource or reservoir definition. A new and major research effort on gas from Devonian Shale is currently underway. The fuels work in geology is often done in cooperation with the West Virginia State Geological and Economic Survey.

In engineering programs, course offerings centered on fuels are extensive. Mining, petroleum, chemical, mechanical, and mineral processing engineering as subject areas are largely committed to design, operation, construction and research dealing with fuels extraction and utilization processes.

Chemical engineering offers two courses on coal conversion at the undergraduate level. Mineral processing engineering offers another sequential undergraduate course on conversion and a graduate course in synthetic liquid fuels. Electrical, mechanical, mining and petroleum engineering have substantial research interest and funding in problems of fuels appropriate to their general charge.

Fuels Research

Before 1970, little activity was apparent in fuel research. From the early 1960's, the state had supported efforts from a semi-autonomous Coal Research Bureau to find, develop, and increase markets for West Virginia coal. The fund supported academic research and technological development to a certain extent. Since 1976, however, a considerable and increasing portion of an ever-larger budget has been allocated under a new charter to academic researchers working in an independent mode. The administration of the research grant procedure has been placed under the direction of a Provost and a committee of university faculty and administrators.

The effect has yet to be evaluated. However, many excellent academicians chose to apply their expertise to the solution on fuels oriented problems. Broad, university-wide, representation among the researchers has become apparent. As part of this effort, the chemistry department and the physics department expanded their research efforts on fuels. Chemistry has aimed toward fuels combustion mechanisms and has additional support from industry and government. Supported by state funds, physics is investigating magnetic effects in pyrite as a function of temperature.

Additional Response to Need

Two goals were visualized for the WVU fuels science and engineering programs in the light of society's need for energy and chemical feedstocks and the students need for preparation in a challenging and rewarding career.

Society's need is likely to be met by utilization of a plentiful fuel resource or by the conversion of a plentiful reserve to a resource. The areas of need to be served are for process plant and utility fuel, metallurgical coke, substitute natural gas and synthetic petroleum. The area of challenge is extended through the science and technology of utilization but with particular attention to the chemical reactions involved.

The fuels science and engineering programs at WVU are career oriented. Orientation for a career is to be viewed within the broad framework of degree candidates who will solve technological problems which are real and present. The expectation is high that the careful selection of students, especially at the graduate levels, and the stress in the programs upon principles and their rigid application will produce future problem solvers.

The educational philosophy at the university has been one of permissiveness, flexibility, and encouragement rather than coercion in the motivation and direction of students.

Organization

Organizational responses have been quite varied. Some programs cross organizational lines while others are within academic units.

Fuels science programs and courses at WVU are concentrated in the College of Mineral and Energy Resources; the College of Engineering, and the College of Arts and Sciences. The College of Mineral and Energy Resources was authorized in January 1975 to offer programs leading to the Bachelor of Science, and Master of Science Degrees in mineral processing engineering, complementing long existing degree programs in mining engineering and petroleum engineering. In 1976, access to the interdisciplinary Ph.D degree with the College of Engineering was authorized. Two options are stressed: one is in coal preparation and the other is in coal conversion. Considerable support in these efforts were required and obtained from the Department of Chemical Engineering.

EDUCATION IN FUELS ENGINEERING
AT THE UNIVERSITY OF UTAH

David M. Bodily

Department of Mining, Metallurgical and Fuels Engineering
University of Utah
Salt Lake City, Ut 84112

The Fuels Engineering Program at the University of Utah was established in 1946. The need was recognized for students with specialized training in fossil fuel technology. The B.S., M.S., and Ph.D. degrees were offered through the Department of Fuel Technology which became part of the State College of Mines and Mineral Industries. The Department rapidly distinguished itself for research and graduate study, although student enrollments were not large. Since its inception, 13 B.S. degrees, 12 M.S. degrees, and 44 Ph.D. degrees have been granted. During recent years, the program has grown in size and the undergraduate program has been revitalized and strengthened. Recent enrollment trends are shown in table 1. The name of the degree has been changed from Fuel Technology to Fuels Engineering and the program is now part of the Department of Mining, Metallurgical and Fuels Engineering.

Undergraduate Program

With the influx of students into the undergraduate program, the curriculum has been revised and new courses have been instituted. Fuels students take a common core program with Chemical and Metallurgical Engineers during the Freshman and Sophomore years and about one-half of the Junior years. This consists of the Liberal Education requirements of the University; general, organic and physical chemistry; mathematics through calculus and differential equations; engineering physics; and engineering courses such as process engineering, thermodynamics, strength of materials, mass transfer, fluid mechanics and heat transfer. During the Junior and Senior years the student takes required advanced undergraduate fuels courses from the list shown in table 2. Eleven of the 17 courses are required. The student also must fill technical elective requirements from fuels or related courses.

The energy problems of the United States have brought attention to energy studies and attracted many students to fuels engineering. Several scholarships are available to outstanding students. This has attracted students of high ability to the program.

"Energy and Man" is a course designed for non-science or engineering students as part of the Liberal Education program. Enrollments were low when it was first introduced in 1970, but in recent years it has been offered each quarter to large enrollments. The purpose of this course is to provide non-technical students with a background concerning energy problems so that they may function more effectively as citizens and as energy consumers.

Graduate Program

Graduate students enter the program with degrees primarily in chemical engineering or chemistry. Chemistry majors must take several basic engineering courses in addition to the graduate degree requirements. About one-third of the course work for an advanced degree must come from outside fuels engineering. The graduate committee of each graduate student must also have representation from outside fuels engineering. Graduate courses are shown in table 2.

Major areas of research for graduate degrees at the present time include liquefaction and gasification of coal, analysis of coal-derived liquids, upgrading of synthetic liquid fuels, tar sand processing, coal structure and reactions, and catalysis.

SUMMARY

The Fuels Engineering program attempts to train professionals with a basic background in engineering and the physical sciences and specialized training in the chemistry and processing of fossil fuels. It is experiencing rapid growth at both the undergraduate and graduate level. The teaching and research faculty has grown to nine persons. Future growth is difficult to predict due to many uncertain factors. The demand for professionals with this type of training is expected to be strong.

TABLE 1. - Fuels Engineering Enrollment

	73/74	74/75	75/76	76/77
Freshman	1	4	12	18
Sophomore	1	6	8	12
Junior	2	2	8	6
Senior	1	2	4	7
Total undergraduate	5	14	32	43
M.S. candidates	7	7	10	15
Ph.D. candidates	14	13	16	17
Total graduate	21	20	26	32

TABLE 2. - Fuels Engineering Courses

Lower Division

Introduction to Process Engineering
Energy and Man
Fundamentals of Process Engineering
Physical Chemistry of Mineral Systems

Advance Undergraduate and Beginning Graduate

Senior Project
Field Trip
Introduction to Heterogeneous Catalysis
Recovery of Fossil Fuels
Chemicals from Petroleum
Catalyst Preparation, Characterization, and Testing
Catalysis Laboratory
Chemistry of Fossil Fuels
Mineral Fuel Testing
Mineral Instrumentation
Conversion of Coal to Other Energy Forms
Energy Resources and Their Utilization
Modern Petroleum Refining
Flames, Combustion and Combustion Reactions
Fuels and Lubricants
Laboratory Safety
Corrosion of Metals, Theory and Practice

Advance Graduate

Theoretical and Applied Aspects of Catalysis
Kinetics and Interpretation of Catalytic Reactions
Chemicals from Petroleum
Fundamental of Coal Liquefaction and Gasification
Properties and Reactions of Coal and Coke
Oil Shale and Bituminous Sands

Education in Fuels and Combustion: Needs for the Future and the
Pennsylvania State University Program

Robert H. Essenhigh

Combustion Laboratory
The Pennsylvania State University
University Park, Pa. 16802

INTRODUCTION

Fuels Science and Engineering is a wide ranging topic that has been described as the interdisciplinary subject par excellence. The total scope is often divided into three prime topics: Production of fuels; Fuel preparation and Benefication; and Utilization. Production covers mining of coal, and petroleum and natural gas reservoir engineering. Preparation covers cleaning, crushing, grinding, and related aspects of coal benefication, with refinery engineering and related operations for oil and gas. Utilization is the facet that fuels education most commonly focuses on, and is primarily concerned with combustion and related uses of all fuels in all applications. The proper content of fuels education is discussed in more detail below: the broad scope of the study of fuels from the scientific to the engineering aspects is often titled Fuel Technology*.

PERSPECTIVE

To the outsider viewing Fuel Technology in the context of today's energy famine it must surely appear to be the subject of greatest technical importance in the curriculum of any university or similar training institute. Such a view is not supported by the facts, however. Fuels education is in a curiously anomalous position. Although fuel technology has been a rewarding subject for study and application for many decades -- one might even say, centuries -- it has still never had the academic prominence or even recognition of other technologies such as chemical engineering, metallurgy, ceramics, and so forth. There are believed to be less than half a dozen universities or institutes in the world with formal academic programs leading to degrees in Fuel Technology. Fuel Science, or Fuels Engineering, and the numbers, in fact, have been declining. There is likewise no central recognized platform or journal for the total range of the topics of concern in Fuel Technology. Interest is scattered over many semi-specialized Society divisions and journals. In a word, Fuel Technology does not, at present, have the recognition of being a formal academic discipline with a formal body of knowledge (even though this exists) that practitioners should know if they are to claim the authority of speaking as fuel technologists. Only in specialized cases such as power and propulsion systems (a minority branch of fuel technology) does something like a formal training exist. Industrial principles and applications, which represent over 40% of national energy use, are mostly unknown and untouched. Industry has therefore had the habit in the past, partly by default, of appointing fuel engineers, managers, supervisors, or controllers, from those in the ranks of other engineering professions such as chemical, metallurgical, ceramic, and mechanical engineering.

The problem has been that since fuels was everyone's business, it was no-one's business. In each individual segment of industry the topic of fuel use was essentially an appendage, with individual solutions to very similar problems being developed in the different process sectors -- ferrous and non-ferrous operations, glass, ceramics, refinery stills, cement manufacture, and so forth.

*"Technology" is used here in the same sense as in M.I. of Technology, or C.I. of Technology, etc.

In university curricula, where process metallurgy and ceramics, and the like, are still thought to be important, fuels are discussed mostly in the context of the single industry. In the other engineering areas, emphasis tends to be solely on power systems and, as observed by Smith and Stinson (1) 25 years ago: "It has been (our) observation that the general treatment of fuels and combustion is many times slighted in engineering curricula, even though the combustion process is a vital link in power cycles. Frequently the topics of fuels and combustion are presented, in part, through courses in steam power, internal-combustion engines, heating and ventilating, and laboratory, with little coordination or continuity of the material presented in the various courses. The result many times is an incomplete coverage of either fuel technology or combustion, and usually a meager concept is obtained of the actual chemical processes of burning." This observation would still seem to be substantially true. Only in the propulsion specialties (gas turbines and rockets) would there seem to have been any significant change.

This fragmentation of fuel technology, however, does not seem to have been too significant in the past; it would be hard to say that industrial development has really been hindered by this. So does it matter for the future? The answer would seem to be a decided: Yes! The pattern of the distant industrial past was a generally accelerating use of fuel, initially of wood and charcoal and subsequently of coal, during which there was ample time (decades) for the most part to develop necessary techniques by essentially untrained inventors and developers (who often became highly skillful by on-the-job training). The pattern of the more recent past (the last 50 years) was then a process of further industrial development based, first, on oil, then on gas. The trend was to more easily used and proportionately cheaper fuels. A return to coal or coal-based fuels means reversing that trend. The fuels will be more expensive and more difficult to use. It is not simply a matter of reverting to past technologies. The use of oil, and particularly gas allowed (largely ad-hoc) improvements in precision of firing furnaces: temperature control, metering, burner cycling, and so forth; and operators will continue to expect, or demand as essential, similar precision and ease of firing. The scale of the problem, in terms of fuel tonnages consumed has also increased: total energy consumption has almost quadrupled in the last half century. There are also environmental constraints that makes return to coal so much more difficult.

As a result of this pattern, there is indeed evidence now of an increasing demand for fuels specialists with a much higher level of education. The past practice of on-the-job training (which led to many re-inventions of the wheel) can be expected to disappear. It takes too long; it can leave too many gaps in knowledge; it is likely to be too specialized which makes for inflexibility; and there is usually time only to attain a relatively elementary level of understanding that can be far short of what is required today.

The demand must increasingly be met by training at the university level, but this presents several problems. There are too few schools at present with even a pretence at a reasonable coverage of the field of knowledge that can be called Fuel Technology, and these schools are almost unknown to large sections of industry, to other universities, and to virtually all prospective students. There is even ignorance in some academic quarters of what academic or formal training coverage can be provided in the field of fuel technology so that plans to expand course coverage can be held up or will be incomplete on account of that lack of knowledge, and lack of necessary teaching manpower. (This, further, ignores the present constraints on university funding that makes curriculum enlargement difficult to impossible in many cases.)

It is understood that this Meeting (on Fuels Science and Engineering Education) at which this paper is presented is designed to develop solutions to these problems. In this paper, contributions to three aspects are presented.

WHAT IS FUEL TECHNOLOGY?

The broad scope of fuel technology (or science and engineering) is outlined in the Introduction. It can be summarized as: the study of fuel in science and practice. For the development of curricula, something with greater precision and more detail is required for setting the boundaries to the field and for identifying individual subject or topics.

Fuel technology is broadly concerned with the utilization of fossil fuels and of their manufactured and related derivatives, including the process of manufacture of the secondary fuels (by gasification and liquefaction). It should also include some degree of study of the sources and reserves of coal, oil, gas, and other potential fuels (including shales, tar sands, solid waste, etc.). Also significant are the physical and chemical properties, methods of analysis, chemical structure, and methods of preparation (cleaning, drying, grinding, distillation, screening, etc.).

Utilization is still the core of fuel technology. This means: production of power; use for processing; and secondary fuel manufacture for ultimate use as gas, liquid, or solid, in power and processing. Utilization depends on knowledge of fuels reactivity -- Reaction Kinetics applied to solid, liquid, or gaseous fuels. It also requires applied knowledge of fluid mechanics (combustion aerodynamics) and heat transfer (mainly radiative). Specific technological subjects of importance that represent application of fundamentals include, in particular: flame chemistry; flame propagation theory; carbon and coal reactions; reactor and flame holding theory; furnace analysis; radiative properties of flames; and scale-up methods for pilot plants.

These topics are set in schematic perspective in Figs. 1 and 2. Figure 1 illustrates the overall process of utilizing fuel to deliver a useful end product. Input includes knowledge of fuel and raw material sources, preparation, and supply to the reactor. Output lists power, process use, manufactured fuels, and effluents. Reactor operation, or requirements for understanding their operation, is illustrated in Fig. 2, which shows the relationship between the basic sciences and their engineering application.

Supplementary to the above, training in fuel technology must also include such sufficient understanding of the power and process operations themselves that the mechanical and other aspects of the furnaces and engines makes sense. This brings in such additional topics as: heat engine thermodynamics; furnace thermodynamics; refractory behavior and selection; heat treatment principles (with emphasis on the iron/carbon diagram); and effluent control (such as, air pollution from combustion sources).

Fuels Education at Penn State

In spite of the wide ranging scope of Fuel Technology, at the Pennsylvania State University all aspects are covered in one Department or another. Relevant Departments or Sections include Chemical Engineering, Mineral Processing, Petroleum and Natural Gas, Mining, Mineral Economics, and the Fuels Science Section of Materials Science and Engineering with some combustion and power aspects in Mechanical Engineering. In addition, the Coal Research Section is a research and administrative unit that ties together a number of closely related research activities on coal and carbons.

Most of the teaching and research activities, however, are centered in the Fuel Science Section of the Materials Science and Engineering Department. The original program started nearly 50 years ago in the Department of Fuel Technology, essentially as an outgrowth of graduate courses in coal carbonization and fuel utilization in the Department of Metallurgy. Over the period 1921-1931 these original courses developed into an Option in Fuel Technology, in that Department, with undergraduate instruction in fuel testing and calorimetry, coking, classification of coals, liquid and gaseous fuels, carbonization and processing of coals, and combustion and utilization of solid, liquid, and gaseous fuels. The strength of this option was such that, in 1932, a separate Department of Fuel Technology was created, granting simultaneously both undergraduate and graduate degrees (B.S., M.S. and Ph.D.). In the years since then, a total of 180 students have graduated with the bachelors degree, 83 with the masters degree, and 115 with the Ph.D.

About 10 years ago the undergraduate curriculum was closed because of very low enrollment. It was then obvious to everyone, except for the faculty in the Fuel Technology Department, that there was no further future in coal, and little further need for fuel technologists dealing with utilization of oil and gas. Reflecting that view, the State Legislature dropped support of a special coal research funding program. In industry, fuel was so easy to burn and so cheap that no special knowledge was required for its (inefficient) use. It is symptomatic of those times that, as remarked above, fuel engineers in industry were almost universally drawn from the ranks of the other engineering professions, without training in fuels, and with little awareness of the body of knowledge that did exist in fuel technology; and this, to some extent, is still the case today.

In 1969, the first (predicted) shortages in interstate pipeline gas supply showed up. In 1970-1971, the (predicted) peaking of native oil supplies from the lower 48 states also occurred. The timing on contraction of support for fuels education was clearly superb. Since then, the well-known controversy has been raging whether the fuel shortages are real or the result of some conspiracy. With the understanding that this is a real problem, the question of what is needed in fuels education is reopened with dramatic force. The central significance of the problem derives from the central significance of energy in driving the industrial machine and modern civilization, and the awareness that without fuel you are out of business.

In spite of the dropping of the undergraduate program, in time for the start of the fuel shortages, (more accurately, the program dropped us), senior level and graduate programs nevertheless continued. In the early years, all the work the Department, both undergraduate and graduate, was focussed almost entirely upon coal and coal-related topics -- what might be called, without prejudice, coal technics. Following World War II, however, the scope of all programs was enlarged to cover the classical range of fuel technology topics: focussing on utilization, but with coverage increased to include gaseous and liquid fuels, and on materials derived from fuels, notably carbons and graphites. Coal preparation and beneficiation that were part of the original Fuel Technology Department program were moved about that time into a new Department of Mineral Preparation.

About the time of the demise of the undergraduate curriculum, the original Department of Fuel Technology ceased to be a Department, and was absorbed (with a small name change) as the Fuel Science Section in the (new) Department of Materials Science and Engineering.

The current scope of the teaching activities in the Fuel Science Section is illustrated by Table 1 which lists, with brief descriptions, the present course offerings of the Section. (The 400 numbers are senior-graduate courses, and the 500 numbers are graduate courses). There are presently 7 faculty in, or associated with the Fuel Science Section (several of whom also have additional teaching requirements in materials and related subjects). There is also a related course in coal petrography (Geol. 421). There are also other closely related courses on combustion, gas turbines, and more conventional mechanical engineering courses on power plants, thermodynamics, and so forth, in other departments. Including aspects of petroleum production and refining, mineral economic aspects and related topics, there is a total of some 15 to 20 courses available at the senior and graduate levels that can be properly defined as part of Fuel Technology.

The research interests are of even wider scope. These include studies of gas/carbon reactions, gasification of carbon and coal, liquefaction of coal, fuel cells, and solar energy converters. The research has been described in about 450 research papers in the past 20 years.

Fuels Education in the Future

If Fuel Technology is sufficiently important for the future, the pattern of the past would suggest that new programs can be expected to come into being, with courses covering part or all of the material outlined in the Section defining Fuel Technology. A decade ago this would already have happened and new Departments would have come into existence. That this has not yet happened is almost certainly due to a number of factors. The most obvious has been lack of funds. There has also been uncertainty as to the real nature and scope of the fuels problem, and uncertainty over the real Federal commitment towards fuels. The topic has lacked activists in the manner of the Environmental Spokesmen of a decade ago -- after all, fuels have been with us a long time: isn't it really a simple problem, and don't we already know all we need to know? Energy activists have tended to promote nuclear electric (which must always be a minor energy source) or new developments in solar, geothermal, and the like. Also, there has not been a recognized combustion engineering community or Institute to speak for the fuels area as a whole.

A more subtle problem derives from the current small size of the fuels community. A program that will attract students, and supporters, must be visible, credible, and viable. Without the existence of a widely-recognized academic discipline a single Department of Fuels lacks visibility, which makes recruiting difficult. The program can also lack credibility: "If it's as important as that, why aren't there more Departments?" is a good question. Without more Departments, the subject is barely viable. It was on these grounds that M.W. Thring on becoming Professor of Fuel Technology at Sheffield University (England) in 1950 immediately entered (successful) negotiations to have the Department recognized as a joint Department of Chemical Engineering.

Counters to these three problems are now forthcoming. The problem of visibility (and significance) was partly solved by the belated recognition by the Network News Anchor men that an energy problem of some sort really did exist. Credibility will appear when a number of fuels departments, options, centers, programs, or sections come into being: this will also confer the necessary viability to the academic programs.

The necessary centers would already appear to be in embryonic existence. This has been established in the following way. We have carried out a search of

the listings on fuels and fuel-related courses in the Course Catalogs of Universities in North America. We have identified a total of about 500 such courses offered in about 120 Universities. Although this averages 4 courses per University about half only offer 3 courses or less. About 1/3 of the courses are offered by only 14 institutions, each offering 9 or more such courses. These Universities are identified in Table 2 together with the total number of courses they offer. Table 2 also shows two other columns. In the Course identification, all conventional (though necessary) courses in transport phenomena, heat transfer, reaction or chemical kinetics, power systems thermodynamics of heat engines, and the like, were omitted. Topics on industrial combustion engineering, flames, propulsion, combustion aerodynamics, pollution from combustion, and so forth, were included. In a first breakdown of the total, the established engine, gas turbine, propulsion, and related power and aerospace topics were designated as a Group II. Subtracting from the total leaves Group I (listed in Table 2), which are mostly the more industrially oriented combustion, pollution, and fundamental flames courses. Inspection of these then shows that fuels and combustion was evidently the major topic in some courses, but was of minor or secondary interest in the rest. Group IA in Table 2 is the number of courses identified as having fuels and combustion as the major topic (within what could be identified by the course descriptions).

Before discussing the breakdown, some caveats and disclaimers are in order. Course offerings of most universities were examined, but not all (we were unable to obtain the Harvard University Catalog, for example). The discrepancy between course description and course content is well known and requires no comment. Selection of the courses (or their omission) involved a value judgment that was difficult to exercise in quite a number of cases, particularly where course descriptions were vague, wide ranging and cut across several topics; members of individual universities may well make a somewhat different selection. The breakdown does not differentiate between senior level courses (that can indicate strength in teaching) from graduate level courses (that can indicate strength in research). A clear pattern nevertheless exists. There is evidently a core of about a dozen Universities with strength in fuels or fuel-related activities. About half are more engine or propulsion oriented (Cal Tech, Michigan, Purdue, Wayne State in particular). The other half are more fundamentally/industrially oriented, or showing equal weight with engine/propulsion aspects (notably Penn State, Georgia Tech, IIT, MIT).

It would appear, then, that a Fuel Technology and Combustion Engineering community and constituency does exist. There can be a question as to how it should grow. There are constraints: funding or the lack of it is the most important, but there is also a shortage of manpower. What else could happen if the subject has been short-changed for so long? It is also not clear whether the center of gravity of Fuel Technology properly lies in the mining, mechanical, chemical, or even metallurgical or some other engineering area. Perhaps the best means of expanding Fuels programs would be by creating Options or Minors in Fuel Technology inside existing Departments of different disciplines. This would not overload the available manpower, and would either provide time for an evaluation of the subject matter to see where it best lies or it would solve the problem by having a different bias -- mechanical, or chemical, or some other -- in different institutions. This may prove indeed to be the only feasible method of providing adequate coverage of the whole area of Fuel Technology. In course of time, such Options and Minors might expand into Sections inside the parent Department, and ultimately the Sections could become Departments. An organic growth based on real need rather than a forced growth based on expectations is obviously a preferred behavior. It is probably not necessary or even desirable for this to be accompanied by the development of the usual paraphernalia of Departments, rigid

curricula, Institutes, Journals, and the like, so long as there are sufficient centers of Fuel Technology that recognize each other and whose standing is acknowledged and made use of. The criteria of visibility, credibility, and viability must be met.

CONCLUSIONS

A coherent, significant, and important body of knowledge representing Fuel Technology does exist, together with a practical reason for its existence. Between half a dozen and a dozen Fuel Technology centers also exist already, at least embryonically. An academic framework for the necessary instruction and research also exists. It would seem that Fuel Technology is ready to come of age and to be recognized as a significant academic and practical discipline in its own right.

Reference

1. Smith, M.L. and Stinson, K.W., "Fuels and Combustion", McGraw Hill, 1962.

Acknowledgements

Preparation of this paper was made possible by support of the Combustion Laboratory Cooperative Fund (Contributors: ALCOA, Combustion Engineering, General Electric, General Motors, Gulf, Mobil, Pittsburgh Plate Glass, Phillips). The selection and compilation of the Fuel Technology courses offerings used as the basis for Table 2 was carried out by Dr. E. Gootzait.

Table 1

Courses in Fuel Science

- F.Sc. 421 Flames. Fundamentals of premixed and diffusional combustion.
- F.Sc. 422 Combustion Engineering. Principles of industrial combustion and gasification engineering.
- F.Sc. 424 Energy and Fuels in Technological Perspective. Critical examination of present-day energy technology.
- F.Sc. 430 Air Pollutants from Combustion. Pollutant-forming processes; pollutant potential of various fuels and combustors; combustion modification and pollution control.
- F.Sc. 431 The Chemistry of Fuels. Origins and properties of the fossil fuels: coals, oils, gas. Coal liquefaction and gasification.
- F.Sc. 506 Carbon Reactions. Heterogeneous reactions of carbons. The scientific base for coal gasification.
- F.Sc. 512 High Temperature Kinetics and Flame Propagation. Equilibria and rate processes in hot gases; flames; detonations.
- F.Sc. 520 Thermodynamics and Kinetics of Fuel Efficiency. Thermodynamic and kinetic constraints on efficiencies of thermal systems; efficiency ratios; furnace analysis; radiation in furnaces, applications and examples.
- F.Sc. 522 Flame Dynamics in Combustors. Analysis of mixing and reaction in high intensity combustion chambers.

Table 2

Number of Course offerings in Fuel Technology
at Different Institutions

T - total Course offerings in Fuel Technology
I - Courses on flames, combustion, pollution, etc.,
and non-engine or propulsion topics
IA - as the major subject

	T	I	IA
Cal Tech	12	5	3
Cincinnati	9	8	8
Georgia Tech	16	13	11
IIT	10	8	7
MIT	13	9	7
Michigan	12	6	3
Minnesota	9	4	4
N. Carolina State	9	4	3
Penn State	20	17	16
Princeton	10	7	7
Purdue	10	4	1
Stevens	8	7	4
Utah	14	14	12
Wayne State	10	7	5
Totals	162	113	91

Note: A total of 500 courses in Fuel Technology were identified offered at 120 different universities and similar teaching institutions. About half offer only 3 courses or less. The 14 institutions listed above offer about 1/3 of all the courses.

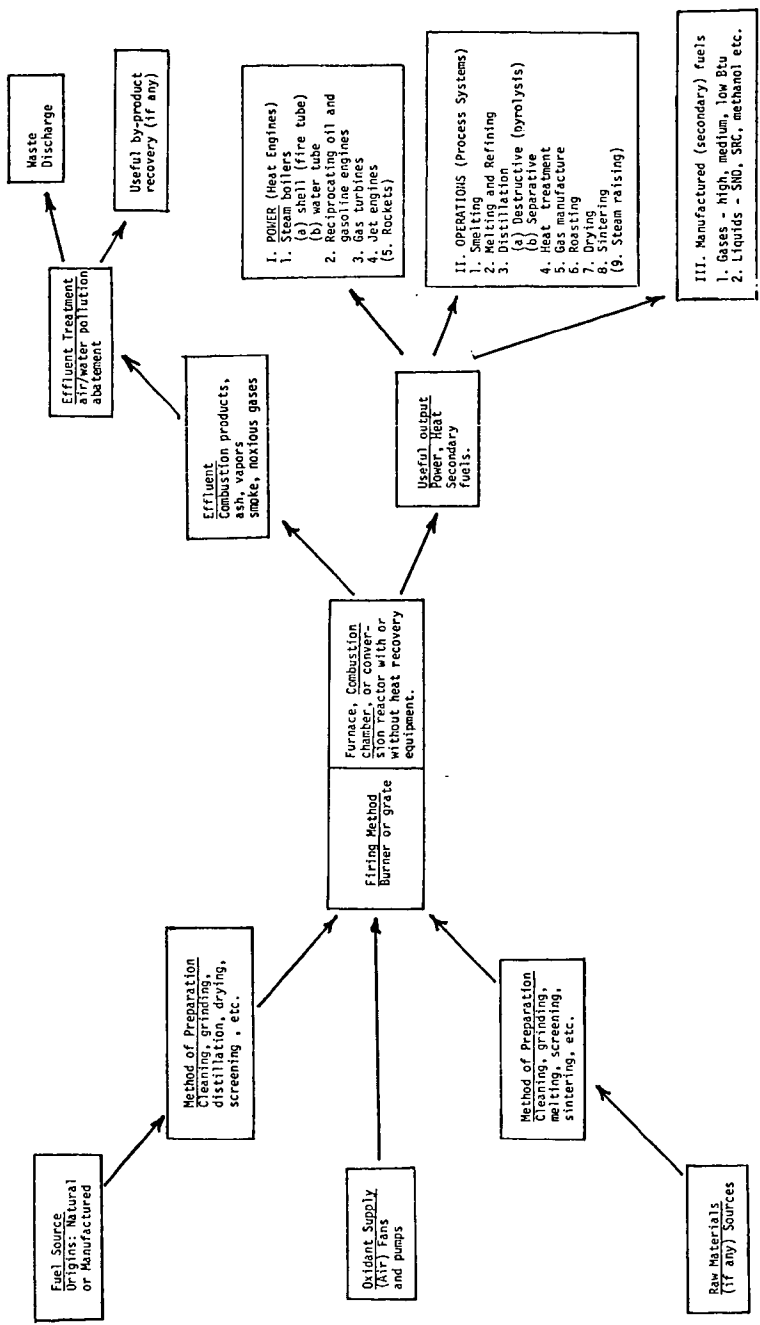


Fig. 1 - Schematic Representation of a Combustion Engineering Operation with Principal Applications (Useful Output)

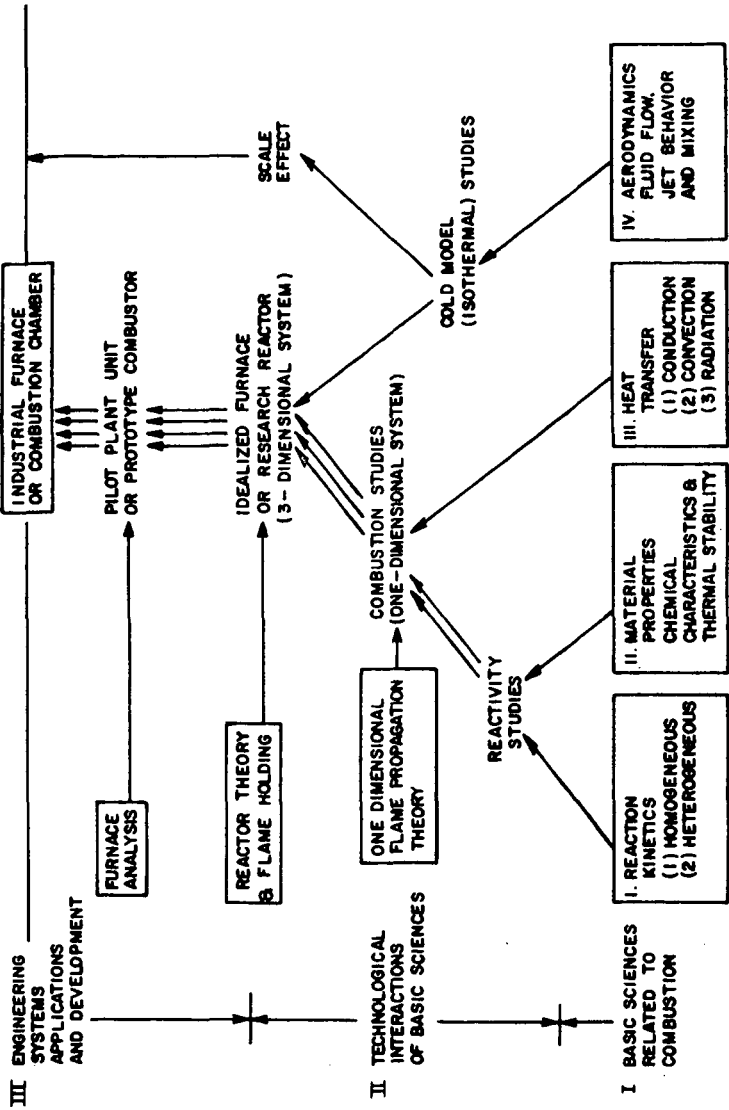


Fig. 2 - Schematic breakdown to illustrate the information flow required for a complete understanding of industrial furnace or combustion chamber behavior. Understanding rests on the four basic sciences: I, Reaction Kinetics; II, Materials Properties; III, Heat Transfer; IV, Aerodynamics. The diagram also illustrates the general relationship between science, technology, and engineering.